Robot aided gait training and assessment

Development of support strategies and assessment methods for LOPES

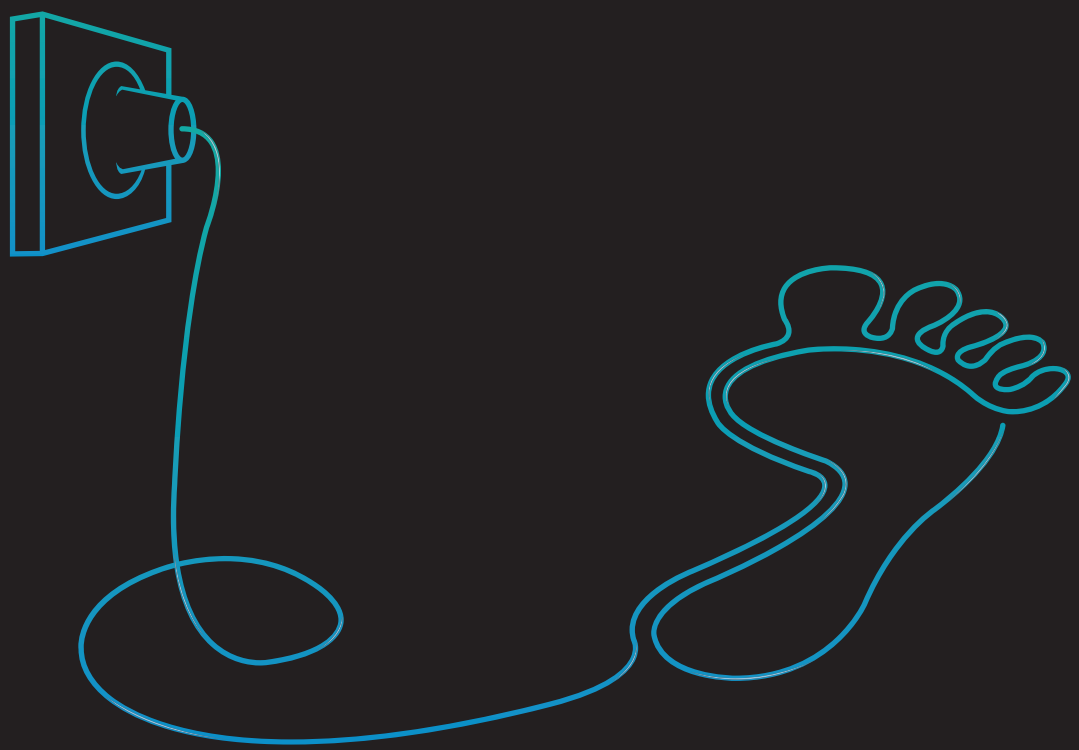

Bram Koopman

Robot aided gait training and assessment

Development of support strategies and assessment methods for LOPES

Bram Koopman

Colofon

The research presented in this thesis is supported by a grant from the Dutch Ministry of Economic affairs and the Province of Overijssel (grant: PID082004), and the EU, within the EVRYON Collaborative Project (Evolving Morphologies for Human-Robot Symbiotic Interaction, Project FP7-ICT-2007-3-231451).

The publication of this thesis was financially supported by:
Department of Biomechanical Engineering of the University of Twente
MOOG BV

Printed by: Koninklijke Wöhrmann

Cover: Dennis Willems, Dezzign

ISBN: 978-90-365-3766-7

ROBOT AIDED GAIT TRAINING AND ASSESSMENT

DEVELOPMENT OF SUPPORT STRATEGIES AND ASSESSMENT METHODS FOR LOPES

PROEFSCHRIFT

ter verkrijging van
de graad van doctor aan de Universiteit Twente,
op gezag van de rector magnificus,
prof. dr. H. Brinksma,
volgens besluit van het College voor Promoties
in het openbaar te verdedigen
op woensdag 10 december 2014 om 16:45

door

Bram Koopman
geboren op 19 augustus 1982
te Twello

Dit proefschrift is goedgekeurd door promotor:
Prof. dr. ir. H. van der Kooij

en door de assistent-promotor:
Dr. E.H.F van Asseldonk

ISBN: 978-90-365-3766-7

Samenstelling promotiecommissie

Voorzitter / Secretaris
Prof. dr. G.P.M.R. Dewulf

Promotor
Prof. dr. ir. H. van der Kooij

Assistent-promotor
Dr. E.H.F. van Asseldonk

Leden
Prof. dr. ing. R. Riener
Prof. dr. ir. J. Harlaar
Prof. dr. ir. S. Stramigioli
Prof. dr. J. S. Rietman

Paranimfen
Pim Koopman
Rob Schoot Uiterkamp

Contents

Chapter 1

General introduction

1.1 Introduction

Many patients with neurological injuries, like stroke or spinal cord injury (SCI), suffer from muscle weakness, loss of independent joint control and spasticity, resulting in reduced walking ability. For many of these patients, relearning to walk is an important goal during the rehabilitation process. The ability to walk also positively affects other activities of daily living and improves general psychological and psychosocial wellbeing. The high demands placed on the therapist during manually assisted gait training has led to the introduction of robotic devices that can provide the required assistance. Robotic gait trainers have the potential to deliver longer, and more intensive, training sessions than that can be achieved during conventional therapies, and enable objective monitoring of the patients' progress. Over the past two decades robot-aided gait training has slowly found its way into the clinics. However, to date, these robotic gait trainers have not fulfilled the high expectations that were raised.

In this introduction the two topics of this thesis are outlined: 1) how can robot-aided gait training be improved to increase its clinical effectiveness, and 2) how can robotic gait trainers be utilized to quantitative measure physiological properties of the patient. The chapter starts with a short introduction on stroke, SCI, body weight supported treadmill training and the rationale for robotic gait training. Next, it provides an overview of the different types of gait trainers and their effectiveness so far. Subsequently, the different control regimes that are currently being developed will be addressed, together with the challenges that they introduce. Finally, the concept of neurological assessment with robotic gait trainers is introduced and the chapter concludes with the aims and outline of this thesis.

1.2 Stroke

Stroke or cerebrovascular accident (CVA) is the third most frequent cause of death worldwide and the second leading cause of death in developed countries [1]. It is among the leading causes of long-term disability in industrialized countries [2-4] and typically affects the elderly population. The age-dependency of stroke is reflected in a progressive increase of incidence with each decade of life. For example, the incidence rate of stroke for those aged <45 years ranges from 0.1-0.3 per 1000 individuals per year, whereas for those aged 75-84 years the rate increases to 12-20 [5]. Similarly, the overall prevalence ranges from 5-10 per 1000 individuals, whereas >65 years it ranges from 46.1-73.3. The prevalence of stroke is higher among men up to the age of approximately 85 years, after which it becomes higher in women [6]. The incidence of stroke has decreased over the past years due to preventive measures but the lifetime risk has not declined to the same degree, perhaps due to improved life expectancy [7-9]. Thus, despite these preventions, the burden of stroke on the healthcare system has not substantially diminished.

Strokes occur due to problems with the blood supply to the brain. Between 70-90% of strokes are ischemic strokes [5,10]. Ischemic strokes are caused by an obstruction in a blood vessel (thrombotic or embolic), which reduce (or block) the blood flow to the brain. The other 10-30% are hemorrhagic strokes, caused by a ruptured blood vessel. Blood accumulated in the surrounding brain tissue will damage the cells, and the brain cells beyond the leak get deprived of oxygen and nutrients. Disrupting the blood supply to the brain for too long can result in loss of specific functions on the contralateral side of the body.

The severity and the kind of function loss depend on the severity of the stroke and on the affected brain region. A typical stroke patient has hemiplegia (paralysis of one side of the body), but loss of sensation, difficulties with speech or visual impairment are also often seen in stroke survivors. The majority of these patients initially lose the ability to walk independently or create abnormal (typically asymmetric) gait patterns, due to muscle weakness and spasticity [11-15]. Partial recovery can be expected within the first 3-6 months. Still, 30-50% of surviving patients do not regain independent walking [16-18].

1.3 Spinal cord injury

Spinal cord injury (SCI) affects between 10.4 and 83 people per million individuals per year (for the developed countries), which leads to an estimated prevalence between 223 and 755 per million inhabitants [19]. The incidence of SCI is relatively high amongst men (men/women: 3.8/1) [19]. The average age of patients sustaining their injury is relatively young (33 years) [19], compared to other neurological disorders like stroke (70 years) [5], [10]. To improve the quality of life of SCI patients, and reduce the financial burden over the remainder of their lifetime, it is therefore important to optimize the recovery process after SCI.

A spinal cord injury is a defect to the spinal cord, resulting in temporary or permanent changes in muscle strength, sensation and other body functions. The cause of spinal cord injuries can be traumatic or non-traumatic. Non-traumatic causes include tumors, ischemia, hemorrhages, or infections to the spinal cord. A lesion to the cervical spinal cord affects all four extremities (quadriplegia), while lesions below that level affect the legs only (paraplegia). Roughly one-third of SCI patients is quadriplegic and two-thirds are paraplegic [19,20]. SCI can be classified using the ASIA scale, which ranges from a complete loss of motor and sensory function in the sacral segments S4-S5 (ASIA A) to a complete restoration of sensation and motor function (ASIA E)[21].

Depending on the extent and the position of the damage, partial or complete loss of motor, sensory, and vegetative function can occur. Symptoms vary widely and may include loss of sensation, (partial) paralysis, incontinence, spasticity or neuropathic pain [22]. Although patients with incomplete lesions [23] have a good prognosis with regard to walking function, they are usually unable to walk at the early stages of recovery due to muscle weakness. For patients with incomplete lesions, one-half to two-thirds of the one-

year motor recovery occurs within the first two months, but recovery can continue up to two years after injury [24,25], or even longer [26]. The recovery of walking in terms of ambulatory function varies from 50% for ASIA B to over 75% for ASIA D classified patients [27,28]. Still, many SCI patients experience limited hip flexion during the swing phase and insufficient knee stability during the stance phase. Consequently, these individuals have reduced ambulation [29], walk slower, with reduced cadence and stride length [30], and often remain reliant on the use of assistive devices [31].

1.4 Neural plasticity

Losing the ability to walk is a major disability for individuals who suffered a SCI or stroke. For most patients, regaining mobility is one of the most important goals during recovery, since walking is a key factor for greater independence [32-35]. Although the location of the trauma obviously differs between stroke and SCI, it is believed that the underlying mechanisms that accompany regaining locomotor function are similar. For stroke, as well as SCI, recovery of function can largely be attributed to spontaneous- and activity-based-neural plasticity [36-39]. Neuroplasticity is defined as the ability of the nervous system to reorganizing its neuronal circuits to compensate for the injury. This emphasizes the need to establish training conditions, such that the nervous system receives the appropriate signals to drive activity-based plasticity. It is believed that, to promote neural plasticity, gait training should be task-specific, repetitive, meaningful, intensive, should start as soon as possible [40-53], and should provide appropriate afferent feedback [54]. For example, afferent feedback from hip extensors, and load receptors in the foot soles, proved to be critical for the generation of rhythmic muscles activation patterns during locomotion [55-57].

1.5 Body weight supported treadmill training

To improve gait performance Body Weight Supported Treadmill Training (BWSTT) has been used for over a decade as a regular form of therapy for neurological patients. BWSTT is a form of training where the patient walks on a treadmill with (partial) support of his body weight, while physiotherapists manually assist the leg movements. It is highly task-specific and repetitive, and allows a greater number of steps to be performed within a single training session compared to conventional physiotherapy. During BWSTT the therapists generally try to guide the legs (where required) towards a “normal” gait pattern [58]. BWSTT has become a well-accepted training approach, and has shown to be successful in improving gait function after SCI [58-61] as well as stroke [48,62-65]. Although several reviews concluded that the effects of BWSTT are equivalent to other training [27,66-68] approaches, or even somewhat smaller [69], it is still considered a valuable tool for locomotor training in neurological patients, as it provides a safer and more convenient way of gait training and enables gait training in the early stages of recovery.

Despite these benefits, BWSTT for SCI patients generally requires two physiotherapists to assist leg movements on both sides of the body. In some cases, even a third therapist is required to stabilize the movement of the trunk [58]. Consequently, it required substantial experience from these therapists to coordinate their movement. Also, the need for multiple therapists might not be financially feasible for every clinic [70]. Although the weight of the patient is partially supported, BWSTT remains a very labour intensive practice, and the position of the therapist, who is seated beside the treadmill, tends to be ergonomically unfavourable. Especially for severely affected SCI or stroke patients, where motor impairments can impede the performance of even a single movement, providing appropriate manual support is physically demanding for the therapist. As a result, the training duration (or the amount of steps practiced) may be limited by the physical fitness of the therapists themselves, and may end up being similar to the amount of steps practices during overground walking sessions [71].

1.6 Rationale for robotic gait training

The repetitive behaviour and task specificity of conventional therapy has stimulated the development of robotic systems that can assist locomotor training for individuals who suffered a SCI or stroke. These robotic systems are attached to the limbs of the patients and can assist locomotion by exerting forces on the limb, much like the manual assistance provided by a therapist. The most important advantage of robotic devices is the ability to increase training intensity and duration, while reducing the workload and discomfort of the therapist [72]. They also enable objective monitoring of the patients performance and progress [73], reduce the number of therapists required to assist the patient [74] and can eliminate the between-trainer variability in terms of the applied supportive forces [75].

Several studies have investigated the adaptive capacity of the nervous system in animals and humans. However, the amount of task-specific repetitions performed during conventional post-stroke therapy is generally substantially smaller than in these studies [76]. By reducing the labour intensive demands (and therapist discomfort) the number of steps can be increased. For example, Schmidt et al. [71] estimated that with robotic gait training up to 1000 steps are performed, whereas during manually assisted training only +/- 100 steps were performed. Regarding training time, Colombo et al. [77] reported that automated gait training could be extended up to 60 minutes, while manually assisted therapy lasted only for about 10-15 minutes. Noteworthy, the limiting factor for the manually assisted training was the therapist, whereas during automated gait training usually the patient became exhausted. In this respect, robotic gait training can provide a safe environment where patients can perform as many step repetitions as they are physically capable of.

1.7 Existing robotic gait trainers

Since the start of the millennium, various robotic gait training devices have been developed. The majority of the robotic gait trainers can roughly be characterized as: 1) exoskeletons, 2) end-effector based systems, or 3) mobile robotic devices that support overground walking (figure 1).

1.7.1 Exoskeletons

In exoskeleton-type robotic gait trainers a mechanical exoskeleton is attached to the limbs and moves in parallel with the patient. These types of gait trainers are usually combined with a treadmill and BWS system. Examples include the Lokomat (Hocoma) [77] and the

Figure 1: Different types of robotic gait trainers. The majority of the robotic gait trainers can roughly be characterized as exoskeletons (top), end-effector based systems (middle), or mobile robotic devices that support overground walking (bottom).

AutoAmbulator (Healthsouth)/ReoAmbulator (Motorika), which are both commercially available. In addition, many experimental exoskeleton-based robotic gait trainers are used at various research institutes, such as the ALEX (Active Leg Exoskeleton) [78], the KNEXO [79], and the LOPES (Lower Extremity Powered Exoskeleton) [80]. These exoskeletons are under continuous development, which has led to new prototypes like the ALEX III [81] and the LOPES II [82] with additional (actuated) degrees of freedom and modified structures to allow arm swing.

1.7.2 End-effector-based systems

Alternatively to the exoskeleton-type robotic gait trainers, which are connected to the patient's leg at multiple points, end-effector-based robotic gait trainers are coupled only to the patient's feet. The harness-secured patient is positioned on a set of footplates, which simulate the stance and swing phases of walking. An example of such a gait trainer is the Gait Trainer 1 (GT1, Reha-Stim), which is commercially available. Compared to exoskeletons, end-effector-based gait trainers lack the ability to control poor joint stability. Also, they modify the sensation at the foot soles that normally occurs during the swing and stance phase. In contrast, they require less time to adjust to the subject's anthropometry, take little time to put on and take off, and do not suffer from the consequences of joint misalignment [83]. Newer versions have fully programmable footplates that allow training of other gait related tasks. Gait trainers like the HapticWalker [71] (commercialized as the GEO, Reha Technologies) or the Gait Master [84] have been developed to assist stair climbing or walking on different terrains. A different type of end-effector gait trainer is the LokoHelp (Woodway) [85], which is fixed onto a motorized treadmill and converts the treadmill movement into a stepping pattern (figure 1).

1.7.3 Mobile robotic devices that support overground walking

Overground walking can be assisted by gait trainers like the KineAssist (Kinea Design), which has a mobile base and provides partial body weight support to the pelvis, whilst leaving the patient's legs unobstructed to allow the therapist to manually support the legs. There are also more complicated mobile systems like the WalkTrainer [86], which consists of a mobile base in combination with a leg and pelvic orthosis to actively assist leg movements. Overground walking can also be assisted by wearable exoskeletons, which can focus on a single joint like the AnkleBOT [87] and the PK100 Bionic Leg Orthosis (Tibion), or which can assist multiple joints like the Ekso (Ekso Bionics), the HAL (Cyberdyne), ReWalk (Argo Medical Technologies) or the Rex (Rex Bionics). These devices were initially designed to assist the users in their daily activities, but can also be used as therapeutic devices, in which patients can practice walking. As these systems provide limited balance- and trunk-support, additional support from a BWSS may be required for more severely impaired patients.

1.8 Robotic gait training after stroke and SCI

Despite the large amount of gait trainers that are under development, so far most of the studies that assessed the effectiveness of robot-aided gait training for patients with SCI or stroke have been performed using the commercially available gait trainers. Despite the reduction in labour intensity, the therapeutic efficacy of these robotic gait trainers is still at an early, rather inconclusive state.

Several studies showed improvements in walking ability between pre- and post-training in acute and chronic SCI patients who trained with the Lokomat [88-92], the Gait Trainer [91,93] or the Lokohelp [85]. However, only a limited number of randomized controlled trials (RCTs) [61,74,94,95], or other study designs [91,96], have been performed to investigate if these improvements are superior to those obtained using conventional approaches. The RCTs that have been performed show contradictory results. Field-Fote et al. [61] concluded that Lokomat training was the only training modality that did not result in significant improvements in walking ability, while others [74,95,96] found no significant differences in functional ambulation between different rehabilitation approaches. Benito-Penalva et al. [91] trained patients with SCI in the LOKOMAT and the Gait Trainer and compared the results with data obtained from the European Multicenter Study about Human Spinal Cord Injury. They reported a significant improvement compared to patients receiving conventional therapy without a robotic systems. Noteworthy, no significant difference in effectiveness of the LOKOMAT and the Gait Trainer was found.

Similar contradicting results have been reported for stroke survivors. Several RCTs demonstrated a significant improvement in overground gait speed, endurance or functional ambulation in the group that used the Gait Trainer [97-99] or the Lokomat [100], compared to conventional physiotherapy. Again, other studies found no significant difference between robotic support and manually assisted treadmill training [101,102] or conventional physiotherapy [103-106]. Hornby et al. [107] even reported that manual support is superior to robotic support. A large multicenter RCT, perfomed by Hidler et al. [108], also concluded that conventional therapy is more effective than robotic-assisted gait training. They also suggested that this may be caused by the diversity of conventional gait training.

A recent meta-analysis by Mehrholz et al. [109] revealed that the observed differences in effectiveness of robotic gait training for stroke patients is most likely due to the types of intervention and the included patient groups. They concluded that robotic gait training in combination with physiotherapy increased the odds of participants becoming independent walkers, compared to robotic gait training alone. They also suggested that, for robotic gait training, greatest benefits with regard to independence in walking can be achieved in participants who are non-ambulatory at the start of the intervention, and in those for whom the intervention is applied early post-stroke. For SCI patients, so far, such trends have not been observed [35,110,111]. These data demonstrate the need to

improve robotic gait training for the less severely affected and chronic patients, so they can also benefit from robot-aided gait training.

1.9 Optimizing robotic gait training

The fact that the therapeutic effect of the "first generation robotic gait trainers" was somewhat disappointing might have been related to the way they were controlled. These early robotic systems used position control to ensure that the patient followed the desired "normal walking pattern" as closely as possible, and did not take the participant's volitional effort into account. This approach proved well suited for patients who are in the early phase of rehabilitation, or who are severely affected, but may not provide the ideal training circumstances for less impaired patients. Although these robotic gait trainers facilitated gait training that was task-specific, repetitive, meaningful, and provided the user with the appropriate afferent feedback, they did not encourage the patient to actively participate. Furthermore, the fixed pattern imposed by the robot reduced the ability to make, and correct, movement errors. Both active participation and movement variability are considered crucial for motor recovery and may play an important role in optimizing robotic gait training.

1.9.1 Active participation

Active patient participation has proven to be an essential component to maximize motor learning and functional improvements in general [112-115], and is suggested to have a strong impact on almost all of the elements of gait recovery in neurological patients as well [116]. However, so far, the voluntary contribution of patients during robot-assisted walking has been rather limited [117]. In SCI patients, moving the legs in a rigid fashion, especially in individuals with some ability to walk, has shown to reduce volitional activity (EMG and VO_2), compared to therapist-assisted BWSTT [74,118,119] or walking without assistance [120]. This phenomenon is also referred to as "slacking", meaning that the user may relax his efforts learns to rely on the support [121,122]. That a patient contributes less than he/she is actually capable of is even seen in manually assisted gait training [117]. Motor learning experiments have confirmed that humans are excellent in minimizing their efforts when given a chance by an assisting robot [122,123]. When active participation is not promoted "the robot may become an analogy of training wheels that will not come off a bicycle" [124].

1.9.2 Movement variability

With position-controlled gait trainers, the consistency of the performed steps is superior to that provided during manually assisted support. However, these trainers also eliminate the natural kinematic variability in the gait pattern and diminish the possibility to make, and correct, movement errors [83]. The problem solving nature associated with learning a new task, or relearning a lost task, is considered the key component for motor learning

[125-127]. In other words, effective practice requires more than just movement repetitions. Animal studies have shown that training with a variable stepping pattern results in higher levels of recovery than walking with a fixed stepping pattren [128,129]. Although recovery mechanisms in mice and rats may not be representative for humans, similar benefits of movement variability are seen in neurological patients, suggesting that training with kinematic variability is advantageous. In line with this, a recent study by Lewek et al. [130] showed that intra-limb coordination after stroke was improved by manually assisted training that allowed natural kinematic variability. In contrast, position-controlled training, which reduced the kinematic variability to a minimum, did not alter intra-limb coordination.

1.10 Assistive controllers

In response to these findings most current robotic gait trainers are designed to make the assistance compliant, either by using impedance- or admittance-control algorithms. They guide the leg by applying a force rather than imposing a trajectory. These strategies allow a certain level of variation in gait kinematics and require active participation of the patient, while still providing sufficient guidance and support to ensure successful walking. In addition, this type of control may increase the patient's motivation, as he/she sees and feels the results of a decreased (and increased) effort. Furthermore, the assistance allows the patients to be more successful with their movement attempts, which encourages them and keeps them interested [131]. Impedance or admittance controllers try to mimic the skills of a trained therapist, who is likely to be compliant, motivational and adaptive to the needs of the patient. Controllers based on this principle are referred to as "assist-as-needed" (AAN), "cooperative" or "interactive" controllers [124,132-135].

1.10.1 Technical implementation

Technical implementation of these control strategies often consists of a predefined reference trajectory (or path) in combination with a "virtual wall" or force field. The stiffness of the virtual wall determines the amount of supportive force that is applied when the individual deviates from the predefined movements (impedance control). These predefined trajectories can be defined in joint space [124,133,136] or in Cartesian space (figure 2) [132,135,137,138]. Impedance (or admittance) control can make the robot's behavior adaptive to the user's needs. That is: the stiffness of the virtual wall/force field can be adapted to the capabilities, progress and current participation of the patient [133]. This allows individuals to benefit from robot-aided gait training throughout the different stages of recovery. At the initial stages of recovery, when the patient is not capable of generating any appropriate activity, the robot will take charge (high impedance) and practically enforce a gait pattern. At the later stages of recovery, when the patient can generate a large part of the required movement himself, the robot will just move along (low impedance).

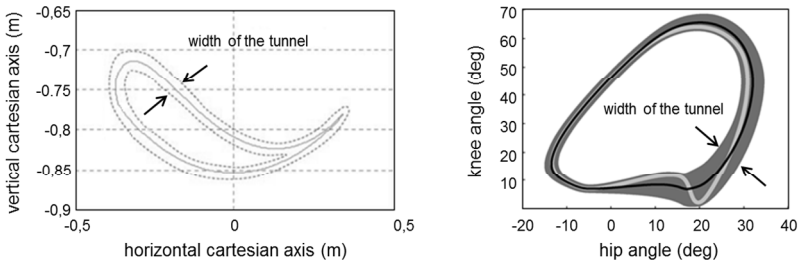

Figure 2: Predefined trajectories in Cartesian and joint space. Left: Predefined trajectories in Cartesian space, adapted from Banala et al. [135]*. The solid line represents the desired trajectory of the ankle, the distance between the dached lines represent the tunnel. Right: Predefined trajectories in joint space, adapted from Duschau-Wicke et al.* [134]*. The solid black line represents the desired trajectory of the hip and knee, the dark gray area represents the tunnel.*

Spatial variation in the gait pattern, and the possibility to make small movement errors, can be increased by lowering the impedance levels or by creating a "virtual tunnel" [135], a "dead band" [134,138] and/or a nonlinear force field [134,135] around the reference trajectory (figure 2). Within the tunnel free movement is allowed, but once the patient hits the wall, supportive forces are applied to assist the patient towards the center of the tunnel. For the Lokomat, the width of the tunnel is a function of the gait phase. It is designed to allow increased spatial variation during the late swing and early stance phase, to account for the large variability in knee flexion at heels strike that was observed in their subjects [134]. Their nonlinear force field enables soft contact with the wall and strong corrections for larger deviations.

In addition to spatial variation, temporal variability can also be implemented, but this requires synchronization between the reference trajectory and the actual trajectory. To account for alterations in cadence, the reference trajectory can be accelerated or decelerated, based on the difference between the current gait phase of the subject and the state of the robot. This may be done continuously [124,134] or on a step-by-step basis [139]. If patients have difficulties initiating the stepping pattern, supportive torques can be applied to assist the patient along the desired path [134]. In some cases a "moving back wall" is introduced, to assist in the timing of the stepping pattern when a patient "falls behind" [134,135]. In most applications, the forward support is related to the deviation from the path, such that the forward force is only applied when the leg is close to the desired path [134,135].

1.10.2 Effectiveness of AAN strategies

While these AAN strategies enable more active patient participation, evidence for better functional outcomes is still limited. In mice and rats it has been demonstrated that locomotor training with AAN algorithms is more effective than position-controlled training [138,140]. In addtition, Cai et al. [138], also concluded that adding a moving back wall, which facilitated alternating inter-limb coordination, was more effective than AAN alone.

The effect of these AAN algorithms in neurologically impaired humans however, is unclear, although some promising results have been reported. In SCI patients, the "patient-cooperative approach" of the Lokomat resulted in increased temporal and spatial variability and increased muscle activation levels, compared to non-cooperative position-controlled training [134,141]. Krishnan et al. [142] added a motor learning task, which required a greater hip and knee motion during the swing phase, on top of this approach, which resulted in a further increase in muscle activation levels. Schück et al. [143] combined the "patient-cooperative approach" with their "Generalized Elastic Path Control" approach, to allow more free movement within the tunnel. They trained two patients with a SCI and two stroke survivors for four weeks (four times per week). However, only one stroke survivor gained a significant and relevant increase in gait speed after training. Krishnan et al. [144] compared the same combination of controllers with conventional (position controlled) robotic gait training in a single stroke subject. The participant trained for four weeks (three times per week) with position-controlled robotic gait support, followed by four weeks of patient-cooperative robotic support. The position-controlled gait training did not produce any meaningful changes in the measured clinical outcomes, whereas the four weeks of cooperative control training resulted in substantial improvements in gait velocity and 6-minute walking distance. In another study by Banala et al. [135] the ALEX was used to train two stroke survivors over 15 sessions (spread over a 6 week period). They used the tunnel approach in combination with the moving back wall and found that, at the end of the training, the gait pattern of the patients became closer to a healthy subject's gait pattern. Also, the patients's walking speed on the treadmill increased. Whether the increased walking speeds translated to an increase in walking speed overground was not reported. Although these data are promising, none of these studies performed a follow-up to see if the participants retained their training-induced functional improvements. Therefore, there is no clinical evidence that these concepts will actually lead to improved walking function in the long term.

1.11 Challenges of AAN strategies

In order to maximally benefit from AAN strategies, a number of new challenges have to be solved first.

1.11.1 Reference trajectories

Although AAN strategies apply supportive forces rather than enforcing a predefined gait pattern, they still require a predefined trajectory to determine the amount of support. Consequently, an important question remains; what should this predefined gait pattern look like. The most common strategy to determine the desired trajectory is based on pre-recorded trajectories from unimpaired volunteers walking on a treadmill or walkway [86,136,145,146]. Alternatively, they can be recorded while unimpaired volunteers walk in the device while it is operated in a transparent mode [124,135,137,139] or with the motors removed [77]. While the reference trajectories are often recorded in the device

out of convenience, in some cases this is done deliberately, to obtain gait patterns that take into account gait modifications that may result from restrictions of the orthosis during walking [77].

In most cases, gait trajectories are recorded at multiple walking speeds, to account for their speed dependency [147,148]. Still, it often remains unclear how to adjust these patterns when the training speed of the patient does not match the speed of one of the pre-recorded patterns. Also, most systems define the reference gait trajectory without considering the patient's anthropometry, although in some cases a healthy control subject is selected, whose dimensions match with the patient receiving the support [135].

Although it is possible to generate gait trajectories that resemble an average pattern, they will never form a perfect match for every individual patient. To modify the reference trajectories to the preferences, and current capabilities, of the patient, different strategies are employed. Some create patient specific patterns by recording the gait trajectory while the patient walks with manual assistance [124,139], while others try to reconstruct gait patterns based on the movements of the unimpaired limb [149]. The reference trajectory can also be personalized by slowly scaling each patient's pre-training gait pattern towards a heathy reference trajectory [135]. Others use reference trajectories that are scalable in time, amplitude and offset [133,136], which allows them to modify the gait pattern based on the subject's height, and range of motion at the joints (e.g. less hip extension when tight hip flexors are present) [83]. Alternatively, the reference trajectories can be optimized online by estimating the human-robot interaction torques and minimizing these by changing certain parameters of the reference trajectory [150,151]. Regretfully, these parameterizations do not take into account the relative timing of the extremes in the gait patterns, which are known to change with walking speed [148].

1.11.2 Setting the proper support level

The majority of the assistive control algorithms discussed above require the therapist to predefine the controller settings. This allows the therapist to modify the impedance level based on qualitative observations of the patient's capabilities and progress, but also introduces challenges. Setting the support levels too low may result in dangerous situations, whereas too much assistance might induce slacking. In fact, Duschau-Wicke et al. [134] experienced that some SCI patients showed slacking behavior by "leaning" on the tunnel wall to keep their legs extended during the stance phase. This limitation may be overcome by adapting the controller settings real time, based on the patient's performance or needs. So far, automated adjustment of the support levels can be achieved in two ways: 1) based on an estimation of the overall patient effort (detected with force sensors) or 2) based on kinematic errors. The first was described by Riener et al. [133], who implemented an algorithm that increases the overall impedance when there is little patient effort detected and vice versa. Emken et al. [139] developed an error-based controller with a forgetting factor. The algorithm systematically reduces the impedance levels when kinematic errors are small, whereas the impedance levels are increased when

the errors are large. The latter algorithm has the advantage that the assistance can be automatically tuned to the participant's individual needs, over the course of the rehabilitation process, but also throughout the gait cycle. They showed that, after convergence of the support levels, each subject obtained a unique set of support levels, which varied with the phase of the gait cycle and correlated with the subjects' needs. Furthermore, it was demonstrated that SCI patients trained with more variability when they used their impedance-shaping algorithm.

1.11.3 Transparency

When these AAN algorithms reduce the support levels, the transparency of the device largely determines the amount of movement variability. Transparency refers to the ability of the robot to "get out of the way" [152], meaning that the robot moves along and does not intervene with the movements of the patient. The transparent mode is essential at the final stages of recovery, when patients only require little support. In that case, a perfectly transparent robot would induce no forces at all, and walking in the robot would resemble normal walking. This transparent mode is also key in training patients with hemiparetic gait, where the paretic-leg needs support, whereas the unaffected leg should be able to move freely. The same applies to specific joints that may not require support.

The overall transparency of a device depends on several properties. Firstly, the device should have sufficient degrees of freedom (DoFs) to move in an unobstructed way. For example, in a perfect transparent robot the patient would have to maintain its own balance. The lack of balance training in most robotic gait trainers is suggested to be one of the contributing factors why robot-aided gait training has not been proven superior to manually assisted treadmill training [153]. When providing manual support an experienced therapist would allow the subject to balance himself as much as possible, providing just enough assistance. Balance training in many robotic gait trainers, however, is not possible due to the constraints on the pelvis that these devices impose. Different studies have shown that constraining the pelvis affects foot placement [154], trunk motion [155], joint kinematics [83], and muscle activation patterns [156]. It also strongly decreases the efforts that subjects have to put in keeping their body upright [157], whereas the goal of the transparent mode is to increase patient participation. Even when sufficient DoFs are provided at the pelvis, the inability to perform sufficient hip abduction in some robotic gait trainers inhibits proper balance training, since lateral foot placement is used to control balance during gait [158]. Consequently, pelvic motions and hip abduction should be incorporated in the device to allow normal walking. These DoFs are incorporated in most experimental gait trainers like the PAM and POGO [124], ALEX III [81] and the LOPES [80], but can also be added to existing gait trainers by adding a dedicated module [159].

The second determinant of the possible level of transparency is the weight of the device. Adding addition mass to the legs (especially at the more distal locations) is known to increase metabolic rate and affect swing and stride times [160,161]. Consequently, bulky

robotic gait trainers will not be able to provide sufficient transparency, and thus, will not be suitable for training patients who require little support. Therefore, in newly designed robotic gait training systems, developers attempt to keep the exoskeleton as lightweight as possible to ensure sufficient transparency [137]. However, mass reductions are often limited when additional degrees of freedom are preferred, or when heavier actuators are required to assist severely impaired patients. In the LOPES, for example, the latter is solved by detaching the motors from the robot frame to decrease the weight and the inertia of the robot [162].

The transparency of the robot can also be increased by means of control algorithms. For the LOPES we use closed-loop force control [162], which allows the robot to be controlled in zero-force control. This enables the subject to move freely with minimal resistance from the robot. Therefore, the LOPES is considered a close-to-transparent robot, and induces only small changes in the kinematic and muscle activation patterns compared to normal walking [163]. These small differences, like a decreased knee range of motion and small changes in muscle activation levels are due to the inertia and mass after the actuators. When the exoskeleton is attached to the leg, not only the mass of the leg has to be accelerated (and decelerated), but also the mass of the exoskeleton leg itself.

The extent to which the dynamics of the robot, in particular its inertia, can be compensated for by means of control algorithms is very limited. Compensating its dynamics would require a precise model for the exoskeleton, accurate torque control and proper estimates of the positions, velocities and accelerations of the subject. However, in most devices, this information is not available in real-time, and the torque tracking is not sufficiently accurate. Attempts have been made to compensate for gravity and/or friction [134,164,165]. However, for the LOPES we experienced that the robot is more transparent without gravity compensation. The exoskeleton legs of the LOPES and the human leg have similar eigenfrequencies. As a result, during the swing phase, the human and robot leg swing in parallel with minimal interaction forces. When the gravity acting on the exoskeleton is compensated, the robot legs tend to continue their swing motion due to the remaining inertia. To end the swing phase, the human has to decelerate the exoskeleton legs without the help of gravity, which actually increases the undesired interaction forces between the robot and user. Similar counterproductive results of gravity compensation, in terms of interaction forces, have also been reported for the LOKOMAT [166]. For position-controlled gait trainers that cannot employ the passive dynamics of the robot, the transparency can also be increased by adapting the predefined gait patterns in real time, such that interaction between the robot and the patient is minimized. This way the robot “yields” to the voluntary exerted patient forces [150], [151]. Alternatively, a certain level of assistive forces can be applied to compensate for the robot dynamics and make it more transparent [142,167]. More recently the concept of “Generalized Elasticities” has been introduced [168]. Here conservative force fields are used that emulate the behavior of optimized passive components. These force fields compensate the mass and inertia of the device when the user moves according to the expected trajectories. A potential limitation of the proposed method is that, since the

force fields are optimized for the expected trajectories, the interaction torques probably increase when the patient moves in an unexpected way.

Despite these efforts most robotic gait trainers that have a dedicated mode for transparent walking still show increased levels of muscle activity in the exoskeleton, compared to "free" treadmill walking [163,167]. Apparently, the transparency of these robots is not sufficient for the user to experience the dynamics of free walking. It is believed that the nervous system must experience such dynamics in order to learn to control them [169]. Improved transparency, therefore, will likely make locomotor training more efficient and facilitate the transfer of the learned abilities to overground walking.

1.11.4 Both recovery and compensation contribute to functional improvements

Kinematic studies have shown that neurological patients that recover towards a normal walking pattern not necessarily reach faster walking speeds, compared to patients that create atypical patterns [13]. This suggests that these patients are able to improve their gait function using behavioural compensation strategies. Here, recovery is characterized as the restitution of pre-injury movement patterns, whereas compensation refers to the appearance of new movement patterns resulting from the adaptation of remaining motor functions [39,170]. For example, SCI patients may walk with greater forward tilt of both trunk and pelvic segments to compensate for a certain degree of instability due to lower-limb deficits [171]. In stroke survivors, these compensatory strategies are very common and well defined. Stroke survivors with reduced knee flexion during the swing phase of the paretic leg (stiff-knee gait) usually show compensatory movements such as pelvic hiking, hip circumduction or vaulting [172,173]. These patients may also create abnormal movements on the non-paretic side in an attempt to compensate for the decreased capabilities of the paretic side [52,174-176]. Although these different compensatory strategies do not contribute to a more symmetric walking pattern, they can increase walking ability.

Thus, functional gains can be achieved by recovery as well as compensation. Despite, all robotic gait trainers focus on recovery, as they impose healthy joint-based reference trajectories. Additionally, imposing symmetrical reference trajectories on both legs also limits the flexibility of the non-paretic leg to compensate for the deficiencies of the paretic leg. Therefore, to facilitate the use of these compensatory strategies, the control of the robot should allow the patient to move with sufficient freedom. Lowering the impedance levels allows such freedom, but also reduces the possibility to support severely affected patients. In fact, when using joint-based reference trajectories, alternative movement strategies can only be used if these movements are defined in the predefined reference trajectories. Although the number of observed compensatory strategies is limited, there is still considerable variation between patients, which complicates a proper definition of such reference trajectories for alternative movement strategies.

Besides the variation in these compensatory strategies and problems with their implementation in reference trajectories, most robotic gait trainers do not have the

appropriate DOFs at the pelvis and hip to allow compensatory strategies. For example, stroke survivors who trained in a robotic gait trainer without hip abduction, showed considerable abduction torques in their impaired leg to overcome their lack of knee flexion during swing [177]. Although the robot enforced a gait pattern that facilitated a save walking pattern, the subjects tried to over-power the robot with their hip circumduction. As highlighted before, restricting important DOFs leads to a situation where training in the robot does not resemble free walking, where the patient can freely employ their compensatory strategies. Overruling these compensatory strategies during gait training may affect the potential increase in walking ability. Thus, to increase the efficacy of robot-aided gait training, the training should not only focus on restoring a normal walking pattern but also allow, and possibly even train, these compensatory strategies.

1.12 Robotic assessment of joint properties

As mentioned before, robotic gait trainers can be used in a wider sense than just for the support of leg movements during treadmill training. Because the majority of the robotic gait trainers are instrumented with sensors that can measure joint angles and forces, these parameters can also be used to objectively monitor the patient's performance and recovery. In addition, well-designed and quantifiable training methods may even reveal some of the mechanisms behind movement recovery and the effects of different types of specific rehabilitation regimes. Eventually, this may lead to the development of more effective treatments [178].

So far, most robotic gait trainers monitor the patient's performance throughout the training sessions by recording gait parameters like stride length, cadence, gait symmetry, joint excursions [135] or joint moments [133,179]. However, gait kinematics and kinetics are not the only important measures in rehabilitation. For example, in current rehabilitation practice the (Modified) Ashworth Scale (AS/MAS) is the most popular clinical measure of spasticity. Spasticity is defined as an unusual tightness of the muscle due to increased tone and reflexes. Spasticity becomes more apparent at faster movements, and is a major source of gait disability in neurological patients [180]. Categorical scales like the MAS are clinically convenient measures, but they rely on the subjective assessment and experience of the clinician. Consequently, the inter- and intra-tester reliability is relatively low [181] and some even suggest that the validity and reliability of the AS is insufficient to be used as a measure of spasticity [182]. Therefore, different types of devices have been suggested for a more objective and quantitative measure of joint spasticity, ranging from simple hand-held dynamometers to automated isokinetic dynamometers, like the KinCom (Isokinetic International) or the BioDex systems (Biodex Medical Systems). There is also a large body of research in which more sophisticated devices are used to study the mechanical abnormalities associated with neuromuscular disorders like SCI [183] or stroke [184]. These systems measure the torques evoked by randomly perturbing the joint. System identification techniques and muscular models are then used to determine the

relative contribution of the intrinsic stiffness (from the spastic muscles) and the apparent stiffness due to reflex behavior. These studies have shown, for example, that SCI and stroke patients have abnormal passive ankle stiffness caused by and increased reflex stiffness [183,184].

Such quantitative measures provide valuable information about the condition of the patients and have demonstrated to have an intra-subject reliability which was as good as, or better than, most clinical measures [185,186]. However, performing such tests during each training session would add time-consuming procedures to existing rehabilitation protocols. Instead, integration of joint assessment within robotic gait trainers would allow convenient testing of joint properties as part of robotic gait training protocols. Tracking joint properties over the course of gait therapy may yield direct insight into how changes in joint properties affect gait function. Promising results of robotic assessment of joint properties like spasticity, muscle strength or joint range of motion have been reported for the Lokomat. To measure the mechanical joint stiffness, Lunenburger et al. [187] applied sine-squared angular motions to the joint, while the subject was suspended in the air. The measured joint torques were compensated for the dynamics of the orthosis and used to calculate the joint stiffness. Generally, a higher mechanical stiffness was observed for joints with higher spasticity levels (MAS 2 to 4), whereas for lower MAS scores the measured stiffness did not vary significantly. A similar setup was used by Bolliger et al. [188] to record maximum voluntary force. Here, subjects were asked to push against the orthosis, while the system recorded the forces acting on the force transducers. They showed that their developed assessment method provides a reliable tool for measuring isometric torques in subjects with and without neurological movement disorders. Although the development of joint assessment tools for robotic gait trainers is in a very early stage, these results demonstrate that it is feasible to obtain objective measures of joint properties in a repeatable and convenient manner.

1.13 Thesis objectives and goals

The goal of this thesis is twofold. The first goal is to develop and evaluate the effectiveness of different controllers based on the assist-as-needed (AAN) principle. The second goal of this thesis is to assess the feasibility of using the LOPES as a measurement tool to quantify joint properties.

Many robotic control strategies require reference trajectories to determine the amount of support. In **Chapter 2** we present and evaluate a novel method to reconstruct body-height and speed-dependent joint trajectories based on regression models for kinematic key events.

Impedance-controlled robotic gait training, where the support is provided on a joint level and the assistive torques are proportional to the deviation from a reference trajectory, can be considered as assist-as-needed. In **Chapter 3**, we evaluate the effectiveness of this

approach in a group of chronic incomplete SCI patients and assess to what extent the participants retain their training-induced functional improvements.

As discussed above, gait training with control on a joint level aims at functional improvements due to restitution of function rather than compensation. To allow the use of compensatory strategies, we developed a method that supports the patient on a subtask level, rather than a joint level. The selection of subtasks that are supported is based on the capabilities and progress of the patient. In this respect subtask-support can be seen as an extension of the AAN principle. In **Chapter 4**, we evaluate this approach in chronic stroke survivors for one specific subtask; toe clearance. By defining the reference trajectory in the coordinate system of the ankle instead of joint angles, the subjects can choose their own strategy to reach sufficient toe clearance. To minimize the patient's reliance on the provided support, we also implemented an adaptive control algorithm that reduces the support levels when kinematic errors are small.

To effectively implement AAN strategies the robot should be able to provide the necessary assistance, but also requires the robot to be transparent when no assistance is needed. In **Chapter 5** we exploit the cyclic behavior of walking to develop two controllers that improve the transparency of the LOPES. The first controller improves the (zero)-torque tracking mode. The second controller compensates for the passive dynamics of the exoskeleton to reduce the interaction forces between the LOPES and the user.

Regular assessment of the patient's joint properties enables objective monitoring of the patient's recovery and may yield direct insight into how changes in joint properties affect gait function. So far, most of these measures are recorded with dedicated equipment and focus on a single joint. In **Chapter 6** we introduce a new method to quantify joint properties using the LOPES. The method is based on Multi Input Multi Output (MIMO) system identification techniques and can be used to estimate multi-joint-impedance.

Chapter 7 includes a general discussion, based on the results of this thesis, followed by recommendations for future developments.

References

[1] "The World Health Report 2002," vol. 16, no. 2, pp. 1-204, 2003.

[2] M. a. Foulkes, P. a. Wolf, T. R. Price, J. P. Mohr, and D. B. Hier, "The Stroke Data Bank: design, methods, and baseline characteristics," *Stroke*, vol. 19, no. 5, pp. 547-554, 1988.

[3] D. Lloyd-Jones, R. J. Adams, T. M. Brown, M. Carnethon, S. Dai, G. De Simone, T. B. Ferguson, E. Ford, K. Furie, C. Gillespie, A. Go, K. Greenlund, N. Haase, S. Hailpern, P. M. Ho, V. Howard, B. Kissela, S. Kittner, D. Lackland, L. Lisabeth, A. Marelli, M. M. McDermott, J. Meigs, D. Mozaffarian, M. Mussolino, G. Nichol, V. L. Roger, W. Rosamond, R. Sacco, P. Sorlie, R. Stafford, T. Thom, S. Wasserthiel-Smoller, N. D. Wong, and J. Wylie-Rosett, "Heart disease and stroke statistics--2010 update: a report from the American Heart Association.," *Circulation*, vol. 121, no. 7, pp. e46-e215, 2010.

[4] C. J. L. Murray and C. Stein, "The Global Burden of Disease 2000 project: aims, methods and data sources," 2001.

[5] V. L. Feigin, C. M. M. Lawes, D. A. Bennett, and C. S. Anderson, "Stroke epidemiology: a review of population-based studies of incidence, prevalence, and case-fatality in the late 20th century," *Lancet Neurol.*, vol. 2, no. 1, pp. 43-53, 2003.

[6] R. E. Petrea, A. S. Beiser, S. Seshadri, M. Kelly-Hayes, C. S. Kase, and P. a Wolf, "Gender differences in stroke incidence and poststroke disability in the Framingham heart study.," *Stroke.*, vol. 40, no. 4, pp. 1032-7, 2009.

[7] P. Thorvaldsen, M. Davidsen, H. Bronnum-Hansen, and M. Schroll, "Stable Stroke Occurrence Despite Incidence Reduction in an Aging Population : Stroke Trends in the Danish Monitoring Trends and Determinants in Cardiovascular Disease (MONICA) Population," *Stroke*, vol. 30, no. 12, pp. 2529-2534, 1999.

[8] R. Carandang, A. Beiser, M. Kelly-hayes, C. S. Kase, W. B. Kannel, and P. A. Wolf, "Trends in Incidence, Lifetime Risk, Severity, and 30-Day Mortality of Stroke Over the Past 50 Years Raphael," vol. 296, no. 24, pp. 2939-2946, 2014.

[9] P. M. Rothwell, a J. Coull, M. F. Giles, S. C. Howard, L. E. Silver, L. M. Bull, S. a Gutnikov, P. Edwards, D. Mant, C. M. Sackley, a Farmer, P. a G. Sandercock, M. S. Dennis, C. P. Warlow, J. M. Bamford, and P. Anslow, "Change in stroke incidence, mortality, case-fatality, severity, and risk factors in Oxfordshire, UK from 1981 to 2004 (Oxford Vascular Study).," *Lancet*, vol. 363, no. 9425, pp. 1925-33, 2004.

[10] M. Brainin, N. Bornstein, G. Boysen, and V. Demarin, "Acute neurological stroke care in Europe: results of the European Stroke Care Inventory.," *Eur. J. Neurol.*, vol. 7, no. 1, pp. 5-10, 2000.

[11] S. J. Olney and C. Richards, "Hemiparetic gait following stroke. Part I: Characteristics," *Gait Posture*, vol. 4, no. 2, pp. 136-148, 1996.

[12] A. L. Hsu, P. F. Tang, and M. H. Jan, "Analysis of impairments influencing gait velocity and asymmetry of hemiplegic patients after mild to moderate stroke," *Arch Phys Med Rehabil*, vol. 84, no. 8, pp. 1185-1193, 2003.

[13] C. M. Kim and J. J. Eng, "Magnitude and pattern of 3D kinematic and kinetic gait profiles in persons with stroke: relationship to walking speed," *Gait Posture*, vol. 20, no. 2, pp. 140-146, 2004.

[14] A. R. Den Otter, A. C. Geurts, T. Mulder, and J. Duysens, "Abnormalities in the temporal patterning of lower extremity muscle activity in hemiparetic gait," *Gait Posture*, vol. 25, no. 3, pp. 342-52, 2006.

[15] N. Arene and J. Hidler, "Understanding motor impairment in the paretic lower limb after a stroke: a review of the literature.," *Top. Stroke Rehabil.*, vol. 16, no. 5, pp. 346-56, 2009.

[16] Skillbeck C.E., Wade D.T., Hewer R.L., and Wood V.A., "Recovery after stroke," *Neurol Neurosurg Psychiatr*, vol. 46, pp. 5-8, 1983.

[17] D. T. Wade and R. L. Hewer, "Functional abilities after stroke: measurement, natural history and prognosis.," *J. Neurol. Neurosurg. Psychiatry*, vol. 50, no. 2, pp. 177-82, 1987.

[18] H. S. Jørgensen, H. Nakayama, H. O. Raaschou, and T. S. Olsen, "Recovery of walking function in stroke patients: the Copenhagen Stroke Study.," *Arch. Phys. Med. Rehabil.*, vol. 76, no. 1, pp. 27-32, 1995.

[19] M. Wyndaele and J.-J. Wyndaele, "Incidence, prevalence and epidemiology of spinal cord injury: what learns a worldwide literature survey?," *Spinal Cord*, vol. 44, no. 9, pp. 523-529, 2006.

[20] J. C. Furlan, M. G. Fehlings, C. H. Tator, and A. M. Davis, "Motor and sensory assessment of patients in clinical trials for pharmacological therapy of acute spinal cord injury: psychometric properties of the ASIA Standards.," *J. Neurotrauma*, vol. 25, no. 11, pp. 1273-301, 2008.

[21] S. C. Kirshblum, W. Waring, F. Biering-Sorensen, S. P. Burns, M. Johansen, M. Schmidt-Read, W. Donovan, D. Graves, A. Jha, L. Jones, M. J. Mulcahey, and A. Krassioukov, "International Standards for Neurological Classification of Spinal Cord Injury.," *J. Spinal Cord Med.*, vol. 34, no. 6, pp. 547-54, 2011.

[22] M. P. Jensen, C. M. Kuehn, D. Amtmann, and D. D. Cardenas, "Symptom burden in persons with spinal cord injury.," *Arch. Phys. Med. Rehabil.*, vol. 88, no. 5, pp. 638-45, 2007.

[23] R. L. Waters, R. H. Adkins, and J. S. Yakura, "Definition of complete spinal cord injury.," *Paraplegia*, vol. 29, no. 9, pp. 573-81, 1991.

[24] J. W. Fawcett, A. Curt, J. D. Steeves, W. P. Coleman, M. H. Tuszynski, D. Lammertse, P. F. Bartlett, A. R. Blight, V. Dietz, J. Ditunno, B. H. Dobkin, L. A. Havton, P. H. Ellaway, M. G. Fehlings, A. Privat, R. Grossman, J. D. Guest, N. Kleitman, M. Nakamura, M. Gaviria, and D. Short, "Guidelines for the conduct of clinical trials for spinal cord injury as developed by the ICCP Panel: clinical trial inclusion/exclusion criteria and ethics.," *Spinal Cord*, vol. 45, no. 3, pp. 190-205, 2007.

[25] Consortium for Spinal Cord Medicine., "Outcomes following traumatic spinal cord injury: clinical practice guidelines for health-care professionals.," *J Spinal Cord Med*, vol. 23, no. 4, pp. 289-316, 2000.

[26] S. Kirshblum, S. Millis, W. McKinley, and D. Tulsky, "Late neurologic recovery after traumatic spinal cord injury," *Arch. Phys. Med. Rehabil.*, vol. 85, no. 11, pp. 1811-1817, 2004.

[27] J. Mehrholz, J. Kugler, and M. Pohl, "Locomotor training for walking after spinal cord injury.," *Spine (Phila. Pa. 1976).*, vol. 33, no. 21, pp. E768-E777, 2008.

[28] J. J. van Middendorp, a J. F. Hosman, M. H. Pouw, and H. Van de Meent, "ASIA impairment scale conversion in traumatic SCI: is it related with the ability to walk? A descriptive comparison with functional ambulation outcome measures in 273 patients.," *Spinal Cord*, vol. 47, no. 7, pp. 555-60, 2009.

[29] K. S. Crozier, L. L. Cheng, V. Graziani, G. Zorn, G. Herbison, and J. F. Ditunno, "Spinal cord injury: prognosis for ambulation based on quadriceps recovery.," *Paraplegia*, vol. 30, no. 11, pp. 762-7, 1992.

[30] A. Pépin, K. E. Norman, and H. Barbeau, "Treadmill walking in incomplete spinal-cord-injured subjects: 1. Adaptation to changes in speed.," *Spinal Cord*, vol. 41, no. 5, pp. 257-70, 2003.

[31] R. L. Waters, R. H. Adkins, J. S. Yakura, and I. Sie, "Motor and sensory recovery following incomplete tetraplegia," in *Archives of Physical Medicine and Rehabilitation*, 1994, vol. 75, no. 3, pp. 306-311.

[32] I. G. L. van de Port, G. Kwakkel, V. P. M. Schepers, and E. Lindeman, "Predicting mobility outcome one year after stroke: a prospective cohort study.," *J. Rehabil. Med.*, vol. 38, no. 4, pp. 218-23, 2006.

[33] K. D. Anderson, "Targeting recovery: priorities of the spinal cord-injured population.," *J. Neurotrauma*, vol. 21, no. 10, pp. 1371-1383, 2004.

[34] P. L. Ditunno, M. Patrick, M. Stineman, and J. F. Ditunno, "Who wants to walk? Preferences for recovery after SCI: a longitudinal and cross-sectional study.," *Spinal Cord*, vol. 47, no. 3, pp. 500-506, 2008.

[35] C. Tefertiller, B. Pharo, N. Evans, and P. Winchester, "Efficacy of rehabilitation robotics for walking training in neurological disorders: A review," *J. Rehabil. Res. Dev.*, vol. 48, no. 4, pp. 387-416, 2011.

[36] S. C. Cramer, M. Sur, B. H. Dobkin, C. O'Brien, T. D. Sanger, J. Q. Trojanowski, J. M. Rumsey, R. Hicks, J. Cameron, D. Chen, W. G. Chen, L. G. Cohen, C. deCharms, C. J. Duffy, G. F. Eden, E. E. Fetz, R. Filart, M. Freund, S. J. Grant, S. Haber, P. W. Kalivas, B. Kolb, A. F. Kramer, M. Lynch, H. S. Mayberg, P. S. McQuillen, R. Nitkin, A. Pascual-Leone, P. Reuter-Lorenz, N. Schiff, A. Sharma, L. Shekim, M. Stryker, E. V Sullivan, and S. Vinogradov, "Harnessing neuroplasticity for clinical applications.," *Brain*, vol. 134, no. Pt 6, pp. 1591-609, 2011.

[37] B. H. Dobkin, "Motor rehabilitation after stroke, traumatic brain, and spinal cord injury: common denominators within recent clinical trials," *Curr Opin Neurol*, vol. 22, no. 6, pp. 563-569, 2014.

[38] A. Curt, H. J. A. Van Hedel, D. Klaus, and V. Dietz, "Recovery from a spinal cord injury: significance of compensation, neural plasticity, and repair.," *J. Neurotrauma*, vol. 25, no. 6, pp. 677-685, 2008.

[39] G. Kwakkel, B. Kollen, and E. Lindeman, "Understanding the pattern of functional recovery after stroke: facts and theories," *Restor Neurol Neurosci*, vol. 22, no. 3-5, pp. 281-299, 2004.

[40] H. Barbeau, S. Nadeau, and C. Garneau, "Physical Determinants, Emerging Concepts, and Training Approaches in Gait of Individuals with Spinal Cord Injury," vol. 23, no. 3, pp. 571-585, 2006.

[41] A. Pollock, G. Baer, P. Langhorne, and V. Pomeroy, "Physiotherapy treatment approaches for the recovery of postural control and lower limb function following stroke: a systematic review.," *Clin. Rehabil.*, vol. 21, no. 5, pp. 395-410, 2007.

[42] R. P. S. Van Peppen, "Towards evidence-based physiotherapy for patients with stroke," *Dissertation*, 2008.

[43] N. A. Bayona, J. Bitensky, K. Salter, and R. Teasell, "The role of task-specific training in rehabilitation therapies," *Top Stroke Rehabil*, vol. 12, no. 3, pp. 58-65, 2005.

[44] C. L. Richards, F. Malouin, S. Wood-Dauphinee, J. I. Williams, J. P. Bouchard -, and D. Brunet, "Task-specific physical therapy for optimization of gait recovery in acute stroke patients," *Arch. Phys. Med. Rehabil.*, vol. 74, no. 6, pp. 612-620, 1993.

[45] B. H. Dobkin, "Strategies for stroke rehabilitation," *Lancet Neurol*, vol. 3, no. 9, pp. 528-536, 2004.

[46] B. French, T. Lh, L. Mj, S. Cj, J. Mcadam, A. Forster, P. Langhorne, A. Walker, W. Cl, L. Connell, J. Coupe, and N. Mcmahon, "Repetitive task training for improving functional ability after stroke (Review)," *Cochrane Database Syst Rev.,* no. 4, 2014.

[47] G. Kwakkel, R. C. Wagenaar, J. W. Twisk, G. J. Lankhorst, and J. C. Koetsier, "Intensity of leg and arm training after primary middle-cerebral-artery stroke: a randomised trial," *Lancet*, vol. 354, no. 9174, pp. 191-196, 1999.

[48] K. J. Sullivan, D. A. Brown, T. Klassen, S. Mulroy, T. Ge, S. P. Azen, and C. J. Winstein, "Effects of task-specific locomotor and strength training in adults who were ambulatory

after stroke: results of the STEPS randomized clinical trial," *Phys Ther*, vol. 87, no. 12, pp. 1580-1602, 2007.

[49] H. Barbeau, "Locomotor training in neurorehabilitation: emerging rehabilitation concepts," *Neurorehabil Neural Repair*, vol. 17, no. 1, pp. 3-11, 2003.

[50] A. L. Behrman, M. G. Bowden, and P. M. Nair, "Neuroplasticity after spinal cord injury and training: an emerging paradigm shift in rehabilitation and walking recovery.," *Phys. Ther.*, vol. 86, no. 10, pp. 1406-1425, 2006.

[51] R. Teasell, J. Bitensky, K. Salter, and N. A. Bayona, "The role of timing and intensity of rehabilitation therapies," *Top Stroke Rehabil*, vol. 12, no. 3, pp. 46-57, 2005.

[52] G. Kwakkel and R. C. Wagenaar, "Effect of duration of upper- and lower-extremity rehabilitation sessions and walking speed on recovery of interlimb coordination in hemiplegic gait," *Phys Ther*, vol. 82, no. 5, pp. 432-48, 2002.

[53] R. W. Teasell, N. C. Foley, S. K. Bhogal, and M. R. Speechley, "An evidence-based review of stroke rehabilitation.," *Top. Stroke Rehabil.*, vol. 10, no. 1, pp. 29-58, 2003.

[54] L. Lunenburger, M. Bolliger, D. Czell, R. Muller, and V. Dietz, "Modulation of locomotor activity in complete spinal cord injury," *Exp Brain Res*, vol. 174, no. 4, pp. 638-646, 2006.

[55] V. Dietz, R. Muller, and G. Colombo, "Locomotor activity in spinal man: significance of afferent input from joint and load receptors," *Brain*, vol. 125, no. Pt 12, pp. 2626-2634, 2002.

[56] S. J. Harkema, S. L. Hurley, U. K. Patel, P. S. Requejo, B. H. Dobkin, and V. R. Edgerton, "Human lumbosacral spinal cord interprets loading during stepping.," *J. Neurophysiol.*, vol. 77, no. 2, pp. 797-811, 1997.

[57] J. Duysens, F. Clarac, and H. Cruse, "Load-regulating mechanisms in gait and posture: comparative aspects.," *Physiol. Rev.*, vol. 80, no. 1, pp. 83-133, 2000.

[58] A. L. Behrman and S. J. Harkema, "Locomotor training after human spinal cord injury: a series of case studies," *Phys Ther*, vol. 80, no. 7, pp. 688-700, 2000.

[59] A. L. Hicks, M. M. Adams, K. Martin Ginis, L. Giangregorio, a Latimer, S. M. Phillips, and N. McCartney, "Long-term body-weight-supported treadmill training and subsequent follow-up in persons with chronic SCI: effects on functional walking ability and measures of subjective well-being.," *Spinal Cord*, vol. 43, no. 5, pp. 291-8, 2005.

[60] B. Dobkin, H. Barbeau, D. Deforge, J. Ditunno, R. Elashoff, D. Apple, M. Basso, A. Behrman, S. Harkema, M. Saulino, M. Scott, and S. C. I. L. Trial, "The evolution of walking-related outcomes over the first 12 weeks of rehabilitation for incomplete traumatic spinal cord injury: The multicenter randomized Spinal Cord Injury Locomotor Trial," *Neurorehabil. Neural Repair*, vol. 21, no. 1, pp. 25-35, 2007.

[61] E. C. Field-Fote and K. E. Roach, "Influence of a locomotor training approach on walking speed and distance in people with chronic spinal cord injury: a randomized clinical trial.," *Phys. Ther.*, vol. 91, no. 1, pp. 48-60, 2011.

[62] H. Barbeau and M. Visintin, "Optimal outcomes obtained with body-weight support combined with treadmill training in stroke subjects," *Arch Phys Med Rehabil*, vol. 84, no. 10, pp. 1458-1465, 2003.

[63] K. J. McCain, F. E. Pollo, B. S. Baum, S. C. Coleman, S. Baker, and P. S. Smith, "Locomotor treadmill training with partial body-weight support before overground gait in adults with acute stroke: a pilot study," *Arch Phys Med Rehabil*, vol. 89, no. 4, pp. 684-691, 2008.

[64] Y. Laufer, R. Dickstein, Y. Chefez, and E. Marcovitz, "The effect of treadmill training on the ambulation of stroke survivors in the early stages of rehabilitation: a randomized study.," *J. Rehabil. Res. Dev.*, vol. 38, no. 1, pp. 69-78, 2001.

[65] S. Hesse, M. Konrad, and D. Uhlenbrock, "Treadmill walking with partial body weight support versus floor walking in hemiparetic subjects.," *Arch. Phys. Med. Rehabil.*, vol. 80, no. 4, pp. 421-7, 1999.

[66] A. M. Moseley, A. Stark, I. D. Cameron, and A. Pollock, "Treadmill training and body weight support for walking after stroke.," *Stroke.*, vol. 34, no. 12, pp.1-3, 3006

[67] J. Mehrholz, M. Pohl, and B. Elsner, "Treadmill training and body weight support for walking after stroke (Review)," *Cochrane Database Syst Rev.*, 2014

[68] T. Lam, J. J. Eng, D. L. Wolfe, J. T. Hsieh, and M. Whittaker, "A systematic review of the efficacy of gait rehabilitation strategies for spinal cord injury.," *Top. Spinal Cord Inj. Rehabil.*, vol. 13, no. 1, pp. 32-57, 2007.

[69] M. Wessels, C. Lucas, I. Eriks, and S. De Groot, "Body weight-supported gait training for restoration of walking in people with an incomplete spinal cord injury: a systematic review.," *J. Rehabil. Med. Off. J. UEMS Eur. Board Phys. Rehabil. Med.*, vol. 42, no. 6, pp. 513-519, 2010.

[70] S. A. Morrison and D. Backus, "Locomotor training: is translating evidence into practice financially feasible?," *J. Neurol. Phys. Ther.*, vol. 31, no. 2, pp. 50-54, 2007.

[71] H. Schmidt, C. Werner, R. Bernhardt, S. Hesse, and J. Kruger, "Gait rehabilitation machines based on programmable footplates," *J Neuroengineering Rehabil*, vol. 4, pp. 1-7, 2007.

[72] S. Freivogel, D. Schmalohr, and J. Mehrholz, "Improved walking ability and reduced therapeutic stress with an electromechanical gait device.," *J. Rehabil. Med. Off. J. UEMS Eur. Board Phys. Rehabil. Med.*, vol. 41, no. 9, pp. 734-739, 2009.

[73] J. Hidler, D. Nichols, M. Pelliccio, and K. Brady, "Advances in the understanding and treatment of stroke impairment using robotic devices," *Top Stroke Rehabil*, vol. 12, no. 2, pp. 22-35, 2005.

[74] T. G. Hornby, D. D. Campbell, D. H. Zemon, and J. H. Kahn, "Clinical and quantitative evaluation of robotic-assisted treadmill walking to retrain ambulation after spinal cord injury," *Top Spinal Cord Inj Rehabil*, vol. 11, pp. 1-17, 2005.

[75] J. A. Galvez, A. Budovitch, S. J. Harkema, and D. J. Reinkensmeyer, "Trainer variability during step training after spinal cord injury: Implications for robotic gait-training device design.," *J. Rehabil. Res. Dev.*, vol. 48, no. 2, pp. 147-160, 2011.

[76] C. E. Lang, J. R. Macdonald, D. S. Reisman, L. Boyd, T. Jacobson Kimberley, S. M. Schindler-Ivens, T. G. Hornby, S. a Ross, and P. L. Scheets, "Observation of amounts of movement practice provided during stroke rehabilitation.," *Arch. Phys. Med. Rehabil.*, vol. 90, no. 10, pp. 1692-8, 2009.

[77] G. Colombo, M. Joerg, R. Schreier, and V. Dietz, "Treadmill training of paraplegic patients using a robotic orthosis," *J Rehabil Res Dev*, vol. 37, no. 6, pp. 693-700, 2000.

[78] S. K. Banala, A. Kulpe, and S. K. Agrawal, "A Powered Leg Orthosis for Gait Rehabilitation of Motor-Impaired Patients," in *Proceedings of the IEEE International Conference on Robotics and Automation*, pp. 4140-4145, 2007.

[79] P. Beyl, M. Van Damme, R. Van Ham, R. Versluys, B. Vanderborght, and D. Lefeber, "An exoskeleton for gait rehabilitation: Prototype design and control principle," in *Proceedings of the I IEEE International Conference on Robotics & Automation*, pp. 2037-2042, 2008.

[80] J. Veneman, "Design and evaluation of the gait rehabilitation robot lopes," *Disseration*, 2007.

[81] D. Zanotto, P. Setgal, and S. K. Agrawal, "Adaptive Assist-As-Needed Controller to Improve Gait Symmetryin Robot-Assisted Gait Training," in Proceedings of the *IEEE International Conference on Robotics & Automation*, pp. 724-729, 2014.

[82] J. Meuleman, E. H. F. Van Asseldonk, and H. Van Der Kooij, "Novel actuation design of a gait trainer with shadow leg approach," in *Proceedings of the IEEE International Conference on Rehabilitation Robotics*, 2013.

[83] J. Hidler, W. Wisman, and N. Neckel, "Kinematic trajectories while walking within the Lokomat robotic gait-orthosis," *Clin Biomech (Bristol, Avon)*, vol. 23, no. 10, pp. 1251-1259, 2008.

[84] H. Iwata, H. Yano, and F. Nakaizumi, "Gait Master: a versatile locomotion interface for uneven virtual terrain," *Proc. IEEE Virtual Real. 2001*, pp. 131-137, 2001.

[85] S. Freivogel, J. Mehrholz, T. Husak-Sotomayor, and D. Schmalohr, "Gait training with the newly developed 'LokoHelp'-system is feasible for non-ambulatory patients after stroke, spinal cord and brain injury. A feasibility study.," *Brain Inj.*, vol. 22, no. 7-8, pp. 625-32, 2008.

[86] Y. Stauffer, Y. Allemand, M. Bouri, J. Fournier, R. Clavel, P. Metrailler, R. Brodard, and F. Reynard, "The WalkTrainer--a new generation of walking reeducation device combining orthoses and muscle stimulation," *IEEE Trans Neural Syst Rehabil Eng*, vol. 17, no. 1, pp. 38-45, 2009.

[87] A. Roy, H. I. Krebs, D. J. Williams, C. T. Bever, L. W. Forrester, R. M. Macko, and N. Hogan, *Robot-Aided Neurorehabilitation: A Novel Robot for Ankle Rehabilitation*, *IEEE Trans. Robot.*, vol. 25, no. 3. IEEE, 2009, pp. 569-582.

[88] P. Winchester, R. McColl, R. Querry, N. Foreman, J. Mosby, K. Tansey, and J. Williamson, "Changes in supraspinal activation patterns following robotic locomotor therapy in motor-incomplete spinal cord injury.," *Neurorehabil Neural Repair*, vol. 19. no. 4, pp. 313-24, 2005.

[89] T. G. Hornby, D. H. Zemon, and D. Campbell, "Robotic-assisted, body-weight-supported treadmill training in individuals following motor incomplete spinal cord injury.," *Phys. Ther.*, vol. 85, no. 1, pp. 52-66, 2005.

[90] M. Wirz, D. H. Zemon, R. Rupp, A. Scheel, G. Colombo, V. Dietz, and T. G. Hornby, "Effectiveness of automated locomotor training in patients with chronic incomplete spinal cord injury: A multicenter trial," *Arch. Phys. Med. Rehabil.*, vol. 86, no. 4, pp. 672-680, 2005.

[91] J. Benito-Penalva, D. J. Edwards, E. Opisso, M. Cortes, R. Lopez-Blazquez, N. Murillo, U. Costa, J. M. Tormos, J. Vidal-Samsó, J. Valls-Solé, and J. Medina, "Gait training in human spinal cord injury using electromechanical systems: effect of device type and patient characteristics.," *Arch. Phys. Med. Rehabil.*, vol. 93, no. 3, pp. 404-12, 2012.

[92] M. van Nunen, "Recovery of walking ability using a robotic device," *Dissertation*, 2013.

[93] S. Hesse, C. Werner, and a Bardeleben, "Electromechanical gait training with functional electrical stimulation: case studies in spinal cord injury.," *Spinal Cord*, vol. 42, no. 6, pp. 346-52, 2004.

[94] C. F. Nooijen, N. Ter Hoeve, and E. C. Field-Fote, "Gait quality is improved by locomotor training in individuals with SCI regardless of training approach," *J. Neuroeng. Rehabil.*, vol. 6, no. 6, pp. 1-11, 2009.

[95] M. Alcobendas-Maestro, A. Esclarín-Ruz, R. M. Casado-López, A. Muñoz-González, G. Pérez-Mateos, E. González-Valdizán, and J. L. R. Martín, "Lokomat robotic-assisted versus overground training within 3 to 6 months of incomplete spinal cord lesion: randomized controlled trial.," *Neurorehabil. Neural Repair*, vol. 26, no. 9, pp. 1058-63, 2012.

[96] I. Schwartz, A. Sajina, M. Neeb, I. Fisher, M. Katz-Luerer, and Z. Meiner, "Locomotor training using a robotic device in patients with subacute spinal cord injury," *Spinal Cord*, vol. 49, no. 10, pp. 1062-1067, 2011.

[97] G. Morone, M. Iosa, M. Bragoni, D. De Angelis, V. Venturiero, P. Coiro, R. Riso, L. Pratesi, and S. Paolucci, "Who may have durable benefit from robotic gait training?: a 2-year follow-up randomized controlled trial in patients with subacute stroke.," *Stroke.*, vol. 43, no. 4, pp. 1140-2, 2012.

[98] M. Pohl, C. Werner, M. Holzgraefe, G. Kroczek, J. Mehrholz, I. Wingendorf, G. Hoolig, R. Koch, and S. Hesse, "Repetitive locomotor training and physiotherapy improve walking and basic activities of daily living after stroke: a single-blind, randomized multicentre trial (Deutsche GangtrainerStudie, DEGAS)," *Clin Rehabil*, vol. 21, no. 1, pp. 17-27, 2007.

[99] R. K. Tong, M. F. Ng, and L. S. Li, "Effectiveness of gait training using an electromechanical gait trainer, with and without functional electric stimulation, in subacute stroke: a randomized controlled trial," *Arch Phys Med Rehabil*, vol. 87, no. 10, pp. 1298-1304, 2006.

[100] A. Mayr, M. Kofler, E. Quirbach, H. Matzak, K. Frohlich, and L. Saltuari, "Prospective, blinded, randomized crossover study of gait rehabilitation in stroke patients using the Lokomat gait orthosis," *Neurorehabil Neural Repair*, vol. 21, no. 4, pp. 307-314, 2007.

[101] K. P. Westlake and C. Patten, "Pilot study of Lokomat versus manual-assisted treadmill training for locomotor recovery post-stroke," *J Neuroeng Rehabil*, vol. 6, pp. 1-11, 2009.

[102] C. Werner, S. Von Frankenberg, T. Treig, M. Konrad, and S. Hesse, "Treadmill training with partial body weight support and an electromechanical gait trainer for restoration of gait in subacute stroke patients: a randomized crossover study," *Stroke*, vol. 33, no. 12, pp. 2895-2901, 2002.

[103] B. Husemann, F. Muller, C. Krewer, S. Heller, and E. Koenig, "Effects of locomotion training with assistance of a robot-driven gait orthosis in hemiparetic patients after stroke: a randomized controlled pilot study," *Stroke*, vol. 38, no. 2, pp. 349-354, 2007.

[104] I. Schwartz, A. Sajin, I. Fisher, M. Neeb, M. Shochina, M. Katz-Leurer, and Z. Meiner, "The effectiveness of locomotor therapy using robotic-assisted gait training in subacute stroke patients: a randomized controlled trial.," *PM R*, vol. 1, no. 6, pp. 516-23, Jun. 2009.

[105] M. van Nunen, K. H. L. Gerrits, M. Konijnenbelt, T. W. J. Janssen, and A. de Haan, "Recovery of walking ability using a robotic device in subacute stroke patients: a randomized controlled study," *Inf. Healthc.*, pp. 1-8, 2014.

[106] S. H. Peurala, O. Airaksinen, P. Huuskonen, P. Jäkälä, M. Juhakoski, K. Sandell, I. M. Tarkka, and J. Sivenius, "Effects of intensive therapy using gait trainer or floor walking exercises early after stroke.," *J. Rehabil. Med.*, vol. 41, no. 3, pp. 166-73, 2009.

[107] T. G. Hornby, D. D. Campbell, J. H. Kahn, T. Demott, J. L. Moore, and H. R. Roth, "Enhanced gait-related improvements after therapist- versus robotic-assisted locomotor training in subjects with chronic stroke: a randomized controlled study," *Stroke*, vol. 39, no. 6, pp. 1786-1792, 2008.

[108] J. Hidler, D. Nichols, M. Pelliccio, K. Brady, D. D. Campbell, J. H. Kahn, and T. G. Hornby, "Multicenter randomized clinical trial evaluating the effectiveness of the Lokomat in subacute stroke," *Neurorehabil Neural Repair*, vol. 23, no. 1, pp. 5-13, 2009.

[109] J. Mehrholz, B. Elsner, C. Werner, J. Kugler, and M. Pohl, "Electromechanical-assisted training for walking after stroke (Review)," C*ochrane Database Syst Rev*., 2013

[110] J. Mehrholz, J. Kugler, and M. Pohl, "Locomotor training for walking after spinal cord injury (Review)," *Cochrane Database Syst Rev.*, 2012.

[111] E. Swinnen, S. Duerinck, J.-P. Baeyens, R. Meeusen, and E. Kerckhofs, "Effectiveness of robot-assisted gait training in persons with spinal cord injury: a systematic review.," *J. Rehabil. Med.*, vol. 42, no. 6, pp. 520-6, 2010.

[112] H. I. Krebs, J. J. Palazzolo, L. Dipietro, B. T. Volpe, and N. Hogan, "Rehabilitation robotics: Performance-based progressive robot-assisted therapy," *Auton. Robots*, vol. 15, no. 1, pp. 7-20, 2003.

[113] N. Hogan, H. I. Krebs, B. Rohrer, J. J. Palazzolo, L. Dipietro, S. E. Fasoli, J. Stein, R. Hughes, W. R. Frontera, D. Lynch, and B. T. Volpe, "Motions or muscles? Some behavioral factors underlying robotic assistance of motor recovery," *J Rehabil Res Dev*, vol. 43, no. 5, pp. 605-618, 2006.

[114] M. Lotze, C. Braun, N. Birbaumer, S. Anders, and L. G. Cohen, "Motor learning elicited by voluntary drive," *Brain*, vol. 126, no. Pt 4, pp. 866-872, 2003.

[115] A. Kaelin-Lang, L. Sawaki, and L. G. Cohen, "Role of voluntary drive in encoding an elementary motor memory," *J Neurophysiol*, vol. 93, no. 2, pp. 1099-1103, 2005.

[116] M. A. Perez, B. K. Lungholt, K. Nyborg, and J. B. Nielsen, "Motor skill training induces changes in the excitability of the leg cortical area in healthy humans," *Exp Brain Res*, vol. 159, no. 2, pp. 197-205, 2004.

[117] A. Wernig, "'Ineffectiveness' of automated locomotor training.," *Arch. Phys. Med. Rehabil.*, vol. 86, no. 12, pp. 2385-6; 2005.

[118] J. F. Israel, D. D. Campbell, J. H. Kahn, and T. G. Hornby, "Metabolic costs and muscle activity patterns during robotic- and therapist-assisted treadmill walking in individuals with incomplete spinal cord injury," *Phys Ther*, vol. 86, no. 11, pp. 1466-1478, 2006.

[119] T. G. Hornby, C. R. Kinnaird, C. L. Holleran, M. R. Rafferty, K. S. Rodriguez, and J. B. Cain, "Kinematic, Muscular, and Metabolic Responses During Exoskeletal-, Elliptical-, or Therapist-Assisted Stepping in People With Incomplete Spinal Cord Injury," *Physical Therapy*, vol. 92, no. 10. pp. 1278-1291, 2012.

[120] P. Coenen, G. Van Werven, M. P. M. Van Nunen, J. H. Van Dieën, K. H. L. Gerrits, and T. W. J. Janssen, "Robot-asisted walking vs overground walking in stroke patients: An evaluation of muscle activity," *J. Rehabil. Med.*, vol. 44, no. 4, pp. 331-337, 2012.

[121] D. J. Reinkensmeyer, O. M. Akoner, D. P. Ferris, and K. E. Gordon, "Slacking by the human motor system: Computational models and implications for robotic orthoses," in *Proceedings of the IEEE International Conference of the Eng Med Biol Soc,* pp. 2129-32, 2009

[122] J. L. Emken, R. Benitez, A. Sideris, J. E. Bobrow, and D. J. Reinkensmeyer, "Motor Adaptation as a Greedy Optimization of Error and Effort," *J Neurophysiol*, vol. 97, no. 6, pp. 3997-4006, 2007.

[123] J. L. Emken, R. Benitez, and D. J. Reinkensmeyer, "Human-robot cooperative movement training: Learning a novel sensory motor transformation during walking with robotic assistance-as-needed," *J Neuroengineering Rehabil*, vol. 4, pp. 1-16, 2007.

[124] D. Aoyagi, W. E. Ichinose, S. J. Harkema, D. J. Reinkensmeyer, and J. E. Bobrow, "A robot and control algorithm that can synchronously assist in naturalistic motion during body-weight-supported gait training following neurologic injury," *IEEE Trans Neural Syst Rehabil Eng*, vol. 15, no. 3, pp. 387-400, 2007.

[125] J. L. Emken and D. J. Reinkensmeyer, "Robot-enhanced motor learning: accelerating internal model formation during locomotion by transient dynamic amplification," *IEEE Trans Neural Syst Rehabil Eng*, vol. 13, no. 1, pp. 33-39, 2005.

[126] R. A. Scheidt, J. B. Dingwell, and F. A. Mussa-Ivaldi, "Learning to move amid uncertainty.," *J. Neurophysiol.*, vol. 86, no. 2, pp. 971-985, 2001.

[127] R. Shadmehr and F. A. Mussa-Ivaldi, "Adaptive representation of dynamics during learning of a motor task.," *J. Neurosci.*, vol. 14, no. 5 Pt 2, pp. 3208-3224, 1994.

[128] L. L. Cai, A. J. Fong, C. K. Otoshi, Y. Q. Liang, J. G. Cham, H. Zhong, R. R. Roy, V. R. Edgerton, and J. W. Burdick, "Effects of consistency vs. variability in robotically controlled training of stepping in adult spinal mice.," in *Proceedings of the IEEE International Conference on Rehabilitation Robotics*, 2005.

[129] M. D. Ziegler, H. Zhong, R. R. Roy, and V. R. Edgerton, "Why variability facilitates spinal learning.," *J. Neurosci.*, vol. 30, no. 32, pp. 10720-6, 2010.

[130] M. D. Lewek, T. H. Cruz, J. L. Moore, H. R. Roth, Y. Y. Dhaher, and T. G. Hornby, "Allowing intralimb kinematic variability during locomotor training poststroke improves kinematic consistency: a subgroup analysis from a randomized clinical trial.," *Phys. Ther.*, vol. 89, no. 8, pp. 829-839, 2009.

[131] D. J. Reinkensmeyer and S. J. Housman, "'If I can't do it once, why do it a hundred times?': Connecting volition to movement success in a virtual environment motivates people to exercise the arm after stroke," *Virtual Rehabilitation,* pp. 44-48, 2007

[132] J. L. Emken, J. E. Bobrow, and D. J. Reinkensmeyer, "Robotic movement training as an optimization problem: designing a controller that assists only as needed," in *Proceedings of the IEEE International Conference on Rehabilitation Robotics*, 2005

[133] R. Riener, L. Lunenburger, S. Jezernik, M. Anderschitz, G. Colombo, and V. Dietz, "Patient-cooperative strategies for robot-aided treadmill training: first experimental results," *IEEE Trans Neural Syst Rehabil Eng*, vol. 13, no. 3, pp. 380-394, 2005.

[134] A. Duschau-Wicke, J. von Zitzewitz, A. Caprez, L. Lunenburger, and R. Riener, "Path control: a method for patient-cooperative robot-aided gait rehabilitation," *IEEE Trans Neural Syst Rehabil Eng*, vol. 18, no. 1, pp. 38-48, 2010.

[135] S. K. Banala, S. H. Kim, S. K. Agrawal, and J. P. Scholz, "Robot Assisted Gait Training With Active Leg Exoskeleton (ALEX)," *IEEE Trans Neural Syst Rehabil Eng*, vol. 17, no. 1, pp. 1-8, 2009

[136] S. Hussain, S. Q. Xie, and P. K. Jamwal, "Adaptive impedance control of a robotic orthosis for gait rehabilitation.," *IEEE Trans. Cybern.*, vol. 43, no. 3, pp. 1025-34, 2013.

[137] M. Wu, T. G. Hornby, J. M. Landry, H. Roth, and B. D. Schmit, "A cable-driven locomotor training system for restoration of gait in human SCI.," *Gait Posture*, vol. 33, no. 2, pp. 256-60, 2011.

[138] L. L. Cai, A. J. Fong, C. K. Otoshi, Y. Liang, J. W. Burdick, R. R. Roy, and V. R. Edgerton, "Implications of assist-as-needed robotic step training after a complete spinal cord injury on intrinsic strategies of motor learning," *J Neurosci*, vol. 26, no. 41, pp. 10564-10568, 2006.

[139] J. L. Emken, S. J. Harkema, J. A. Beres-Jones, C. K. Ferreira, and D. J. Reinkensmeyer, "Feasibility of manual teach-and-replay and continuous impedance shaping for robotic locomotor training following spinal cord injury," *IEEE Trans Biomed Eng*, vol. 55, no. 1, pp. 322-334, 2008.

[140] C. Lee, D. Won, M. J. Cantoria, M. Hamlin, and R. D. de Leon, "Robotic assistance that encourages the generation of stepping rather than fully assisting movements is best for learning to step in spinally contused rats.," *J. Neurophysiol.*, vol. 105, no. 6, pp. 2764-71, 2011.

[141] A. Duschau-Wicke, A. Caprez, and R. Riener, "Patient-cooperative control increases active participation of individuals with SCI during robot-aided gait training," *J. Neuroeng. Rehabil.*, vol. 7, no. 43, pp. 1-13, 2010.

[142] C. Krishnan, R. Ranganathan, Y. Y. Dhaher, and W. Z. Rymer, "A pilot study on the feasibility of robot-aided leg motor training to facilitate active participation.," *PLoS One*, vol. 8, no. 10, p. e77370, Jan. 2013.

[143] A. Schück, R. Labruyère, H. Vallery, R. Riener, and A. Duschau-Wicke, "Feasibility and effects of patient-cooperative robot-aided gait training applied in a 4-week pilot trial.," *J. Neuroeng. Rehabil.*, vol. 9, no. 1, pp. 1-14, 2012.

[144] C. Krishnan, D. Kotsapouikis, Y. Y. Dhaher, and W. Z. Rymer, "Reducing robotic guidance during robot-assisted gait training improves gait function: a case report on a stroke survivor.," *Arch. Phys. Med. Rehabil.*, vol. 94, no. 6, pp. 1202-6, 2013.

[145] H. Yano, K. Kasai, H. Saitou, and H. Iwata, "Development of a gait rehabilitation system using a locomotion interface," *J. Vis. Comput. Animat.*, vol. 14, no. 5, pp. 243-252, 2003.

[146] S. Hesse, H. Schmidt, and C. Werner, "Machines to support motor rehabilitation after stroke: 10 years of experience in Berlin," *J Rehabil Res Dev*, vol. 43, no. 5, pp. 671-678, 2006.

[147] J. L. Lelas, G. J. Merriman, P. O. Riley, and D. C. Kerrigan, "Predicting peak kinematic and kinetic parameters from gait speed.," *Gait Posture*, vol. 17, no. 2, pp. 106-12, 2003.

[148] G. Stoquart, C. Detrembleur, and T. Lejeune, "Effect of speed on kinematic, kinetic, electromyographic and energetic reference values during treadmill walking," *Neurophysiol Clin*, vol. 38, no. 2, pp. 105-116, 2008.

[149] H. Vallery, E. H. van Asseldonk, M. Buss, and H. van der Kooij, "Reference trajectory generation for rehabilitation robots: complementary limb motion estimation," *IEEE Trans Neural Syst Rehabil Eng*, vol. 17, no. 1, pp. 23-30, 2009.

[150] S. Jezernik, R. Scharer, G. Colombo, and M. Morari, "Adaptive robotic rehabilitation of locomotion: a clinical study in spinally injured individuals," *Spinal Cord*, vol. 41, no. 12, pp. 657-666, 2003.

[151] S. Jezernik, G. Colombo, and M. Morani, "Automatic Gait-Pattern Adaptation Algorithms for Rehabilitation With a 4-DOF Robotic Orthosis," *IEEE Trans. Robot. Autom.*, vol. 20, no. 3, pp. 574-582, 2004.

[152] A. Duschau-wicke, T. Brunsch, S. Felsenstein, H. Vallery, and R. Riener, "Patient-Cooperative Control : Adapting Robotic Interventions to Individual Human Capabilities," pp. 271-274, 2009.

[153] T. G. Hornby, D. J. Reinkensmeyer, and D. Chen, "Manually-assisted versus robotic-assisted body weight-supported treadmill training in spinal cord injury: what is the role of each?," *PM R*, vol. 2, no. 3, pp. 214-21, 2010.

[154] C. E. Bauby and A. D. Kuo, "Active control of lateral balance in human walking," *J Biomech*, vol. 33, no. 11, pp. 1433-1440, 2000.

[155] J. F. Veneman, J. Menger, E. H. F. van Asseldonk, F. C. T. van der Helm, and H. van der Kooij, "Fixating the pelvis in the horizontal plane affects gait characteristics.," *Gait Posture*, vol. 28, no. 1, pp. 157-63, 2008.

[156] J. M. Hidler and A. E. Wall, "Alterations in muscle activation patterns during robotic-assisted walking," *Clin Biomech (Bristol, Avon)*, vol. 20, no. 2, pp. 184-193, 2005.

[157] J. M. Donelan, D. W. Shipman, R. Kram, and A. D. Kuo, "Mechanical and metabolic requirements for active lateral stabilization in human walking," *J Biomech*, vol. 37, no. 6, pp. 827-835, 2004.

[158] A. L. Hof, "The 'extrapolated center of mass' concept suggests a simple control of balance in walking.," *Hum. Mov. Sci.*, vol. 27, no. 1, pp. 112-25, 2008.

[159] Hocoma, "Lokomat® Pro with FreeD." [Online]. Available: http://www.hocoma.com/fileadmin/user/Dokumente/Lokomat/fly_L6freeD_140128_en.pdf. [Accessed: 10-Sep-2014].

[160] T. D. Royer and P. E. Martin, "Manipulations of leg mass and moment of inertia: Effects on energy cost of walking," *Med. Sci. Sports Exerc.*, vol. 37, no. 4, pp. 649-656, 2005.

[161] R. C. Browning, J. R. Modica, R. Kram, and A. Goswami, "The Effects of Adding Mass to the Legs on the Energetics and Biomechanics of Walking," *Med. Sci. Sport. Exerc.*, vol. 39, no. 3, pp. 515-525, 2007.

[162] J. F. Veneman, R. Ekkelenkamp, R. Kruidhof, F. C. T. van der Helm, and H. van der Kooij, "A Series Elastic- and Bowden-Cable-Based Actuation System for Use as Torque Actuator in Exoskeleton-Type Robots," *Int. J. Rob. Res.*, vol. 25, no. 3, pp. 261-281, 2006.

[163] E. H. F. van Asseldonk, J. F. Veneman, R. Ekkelenkamp, J. H. Buurke, F. C. T. van der Helm, and H. van der Kooij, "The Effects on Kinematics and Muscle Activity of Walking in a Robotic Gait Trainer During Zero-Force Control.," *IEEE Trans. Neural Syst. Rehabil. Eng.*, vol. 16, no. 4, pp. 360-370, 2008.

[164] J. L. Emken, J. H. Wynne, S. J. Harkema, and D. J. Reinkensmeyer, "A robotic device for manipulating human stepping," *IEEE Transactions on Robotics*, vol. 22, pp. 185-189, 2006

[165] R. Ronsse, B. Koopman, N. Vitiello, T. Lenzi, S. M. M. De Rossi, J. van den Kieboom, E. van Asseldonk, M. C. Carrozza, H. van der Kooij, and A. J. Ijspeert, "Oscillator-based walking

assistance: a model-free approach.," in *Proceedings of the IEEE International Conference on Rehabilitation Robotics*, 2011.

[166] H. Vallery, A. Duschau-wicke, and R. Riener, "Optimized Passive Dynamics Improve Transparency of Haptic Devices," in *Proceedings of the IEEE International Conference on Robotics and Automation*, pp. 301-306, 2009.

[167] K. Van Kammen, A. Boonstra, H. Reinders-Messelink, and R. den Otter, "The Combined Effects of Body Weight Support and Gait Speed on Gait Related Muscle Activity: A Comparison between Walking in the Lokomat Exoskeleton and Regular Treadmill Walking.," *PLoS One*, vol. 9, no. 9, p. e107323, Jan. 2014.

[168] H. Vallery, A. Duschau-Wicke, and R. Riener, "Generalized elasticities improve patient-cooperative control of rehabilitation robots," in *Proceedings of the IEEE International Conference on Rehabilitation Robotics*, pp. 535-541, 2009

[169] D. J. Reinkensmeyer, D. Aoyagi, J. L. Emken, J. A. Galvez, W. Ichinose, G. Kerdanyan, S. Maneekobkunwong, K. Minakata, J. A. Nessler, R. Weber, R. R. Roy, R. de Leon, J. E. Bobrow, S. J. Harkema, and V. R. Edgerton, "Tools for understanding and optimizing robotic gait training," *J Rehabil Res Dev*, vol. 43, no. 5, pp. 657-670, 2006.

[170] M. F. Levin, J. a Kleim, and S. L. Wolf, "What do motor 'recovery' and 'compensation' mean in patients following stroke?," *Neurorehabil. Neural Repair*, vol. 23, no. 4, pp. 313-9, 2009.

[171] A. Leroux, J. Fung, and H. Barbeau, "Postural adaptation to walking on inclined surfaces: II. Strategies following spinal cord injury.," *Clin. Neurophysiol.*, vol. 117, no. 6, pp. 1273-82, 2006.

[172] G. Chen, C. Patten, D. H. Kothari, and F. E. Zajac, "Gait differences between individuals with post-stroke hemiparesis and non-disabled controls at matched speeds," *Gait Posture*, vol. 22, no. 1, pp. 51-56, 2005.

[173] D. C. Kerrigan, E. P. Frates, S. Rogan, and P. O. Riley, "Hip hiking and circumduction: quantitative definitions," *Am J Phys Med Rehabil*, vol. 79, no. 3, pp. 247-252, 2000.

[174] I. A. K. DeQuervain, S. R. Simon, S. Leurgans, W. S. Pease, and D. McAllister, "Gait pattern in the early recovery period after stroke," *J. Bone Jt. Surgery-American Vol.*, vol. 78A, no. 10, pp. 1506-1514, 1996.

[175] M. G. Bowden, C. K. Balasubramanian, R. R. Neptune, and S. A. Kautz, "Anterior-posterior ground reaction forces as a measure of paretic leg contribution in hemiparetic walking," *Stroke*, vol. 37, no. 3, pp. 872-876, 2006.

[176] J. H. Buurke, A. V Nene, G. Kwakkel, V. Erren-Wolters, M. J. IJzerman, and H. J. Hermens, "Recovery of Gait After Stroke: What Changes?," *Neurorehabil. Neural Repair*, vol. 22, no. 6, pp. 676-683, 2008.

[177] N. D. Neckel, N. Blonien, D. Nichols, and J. Hidler, "Abnormal joint torque patterns exhibited by chronic stroke subjects while walking with a prescribed physiological gait pattern.," *J. Neuroeng. Rehabil.*, vol. 5, pp. 1-11, 2008.

[178] D. J. Reinkensmeyer, J. L. Emken, and S. C. Cramer, "Robotics, motor learning, and neurologic recovery," *Annu Rev Biomed Eng*, vol. 6, pp. 497-525, 2004.

[179] J. Hidler, "Robotic-assessment of walking in individuals with gait disorders.," in *Proceedings of the IEEE International Conference of the Eng Med Biol Soc*, pp. 4829-31, 2004.

[180] A. Lamontagne, F. Malouin, and C. L. Richards, "Locomotor-specific measure of spasticity of plantarflexor muscles after stroke," *Arch Phys Med Rehabil*, vol. 82, no. 12, pp. 1696-1704, 2001.

[181] J. Mehrholz, K. Wagner, D. Meißner, K. Grundmann, C. Zange, R. Koch, and M. Pohl, "Reliability of the Modified Tardieu Scale and the Modified Ashworth Scale in adult patients with severe brain injury: a comparison study," *Clin. Rehabil.*, vol. 19, no. 7, pp. 751-759, 2005.

[182] Fleuren JF, G. Voerman, C. Erren-Wolters, G. Snoek, J. S. Rietman, H. J. Hermens, and N. AV., "Stop using the Ashworth Scale for the assessment of spasticity," *J Neurol Neurosurg Psychiatry*, vol. 81, no. 1, pp. 46-52, 2009.

[183] M. M. Mirbagheri, H. Barbeau, M. Ladouceur, and R. E. Kearney, "Intrinsic and reflex stiffness in normal and spastic, spinal cord injured subjects.," *Exp. Brain Res.*, vol. 141, no. 4, pp. 446-59, 2001.

[184] L. Galiana, J. Fung, and R. Kearney, "Identification of intrinsic and reflex ankle stiffness components in stroke patients," *Exp Brain Res*, vol. 165, no. 4, pp. 422-434, 2005.

[185] R. E. Kearney, P. L. Weiss, and R. Morier, "System identification of human ankle dynamics: intersubject variability and intrasubject reliability.," *Clin. Biomech. (Bristol, Avon)*, vol. 5, no. 4, pp. 205-17, 1990.

[186] M. Boiteau, F. Malouin, and C. L. Richards, "Use of a Hand-held Dynamometer and a Kin-Com Dynamometer for Evaluating Spastic Hypertonia in Children : A Reliability Study," pp. 796-802, 1995.

[187] L. Lunenburger, G. Colombo, R. Riener, and V. Dietz, "Clinical assessments performed during robotic rehabilitation by the gait training robot Lokomat," in *Proceedings of the IEEE International Conference on Rehabilitation Robotics*, pp. 345-348, 2005.

[188] M. Bolliger, R. Banz, V. Dietz, and L. Lünenburger, "Standardized voluntary force measurement in a lower extremity rehabilitation robot.," *J. Neuroeng. Rehabil.*, vol. 5, p. 23, 2008.

Chapter 2

Speed-dependent reference joint trajectory generation for robotic gait support

Published as:
B. Koopman, E. H. F. van Asseldonk, H. van der Kooij, "Speed-dependent reference joint trajectory generation for robotic gait support", *J. Biomech.,* vol. 47, pp. 1447-1458, 2014.

Abstract

For the control of actuated orthoses, or gait rehabilitation robotics, kinematic reference trajectories are often required. These trajectories, consisting of joint angles, angular velocities and accelerations, are highly dependent on walking speed. We present and evaluate a novel method to reconstruct body height- and speed-dependent joint trajectories. First, we collected gait kinematics in fifteen healthy (middle) aged subjects (47-68), at a wide range of walking speeds (0.5-5 km/h). For each joint trajectory multiple key-events were selected (among which its extremes). Second, we derived regression-models that predict the timing, angle, angular velocity and acceleration for each key-event, based on walking speed and the subject's body height. Finally, quintic splines were fitted between the predicted key-events to reconstruct a full gait cycle. Regression-models were obtained for hip ab-/adduction, hip flexion/extension, knee flexion/extension and ankle plantar-/dorsiflexion. Results showed that the majority of the key-events were dependent on walking speed, both in terms of timing and amplitude, whereas the body height had less effect. The reconstructed trajectories matched the measured trajectories very well, in terms of angle, angular velocity and acceleration. For the angles the *RMSE* between the reconstructed and measured trajectories was 2.6°. The mean correlation coefficient between the reconstructed and measured angular trajectories was 0.91. The method and the data presented in this paper can be used to generate speed-dependent gait patterns. These patterns can be used for the control of several robotic gait applications. Alternatively they can assist the assessment of pathological gait, where they can serve as a reference for "normal" gait.

2.1 Introduction

During the last decade a lot of effort has been put in the development of actuated orthoses. They can enable neurological patients to walk again, assist physical therapy, or increase human performance above normal levels [1-4]. Independent of whether these devices are position or force controlled they often require reference trajectories to define the motion, or determine the amount of assistance.

Generally, these reference patterns are based on pre-recorded trajectories from unimpaired volunteers walking on a treadmill or walkway [5,6], or based on walking in the device while it is operated in a transparent mode [7,8] or with the motors removed [11]. Others create patient specific patterns by recording the gait trajectory while the patient walks with manual assistance [9,10], or by reconstructing joint patterns based on movements of the unimpaired limb [12].

Most methodologies however, have certain considerations that limit the use of the recorded trajectories to specific applications. Firs, due to the mass and inertia of a device and/or imperfections of the transparent mode, gait patterns recorded in the device might not match with the ones recorded during free walking [13,14]. Second, the recorded patterns obtained during manual assistance will only be valid for that specific subject (and speed) and still require initial manual support from the therapist. Third, coupling the movement of the disabled leg to the movement of the unimpaired leg is only applicable to patients with one affected leg, which is often true for stroke survivors, but not for many other neurological injuries. Thus, obtaining pre-recorded trajectories from unimpaired volunteers seems the most suitable approach to create a set of reference patterns that can be used in a variety of gait-support applications.

Still, their use is constrained to the limited number of speeds they are recorded on. Most studies include slow, normal and fast walking [15-17], while the progress of the patients' preferred walking speed can be as small as 0.1 km/h. Additionally, even the slow walking speeds of healthy controls, ranging from 0.9 to 1.4 m/s [16,17], are typically higher than the preferred walking speed of patients with neurological injuries like stroke, ISCI or Parkinson (0.5-1.1 m/s) [18-22].

To eliminate the need to record joint trajectories at a high number of different walking speeds a method is required that can reconstruct joint trajectories for any given speed. Several studies already tried to quantify the speed-dependencies of joint trajectories for some key features like peak sagittal plane parameters [15,16,23,24].

However, for robotic control purposes these peak parameters, consisting of one or two specific key-events per joint, are not sufficient to reconstruct a full gait cycle. Information about the velocity and acceleration of these key-events, which are never reported, would also allow for more accurate joint trajectory reconstruction. Additionally, the relative timing of these peak parameters, which is not included in most regression-models, is also shown to be largely dependent on speed [25]. Finally, all studies that provide regression-

models for the speed-dependency of kinematic gait parameters are limited to the sagittal plane kinematics, whereas also hip ab-/adduction is incorporated in the more advanced orthoses.

The objective of this study was to present and evaluate a novel method for reconstructing body height and speed-dependent angular trajectories (sagittal and frontal). We propose to use piece-wise quintic spline fitting between different key-events. The key-events consist of a selection of extreme values in position and velocity data. The timing, angle, angular velocity and acceleration of these key-events are predicted, based on walking speed and body height, using regression-models. The presented method and data provide a reference for generating speed-dependent joint trajectories for several robotic gait applications.

2.2 Methods

2.2.1 Subjects

Fifteen healthy (middle) aged subjects in the age range 47-68 (age 59.3 ± 6.4, seven men, eight women, weight 74.0 kg ± 11.0, body height 1.69 m ± 0.10, BMI 25.8 ± 2.4) participated in this study. No subject had symptoms of orthopedic or neurological disorders and all gave informed consent, according to the recommendations of the declaration of Helsinki.

2.2.2 Experimental protocol and recordings

Subjects walked on a treadmill, starting with a familiarization period of 3 min followed by a 3 min walking trial. This was repeated for seven different speeds (0.5, 1, 1.5, 2, 3, 4 and 5 km/h) with 1-min breaks between trials. No specific instructions on how to walk on the treadmill were given. Gait kinematics were recorded with an optical tracking system (Vicon Oxford Metrics, Oxford, UK) at a frequency of 120 Hz. To track the motion of the subject, 21 passive reflective markers were attached to bony landmarks and segments on the legs and trunk (figure 1).

2.2.3 Data analysis

Conventional methods that determine normative gait patterns take the average across individual subjects. This may result in an underestimation of the extremes in the gait pattern, when subjects have a different distribution of the extremes throughout the gait cycle [26,27]. Therefore, we developed a method where the pattern is parameterized with different key-events (minima, maxima etc.). This way, the extreme value in the reconstructed pattern is actually the mean of the extreme values of the individual patterns, even when the extremes occur at another percentage in the gait cycle. A piece-wise quintic spline is fitted between the different key-events to create subject- and speed-

Figure 1: Marker placement. To track the motion of the subject, twenty one passive reflective markers (gray circles) were attached to bony landmarks and segments on the legs and trunk. Joint angles are defined according to the classical method used in clinical examination, where (dorsi-) flexion and abduction are defined positive.

dependent reference patterns. The following paragraphs describe these different steps in more detail.

2.2.4 Kinematics

Custom-written Matlab software was used to convert the marker positions into hip ab-/adduction, hip flexion/extension, knee flexion/extension and ankle plantar-/dorsiflexion (figure 2). This program can be seen as a variant of the Conventional Gait Model. It uses the minimum number of markers possible to determine 3-dimensional kinematics. All joints are modeled as potential ball-hinges, with three independent rotational degrees of freedom. The model is hierarchical, indicating that the proximal segments have to be detected before the distal segments can be defined. Joint positions are based on the location of some anatomical landmarks and regression equations. In the software additional constrains, primarily during the double stance phase, and optimization routines are used to reduce measurement errors [28].

To prevent habituation from affecting the gait patterns, only the last minute of each trial was selected for data analysis. The joint angular data was split into individual strides, and normalized as a percentage of the gait cycle, 0% corresponding to heel contact of the concerned leg. Heel-contact and toe-off events were detected with a phase detection method developed by Zeni et al. [29] that used the local maxima in the anterio-posterior position of the heel marker. Outliers, due to missing marker data, bad interpolation or a misplaced step by the subject, were removed. A step was defined as outlier when the whole trajectory, or part of it, fell outside the boundaries, which was set at 3 times the interquartile range away from the 25 and 75 percentile. Because the intra-subject

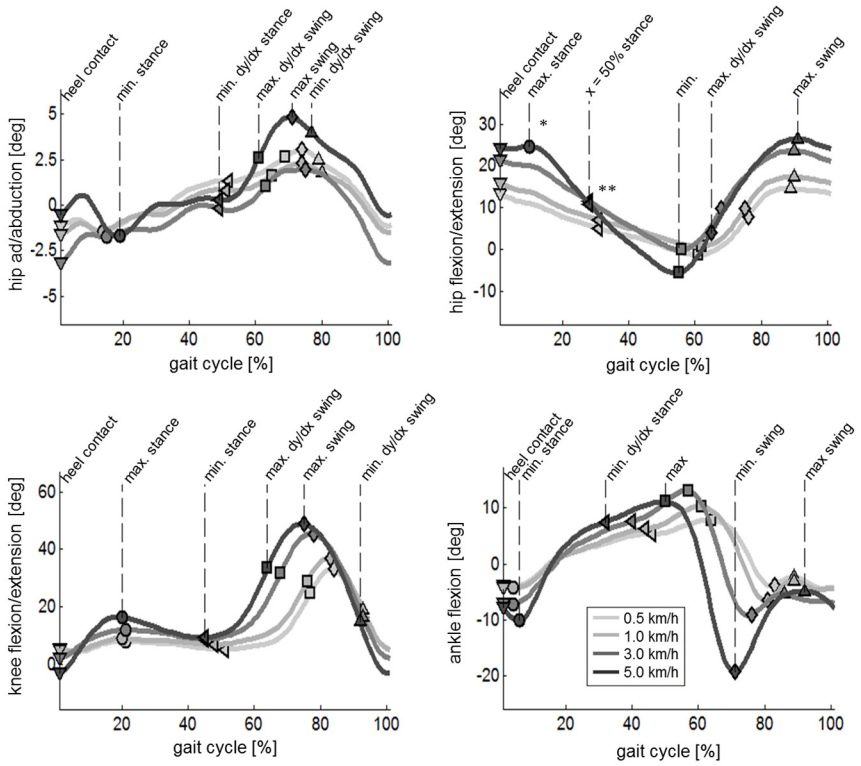

Figure 2: Selected key-events for the different joint trajectories. Example of the average trajectories of a typical subject at 0.5, 1, 3 and 5 km/h, together with the extracted key-events. We selected 6 key-events that described the individual's gait pattern. The key-events include the start of the gait cycle (heel contact) and its extreme values. Between some extreme values additional key-events were placed at maxima/minima in velocity data to obtain an adequate distribution of key-events throughout the gait cycle. The key-events of the average left and right joint trajectories were extracted separately. At lower walking-speeds this key-event is not present for every subject. If this is true for the majority the subjects (at a specific speed), then this particular key-event is not included in the spline fitting procedure at that speed (Table 2). ** Key-event added to improve spline fitting. This key-event does not represent a maxima or minima in position or velocity, but is defined at the middle of the stance phase.*

variation (in amplitude and timing) was small we calculated average trajectories for each individual subject. Still, average trajectories were calculated for the left and right leg separately.

The detected heel-contact and toe-off events were also used to calculate other spatiotemporal parameters like cadence, stride length and relative gait phases. Although one can walk with infinite combinations of stride lengths and cadences, Sekiya et al. [30] demonstrated that step-length divided by step-rate ("step-ratio") is relatively constant over a wide range of walking speeds. Therefore we used this ratio as a simple descriptor for temporal and spatial co-ordination.

The step-ratio is calculated according to:

$$step\ ratio = \frac{step\ length\ (m)}{step\ frequency\ (\frac{steps}{s})} = \frac{1}{4} \cdot \frac{stride\ length}{stride\ frequency} \quad [1]$$

2.2.5 Key-events

From each joint trajectory we extracted 6 key-events, including the start of the joint trajectory (heel contact) and a selection of extreme values in position and velocity data (figure 2). We parameterized each key-event with an x parameter, representing the percentage of the gait cycle at which the key-event occurred, its angle (y), angular velocity (dy/dx) and acceleration (d^2y/dx^2).

2.2.6 Regression-models

The extracted parameters of the key-events were used to construct a set of regression-models. These models were used to predict the parameter values for each key-event, based on a set of predictor variables. We used the following regression formula.

$$Y = \beta_0 + \beta_1 v + \beta_2 v^2 + \beta_3 l \quad [2]$$

Where v represents walking speed, l body height and Y represents the x, y, dy/dx, or d^2y/dx^2 parameter of a particular key-event. Both v and v^2 are included in the regression formula, since Lelas et al. [15] already showed that most common peak sagittal plane parameters have a linear and/or quadratic relationship with walking speed. We used stepwise regression [31] to test the statistical significance of the predictor variables, using entrance/exit tolerances with $p<0.01$. After selecting the appropriate predictor variables for the regression-model, we used robust regression [32], with a 'bisquare' weighing function, to retrieve the final set of regression coefficients (β_x). Regression-models (figure 3) were derived for all 4 parameters of all 6 key-events, creating 24 regression-models for each joint. We also obtained regression-models for the step-ratio and the relative duration of the different gait phases, using the same predictor variables.

2.2.7 Spline fitting

The obtained regression-models were used to reconstruct the reference patterns (for each subject and walking speed). First, the x, y, dy/dx, or d^2y/dx^2 parameters of the key-events (for a certain speed and body height) were calculated. Subsequently, a quintic spline was fitted between every pair of consecutive key-events, resulting in 6 (5^{th} order) polynomials (figure 4 and Supplementary material A). Piece-wise quintic spline fitting was used because it creates continuous trajectories (in terms of position, velocity and acceleration), which is preferable for robotic control.

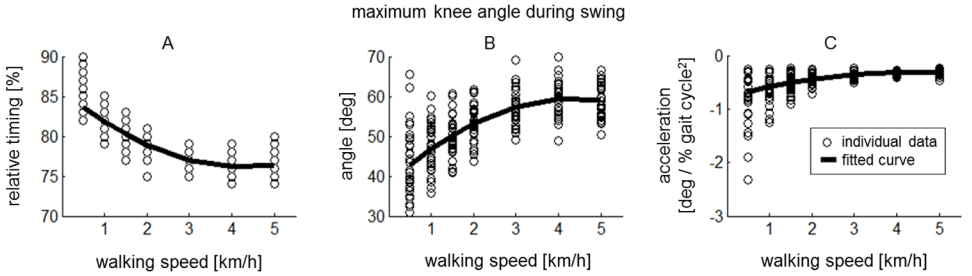

Figure 3: Typical example of speed- and body height-dependency of the parameters of a key-event. Relation between walking speed and the relative timing (A), angle (B), and angular acceleration (C) of the "max. swing" key-event of the knee joint, referring to the maximum knee flexion during the swing phase. Each circle represents the parameter value of the key-event at a specified walking speed for one subject. The solid line indicates the fitted regression-model. Since this key-event represents a maximum in the joint angular data, the angular velocity parameter is zero by definition, and is not shown. For the parameters of this key-event the body height did not significantly add to the predictability of the regression-model (table 3).

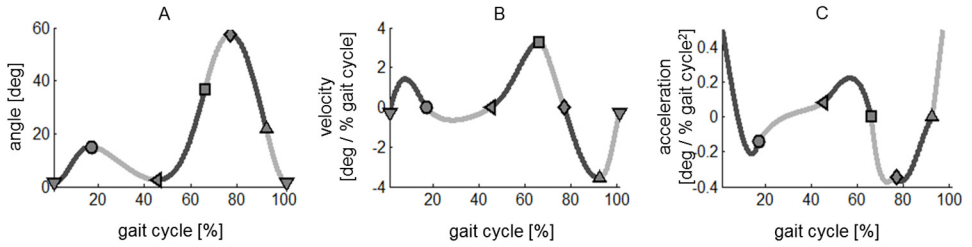

Figure 4: Reconstruction of the joint trajectories. Typical example of the reconstruction of a joint trajectory using piece-wise quintic splines. Here a trajectory for the knee joint is reconstructed. Six quintic splines are fitted between the 7 key-events. The values for the x, y, dy/dx or d^2y/dx^2 parameter of the first 6 key-events are calculated for a specific speed and body height with the regression equations provided in table 3. To ensure continuity in the reconstructed trajectory the y, dy/dx and d^2y/dx^2 parameter of the 7^{th} key-event (at 100% of the gait cycle) is equal to the first 1^{st} key-event (at 0 % of the gait cycle). The resulting trajectory is continuous in the position (A), velocity (B) and acceleration (C).

2.2.8 Validation

To determine the accurateness of the spline fitting procedure we evaluated the Root Mean Square Error (*RMSE*) and the correlation coefficient (*r*) between the actual (left and right) joint trajectories and the reconstructed spline, using the leave-one-out method of cross-validation (or rotation estimation) [33,34] (figure 5). Next, the results were averaged over left and right trajectories and across subjects ($RMSE_{act\text{-}rec}$ and $r_{act\text{-}rec}$) and reported for every walking speed (figure 6). To assess the quality of the fit during the different gait phases, the *RMSE* between the actual and reconstructed trajectories was also expressed

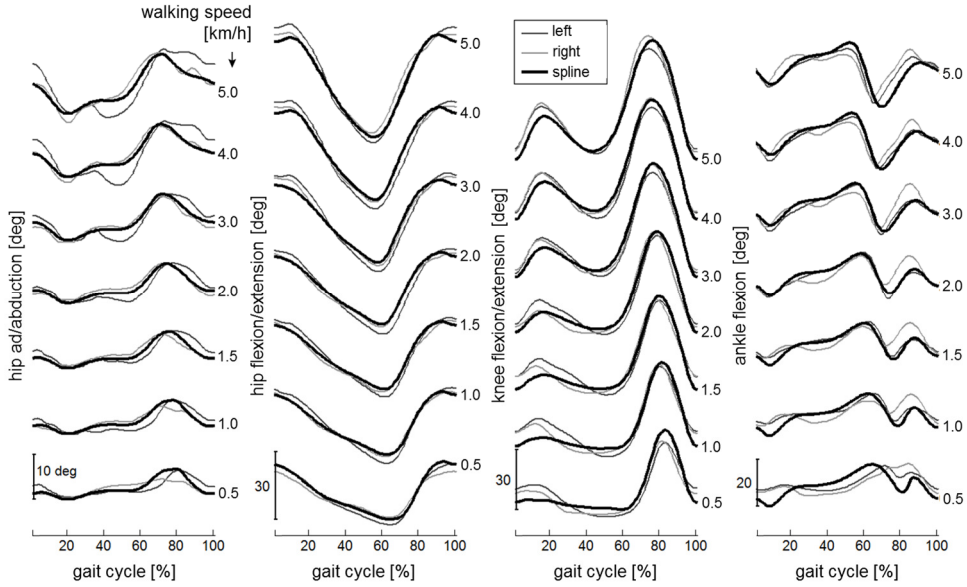

Figure 5: Cross-validation of the reconstructed trajectories. Example of the results of one round of cross-validation for a typical subject. It shows the left (thin light gray line) and right (thin dark gray line) joint trajectories, together with the reconstructed trajectories (thick black line). Here the key-events for the splines are based on regression-models that do not include data from this particular subject. Subsequently, the $RMSE_{act\text{-}rec}$ and correlation coefficient ($r_{act\text{-}rec}$) are calculated for every speed. This procedure was repeated 15 times (once for each subject), and the results were averaged over the rounds.

as a percentage of the gait cycle. As a reference for the obtained model error, we calculated the natural deviation ($RMSD_{l\text{-}r}$) and correlation coefficient ($r_{l\text{-}r}$) between the left and right joint trajectories. Another reference for the model error was provided by the inter-subject variability, which was calculated by the standard deviation (*STD*) across subjects, for every percentage of the gait cycle.

2.3 Results

2.3.1 Regression-models

Most key-events showed a dependency on walking speed, whereas body height influenced the parameters of the key-events to a lesser extent (table 1-4). For the angle (y) only 7 of the 24 key-events were dependent ($p<0.01$, see "Regression-models") on body height, whereas 19 key-events were linearly and/or quadratically dependent on speed. For the timing (x), only 10 key-events were dependent on body height, whereas 15 key-events were linearly and/or quadratically dependent on speed.

Table 1: Regression equations and RMSE for the parameter values of the key-events of the hip ab-/adduction.

	Key-event	**β_0 (intercept)**	**β_1 (speed)**	**β_2 (speed^2)**	**β_3 (body height)**	***RMSE***
Index (x parameter)	heel contact	1	-	-	-	
	min. stance	33,360	-	-	-7,319	4,206
	min. dy/dx stance	30,158	-2,038	-	11,832	4,494
	max. dy/dx swing	52,727	-1,613	-	9,393	3,704
	max. swing	83,318	-6,031	0,762	-	2,840
	min. dy/dx swing	68,490	-1,847	-	10,898	3,523
		β_0 (intercept)	β_1 (speed)	β_2 (speed^2)	β_3 (body height)	*RMSE*
Angle (y parameter)	heel contact	-0,783	-	0,056	-	1,457
	min. stance	-1,641	-0,879	-	-	1,129
	min. dy/dx stance	0,121	-0,652	-	-	1,403
	max. dy/dx swing	3,090	-	-	-	1,419
	max. swing	4,441	0,557	-	-	1,820
	min. dy/dx swing	1,860	0,657	-	-	1,674
		β_0 (intercept)	β_1 (speed)	β_2 (speed^2)	β_3 (body height)	*RMSE*
Velocity ($\frac{dy}{dx}$ parameter)	heel contact	-0,689	-	-0,010	0,424	0,119
	min. stance	0	-	-	-	
	min. dy/dx stance	-0,015	-	-	-	0,092
	max. dy/dx swing	0,350	0,075	-	-	0,215
	max. swing	0	-	-	-	
	min. dy/dx swing	-0,399	-	-	-	0,153
		β_0 (intercept)	β_1 (speed)	β_2 (speed^2)	β_3 (body height)	*RMSE*
Acceleration ($\frac{d^2y}{dx^2}$ parameter)	heel contact	0,019	-	-	-	0,047
	min. stance	0,043	-	0,002	-	0,027
	min. dy/dx stance	0	-	-	-	
	max. dy/dx swing	0	-	-	-	
	max. swing	-0,082	-	-	-	0,039
	min. dy/dx swing	0	-	-	-	

Here the regression formulas are shown that include the data from all 15 subjects.
Speed is defined in km/h and body height in m.
1 one by default (% of gait cycle of heel contact key-event).
0 zero by default (minimum or maximum in joint angle or angular velocity).
- no significant contribution to the regression-model.

Table 2: Regression equations and RMSE for the parameter values of the key-events of the hip flexion/extension.

	Key-event	**β_0 (intercept)**	**β_1 (speed)**	**β_2 (speed^2)**	**β_3 (body height)**	***RMSE***
Index (x parameter)	heel contact	1	-	-	-	
	max. stance*	-10,809	-	-	11,762	1,755
	x=50% stance**	24,512	-2,021	0,195	5,109	1,017
	min.	48,879	-3,854	0,355	9,891	1,943
	max. dy/dx swing	80,562	-6,432	0,885	-	2,058
	max. swing	94,280	-0,601	-	-	2,183
		β_0 (intercept)	β_1 (speed)	β_2 (speed^2)	β_3 (body height)	*RMSE*
Angle (y parameter)	heel contact	20,354	1,934	-	-	2,424
	max. stance*	18,917	2,583	-	-	2,022
	x=50% stance**	4,845	1,718	-	-	1,964
	min.	-2,026	-2,090	-	-	2,328
	max. dy/dx swing	20,030	-	-	-7,732	2,508
	max. swing	21,447	2,318	-	-	2,388
		β_0 (intercept)	β_1 (speed)	β_2 (speed^2)	β_3 (body height)	*RMSE*
Velocity ($\frac{dy}{dx}$ parameter)	heel contact	-2,062	-	-	1,112	0,234
	max. stance*	0	-	-	-	
	x=50% stance**	-0,240	-0,224	-	-	0,149
	min.	0	-	-	-	
	max. dy/dx swing	0,472	0,096	-	0,633	0,246
	max. swing	0	-	-	-	
		β_0 (intercept)	β_1 (speed)	β_2 (speed^2)	β_3 (body height)	*RMSE*
Acceleration ($\frac{d^2y}{dx^2}$ parameter)	heel contact	-0,068	0,031	-	-	0,059
	max. stance*	-0,112	-	-	-	0,041
	x=50% stance**	0,026	-0,010	-	-	0,024
	min.	-0,117	0,059	-0,007	0,098	0,036
	max. dy/dx swing	0	-	-	-	
	max. swing	-0,083	-	-0,002	-	0,044

** For walking speeds below 3.5 km/h this key-event is not included in the spline fitting procedure.*

*** Key-event added to improve spline fitting. This key does not represent a maxima or minima in position or velocity, but is defined at the middle of the stance phase.*

Table 3: Regression equations and RMSE for the parameter values of the key-events of the knee flexion/extension.

	Key-event	**β_0 (intercept)**	**β_1 (speed)**	**β_2 (speed^2)**	**β_3 (body height)**	***RMSE***
Index (x parameter)	heel contact	1	-	-	-	
	max. stance	17,103	-	-	-	2,487
	min. stance	48,542	-0,998	-	-	2,789
	max. dy/dx swing	68,947	-6,096	0,611	5,967	1,623
	max. swing	85,816	-4,480	0,519	-	1,301
	min. dy/dx swing	92,489	-	-	-	1,553
		β_0 (intercept)	β_1 (speed)	β_2 (speed^2)	β_3 (body height)	*RMSE*
Angle (y parameter)	heel contact	31,595	-4,311	0,494	-13,050	3,596
	max. stance	5,995	3,028	-	-	3,481
	min. stance	-10,037	-	-	7,594	2,291
	max. dy/dx swing	29,618	3,803	-0,486	-	3,556
	max. swing	38,110	9,744	-1,105	-	4,354
	min. dy/dx swing	24,631	-0,967	-	-	3,866
		β_0 (intercept)	β_1 (speed)	β_2 (speed^2)	β_3 (body height)	*RMSE*
Velocity ($\frac{dy}{dx}$ parameter)	heel contact	-3,581	-	-	1,977	0,525
	max. stance	0	-	-	-	
	min. stance	0	-	-	-	
	max. dy/dx swing	3,276	-	-	-	0,447
	max. swing	0	-	-	-	
	min. dy/dx swing	-0,446		-0,032	-1,696	0,629
		β_0 (intercept)	β_1 (speed)	β_2 (speed^2)	β_3 (body height)	*RMSE*
Acceleration ($\frac{d^2y}{dx^2}$ parameter)	heel contact	0,301	0,073	-	-	0,171
	max. stance	-0,094	-	-0,005	-	0,051
	min. stance	0,042	-	0,004	-	0,029
	max. dy/dx swing	0	-	-	-	
	max. swing	-0,784	0,225	-0,026	-	0,125
	min. dy/dx swing	0	-	-	-	

Table 4: Regression equations and RMSE for the parameter values of the key-events of the ankle plantar-/dorsiflexion.

	Key-event	β_0 (intercept)	β_1 (speed)	β_2 (speed^2)	β_3 (body height)	*RMSE*
Index (x parameter)	heel contact	1	-	-	-	
	min. stance	8,145	0,331		-	1,915
	min. dy/dx stance	12,005	-	-	13,754	4,307
	max.	67,686	-5,469	0,493	-	3,333
	min. swing	73,460	-6,699	0,744	6,463	1,673
	max. swing	87,621	-	0,132	-	3,150
		β_0 (intercept)	β_1 (speed)	β_2 (speed^2)	β_3 (body height)	*RMSE*
Angle (y parameter)	heel contact	18,645	0,554	-	-13,246	2,357
	min. stance	17,309	-	-	-14,173	2,517
	min. dy/dx stance	0,836	0,812	-	-	2,328
	max.	-15,523	-	-	14,494	2,494
	min. swing	21,984	-3,425	-	-12,522	4,848
	max. swing	4,860	-0,655	-	-	2,687
		β_0 (intercept)	β_1 (speed)	β_2 (speed^2)	β_3 (body height)	*RMSE*
Velocity ($\frac{dy}{dx}$ parameter)	heel contact	-0,145	-	-0,020	-	0,267
	min. stance	0	-	-	-	
	min. dy/dx stance	-0,991	-	-	0,620	0,172
	max.	0	-	-	-	
	min. swing	0	-	-	-	
	max. swing	0	-	-	-	
		β_0 (intercept)	β_1 (speed)	β_2 (speed^2)	β_3 (body height)	*RMSE*
Acceleration ($\frac{d^2y}{dx^2}$ parameter)	heel contact	0,145	-0,137	0,015	-	0,109
	min. stance	-0,556	-	-	0,492	0,111
	min. dy/dx stance	0	-	-	-	
	max.	0,055	-0,019	-	-0,089	0,059
	min. swing	0,433	-	-	-	0,235
	max. swing	0,412	0,087	-0,012	-0,425	0,098

Table 5: Regression equations and RMSE for spatiotemporal parameters.

		β_0 (intercept)	β_1 (speed)	β_2 (speed^2)	β_3 (body height)	*RMSE*
Spatiotemporal parameters	Step-ratio	-0.532	0,020	-	0,47	0,073
	Relative double support phase (%)	26,485	-7,230	0,795	-	1,771

Table 6: RMSE for the reconstructed trajectories and the estimated key-events.

	$RMSE_{y\ key\text{-}event}$ [1]	$RMSE_{act\text{-}rec}$ [3]	$RMSD_{l\text{-}r}$ [3]	STD [4]	ROM [3]
Hip ab-adduction	1.48	1,46	1,35	1.41	9,94
Hip flexion/extension	2.27	2,42	1,64	2.34	34,22
Knee flexion/extension	3.52	3,49	2,82	3.42	52,76
Ankle plantar-/dorsiflexion	2.87	2,84	2,60	2.79	20,04
Average	2.53	2.55	2.10	2.49	
	$RMSE_{x\ key\text{-}event}$ [2]	$r_{act\text{-}rec}$ [3]	$r_{l\text{-}r}$ [3]		
Hip ab-/adduction	3.75	0,87	0,88		
Hip flexion/extension	1.79	0,98	0,99		
Knee flexion/extension	1.95	0,97	0,98		
Ankle plantar-/dorsiflexion	2.88	0,80	0,84		
Average	2.59	0.91	0.92		

[1] *$RMSE_{y\ key\text{-}event}$ = Mean RMSE between measured y-parameters of the key-events and the y-parameters estimated with the regression-models (Table 1-4). The $RMSE_{y\ key\text{-}event}$ is averaged over the 6 key-events for every joint.*
[2] *$RMSE_{x\ key\text{-}event}$ = Mean RMSE between measured x-parameters of the key-events and the x-parameters estimated with the regression-models (averaged over the 6 key-events).*
[3] *These measures are averaged over the different walking speeds.*
[4] *The standard deviation (STD) is averaged across the gait cycle and subsequently over the different walking speeds.*

For instance, the maximal knee flexion during swing, which is a commonly reported gait feature, showed a decrease in relative timing at higher walking speeds, whereas the maximum angle itself, and its acceleration, increased with speed (figure 3). Stepwise regression showed that these effects are nonlinear and that the body height has no significant contribution to the predictability of any of the parameters of this key-event. Therefore, the regression-models for the x, y, and d^2y/dx^2 parameter of this particular key-event only include coefficients for the walking speed and walking speed squared (table 3).

The regression-models for the parameter values of the individual key-events for the different joints are presented in table 1-4. Generally, different subjects show similar dependencies. However, there was considerable variation between subjects in the parameter values of the key-events (figure 3), as reflected by the *RMSE* of the prediction of the different parameter values of the key-events (table 1-4).

To determine the time in which a reference trajectory needs to be replayed (for robotic control), or transform the relative duration of the different gait phases (% of gait cycle), to absolute timing (s), the cycle time is required. The cycle time can be obtained from the regression-models for the step-ratio (table 5) according to:

$$cycle\ time = 2 \cdot step\ time = 2 \cdot \sqrt{\frac{step\ ratio}{v / 3.6}} \quad , \quad \text{(with } v \text{ in km/h)} \qquad [3]$$

2.3.2 Validation

With the obtained regression-models a set of reference trajectories was reconstructed for every subject (at each walking speed). The reconstructed patterns matched the measured data well (figure 5). Generally, the largest errors are found at the lower walking speeds, and are located during the parts of the gait cycle where the joint excursions are largest or where joint angles change rapidly (figure 6A). The quality of the fit was also reflected in the calculated *RMSE* (figure 6B). For the hip abduction the $RMSE_{act\text{-}rec}$ (averaged over all walking speeds) was smallest (±1.5°). This joint also had the smallest range of motion of the considered joints (±10°, table 6). Reversely, the knee joint, which has the largest

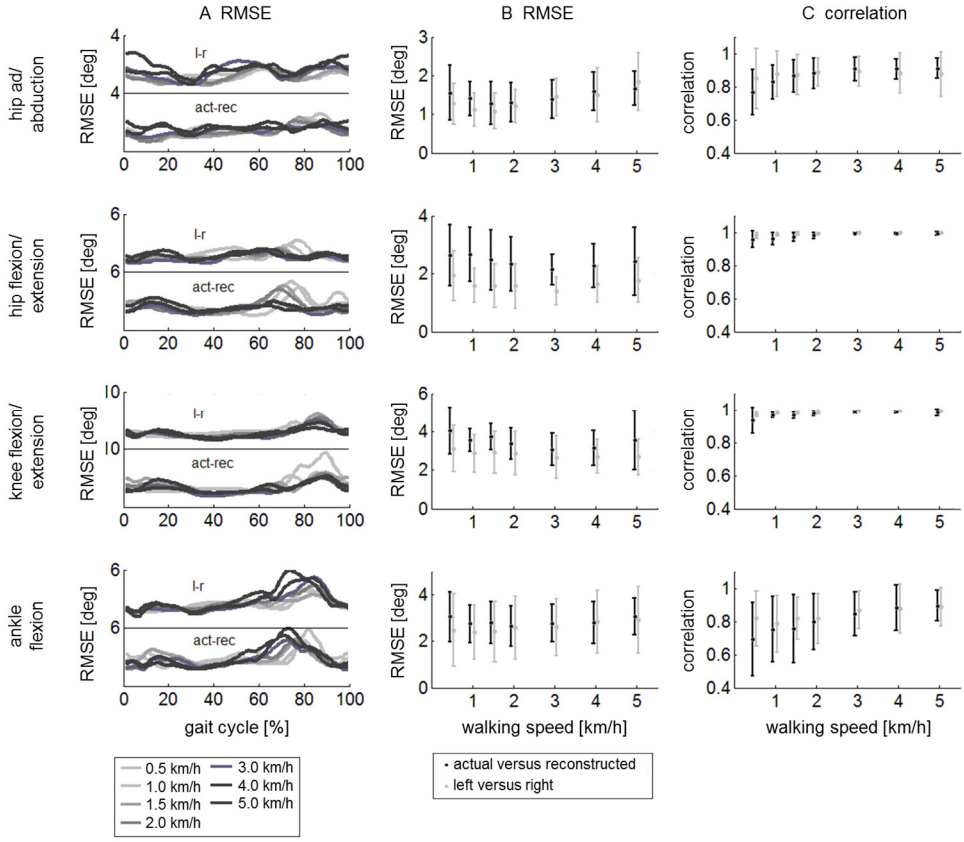

Figure 6: Validation of the reconstructed reference trajectories. A: RMSE between actual and reconstructed trajectories for the different joints ("act-rec", bottom part of the graphs), expressed as a function of the gait cycle for every walking speed. As a reference for the model error the natural deviation between the left and right joint trajectories are also provided ("l-r", top part of the graphs). B: RMSE between actual and reconstructed trajectories ($RMSE_{act\text{-}rec}$ black lines) and natural deviation between the left and right joint trajectories ($RMSD_{l\text{-}r}$ gray lines). Both measures are averaged across subjects for each walking speed. The error bars indicate the standard deviation. C: Correlation coefficients between actual and reconstructed trajectories ($r_{act\text{-}rec}$ black lines) and correlation coefficients between the left and right joint trajectories ($r_{l\text{-}r}$ gray lines).

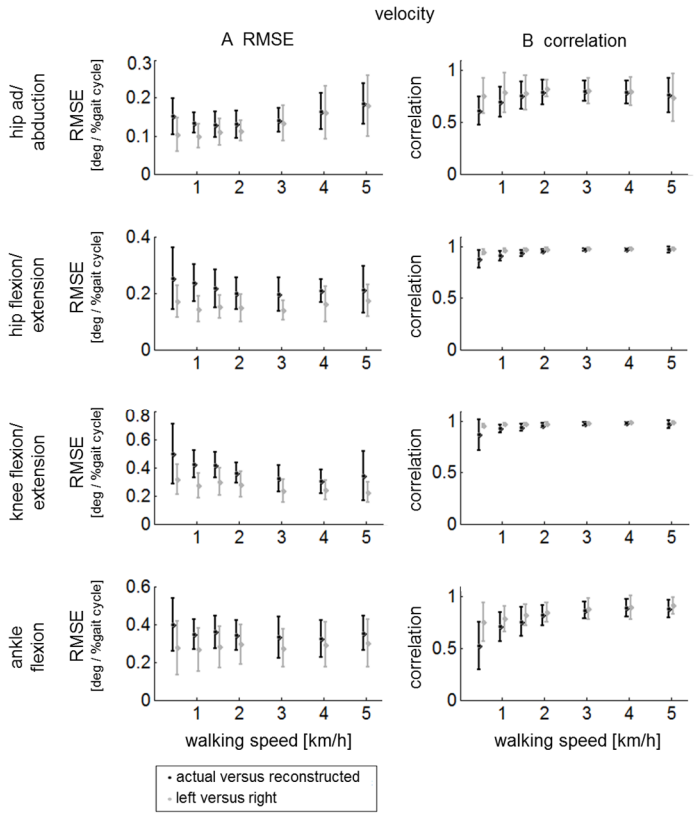

Figure 7: Validation of the reconstructed reference velocity trajectories. A: RMSE between actual and reconstructed angular velocity profiles ($RMSE_{act\text{-}rec}$ black lines) and natural deviation between left and right angular velocity profiles ($RMSD_{l\text{-}r}$ gray lines). Both measures are averaged across subjects for each walking speed. The error bars indicate the standard deviation. B: Correlation coefficients between actual and reconstructed angular velocity profiles ($r_{act\text{-}rec}$ black lines) and correlation coefficients between the left and right joint angular velocity profiles ($r_{l\text{-}r}$ gray lines).

range of motion (±53°), shows the highest average $RMSE_{act\text{-}rec}$ (±3.5°). The $RMSE_{act\text{-}rec}$ results are in line with the *RMSE* values of the predicted angles of the key-events. That is; the *RMSE* in the predicted angles (y) of the key-events ($RMSE_{y\ key\text{-}event}$) is very similar to the $RMSE_{act\text{-}rec}$ for all joints (table 6). Additionally, the correlation coefficient was used to quantify the similarity between the reconstructed and actual patterns. For hip- and knee flexion the $r_{act\text{-}rec}$ was above 0.93 at low walking speeds, with even larger correlations for higher speeds (figure 6C). For hip abduction and ankle flexion, the $r_{act\text{-}rec}$ was lowest, ranging from 0.69 at 0.5 km/h to 0.89 at 5 km/h. The $r_{act\text{-}rec}$ of the different joints are in line with the *RMSE* values in predicting the relative timing of the key-events. That is; the *RMSE* in the predicted timing (x) of the key-events ($RMSE_{x\ key\text{-}event}$) is also highest for the ankle flexion and hip abduction (table 6). As a reference for the obtained fitting quality, we compared the model error with the natural deviation between the left and right leg.

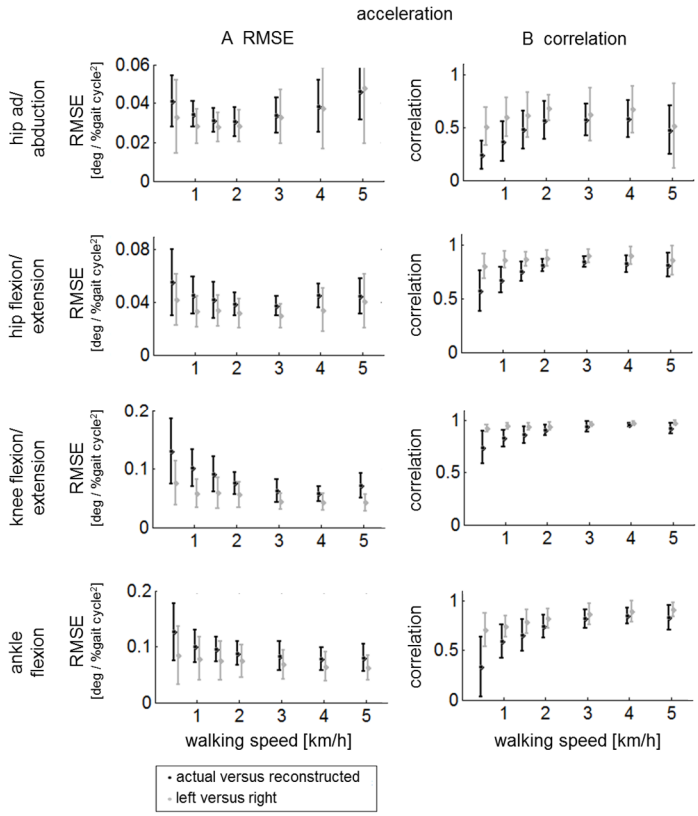

Figure 8: Validation of the reconstructed reference acceleration trajectories. A: RMSE between actual and reconstructed angular acceleration profiles ($RMSE_{act\text{-}rec}$ black lines) and natural deviation between left and right angular acceleration profiles ($RMSD_{l\text{-}r}$ gray lines). Both measures are averaged across subjects for each walking speed. The error bars indicate the standard deviation. B: Correlation coefficients between actual and reconstructed angular acceleration profiles ($r_{act\text{-}rec}$ black lines) and correlation coefficients between the left and right joint angular acceleration profiles ($r_{l\text{-}r}$ gray lines).

Here the model error ($RMSE_{act\text{-}rec}$) was only slightly higher than the left-right deviation ($RMSD_{l\text{-}r}$) and the $r_{act\text{-}rec}$ was only slightly lower than the $r_{l\text{-}r}$ (figure 6, table 6). Both measures indicates that the error in the reconstructed spline is only marginally larger compared to the error when the trajectory of one leg is taken as a reference for the other. Similar results were obtained for the reconstructed angular velocity (figure 7) and acceleration profiles (figure 8), though the correlation measures decrease for the velocity and acceleration. Another reference for the model error was provided by the inter-subject variability (STD). Generally, the model error is close to the natural variability between subjects (table 6).

The spline fitting methodology was also compared to the traditional averaging method, where we calculated the average trajectories across subjects. Generally, the amplitude of

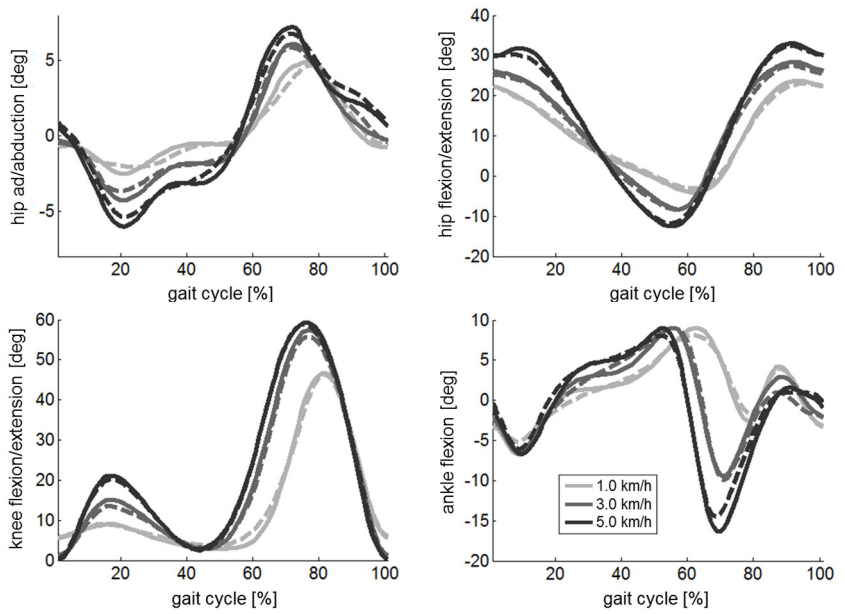

Figure 9: Reconstructed trajectories versus averaged trajectories. The reconstructed trajectories (solid line) are based on the predicted key-events and the average trajectories are averaged across subjects (dashed line). The trajectories are presented at 3 different speeds. Averaging over multiple subjects has a dampening effect on the extreme values in the average pattern, especially for the hip abduction and ankle flexion. The reconstructed trajectories are generated for a subject with a body height that equals the mean body height of our subject population (1.69 m).

the average trajectories was smaller than the amplitude of the reconstructed trajectories (figure 9), especially for the hip abduction and ankle flexion.

2.4 Discussion and conclusion

In this study we present a method to parameterize joint trajectories and generate walking speed- and body height dependent reference joint trajectories. The generated trajectories are continuous in terms of position, velocity and acceleration, and especially suitable for the control of robotic gait applications. The method is based on fitting quintic splines between different key-events, which are estimated with regression-models. The reconstructed trajectories matched the measured trajectories very well. The obtained regression-models also show that: 1) the majority of the key-events are speed-dependent, both in terms of amplitude and timing, 2) walking speed has a larger effect on the key-events than body height, 3) there is considerable inter-subject variability in the extracted key-events, especially at lower walking speeds. This section discusses these findings in further detail.

2.4.1 Extreme values in joint angles

Previous studies on speed-dependencies in joint trajectories mainly focused on the extreme values. In this study we observed similar changes in all commonly reported extreme values [15,17,24,25,35-37]. For the knee joint we found a speed-dependent increase in knee flexion during the swing phase, as well as during the loading response. Maximum hip flexion and extension also increased with walking speed, in a similar manner as reported by others. The ankle joint also contained multiple extreme values that changed with walking speed, like an increase in maximum plantar flexion and a reduction in dorsiflexion during swing. Generally, the effect of speed on these kinematic changes was largest at lower walking speeds [38]. An in-depth comparison between our findings and related studies, for all commonly reported extreme values, is provided in Supplementary material B. For the extreme values in the hip ab/adduction we observed an increase with speed. Schwartz et al. [39] are one of the few reporting hip ab/adduction angular patterns at different speeds. Although they focused on growing children, rather than elderly, they report similar changes in terms of angular amplitude at increasing speeds.

2.4.2 Timing of extreme values in joint angles

The relative timing of the majority of the extreme values showed a clear dependency on walking speed. They occurred earlier during the gait cycle with increasing speed. These changes in timing are strongly related to changes in the duration of the different gait phases. At higher walking speeds the relative duration of the double support phase decreases (table 5), shifting most extreme values forward. Stoquart et al. [25] are one of the few who reported the relative timing of the maximum hip extension, maximum knee flexion and maximum ankle plantar flexion, and demonstrated similar changes (Supplementary material B). Van Hedel et al. [38] did not quantify the changes in timing, still their normalized joint trajectories showed very similar trends in relative timing at increasing speeds.

2.4.3 Inter-subject variability in the extracted key-events

We clearly demonstrated the speed-dependency of the key-events, but the *RMSE* between the measured and predicted key-events was considerable, up to 15% of the mean ROM for the hip abduction. This is primarily caused by the high inter-subject variability, which was also reported by others [15-17,23,24]. For most key-events the variation in the parameters decreased with walking speed, suggesting a more consistent walking pattern at higher speeds. Nonetheless, most key-events show significant correlations with walking speed, underlining the need to adjust angular trajectories to walking speed.

2.4.4 Influence of body height on key-events

In accordance with other studies we found that body height has a limited effect on the key-events, compared to walking speed. Hanlon et al. [16] did not demonstrate any improvement in the correlation between gait patterns and walking speed when using normalized walking speed (normalized to leg length), compared to using absolute speed. Additionally, Lelas et al. [15], who performed regressions with normalized walking speed, and multiple regression with walking speed and leg-length, did not show overall improvement compared to regressing on walking speed only. Finally, Kirtley et al. [24] did not find significant correlation between body height and any of their reported kinematic parameters. Still, it should be mentioned that, in most studies, including ours, the variability in body height is much smaller than the variability in walking speed. If a wider range of body heights were included, for instance by including extremely short or tall persons, the effect of body height may be larger.

2.4.5 Comparison with traditional averaging methods

As mentioned before, most studies that report normative gait patterns take the average of individual normalized datasets. Molloy et al. [26] and Sadeghi et al. [27] showed that averaging over subjects can have a dampening effect on the extremes in the gait pattern, when the datasets have a different distribution of the extremes throughout the gait cycle. Figure 8 demonstrates that the method proposed here compensates for this effect, which is most noticeable in joint trajectories that have large inter-subject variability in the timing of the key-events (hip abduction and ankle flexion, table 6). Molloy et al., who did not assess hip abduction, also reported that the largest errors were found for the ankle joint (maximum plantar flexion).

2.4.6 Limitations

This study is not without limitations. Due to the small number of subjects (15), we did not derive separate regression equations for male and female subjects, although small gender differences have been reported. Females are reported to have a moderately increased hip flexion [17,40], and less knee flexion during swing [17] and loading response [17,41]. Here, we focused on (middle) aged subjects, since many neurological gait disorders occur in this group. Studies on age-related gait alterations demonstrated a moderate increase in knee flexion at mid-stance, a decrease of the maximum knee flexion [17], reduced hip extension [35,42], and reduced ankle plantar flexion [35,36]. Others, however, reported no clear effect of age [43]. Although most of the reported changes in gait kinematics in elderly are related to aging per se, and not to reduced walking speed, they are small and inconsistent. Therefore, we suggest that, in practice, the same reference data can be used for all adults. In future studies (including more subjects), all these variables can be added to the regression-models in order to investigate their potential contribution towards more accurate joint trajectory estimations.

In this study 6 key-events were selected for every joint. These key-events (figure 2) were chosen based on the experience of the authors. Visual comparison of the reconstructed patterns and the measured patterns showed that these key-events sufficed to capture the main characteristics of the joint trajectories. We did not perform an optimization on the number of key-events to achieve the best possible fit. Consequently, another set (or amount) of key-events could possibly produce a better fit. However, based on the high correlation coefficients and low *RMSE* values, we do not see much room for improvement.

Another potential limitation of this study is that the gait kinematics were recorded on a treadmill. Although small kinematic (and spatiotemporal) differences have been recorded in the past [44,45], more recent studies show that these differences are typically smaller than 3°, and fall within the normal variability and repeatability of these kinematic parameters [46-48]. They concluded that humans do not make any significant gait adjustments when walking on a treadmill, taking into account an appropriate familiarization period [49,50]. Therefore, we suggest that, in practice, the same reference data can be used for overground- and treadmill-walking.

2.4.7 Utility

The obtained regression-models (table 1-4) can be used to reconstruct subject- and speed-dependent reference trajectories, within the provided range (0.5-5 km/h). For the control of robotic orthoses, the trajectories can be replayed with a user specific cycle time, or with an estimate of the cycle time (table 5). The fitted splines also provide continuous angular velocity and acceleration patterns, which can be used for friction and/or inertia compensation of a robotic device. Although our primary goal was to create reference trajectories that can be used for robotic gait applications they can also serve a clinical purpose. They can help discriminating between gait changes due to a reduction in self-selected walking speed and effects actually caused by underlying pathologies. Supplementary material C discusses the clinical and robotic applications (and limitations) in more detail.

Acknowledgments

This study was supported by a grant from Dutch Ministry of Economic affairs and Province of Overijssel, the Netherlands (grant: PID082004), and the EU, within the EVRYON Collaborative Project (Evolving Morphologies for Human-Robot Symbiotic Interaction, Project FP7-ICT-2007-3-231451).

References

[1] I. Diaz, J. J. Gil, and E. Sanchez, "Lower-Limb Robotic Rehabilitation: Literature Review and Challenges," *Journal of Robotics,* vol. 2011, pp. 1-11, 2011.

[2] A. Pennycott, D. Wyss, H. Vallery, V. Klamroth-Marganska, and R. Riener, "Towards more effective robotic gait training for stroke rehabilitation: a review," *J Neuroeng Rehabil,* vol. 9, pp. 1-13, 2012.

[3] D. P. Ferris, G. S. Sawicki, and A. Domingo, "Powered lower limb orthoses for gait rehabilitation," Top Spinal Cord Inj Rehabil, vol. 11, pp. 34-49, 2005.

[4] A. M. Dollar and H. Herr, "Lower Extremity Exoskeletons and Active Orthoses: Challenges and State-of-the-Art," IEEE Transactions on Robotics and Automation, vol. 24, pp. 144-158, 2008.

[5] H. Yano, K. Kasai, H. Saitou, and H. Iwata, "Development of a gait rehabilitation system using a locomotion interface," Journal of Visualization and Computer Animation, vol. 14, pp. 243-252, 2003.

[6] Y. Stauffer, Y. Allemand, M. Bouri, J. Fournier, R. Clavel, P. Metrailler, R. Brodard, and F. Reynard, "The WalkTrainer--a new generation of walking reeducation device combining orthoses and muscle stimulation," *IEEE Trans Neural Syst Rehabil Eng,* vol. 17, pp. 38-45, 2009.

[7] S. K. Banala, S. H. Kim, S. K. Agrawal, and J. P. Scholz, "Robot assisted gait training with active leg exoskeleton (ALEX)," *IEEE Trans Neural Syst Rehabil Eng,* vol. 17, pp. 2-8, Feb 2009.

[8] M. Wu, T. G. Hornby, J. M. Landry, H. Roth, and B. D. Schmit, "A cable-driven locomotor training system for restoration of gait in human SCI," *Gait Posture,* vol. 33, pp. 256-60, 2011.

[9] J. L. Emken, S. J. Harkema, J. A. Beres-Jones, C. K. Ferreira, and D. J. Reinkensmeyer, "Feasibility of manual teach-and-replay and continuous impedance shaping for robotic locomotor training following spinal cord injury," *IEEE Trans Biomed Eng,* vol. 55, pp. 322-34, 2008.

[10] D. Aoyagi, W. E. Ichinose, S. J. Harkema, D. J. Reinkensmeyer, and J. E. Bobrow, "A robot and control algorithm that can synchronously assist in naturalistic motion during body-weight-supported gait training following neurologic injury," *IEEE Trans Neural Syst Rehabil Eng,* vol. 15, pp. 387-400, 2007.

[11] G. Colombo, M. Joerg, R. Schreier, and V. Dietz, "Treadmill training of paraplegic patients using a robotic orthosis," *J Rehabil Res Dev,* vol. 37, pp. 693-700, 2000.

[12] H. Vallery, E. H. van Asseldonk, M. Buss, and H. van der Kooij, "Reference trajectory generation for rehabilitation robots: complementary limb motion estimation," *IEEE Trans Neural Syst Rehabil Eng,* vol. 17, pp. 23-30, 2009.

[13] J. L. Emken, J. H. Wynne, S. J. Harkema, and D. J. Reinkensmeyer, "A robotic device for manipulating human stepping," *IEEE Transactions on Robotics,* vol. 22, pp. 185-189, 2006.

[14] E. H. van Asseldonk, J. F. Veneman, R. Ekkelenkamp, J. H. Buurke, F. C. van der Helm, and H. van der Kooij, "The Effects on Kinematics and Muscle Activity of Walking in a Robotic Gait Trainer During Zero-Force Control," *IEEE Trans Neural Syst Rehabil Eng,* vol. 16, pp. 360-370, 2008.

[15] J. L. Lelas, G. J. Merriman, P. O. Riley, and D. C. Kerrigan, "Predicting peak kinematic and kinetic parameters from gait speed," *Gait Posture,* vol. 17, pp. 106-12, 2003.

[16] M. Hanlon and R. Anderson, "Prediction methods to account for the effect of gait speed on lower limb angular kinematics," *Gait Posture,* vol. 24, pp. 280-7, 2006.

[17] T. Oberg, A. Karsznia, and K. Oberg, "Joint Angle Parameters in Gait - Reference Data for Normal Subjects, 10-79 Years of Age," *Journal of Rehabilitation Research and Development,* vol. 31, pp. 199-213, 1994.

[18] P. A. Goldie, T. A. Matyas, and O. M. Evans, "Deficit and change in gait velocity during rehabilitation after stroke," *Arch Phys Med Rehabil,* vol. 77, pp. 1074-82, 1996.

[19] C. B. Beaman, C. L. Peterson, R. R. Neptune, and S. A. Kautz, "Differences in self-selected and fastest-comfortable walking in post-stroke hemiparetic persons," *Gait Posture,* vol. 31, pp. 311-6, 2010.

[20] U. S. Witte and J. Y. Carlsson, "Self-selected walking speed in patients with hemiparesis after stroke," *Scand J Rehabil Med,* vol. 29, pp. 161-5, 1997.

[21] H. J. A. van Hedel, V. Dietz, and A. Curt, "Assessment of walking speed and distance in subjects with an incomplete spinal cord injury," *Neurorehabilitation and Neural Repair,* vol. 21, pp. 295-301, 2007.

[22] A. Delval, J. Salleron, J. L. Bourriez, S. Bleuse, C. Moreau, P. Krystkowiak, L. Defebvre, P. Devos, and A. Duhamel, "Kinematic angular parameters in PD: reliability of joint angle curves and comparison with healthy subjects," *Gait Posture,* vol. 28, pp. 495-501, 2008.

[23] B. W. Stansfield, S. J. Hillman, M. E. Hazlewood, and J. E. Robb, "Regression analysis of gait parameters with speed in normal children walking at self-selected speeds," *Gait Posture,* vol. 23, pp. 288-94, 2006.

[24] C. Kirtley, M. W. Whittle, and R. J. Jefferson, "Influence of walking speed on gait parameters," *J Biomed Eng,* vol. 7, pp. 282-8, 1985.

[25] G. Stoquart, C. Detrembleur, and T. Lejeune, "Effect of speed on kinematic, kinetic, electromyographic and energetic reference values during treadmill walking," *Neurophysiol Clin,* vol. 38, pp. 105-16, 2008.

[26] M. Molloy, J. Salazar-Torres, C. Kerr, B. C. McDowell, and A. P. Cosgrove, "The effects of industry standard averaging and filtering techniques in kinematic gait analysis," *Gait Posture,* vol. 28, pp. 559-62, 2008.

[27] H. Sadeghi, P. A. Mathieu, S. Sadeghi, and H. Labelle, "Continuous curve registration as an intertrial gait variability reduction technique," *IEEE transactions on neural systems and rehabilitation engineering,* vol. 11, pp. 24-30, 2003.

[28] B. Koopman, H. J. Grootenboer, and H. J. de Jongh, "An inverse dynamics model for the analysis, reconstruction and prediction of bipedal walking," *J Biomech,* vol. 28, pp. 1369-76, 1995.

[29] J. A. Zeni, Jr., J. G. Richards, and J. S. Higginson, "Two simple methods for determining gait events during treadmill and overground walking using kinematic data," *Gait Posture,* vol. 27, pp. 710-4, 2008.

[30] N. Sekiya and H. Nagasaki, "Reproducibility of the walking patterns of normal young adults: test-retest reliability of the walk ratio(step-length/step-rate)," *Gait Posture,* vol. 7, pp. 225-227, 1 1998.

[31] N. R. Draper and H. Smith, *Applied Regression Analysis*. Hoboken, NJ: Wiley-Interscience, 1998.

[32] J. O. Street, R. J. Carroll, and D. Ruppert, "A Note on Computing Robust Regression Estimates via Iteratively Reweighted Least Squares," *The American Statistician,* vol. 42, pp. 152–154, 1988.

[33] M. Stone, "Cross-Validatory Choice and Assessment of Statistical Predictions," *Journal of the Royal Statistical Society Series B-Statistical Methodology,* vol. 36, pp. 111-147, 1974.

[34] S. Geisser, *Predictive Inference*. New York, NY: Chapman and Hall, 1993.

[35] D. C. Kerrigan, M. K. Todd, U. Della Croce, L. A. Lipsitz, and J. J. Collins, "Biomechanical gait alterations independent of speed in the healthy elderly: Evidence for specific limiting impairments," *Archives of Physical Medicine and Rehabilitation,* vol. 79, pp. 317-322, 1998.

[36] A. Silder, B. Heiderscheit, and D. G. Thelen, "Active and passive contributions to joint kinetics during walking in older adults," *J Biomech,* vol. 41, pp. 1520-7, 2008.
[37] A. Pepin, K. E. Norman, and H. Barbeau, "Treadmill walking in incomplete spinal-cord-injured subjects: 1. Adaptation to changes in speed," *Spinal Cord,* vol. 41, pp. 257-70, 2003.
[38] H. J. Van Hedel, L. Tomatis, and R. Muller, "Modulation of leg muscle activity and gait kinematics by walking speed and bodyweight unloading," *Gait Posture,* vol. 24, pp. 35-45, 2006.
[39] M. H. Schwartz, A. Rozumalski, and J. P. Trost, "The effect of walking speed on the gait of typically developing children," *J Biomech,* vol. 41, pp. 1639-50, 2008.
[40] D. C. Kerrigan, M. K. Todd, and U. Della Croce, "Gender differences in joint biomechanics during walking: normative study in young adults," *Am J Phys Med Rehabil,* vol. 77, pp. 2-7, 1998.
[41] D. B. Kettelkamp, R. J. Johnson, G. L. Smidt, E. Y. Chao, and M. Walker, "An electrogoniometric study of knee motion in normal gait," *J Bone Joint Surg Am,* vol. 52, pp. 775-90, 1970.
[42] R. D. Crowinshield, R. A. Brand, and R. C. Johnston, "The effects of walking velocity and age on hip kinematics and kinetics," *Clin Orthop Relat Res,* pp. 140-4, May 1978.
[43] M. P. Murray, A. B. Drought, and R. C. Kory, "Walking Patterns of Normal Men," *J Bone Joint Surg Am,* vol. 46, pp. 335-60, 1964.
[44] G. M. Strathy, E. Y. Chao, and R. K. Laughman, "Changes in knee function associated with treadmill ambulation," *J Biomech,* vol. 16, pp. 517-22, 1983.
[45] F. Alton, L. Baldey, S. Caplan, and M. C. Morrissey, "A kinematic comparison of overground and treadmill walking," *Clinical Biomechanics,* vol. 13, pp. 434-440, 1998.
[46] P. O. Riley, G. Paolini, U. Della Croce, K. W. Paylo, and D. C. Kerrigan, "A kinematic and kinetic comparison of overground and treadmill walking in healthy subjects," *Gait Posture,* vol. 26, pp. 17-24, 2007.
[47] K. Parvataneni, L. Ploeg, S. J. Olney, and B. Brouwer, "Kinematic, kinetic and metabolic parameters of treadmill versus overground walking in healthy older adults," *Clin Biomech (Bristol, Avon),* vol. 24, pp. 95-100, 2009.
[48] S. J. Lee and J. Hidler, "Biomechanics of overground vs. treadmill walking in healthy individuals," *J Appl Physiol,* vol. 104, pp. 747-55, 2008.
[49] A. Matsas, N. Taylor, and H. McBurney, "Knee joint kinematics from familiarised treadmill walking can be generalised to overground walking in young unimpaired subjects," *Gait Posture,* vol. 11, pp. 46-53, 2000.
[50] E. Wass, N. F. Taylor, and A. Matsas, "Familiarisation to treadmill walking in unimpaired older people," *Gait & Posture,* vol. 21, pp. 72-79, 2005.
[51] T. Oberg, A. Karsznia, and K. Oberg, "Basic Gait Parameters - Reference Data for Normal Subjects, 10-79 Years of Age," *Journal of Rehabilitation Research and Development,* vol. 30, pp. 210-223, 1993.
[52] T. Mcgeer, "Passive Dynamic Walking," *International Journal of Robotics Research,* vol. 9, pp. 62-82, 1990.
[53] F. C. Anderson, S. R. Goldberg, M. G. Pandy, and S. L. Delp, "Contributions of muscle forces and toe-off kinematics to peak knee flexion during the swing phase of normal gait: an induced position analysis," *J Biomech,* vol. 37, pp. 731-7, 2004.
[54] W. Zijlstra, A. W. F. Rutgers, A. L. Hof, and V. W. T. W., "voluntary and involuntary adaptation of walking to temporal and spatial constrains," *Gait & Posture,* vol. 3, pp. 13-18, 1995.
[55] H. Nagasaki, H. Itoh, K. Hashizume, T. Furuna, H. Maruyama, and T. Kinugasa, "Walking patterns and finger rhythm of older adults," *Percept Mot Skills,* vol. 82, pp. 435-47, 1996.

[56] D. W. Grieve and R. J. Gear, "The relationships between length of stride, step frequency, time of swing and speed of walking for children and adults," *Ergonomics,* vol. 9, pp. 379-99, 1966.

[57] P. O. Riley, U. DellaCroce, and D. C. Kerrigan, "Effect of age on lower extremity joint moment contributions to gait speed," *Gait Posture,* vol. 14, pp. 264-70, 2001.

[58] B. W. Stansfield, S. J. Hillman, M. E. Hazlewood, A. A. Lawson, A. M. Mann, I. R. Loudon, and J. E. Robb, "Normalized speed, not age, characterizes ground reaction force patterns in 5-to 12-year-old children walking at self-selected speeds," *Journal of Pediatric Orthopaedics,* vol. 21, pp. 395-402, 2001.

[59] M. L. van der Linden, A. M. Kerr, M. E. Hazlewood, S. J. Hillman, and J. E. Robb, "Kinematic and kinetic gait characteristics of normal children walking at a range of clinically relevant speeds," *J Pediatr Orthop,* vol. 22, pp. 800-6, 2002.

[60] G. Chen, C. Patten, D. H. Kothari, and F. E. Zajac, "Gait differences between individuals with post-stroke hemiparesis and non-disabled controls at matched speeds," *Gait Posture,* vol. 22, pp. 51-6, 2005.

[61] G. I. Turnbull, J. Charteris, and J. C. Wall, "A comparison of the range of walking speeds between normal and hemiplegic subjects," *Scand J Rehabil Med,* vol. 27, pp. 175-82, 1995.

[62] L. M. Schutte, U. Narayanan, J. L. Stout, P. Selber, J. R. Gage, and M. H. Schwartz, "An index for quantifying deviations from normal gait," *Gait & Posture,* vol. 11, pp. 25-31, 2000.

[63] M. H. Schwartz and A. Rozumalski, "The gait deviation index: A new comprehensive index of gait pathology," *Gait & Posture,* vol. 28, pp. 351-357, 2008.

[64] A. Duhamel, J. L. Bourriez, P. Devos, P. Krystkowiak, A. Destee, P. Derambure, and L. Defebvre, "Statistical tools for clinical gait analysis," *Gait & Posture,* vol. 20, pp. 204-212, 2004.

[65] G. E. Gorton, D. A. Hebert, and M. E. Gannotti, "Assessment of the kinematic variability among 12 motion analysis laboratories," *Gait & Posture,* vol. 29, pp. 398-402, 2009.

[66] M. H. Schwartz, J. P. Trost, and R. A. Wervey, "Measurement and management of errors in quantitative gait data," *Gait & Posture,* vol. 20, pp. 196-203, 2004.

Supplementary material

Supplementary material A: Spline fitting procedure

This appendix summarizes the reconstruction procedure of the reference trajectories. Between each consecutive pair of key-events a quintic spline is formulated. Each spline is based on 6 constrains (initial and final position, velocity and acceleration) and requires a fifth order polynomial:

$$\begin{aligned} S(x) &= A_i + B_i x + C_i x^2 + D_i x^3 + E_i x^4 + F_i x^5 \\ \frac{dS}{dx}(x) &= B_i + C_i 2x^1 + D_i 3x^2 + E_i 4x^3 + F_i 5x^4 \qquad \text{for } x_i \le x \le x_{i+1} \\ \frac{d^2S}{dx^2}(x) &= C_i 2 + D_i 6x^1 + E_i 12x^2 + F_i 20x^3 \end{aligned} \qquad [1]$$

where $S(x)$ represents the spline (between key-event i and key-event $i+1$) and A-F its coefficients. Filling in these equations for 2 subsequent key-events yields:

$$\begin{bmatrix} 1 & x_i & x_i^2 & x_i^3 & x_i^4 & x_i^5 \\ 0 & 1 & 2x_i & 3x_i^2 & 4x_i^3 & 5x_i^4 \\ 0 & 0 & 2 & 6x_i & 12x_i^2 & 20x_i^3 \\ 1 & x_{i+1} & x_{i+1}^2 & x_{i+1}^3 & x_{i+1}^4 & x_{i+1}^5 \\ 0 & 1 & 2x_{i+1} & 3x_{i+1}^2 & 4x_{i+1}^3 & 5x_{i+1}^4 \\ 0 & 0 & 2 & 6x_{i+1} & 12x_{i+1}^2 & 20x_{i+1}^3 \end{bmatrix} \cdot \begin{bmatrix} A_i \\ B_i \\ C_i \\ D_i \\ E_i \\ F_i \end{bmatrix} = \begin{bmatrix} y_i \\ \frac{dy}{dx}_i \\ \frac{d^2y}{dx^2}_i \\ y_{i+1} \\ \frac{dy}{dx}_{i+1} \\ \frac{dy}{dx^2}_{i+1} \end{bmatrix} \qquad [2]$$

which can be written as:

$$\begin{bmatrix} A_i \\ B_i \\ C_i \\ D_i \\ E_i \\ F_i \end{bmatrix} = inv \begin{bmatrix} 1 & x_i & x_i^2 & x_i^3 & x_i^4 & x_i^5 \\ 0 & 1 & 2x_i & 3x_i^2 & 4x_i^3 & 5x_i^4 \\ 0 & 0 & 2 & 6x_i & 12x_i^2 & 20x_i^3 \\ 1 & x_{i+1} & x_{i+1}^2 & x_{i+1}^3 & x_{i+1}^4 & x_{i+1}^5 \\ 0 & 1 & 2x_{i+1} & 3x_{i+1}^2 & 4x_{i+1}^3 & 5x_{i+1}^4 \\ 0 & 0 & 2 & 6x_{i+1} & 12x_{i+1}^2 & 20x_{i+1}^3 \end{bmatrix} \cdot \begin{bmatrix} y_i \\ \frac{dy}{dx}_i \\ \frac{d^2y}{dx^2}_i \\ y_{i+1} \\ \frac{dy}{dx}_{i+1} \\ \frac{dy}{dx^2}_{i+1} \end{bmatrix} \qquad [3]$$

where x_i, y_i, dy/dx_i, and $d^2y/dx^2{}_i$ represent the x, y, dy/dx, and d^2y/dx^2 parameters of the i^{th} key-event. These parameters are calculated for a specific speed and body height with the

regression equations provided in table 1-4. For example: the x parameter of the 6 key-events for the knee joint trajectory are calculated according to:

$$\begin{bmatrix} x_1 \\ x_2 \\ x_3 \\ x_4 \\ x_5 \\ x_6 \end{bmatrix} = \begin{bmatrix} 1 & 0 & 0 & 0 \\ 17{,}103 & 0 & 0 & 0 \\ 48{,}542 & -0{,}998 & 0 & 0 \\ 68{,}947 & -6{,}096 & 0{,}611 & 5{,}9067 \\ 85{,}816 & -4{,}480 & 0{,}519 & 0 \\ 92{,}489 & 0 & 0 & 0 \end{bmatrix} \bullet \begin{bmatrix} l & v & v^2 \end{bmatrix} \quad \begin{matrix} \Rightarrow \\ v = 3 \text{ km/h} \\ l = 1.75 \text{ m} \end{matrix} \quad \begin{bmatrix} x_1 \\ x_2 \\ x_3 \\ x_4 \\ x_5 \\ x_6 \end{bmatrix} = \begin{bmatrix} 1.00 \\ 17.10 \\ 45.55 \\ 66.60 \\ 77.04 \\ 92.49 \end{bmatrix} \quad [4]$$

where v represents the walking speed and l the body height. Here the x parameters are calculated for a walking speed of 3 km/h and for a subject with a body height of 1.75 m. The y, dy/dx, and d^2y/dx^2 parameters are calculated in a similar way (table 3). To ensure continuity of the spline we define the angle, velocity and acceleration at the end of the sixth last spline to be equal to the start of the first spline:

$$x_7 = 101,\ y_7 = y_1,\ \frac{dy}{dx_7} = \frac{dy}{dx_1},\ \frac{d^2y}{dx^2{}_7} = \frac{d^2y}{dx^2{}_1} \quad [5]$$

Filling in the obtained x, y, dy/dx, and d^2y/dx^2 parameters in a pairwise fashion in equation 3 yields the coefficients for the 6 splines.

$$S(x) = 6.67 \cdot 10^{-1} - 6.85 \cdot 10^{-1} x + 3.04 \cdot 10^{-1} x^2 - 1.45 \cdot 10^{-2} x^3 - 2.86 \cdot 10^{-5} x^4 + 8.45 \cdot 10^{-6} x^5 \quad [6]$$

for $1 \le x \le 17.1$

$$S(x) = -3.23 \cdot 10^{1} + 7.72 x - 4.57 \cdot 10^{-1} x^2 + 1.24 \cdot 10^{-2} x^3 - 1.70 \cdot 10^{-4} x^4 + 9.73 \cdot 10^{-6} x^5 \quad [7]$$

for $17.1 \le x \le 45.5$

etc.

Combining these splines creates the reference trajectory as shown in figure 4. The same approach is used to generate the trajectories for the others joint (table 1-4).

The method described above is also provided in matlab code (see "createRefTrajectories.m") in the online version of this supplementary material, which can be found at doi:10.1016/j.jbiomech.2014.01.037.

Supplementary material B: Peak sagittal parameters: comparison with literature

As mentioned before most studies on speed-dependencies in joint trajectories mainly focused on the extreme values. The goal of this supplementary material is to provide a quantitative comparison between our findings and previous studies. This is done for all commonly reported extreme values for the knee, hip and ankle joint. The study characteristics of the studies included in this comparison are summarized in table 7.

Similar to previous studies we observed a speed-dependent increase in maximum hip extension and flexion (figure 10 B, D). At higher walking speeds the step size increases [24, 37, 38, 51] (figure 12 B), and an increased hip angular range is a requirement to make larger steps. The percentage of the gait cycle at which the maximum hip extension occurs decreased at higher walking speeds (figure 10 A, C), which is related to the reduction of the double support phase at higher walking speeds (figure 13 C).

The maximum knee flexion during the swing phase and the loading response are also well-documented extreme values. The increased knee flexion during the loading response (figure 11 B) is suggested to be due to the need for greater shock absorption at higher speeds [15,37]. The maximum knee flexion during the swing phase also increased with walking speed, and occurred earlier in the gait cycle, similar to data reported by several authors (figure 11 C, D). The swing phase is often described as “ballistic”, and is achieved passively [52]. Consequently, the increased knee flexion during the swing phase is thought

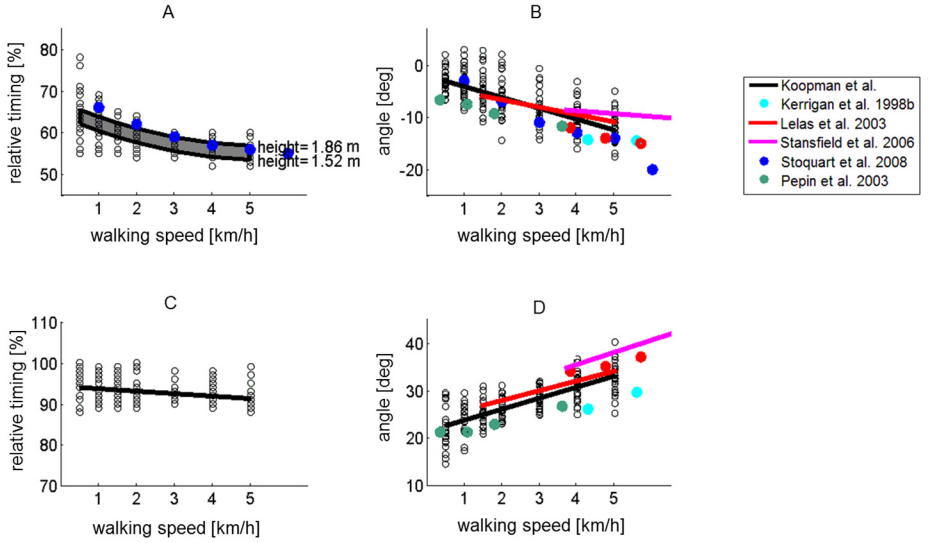

Figure 10: Comparison with literature for the peak sagittal parameters of the hip joint. Relative timing and amplitude of the maximum hip extension (A, B) and hip flexion (C, D). Each black circle represents the parameter value of the key-event at a specified walking speed for one subject, whereas the black line indicates the regression model. The shaded area indicates the fitted regression model for the range of body heights that are included in this study (1.52-1.86 m). The colored lines indicate regression models, and the circles mean values, for different studies.

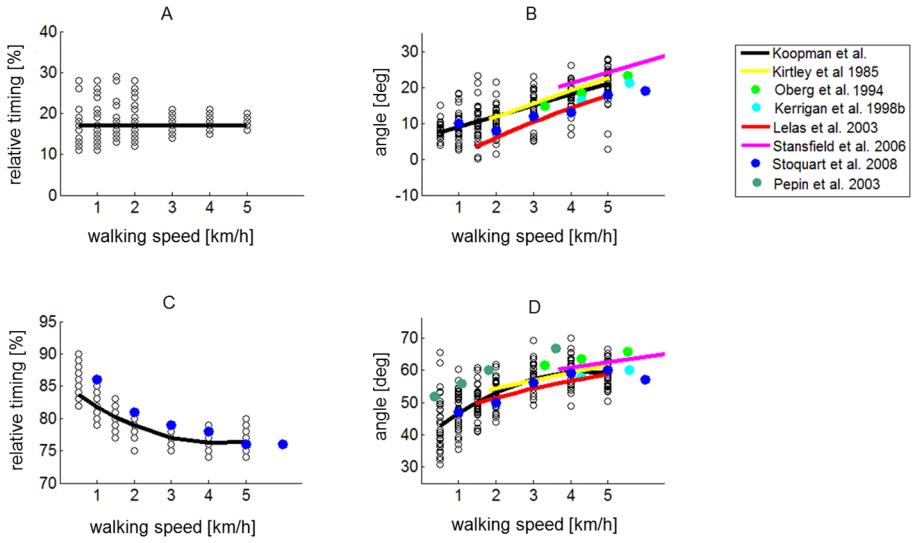

Figure 11: Comparison with literature for the peak sagittal parameters of the knee joint. Relative timing and amplitude of the maximum knee flexion during the stance phase (A, B) and the swing phase (C, D). Each black circle represents the parameter value of the key-event at a specified walking speed for one subject, whereas the black line indicates the regression model. The colored lines indicate regression models, and the circles mean values, for different studies.

to be related to a larger knee angular velocity at toe-off at higher walking speeds [53].

The ankle joint also contains multiple extreme values that have been studied before. In this study the peak plantar flexion increased with walking speed and occurred earlier in the gait cycle, which is as also reported in previous studies (figure 12 A, B). This increase is suggested to be associated with an increased ankle power, in order to produce adequate push-off at higher speeds [15,25,36]. For the peak dorsiflexion during the stance phase we did not find a correlation with walking speed, whereas others reported a mild reduction (figure 12 D). For the peak dorsiflexion during swing we observed a modest reduction with walking speed, similar to others (figure 12 F).

The majority of the studies used in this comparison (table 7) also provide mean values, or regression equations, for common spatiotemporal parameters like cadence, step length or the relative duration of the different gait phases. Similar to previous studies, the increase in walking speed is achieved by increases in both cadence and step length (figure 13 A, B). Since this was anticipated we calculated the step-ratio. Sekiya et al. [30] found this parameter to be relatively constant over a wide range of walking speeds. Others also showed a linear relationship between step frequency and step length [54]. Compared to our results Sekiya et al. [30] reported higher values for the step-ratio (figure 13 A, B). This might be explained by the difference in age. Elderly are known to walk with a higher cadence and shorter step length at similar speeds, resulting in a lower step-ratio [55]. The regression analysis revealed a small positive dependency of the step-ratio on walking

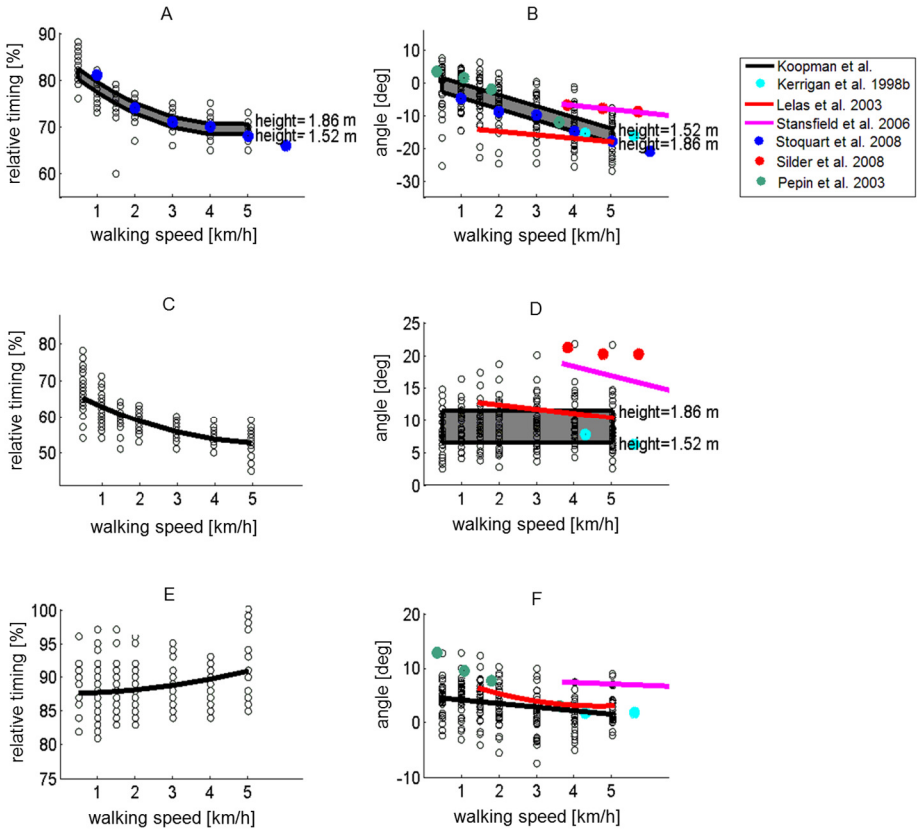

Figure 12: Comparison with literature for the peak sagittal parameters of the ankle joint. Relative timing and amplitude of the maximum plantar flexion (A, B), maximum dorsiflexion during the stance phase (C, D) and maximum dorsiflexion during swing (E, F). Each black circle represents the parameter value of the key-event at a specified walking speed for one subject, whereas the black line indicates the regression model. The shaded area indicates the fitted regression model for the range of body heights that are included in this study (1.52-1.86 m). The colored lines indicate regression models, and the circles mean values, for different studies.

speed and body height. In contrast, Zijlstra et al. [54] reported a reduction in step-ratio at higher speeds. However, their reduction in step-ratio is seen at walking speeds that exceed our maximum speed. A reduction of the step-ratio at extreme speeds may be caused by biomechanical factors limiting a further increase in step length. At higher walking speeds the relative double support phase decreased (figure 13 C) and, consequently, the swing phase increases. As mentioned above, the swing phase is often assumed to be achieved passively and maintains approximately the same duration at different speeds, leading to an increase in the relative duration at higher walking speeds (where the cycle time decreases). At even higher walking speeds the double support phase will continue to decrease until the subject starts running and the double support phase becomes absent [56].

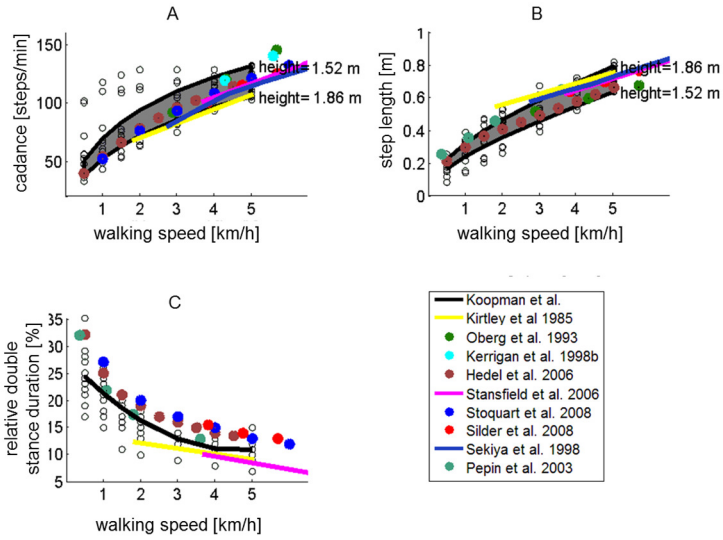

Figure 13: Comparison with literature for spatiotemporal parameters. Cadence (A), step length (B) and relative double support phase duration (C). Each black circle represents the spatiotemporal parameter at a specified walking speed for one subject, whereas the black line indicates the regression model. The shaded area indicates the fitted regression model for the range of body heights that are included in this study (1.52-1.86 m). The colored lines indicate regression models, and the circles mean values, for different studies.

Table 7: Study characteristics and reported parameters of related studies on speed-dependent gait characteristics.

Study	Type of data	Provided data[1] joints/spatio-temporal data	Age range (mean ± std)	Subjects men-women	Treadmill /Walkway	Walking speeds[3]
Kirtley et al. [24]	Regression lines	Knee flexion Cadence Step length Gait phases	18-63 (37)	10-0	Walkway	Normal [3], 2 below normal, 2 above normal
Oberg et al. [51]	Mean values	Cadence Step length	10-79	116 - 117	Walkway	Slow, normal and fast
	Note: Parameters averaged over the age groups 50-59 and 60-69.					
Oberg et al. [17]	Regression lines Mean values	Hip flexion Knee flexion	10-79	116 - 117	Walkway	Slow, normal and fast
	Note: Regression lines are only provided for the total subject population. Values used here are averaged over the age groups 50-59 and 60-69. Corresponding walking speeds are not reported for the different age groups. The used values are the means of all subjects. For the hip only the ROM is provided, and not the peak flexion/extension separately.					
Kerrigan et al. [35]	Mean values Mean trajectories	Hip flexion Knee flexion Ankle flexion Cadence	65 - 84 (72.7±5.5)	14 - 17	Walkway	Normal and fast.
Van Hedel et al. [38]	Mean trajectories	Cadence Step length Gait phases	19-32 (23.8±3.4)	10 - 10	Treadmill	10 pre-defined speeds (0.5-5 km/h)
	Note: Mean values for the cadence, step length and gait phases obtained from figure 2. Normalized step length is reported. Here the step length is calculated for a subject with a body height of 1.69m.					
Lelas et al. [15]	Regression lines	Hip flexion Knee flexion Ankle flexion	19 -40 28.1±5.9	64 (un-known gender)	Walkway	Normal, fast, slow and very slow
Stansfield et al. [23][2]	Regression lines	Hip flexion Knee flexion Ankle flexion Cadence Step length Gait phases	7 – 12	8 - 8	Walkway	Normal
	Note: Prospective 5-year study. Regression formulas are expressed in normalized speed. The reported spatiotemporal parameters are also normalized to dimensionless quantities. Here the parameters are calculated for a subject with a body height of 1.69m.					
Stoquart et al. [25]	Mean values Mean trajectories	Hip flexion Knee flexion Ankle flexion Cadence Gait phases Timing of key features	23±2	4 - 8	Treadmill	6 pre-defined speeds (1-6km/h)
Silder et al. [36]	Mean values	Hip flexion Ankle flexion	Young 18–35	Young 9 - 11	Walkway	80%, 100%, and 120% of

		Cadence Step length Gait phases	Elderly 65 - 85	Elderly 7 - 13		normal
	Note: Only the data from the elderly is used for comparison. Normalized step length is reported. Here the step length is calculated for a subject with a body height of 1.69m.					
Pepin et al. [37]	Mean values Mean trajectories	Hip flexion Knee flexion Ankle flexion Cycle time Step length Gait phases	28 -40	7-0	Treamill	0.1, 0.3, 0.5 and 1.0 m/s
Sekiya et al. [30]	Mean values	Step-ratio	Males 22.4±3.7 Females 22.5±3.9	8-17	Walkway	Slowest, slow preferred fast, fastest
	Note: Step-ratio used to calculate step length and cadence. Values are averaged over male and females.					
Koopman et al.	Regression lines	Hip abduction Hip flexion Knee flexion Ankle flexion Cadence Gait phases	47-69 (59.4±6.3)	7 - 8	Treadmill	7 pre-defined speeds (0.5-5 km/h)

[1] *Only the reported data that is used for the comparison with this study is mentioned in the table.*
[2] *Although this study present data for growing children it is shown that the change in self-selected speed, not age, is the primary determinant of kinematic and kinetic changes observed in growing children and elderly [35,57-59]. Therefore the provided normalized parameters (and walking speed) are scaled to a subject with a body height of 1.69m.*
[3] *Normal refers to the self–selected walking speed.*

Supplementary material C: Clinical and robotic applications and limitations

Clinical applications

Although our primary goal was to create reference trajectories that can be used for robotic gait applications they can also serve a clinical purpose. Our results clearly show that walking speed should be taken into account when judging whether a reduction in joint excursions can be considered pathological. Stroke survivors, for example, often show a reduced hip extension and a reduction in knee flexion during swing [60]. These patients are also known to walk at reduced speeds. Reversely, when patients, during their rehabilitation process, increase their knee flexion, this could (partly) be explained by their increase in walking speed. Similarly, in ISCI it has been shown that observed gait alterations are related to both their reduced walking speed and to their neural deficits [37].

Consequently, gait patterns of neurological patients should be compared with healthy subjects walking at matched speeds in order to differentiate between gait adaptations that are due to a reduced walking speed and gait adaptations that are a direct consequence of the injury. The reference patterns presented in this study can be used for this purpose. Traditionally, reference patterns are recorded at a limited number of speeds. The obtained regression models in this study allow the reconstruction of reference patterns for any speed, within the given range (0.5-5 km/h). This is crucial for the kinematic comparison of patients who are less capable of walking at a gait speed that differs from their 'preferred' or 'comfortable' one [37,61]. During the actual gait therapy, the speed dependent trajectories can also provide the therapist with kinematic references (maximum joint excursions) that are appropriate, and achievable, for the patient (taking into account his current walking speed).

To employ the provided reference patterns in a meaningful manner a measure of the model error is required. In this study the model error (defined by the *RMSE* between the model prediction and the actual joint trajectories) is 2.6 degrees (table 6). This is very close to the inter-subject variability, which is 2.5 degrees (table 6). This indicates that the model error is equally large as the error that occurs when average trajectories (averaged across subjects) are used. Generally, the largest model errors are found at the lower walking speeds, and are located during the parts of the gait cycle where the joint excursions are largest, or joint angles change rapidly. At 0.5 km/h the *RMSE* (averaged over the different joint) is 2.8 degrees. Still, this is only marginally larger than the inter-subject variability at that speed (2.7 degrees). At low walking speeds the subjects also showed more variability in cadence. This indicates that the subjects chose different walking strategies at lower speeds, resulting in variability in their angular trajectories. The agreement between the model error and the inter-subject variability was expected since the reconstructed trajectories greatly resemble the average trajectories (figure 9). Thus, for clinical use the reconstructed trajectories can be used in the same way as average trajectories are being used.

Throughout the literature several methods are proposed to quantify gait deviations and detect actual gait deviations [62-64]. Here the relatively large inter-subject variability indicates that a patient has to deviate considerable from the average trajectory (or reconstructed trajectories) in order to fall outside the range of natural variability. Still, an actual gait deviation does not necessarily reflect a clinical relevant gait impairment. Consequently, results from quantitative gait data analysis still require the clinician to make an objective assessment of the functional impact of the observed gait alterations. In this process the gait patterns provided in this study can highlight parts of the gait cycle where problems are dominant or determine whether treatment, directed at those problems, show improvements in the right direction.

When the provided reference patterns are used for kinematic comparisons, one should keep in mind that small differences can occur due to different experimenters, gait analysis systems, biomechanical models and testing protocols [65,66]. Still, we believe that these differences are small. Supplementary material B shows kinematic parameters that are reported in different studies, using different protocols, biomechanical models etc. Although there exists some variability, most results fall within the variability observed in our study, indicating that the experimental factors do not affect the generalizability of our results.

Finally, this study shows that one should be careful when comparing mean extreme values and observed extremes in averaged joint trajectories. Most studies present a limited number of specific gait features (often angular extremes) to quantify the effect of different pathologies, whereas other present average joint trajectories. This study shows that these angular extremes usually have a slightly different distribution throughout the gait cycle between subjects, causing lower extreme values in the averaged joint trajectories, compared to the averaged peak values themselves.

Robotic gait applications

Because the model error is in the same order as the natural variability between subjects we concluded that the accuracy of the reconstructed reference trajectories was acceptable. However, for the implementation of these trajectories in robotic gait applications there remain some considerations.

First, some patients might feel hindered when the applied trajectories are slightly different from their own trajectories. Also, applying a “normal gait pattern” might not be feasible (or preferable) for some patients. However, because of the natural variability between subjects it is practically impossible to create a 100% match for every individual patient a priori. Therefore, we consider the reconstructed trajectories as an initial guess of the patient’s walking pattern. When the therapist observes that the reference trajectory is not adequate for the patient, it can easily be modified by changing some key-events. For instance; if a patient requires more knee flexion, this can be accomplished by increasing the y parameter of the “max. swing” key-event (figure 2) and reconstructing a new trajectory. In fact, this “reference pattern tuning” approach is implemented in the control

software of a robotic gait trainer that is developed at our department. Currently, this robotic gait trainer (LOPES) is getting installed into two Dutch rehabilitation centers, and therapists have indicated that they greatly value this approach. They also value that the reference trajectories are automatically adjusted to the current walking speed.

Second, robots can potentially harm the user when the reference trajectories (and consequently the robot and user) reach angles that are not within the user's range of motion. In this study the reconstructed reference trajectories are all within the normal range of motion of the different joints.

Finally, the reference trajectories have to be checked to ensure that there does not exists a combination of angles where the feet will hit the treadmill, or each other. This is more crucial in certain phases (in this case the swing phase). Whether or not the feet will hit the treadmill during the swing phase is a bit more difficult to assess because it depends on the degrees of freedom of the device. If, for instance, the device allows natural pelvis motions (normal lateral pelvic tilt etc.), the patterns are not expected to pose any problems. However, in some robotic gait trainers pelvis motions are restricted or limited. Then, the reference patterns will need a more thorough check before being used. Still, most robotic gait trainers already have (device-) specific safety implementations which will prevent stumbling or other unsafe situations.

Chapter 3

The effect of impedance-controlled robotic gait training on walking ability and quality in individuals with chronic incomplete spinal cord injury: an explorative study

Published as:
B. Koopman†, B. Fleerkotte†, J. H. Buurke, E. H. F. van Asseldonk, H. van der Kooij, J. S. Rietman, "The effect of impedance-controlled robotic gait training on walking ability and quality in individuals with chronic incomplete spinal cord injury: an explorative study", *J. Neuroeng. Rehabil.*, vol. 11, pp. 11-26, 2014.
† Authors contributed equally

Abstract

There is increasing interest in the use of robotic gait-training devices in walking rehabilitation of incomplete spinal cord injured (iSCI) individuals. These devices provide promising opportunities to increase the intensity of training and reduce physical demands on therapists. Despite these potential benefits, robotic gait-training devices have not yet demonstrated clear advantages over conventional gait-training approaches, in terms of functional outcomes. This might be due to the reduced active participation and step-to-step variability in most robotic gait-training strategies, when compared to manually assisted therapy. Impedance-controlled devices, that allow more freedom of movement and only intervene when the movement cannot be performed independently, can increase active participation and step-to-step variability. The aim of this study was to assess the effect of impedance-controlled robotic gait training on walking ability and quality in chronic iSCI individuals. A group of 10 individuals with chronic (mean: 47 months post injury) iSCI participated in an explorative clinical trial. Participants trained three times a week for eight weeks using an impedance-controlled robotic gait trainer (LOPES: LOwer extremity Powered ExoSkeleton). Primary outcomes were the 10-meter walking test (10MWT), the Walking Index for Spinal Cord Injury (WISCI II), the six-meter walking test (6MWT), the Timed Up and Go test (TUG) and the Lower Extremity Motor Scores (LEMS). Secondary outcomes were spatiotemporal and kinematics measures. All participants were tested before, during, and after training and during a follow-up (eight weeks after the training). Participants experienced significant improvements in walking speed (0.06 m/s, p=0.008), distance (29m, p=0.005), TUG (3.4, p=0.012) and LEMS (3.4, p=0.017) after eight weeks of training with the LOPES. At the eight-week follow-up, participants retained the improvements measured at the end of the training period. Significant improvements were also found in spatiotemporal measures and hip range of motion. Robotic gait training using an impedance-controlled robot is feasible in gait rehabilitation of chronic iSCI individuals. It leads to improvements in walking ability, muscle strength, and quality of walking. Improvements observed at the end of the training period persisted at the eight-week follow-up. Slower walkers benefit the most from the training protocol and achieve the greatest relative improvement in speed and walking distance.

3.1 Introduction

Spinal cord injury (SCI) affects 10.4 [1] to 83 [2] per million individuals per year (in developed countries), leading to an estimated prevalence that ranges between 223 and 755 per million inhabitants [3]. Learning to walk again is a major goal during SCI rehabilitation [4,5]. Generally, more than 50 percent of patients have motor incomplete lesions (iSCI) [3], of which around 75 percent regain some ambulatory function [6]. Still, many iSCI individuals experience limited hip flexion during swing phase and insufficient knee stability during the stance phase. Consequently, these individuals walk slower and often remain reliant on assistive devices. Over the last decades, many rehabilitation strategies have been explored to improve functional outcomes. Most are based on evidence suggesting that task-specific and intensive training, consisting of repetitive active movements and providing appropriate afferent feedback, engages spinal and supraspinal circuits, promoting neural plasticity (cortical reorganization) and increasing functional improvement [7-14].

Robotic gait-training devices have the potential to provide training sessions that support these key components. These devices reduce the labour-intensive demands on therapists and their discomfort, compared to manually assisted body-weight-supported treadmill training (BWSTT) [15]. They also enable objective monitoring of a patient's performance and progress and reduce the between-trainer variability in terms of the applied supportive forces [16]. In the last decade, different robotic gait-training devices have been developed that are also used for other motor impairments, like stroke or multiple sclerosis. These robotic devices consist of a driven exoskeleton orthosis, like the Lokomat (Hocoma AG, Switzerland) or Auto/ReoAmbulator (HealthSouth/Motorika, USA) that drives the hip and knee joint, or driven footplates that facilitate a stepping motion like the Gait Trainer (Reha-Stim, Germany), G-EO (RehaTechnologies) or LokoHelp (LokoHelp Group, Germany).

Although these robotic gait-training devices have been on the market for more than a decade, research on their efficacy is still at an early and rather inconclusive state. On the one hand several studies showed improvements in walking ability between pre- and post-training in acute and chronic iSCI individuals who trained with the Lokomat [14,17-20] or Gait Trainer [19,21]. On the other hand, only very few randomized controlled trials (RCTs) [22-25] or other study designs [19,26], were performed to investigate whether these improvements are superior to those obtained using conventional approaches. Results from these studies, however, show contradictory results. Recent reviews have also concluded that robotic gait-training devices have not yet demonstrated clear advantages over conventional gait-training approaches in terms of clinical effectiveness [27-29].

The limited effectiveness of the first-generation robotic gait-training devices could be attributed to some inherent limitations of these devices, which were mainly position-controlled. This type of assistance may promote "slacking", where the user starts to rely on the robot to perform the movement and reduces his muscular activity [30,31]. In iSCI individuals, position-controlled robotic guidance, especially in individuals with some ability

to walk, has been shown to actually reduce volitional activity (EMG and VO2) compared to therapist-assisted BWSTT [25,32]. For motor learning in general, active subject participation is considered a very important factor [33,34]. If, conversely, participants are encouraged to actively participate, they could be resisted by the position-controlled robot, causing abnormal alternations in muscle-activation patterns [35].

Another limiting factor of position-controlled robots is that they reduce movement variability to a minimum [36]. Kinematic variability, and the possibility to make movement errors is necessary to (re)learn any new task [37,38]. In this respect, traditional robotic gait-training devices only partly meet the requirement for task-specific, intensive, active, and variable training. In other words, they do not resemble the manual assistance provided by a therapist who is likely to be compliant, motivational, and intuitively adaptive to the needs of the individual and who inherently introduces a natural sense of variability.

This situation demonstrates the need to develop and improve control approaches that increase active participation and natural movement variability. This can be achieved by only providing assistance when needed, and not supporting the subject's movements that are unimpaired. Technical implementation of this strategy often consists of controlling the interaction forces between the robot and the patient. Generally, these control strategies use a healthy control spatial path to define the desired motion, in combination with a "virtual wall"/force field that determines the amount of supportive force when the individual deviates from the template (impedance control). In some cases a "moving back wall" is introduced to assist the timing of the stepping pattern [39,40].

This kind of control strategy can overcome the main criticisms against robot-aided gait training by making the robot's behavior more flexible and adaptive to the user's needs. That is, the stiffness of the "virtual wall"/force field can be adapted to the capabilities, progress, and current participation of the user. This allows individuals to benefit from robot-aided treadmill training throughout the different stages of their recovery. At the initial stages of recovery, the robot can take charge (high impedance), whereas at the concluding stages of recovery, the user must contribute more to the prescribed motion (low impedance). To reduce the chance of the user becoming reliant on the support, some robotic gait-training devices use adaptive ("impedance shaping") algorithms that reduce the stiffness of the virtual wall when kinematic errors are small [41,42]. Flexibility between steps and the possibility of making small movement errors can be increased by lowering the impedance levels or by creating a "virtual tunnel," "dead band," or nonlinear force-field around the healthy control template [39,40].

Lowering impedance levels might also increase motivation during training sessions. At lower impedance levels, the user has more control over his gait pattern, and additional effort/voluntary movement is reflected in the gait pattern. This way, individuals are aware of their increased activity, a sensation that can positively contribute to their active involvement. These types of controllers, that 1) provide more freedom of movement, 2) only focus on the impaired aspects of gait, 3) promote active participation and 4) allow

online modification of the amount of assistance (either manually or automatically), are referred to as "assist-as-needed" (AAN), "cooperative," "adaptive," or "interactive" controllers [39-47]

Despite the potential of AAN strategies, the superiority of this approach for iSCI individuals has not been demonstrated. In animal studies, Cai et al. and Ziegler et al. showed that AAN control algorithms allow more variation between steps and result in larger walking recovery than position-control algorithms [48-50]. Despite numerous experimental robotic gait-training devices that have been developed [51], very few of the new compliant-control strategies have been tested on iSCI individuals in multisession training protocols. In single-session experiments, Emken et al. [41] showed that iSCI individuals trained with more variability when they used their "impedance-shaping algorithm". Duschau-Wicke et al. [40] evaluated their "patient-cooperative approach" in a single training session and showed that iSCI individuals trained with larger kinematic variability, and with larger muscle activity, compared to non-cooperative position-controlled training. Schück et al. [52] evaluated this approach in a multisession training protocol. They used the Lokomat to train two iSCI (and two stroke) individuals for four weeks, with four training sessions of 45 minutes per week, However, they did not find a relevant increase in gait speed for iSCI individuals.

Most studies on robotic gait training only assess walking ability. They report functional outcome measures and clinical scales, like walking speed (10-Meter Walking Test), distance (Six-Minute Walking Test), or walking ability (WISCI II). Only a few studies assess the effect of robotic gait training on walking quality, in terms of spatiotemporal and kinematic measures [23,25]. Assessment of walking quality can provide useful insights into whether gait training restores walking function by restoration of function (using more normal movement patterns) or by compensatory strategies.

The aim of this study was to evaluate the feasibility and effect of an eight-week, multi-session training protocol using an impedance-controlled gait trainer. The effect of training was assessed in terms of walking ability and walking quality. Individual assessments were used to determine which individuals were most likely to benefit from the training protocol. To evaluate if training effects were retained post-training, we performed follow-up testing eight weeks after completion of the training protocol.

3.2 Methods

3.2.1 Participants

Subjects with chronic, motor-incomplete SCI (iSCI) were recruited from Het Roessingh Centre for Rehabilitation in Enschede, The Netherlands. Inclusion criteria were iSCI sustained at least a half year prior to enrolment, age above 18 years, a stable medical condition, a physical condition that allows for three minutes of supported walking, the ability to bear their own body weight while standing, not currently enrolled in gait training

therapy, and a stable dose of anti-spastic medicine during the study. Exclusion criteria were current orthopedic issues causing problems in walking or balance, the presence of other neurological disorders, a history of cardiac conditions that interfere with physical load, the absence of independent ambulation prior to SCI, chronic joint pain and inappropriate/ unsafe fit of the robotic trainer due to the participant's body size (bodyweight > 100 kg) and/or joint contractures. All subjects provided written informed consent including permission for publication, prior to admittance to the study. The study protocol was approved by the local medical ethics committee, METC Twente (Enschede, The Netherlands).

3.2.2 Experimental apparatus

Rehabilitation device

Gait training was done with the prototype of the LOPES gait rehabilitation robot (figure 1). The LOPES consists of a bilateral exoskeleton-type rehabilitation robot above an instrumented treadmill. It is lightweight and impedance controlled using Bowden-cable-driven series-elastic actuators. The exoskeleton offers a freely translatable (3D) pelvis, where the sideways and forward/backward motion is actuated. Furthermore, it contains two actuated rotation axes in the hip joints and one at the knee (abduction/adduction of the hip and flexion/extension of hip and knee). Passive foot lifters can be added to induce ankle dorsiflexion, if required. An external bodyweight-support system can relieve a definable percentage of body weight via a harness. A more detailed description of the exoskeleton design is presented in [53].

Joint-trajectory controller

In this study, the amount of assistance that the participant receives is proportional to the deviation from a template or "reference walking pattern". This reference walking pattern is derived from speed-dependent walking patterns in healthy participants. Details about the derivation of these reference patterns can be found in [54]. In short, the patterns were derived in the following way. Joint trajectory data from 15 healthy participants was parameterized by defining different key events (minima, maxima in angular position or velocity) that were extracted from the individual patterns. Next, the walking speed and body-height dependency of these parameters were determined by regression equations.

These regression equations form the basis to reconstruct a desired joint trajectory pattern for every walking speed, and for participants with different body heights. First, the regression equations are used to estimate the different key events for a specific participant height and the selected walking speed. Next, quintic splines are fitted through the predicted key events to create a joint-trajectory. This is done for the hip and knee joint, creating the reference walking pattern (figure 2). This method was implemented such that, when the therapist changed the treadmill speed, the joint trajectories were automatically adjusted to that specific walking speed.

Figure 1: The LOPES robotic gait trainer.

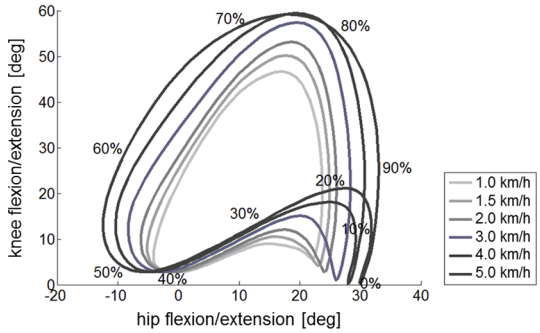

Figure 2: Hip and knee reference trajectories for the different walking speeds [54].

The amount of robotic support was adjusted by changing the stiffness of the impedance controller. The impedance levels were set to a participant-specific percentage of the maximum stiffness that could be controlled by the LOPES (300 Nm/rad). In this study, the same percentage was used for hip and knee joints and for the left and right leg. To enable the participant to stay in control of his cadence, the reference walking pattern is not replayed as a function of time but is synchronized to the cadence of the participant [43].

3.2.3 Training protocol

Subjects participated in an eight-week training program. Participants trained three times per week, for a maximum of 60 minutes per session. The training period was divided in two four-week periods, with one week scheduled for clinical tests in between. During training sessions, rest intervals were introduced if required by the participant or suggested by the therapist. The first training session was used to 1) fit the LOPES to the subject, 2) let participants get used to walking in the device and 3) select their preferred walking speed.

To fit the LOPES to the subject, different anthropometric measurements were taken to adjust the exoskeleton segment lengths. Next, the subject was positioned into the LOPES

and the trunk and lower extremities were secured. Three adjustable cuffs (one at the thigh, two at the shank) attached the lower extremities to the LOPES frame. Final adjustments were made to the cuffs to align the subject's hip and knee joints with the axes of the exoskeleton joints. Bodyweight support was set at a minimal amount for each participant, preventing excessive knee flexion during stance phase or toe dragging during swing phase. Foot lifters were used in case of insufficient ankle dorsiflexion during swing phase.

During all training sessions, the LOPES operator was paired with an experienced physical therapist. Over the training period, different parameters were adjusted to increase training intensity. Walking speed was the first parameter to be increased when possible. Subsequently, the total training time per session was increased and BWS levels were decreased. To promote active patient participation, the impedance levels of the LOPES were reduced when possible. This controller could vary between very stiff (robot-in-charge) to very flexible (patient-in-charge). Lower impedance levels also allowed more variability in the stepping trajectory (figure 3) [41].

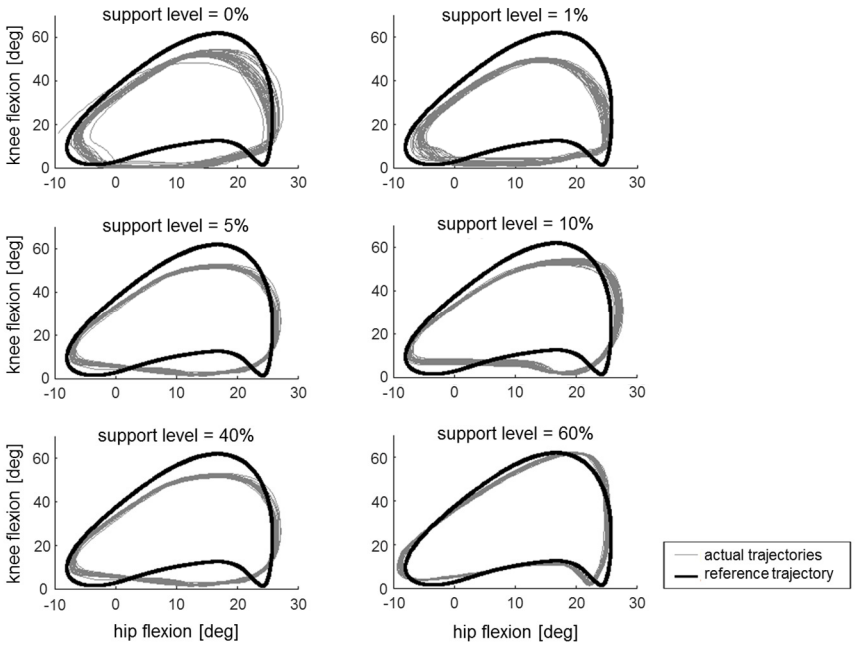

Figure 3: Typical example of hip and knee reference trajectories and actual joint trajectories for a healthy subject walking at 2 km/h using different impedance levels. Increasing the impedance levels results in a closer approximation of the reference trajectory and a reduction in the movement variability between steps. Here, the reference knee angle is enlarged by 10 percent to ensure that the robot provides support (since the healthy subject is expected to walk according to the healthy reference trajectory).

Adjustments of training parameters were done by the physical therapist based on the quality of walking (adequate step height during swing phase and adequate knee stability during stance phase), current physical condition (observation of breathing rate and degree of transpiration), and motivation (as verbally indicated by the participant). All changes were made in agreement with the participant. All training parameters were stored for later analysis.

3.2.4 Outcome measures

Primary outcome measures

To assess changes in muscle strength and walking ability, clinical tests were performed before (pre), during (mid), and after (post) eight weeks of training. To examine whether the training effects were retained, we also performed a follow-up, eight weeks after the completion of the training protocol.

Walking speed was measured using the 10-Meter Walk Test (10MWT). Participants were instructed to walk in a straight line at their own comfortable speed. Distance/endurance was tested with the Six-Minute Walk Test (6MWT), where participants ambulated for six minutes at their self-selected speed. The Timed Up and Go (TUG) test assessed the combination of balance during walking, gait speed, and sit-to-stand transitions. In this composite test, the patient must get up from a chair, walk 3 meters, return, and sit down again. For these three tests, participants were permitted to use braces and walking devices. The Walking Index for Spinal Cord Injury II (WISCI-II) was used to quantify the amount of assistance required during over-ground ambulation and to assess the use of assistive devices and/or orthoses. Category 0 indicates the participant could not walk or stand, category 20 indicates the participant could walk at least 10 m without assistance or use of assistive devices. All of these measures were taken according to van Hedel et al. [55]. Muscle strength was determined by the Lower Extremity Motor Scores (LEMS), utilized by the American Spinal Injury Association (ASIA). The strength of five key muscles are graded from 0 to 5 (0 indicates absence of muscle contraction and 5 is a normative active movement with full range of motion against full resistance). The cumulative score for lower extremities is between 0 and 50 [56]. All measures were recorded by an experienced physical therapist, not involved in the training.

Secondary outcome measures

To assess changes in gait quality, kinematic data and spatiotemporal measures were taken pre- and post-training. Gait kinematics were recorded using an optical tracking system, consisting of six infrared cameras (Vicon PlugIn Gait Model, VICON, Oxford Metrics, Oxford, UK) and reflective markers. Participants walked at their preferred speed across a 7-meter walkway approximately 10 times and were allowed to rest between rounds. Kinematic data from right and left limbs of each participant were extracted and averaged over at least 10 steps, using custom-written software (MATLAB, Mathworks Inc., Natick,

MA, USA). The use of assistive walking devices and orthotic devices for safe over-ground walking was allowed (and kept constant during the pre- and post-measurements).

A total of nine parameters were extracted from the kinematic data: walking speed, cycle time, step symmetry index, step length, step width, relative stance phase duration, maximum knee flexion during the swing phase, range of motion (ROM) of the knee during the stance phase (initial- and mid-stance) and hip ROM. These parameters were used for comparison between pre- and post-training.

Cycle time was defined as the time between two consecutive heel strikes of the same leg. Range of motion of the knee during the stance phase was used to assess knee stability during the stance phase. Step width was determined as a measure of gait stability [57]. The step symmetry index was calculated according to equation 1.

$$SI = \frac{SLs\text{-}SLw}{0.5(SLs+SLw)} \cdot 100\% \quad [1]$$

SLs represents the step length of the stronger leg and SLw the step length of the weaker leg. Here, a symmetry index of zero indicates perfect symmetry between the two legs. Similarly to Nooijen et al. [23] the stronger leg was defined as the leg that, on average, made the largest steps during the pre-test. In all participants, the weak leg during the pre- and post-training remained the same.

The step length, relative stance phase duration, maximum knee flexion during the swing phase, ROM of the knee during the stance phase and the hip ROM were also separately calculated for the weaker and stronger leg.

3.2.5 Statistics

Measurements of walking ability were assessed pre-, mid-, and post-training and at follow-up. Because of the lack of normally distributed data (determined by Shapiro-Wilk test) and the relatively small number of participants, nonparametric statistical tests were used to detect changes throughout the training period. Statistical analysis was done on the absolute values for all measurements. To assess the effect of the training protocol on functional outcome (10MWT, 6MWT, WISCI II, TUG and LEMS), the Friedman analysis of variance by ranks was used, with $P<0.05$. *Post-hoc* comparisons were performed using the Wilcoxon signed-rank test, with a Bonferroni correction to account for multiple comparisons ($P<0.017$). To assess retention of the functional level at follow-up, a Wilcoxon signed-rank test was performed to detect changes between post-training and follow-up with significance $P<0.05$. Spearman correlation coefficients were calculated to identify possible correlations between the initial performance on the walking ability tests and the absolute change in these measures ($P<0.05$). Measurements of walking quality (kinematic and spatiotemporal measures) were only assessed pre- and post-training. Changes in walking quality between pre- and post-training were determined with the Wilcoxon signed-rank test ($P<0.05$) All statistical tests were performed with SPSS Statistics (IBM Corp., Armonk, NY, USA).

3.3 Results

3.3.1 Participants

A total of 12 participants with iSCI were included. Participant characteristics are listed in table 1. Two participants dropped out (subjects 6 and 12). They did not complete the training due to medical reasons not related to the gait training.

3.3.2 Training parameters

Over the eight-week period, a mean number of 20.2 (range, 18-24) training sessions were completed by the 10 participants. Due to reasons unrelated to the gait training, some participants had to cancel some training sessions. The average time ambulated during a session increased from 14.5 minutes at the start of the training protocol to 22.7 minutes at the end. Gait speed increased from 0.43 to 0.58 m/s. BWS was only used in five participants, and decreased from 8.5 percent to 7.4 percent. The average impedance levels/support levels decreased from 56.9 percent to 37.4 percent. Individual changes in the training parameters over the course of the training period are shown in figure 4.

3.3.3 Primary outcome measures

Training period

The Friedman analysis showed a significant training effect in all walking ability and

Table 1: Descriptive information of participants.

Subject	Age	Gender	Motor level of injury*	ASIA class	Post-injury time (months)
1	37	F	Th9	C	14
2	50	M	Th4	D	22
3	29	F	L2	B **	36
4	60	F	Th1	C	16
5	48	F	L2/ Th12	D	122
*6****	61	M	C5	D	14
7	56	F	L1/ L2	C	14
8	31	M	C5	C	120
9	63	M	C3/ C2	C	16
10	46	F	C5	D	41
11	51	M	Th12	D	62
*12****	53	M	Th12	C	84
Mean	48,75 ± 11.3				46,75 ± 41.03

**Levels separated by a "/" indicate a difference in right and left level of injury. It is noted Right/Left.*
***Diagnosed with a cauda equine syndrome.*
****Dropout.*

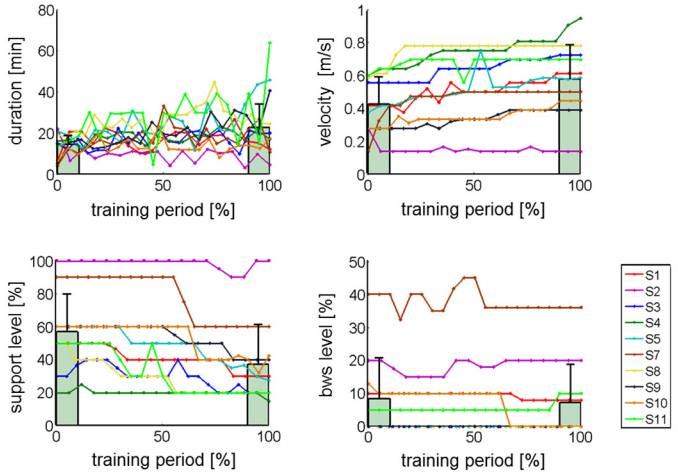

Figure 4: Training parameters as a function of the training duration. Training sessions are normalized to the total training time (0 percent start of training, 100 percent completion of training). Training duration refers to the actual total training time per session (excluding setup time and rest periods). Support levels are expressed as a percentage of the maximum stiffness that could be controlled by the LOPES (300 Nm/rad). BWS was only required in five of the 10 participants. The bars indicate the mean training parameters, averaged across participants, at the start of the training (0-10 percent) and at the end of the training period (90-100 percent). The error bars indicate the standard deviation.

Table 2: Statistical results of primary outcome measures.

	Improvement in % of subjects (pre-post)	Pre mean (median)	Post mean (median)	Main effect of time p	Post-hoc comparison			
					Pre-mid p	Mid-post p	Pre-post p	Post-follow up p
Walking speed (m/s)	90	0.61 (0.64)	0.67 (0.67)	$\chi^2(2)=8.7$ 0.013*	0.411	0.023	0.008*	0.797
Walking distance (m)	100	184.4 (184)	212.9 (216)	$\chi^2(2)=12.8$ 0.002*	0.022	0.012*	0.005*	0.507
TUG [1] (s)	100	19.5 (14.5)	16.1 (12.4)	$\chi^2(2)=10.8$ 0.005*	0.017*	0.208	0.012*	0.779
WISCI-II	30	13.5 (13)	14.4 (14.5)	$\chi^2(2)=6.5$ 0.039*	0.046	0.317	0.083	0.157
LEMS	90	34.4 (34.5)	37.8 (39)	$\chi^2(2)=6.9$ 0.032*	0.210	0.258	0.017*	0.365

[*] *Significant difference. The Friedman analysis of variance by ranks was used, with P<0.05. Post-hoc comparisons were performed using the Wilcoxon signed-rank test and a Bonferroni correction was used to account for multiple comparisons (P<0.017).*

[1] *The TUG was assessed in eight of 10 participants. Participants 7 and 9 were unable to stand up from the chair independently during the entire study.*

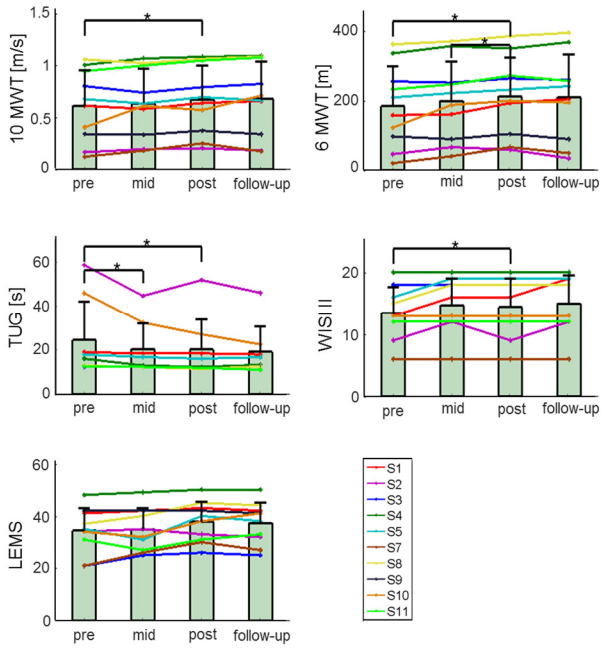

Figure 5: Primary outcomes. Measurements of walking ability were assessed pre-, mid-, and post-training and at follow-up. TUG could not be measured for subject 7 and 9. The bars indicate the mean clinical measures, averaged across participants, at each period. The error bars indicate the standard deviation.

strength scores (table 2). Subsequent post-hoc pairwise comparisons between the different evaluation periods showed that significant improvements were primarily found between pre- and post-training. The post-hoc test between pre- and post-training revealed that eight weeks of LOPES training resulted in significant improvements in walking speed (10MWT), distance (6MTW), TUG score, and LEMS (table 2). No significant difference was found for the WISCI II score between pre- and post-training. Figure 5 shows the individual changes in the primary-outcome measures at the different evaluation periods.

Follow-up

All participants retained the functional level reached at completion of their training. No significant differences were found between follow-up and post-training in any of the primary outcome measures (table 2).

Relationship between initial impairment levels and absolute increase

There were no significant correlations between the initial performance on walking ability tests and the absolute increase in test performance. Still, for walking speed and distance, for example, assuming an equal increase in absolute performance suggests that slower

Table 3: Statistical results of secondary outcome measures.

		Increase in % of subjects (pre-post)	Pre mean (median)	Post mean (median)	Pre-post *p*
Walking speed (m/s)		89	0.49 (0.57)	0.56 (0.64)	0.015*
Cycle time (s)		11	2.24 (1.79)	2.04 (1.58)	0.032*
Step symmetry index (%)		22	8.46 (6.92)	4.38 (3.28)	0.021*
Step width (m)		33	0.11 (0.11)	0.10 (0.11)	0.114
Step length (m)	Strong and weak	89	0.44 (0.44)	0.47 (0.44)	0.017*
	Strong	78	0.46 (0.46)	0.48 (0.47)	0.027*
	Weak	100	0.42 (0.42)	0.46 (0.44)	0.007*
Rel. stance phase duration (%)	Strong and weak	11	74.5 (70.6)	72.3 (68.8)	0.011*
	Strong	11	74.6 (71.2)	73.0 (69.6)	0.028*
	Weak	0	74.4 (70.6)	71.5 (68.4)	0.008*
Maximum knee flexion (swing) (deg)	Strong and weak	56	48.6 (49.1)	48.4 (48.9)	0.859
	Strong	56	49.3 (48.5)	50.7 (51.2)	0.314
	Weak	33	47.8 (52.2)	46.0 (47.9)	0.374
Knee ROM (initial and mid stance) (deg)	Strong and weak	67	22.5 (21.0)	23.5 (23.2)	0.441
	Strong	78	23.6 (26.8)	26.0 (22.8)	0.110
	Weak	67	21.5 (19.2)	21.8 (14.8)	0.953
Hip ROM (deg)	Strong and weak	100	36.7 (34.9)	38,8 (38.9)	0.008*
	Strong	67	37.0 (38.2)	39.0 (37.5)	0.051
	weak	89	36.4 (34.5)	38.7 (40.3)	0.011*

** Significant difference, Wilcoxon signed-rank test (P<0.05)*
Participant 7 was excluded for analysis of kinematic and spatiotemporal data because of the use of orthotic devices, limiting accurate 3D kinematic data collection.

ambulators experience the greatest relative improvement. Indeed, the relative improvement in 10 MWT (ρ =-0.68, *p*=0.04) and 6 MWT (ρ =-0.79, *p*=0.01) showed a significant negative correlation with the initial score on these tests. The initial score on the TUG, WISI-II and LEMS did not prove to be an indicator of the relative increase in the corresponding score.

3.3.4 Secondary outcome measures

Significant changes were observed in most spatiotemporal parameters (table 3). The maximum knee flexion during swing, the knee ROM during the stance phase, and the step width did not show significant changes. For the step length and hip ROM, the mean changes in the weak leg exceeded the changes observed in the strong leg.

3.4 Discussion

The aim of the present study was to examine the effects of an eight-week training program on the walking ability and quality in iSCI individuals, using an impedance-control

strategy. In this study, we used a prototype of the LOPES gait trainer. The training protocol was tolerated well by all 10 participants and was performed without difficulties for eight weeks. Participants improved significantly on functional outcomes, muscle strength, kinematics, and spatiotemporal measures after eight weeks of LOPES training. Subsequent follow-up evaluations revealed that participants retained their training-induced functional improvements. The main improvement in kinematics occurred at the hip. The range of motion of the hip joint increased, whereas the different measures for the knee joint were unaffected by the training protocol. Participants with the most limited initial walking function showed the largest relative improvements.

3.4.1 Functional outcomes

Our main findings were a significant functional improvement and an increased muscle strength. Comparing our results with those of others is hampered because of differences in robotic devices, protocols, patient characteristics, outcome measures, and the number of individuals. Furthermore, most robotic gait-training devices are rapidly evolving with increasing functionalities, making robotic gait-training strategies hard to categorize.

We found significant changes in 10MWT, 6MWT, and TUG performance that were relatively small compared to other studies (table 4). A likely explanation for this difference is the included participants. Both Alcobendas et al. [24] and Benito-Penalva et al. [19] included acute iSCI individuals. Benito-Penalva et al., [19] who included a very wide range of participants, showed that the greatest rate of improvement was seen when training started early in rehabilitation, defined as less than six months post-injury. It is very likely that the improvements in these participants are partly due to underlying spontaneous recovery [58], rather than therapy effects. These findings agree with other pilot studies, showing that individuals with the smallest time since onset of injury show the largest improvements in over-ground walking ability [14,17,21]. Additionally, most studies that include sub-acute iSCI individuals also allow their participants to receive additional gait-related therapies [19,20,24], whereas these therapies for chronic individuals have stopped, effectively increasing the intensity of the training protocol.

Table 4: Overview of studies using robotic gait training in patients with spinal cord injury. Part 1

	Participants Time since onset Device	ASIA C/D (%)	Training parameters (average number of sessions)	10 MWT speed (m/s) (pre - post)
Wirz et al. [18]	N= 20 (4) Chronic Average: 70.8 months Lokomat	45/55	8 weeks; 45 min; 3-5 x/wk; (26 sessions)	0.38 - 0.49*
Field-Fote et al. [22]	N = 14 Chronic ≥ 12 month Lokomat	C and D	12 weeks; 45 min; 5 x/wk; (49 sessions)	0.17 - 0.18
Alcobendas-Maestro	N = 37 (23)	68/32	8 weeks; 30 min; 5 x/wk;	*0.3 - 0.4*[5]

et al. [24]	Sub-acute Average: 4 months Lokomat		(40 sessions) [3]	
Benito-Penalva et al. [19]	N = 105 Sub-acute <6 month N=81 6-12 month N=8 >12 month N=16 Lokomat (N=39) GT (N=66)	42/48 (10% A or B)	8 weeks; 45 min; 5 x/wk; (40 sessions) [3]	0.08 - 0.26*
Van Nunen et al. [20]	N=18 (9) Sub-acute and chronic <12 month N=7 >12 month N=11 Median: 28.8 months Lokomat	44/39 (17% B)	12 weeks; 60 min; 2 x/wk; (24 sessions) (20-45 min) [2,4]	*0.09-0.15**
Fleerkotte et al.	N = 10 Chronic Average: 45.3 months LOPES	50/40 (10% B)	8 weeks; 60 min; 3 x/wk; (20 sessions) (19 min) [2]	0.61 - 0.67*

Table 4: Part 2

	6MWT Distance (mtr) (pre - post)	TUG (sec) (pre - post)	WISCI II (pre - post)	LEMS (pre - post)
Wirz et al. [18]	121 - 165*	61 - 36*	No significant increase	32 - 35* (N=10)
Field-Fote et al. [22]	50.4 - 53.7[1]	-	-	Left leg 12.7 - 13.9 Right leg 12.9 - 14.1*
Alcobendas-Maestro et al. [24]	*110 -169*[5]	-	*4 - 16*[5]	*33 - 40*[5]
Benito-Penalva et al. 2012 [19]	-	-	4.0-9.2*	22.1-30.6*
Van Nunen et al. [20]	-	No significant increase (N=6)	No significant increase	-
Fleerkotte et al.	184.4 - 212.9*	24.4 - 20.2*	13.5 - 14.4	34.4 - 37.8*

** Indicates a significant change.*
N indicates the number of participants, (..) the number of individuals initially unable to walk over the full 10 m walkway.
Median, mean.
[1] *Actually performed a 2MWT, here linearly extrapolated to six minutes.*
[2] *Average/range of the pure training time (excluding setup time and rest periods).*
[3] *Also received standard daily therapy (except for over-ground gait training).*
[4] *Also received other gait related therapies (including over-ground gait training).*
[5] *Not tested for significant differences between pre and post, only for significant differences in gains obtained with Lokomat or conventional therapy.*

From the studies including chronic iSCI individuals, Nunen et al. [20] reported similar improvements in walking speed. Wirz et al. [18], who also included only chronic iSCI survivors, observed larger improvements in walking speeds. Possible explanations for their higher gains are a greater number of training sessions (26 vs. 20) , longer session durations (45 vs. 19 min), and lower initial walking speeds (0.38 vs. 0.61 m/s). A lower initial walking speed possibly allows more room for improvement. Although not discussed by Nunen et al., [20] their results indicate that participants with initial walking speeds around 0.4 m/s show the largest improvements in walking speeds. Therefore, it seems reasonable to assume that the greater effect sizes found by Wirz et al., [18] can be explained by the initial functional level of their participants [18]. Field-Fote et al. [22], who trained chronic iSCI individuals with very low initial walking speeds, did not find any significant effects of robotic gait training on walking speed. Apparently, iSCI individuals must have a certain level of initial walking speed/function to benefit from robotic gait training. Their subjects also have lower initial LEMS scores.

Although the Friedman analysis showed a significant training effect on the WISCI II score, there was no significant improvement in WISCI II scores between pre-and post-training. This is in line with other studies, taking into account the types of participants. It is known that the WISCI II is more sensitive in monitoring recovery of walking capacity in iSCI subjects during the acute stage of recovery rather than the chronic stage [59]. Similar to Wirz et al. [18], Nunen et al. [20] and others [14,17,21], we did not find an increase in WISCI II score in chronic individuals, whereas Alcobendas et al. [24] and Benito-Penalva et al. [19] reported significant increases in acute patients. Improvement in LEMS scores are similar to the results found in other studies among chronic iSCI individuals [18].

3.4.2 Retention

Follow-up measurements revealed that participants in our study retained the level of functional improvement measured at the end of the training period. Studies on robotic gait training in iSCI individuals rarely include a follow-up. Field-Fote et al. [22] did perform a follow-up among 10 individuals whose improvements exceeded 0.05 m/s to assess their retention of relearned gait abilities. They concluded that walking speeds declined between the conclusion of the training and follow-up, but remained above pre-training levels. However, their follow-up group included only two chronic iSCI participants who received robotic gait training, hampering a fair comparison.

It is important to note the timing of follow-up, which was, on average, 20.3 months in their study and only eight weeks in ours. Although Field-Fote et al. [22] did not find a correlation between time since the conclusion of training and the decline in walking speed, it seems likely that participants lose some of their relearned walking abilities over time, especially if they do not exploit their relearned walking abilities in daily life [60,61].

In future studies that assess the efficacy of different rehabilitation strategies, it is important to include follow-up testing. For example, in stroke survivors, it has been shown that at six months, a specific intervention seemed superior, whereas at one year, all

participants reached the same levels of functional walking [62]. This emphasizes the importance of long-term follow-up measurements to prevent incorrect conclusions.

3.4.3 Spatiotemporal and kinematic measures

To our knowledge, this is the first study reporting significant changes in spatiotemporal and kinematic measures associated with increased walking ability due to robotic gait training. We found significant changes in most spatiotemporal and kinematic measures after robotic gait training. Previous studies showed small increases in cadence, step and stride length, and step-length symmetry [23] or sagittal plane excursions [25], but these were not significant. In this study, most of these measures were significantly higher after training. It is important to note that Nooijen et al. [23] and Hornby et al. [25] used the LOKOMAT without the option to decrease guidance forces, as this option was unavailable on the device at the time of their study. Although both studies encouraged participants to "walk with the machine," they both state that constant guidance may minimize the voluntary effort during training and subsequently limit improvements in gait function.

In this study, improvements in spatiotemporal and kinematic measures were greater in the weaker leg. For the step length and hip ROM, the improvements were larger for the weaker leg, which resulted in significant increases in symmetry between the two legs. This may indicate that gait training restores walking function by restoration of function using more normal movement patterns, rather than compensation.

Improvements in walking speed were caused by improvements in step length as well as cadence. The increased walking speed might explain some of the observed changes in other spatiotemporal measures. Here, the increase in walking speed probably explains the decrease in stance phase duration [63] and the decrease in step width [64]. Also, whether the increased hip flexion is enabled by an increased hip flexion strength (mean increase in LEMS score of 3,4), or is simply a consequence of the increased walking speed [65] cannot be answered.

3.4.4 Intensity

Most current rehabilitation strategies focus on recovery through intense practice of a specific task. In BWSTT training, intensity depends on a combination of duration (time or number of steps), speed, training frequency, and the amount of BWS. In this study training intensity was maximized by increasing training speed and duration, and lowering the BWS levels when possible. With the development of robotic gait trainers that can potentially support the whole movement, the amount of robotic support is also an important parameter that affects training intensity. Often the precise setting of these parameters is based on a therapist's clinical judgment and not on experimental evidence [22]. For some parameters, the effects on training outcome are known, but for many they are not. Furthermore, the interaction among the different parameters is not being investigated. For example, reducing the amount of BWS and training at higher treadmill speeds increases efferent input. This is known to affect the neural control of stepping and is

suggested to promote functional recovery [66, 11]. Still, the interactive effect of BWS and walking speed in individuals following SCI is unknown. Also the tradeoff between training duration and frequency remains unknown.

For robotic gait training, the optimal amount of support also remains unclear, although reducing the amount of support according to the AAN principle seems most suitable. Here, one might follow the concepts provided in the "Challenge-Point Framework" [67]. This framework states that, for each skill level, there exists an optimal level of task difficulty. When skill levels increase, further learning will be best facilitated by increasing task difficulty. In this study, task difficulty was increased by lowering theimpedance levels.

To gain a better understanding of the combined effect of training duration, speed, frequency, the amount of BWS and robotic support levels, these intensity parameters should be carefully reported in future studies [68]. For example, average walking speed and BWS levels in the robotic device are rarely reported in robotic gait-training studies. Additionally, often only the total session duration is reported, which does not represent the actual training time (excluding setup time and rest periods). With the increasing interest in robotic gait-training devices that have (adaptive) impedance levels, it is also advised to also report impedance levels of the robot.

The importance of properly quantifying and reporting and intensity is also pointed out in a reported discussion between Hornby and Reinkensmeyer [69]. Hornby suggests that improvements seen in many clinical studies involving robot-assisted, manual-assisted, and even over-ground therapy strategies may, in fact, be largely attributed to the relatively high levels of training intensity of these forms of therapy, which are not typically provided in more traditional forms of therapy.

Among the different robotic gait-training studies, there is a great diversity in training frequency, ranging between three to five sessions per week, and duration, ranging from 30-45 minutes per session (table 4). These parameters are often based on financial and practical reasons [20]. In this study, training frequency fell within this range but the mean training duration (19 minutes) was considerably lower. The relatively low training duration is thought to be the result of the use of the impedance control. By lowering the impedance levels when possible, the active contribution required from participants was relatively high. As a result, some participants, especially the slowest walkers, could not train for the same duration as seen in other position-controlled gait-training studies. Still, we showed that similar gains in walking ability can be accomplished with less training time. Actually, the biggest gains in walking ability were observed in slow walkers with the lowest training duration, suggesting that active participation is equally important as training duration.

3.4.5 Clinical relevance

In this study, 90 percent of participants increased their walking speed on the 10MWT, 100 percent increased their distance on the 6MWT, and 100 percent reduced their TUG.

Although this resulted in an average significant change of 0.6 m/s, 29 m and 3.4 s (figure 5), it should be noted that there was considerable variation among subjects. Also, whether these improvements represent a detectable (and clinically relevant) change is debatable. The minimally detectable change (MDC), which defines the minimal amount of change required to distinguish (with 95 percent confidence) a "true" performance change from a change due to variability in performance or measurement error, is reported to be around 0.13 m/s, 45.8 m, and 10.8 s [70]. Criteria for what clinicians define as "clinically relevant" or "meaningful" can be even higher. Although MDC criteria for detecting "true" improvements are conservative, according to them, only one participant showed a "true" improvement on the 10MWT, 6MWT and TUG tests. Still, small gains in functional improvement that can lead to reduced reliance on assistive devices could be of great personal relevance to these individuals [71].

Additionally, walking function may not be the only appropriate outcome measure for iSCI individuals. Hicks et al. [72] suggest that whole-body upright exercise has additional physiological and psychological benefits beyond improvements in functional ambulation, especially for wheelchair-dependent individuals. It may decrease the risk of secondary health complications, such as cardiovascular disease, diabetes, or depression. Although we did not systematically assess these physiological and psychological benefits, some patients indicated they had reduced occurrence of urinary tract infections or mentioned that they experienced positive psychological effects from the training. Thus, to assess the full potential of robotic gait training and other forms of therapy, additional measures of functional performance should be used, rather than just walking ability and quality [73].

3.4.6 Limitations and future perspectives

The major limitation of this pretest-posttest study is the lack of a control group, or the use of a crossover design. The rationale for not including a control group was that this "stage 1 pilot study" was set up to assess the possible effect of impedance-controlled robotic gait training, how well it can be applied, the utility of the outcome measures chosen, and the variability in patient responses [68]. It was not intended to afford a basis on which to claim that this kind of training can produce greater functional improvements than those achieved through manually assisted gait training or other forms of conventional therapy. It only shows that chronic iSCI individuals still have the capacity to improve their walking function when provided with an intensive robotic gait-training program. Pretest-posttest study design are considered a useful step before setting up large scale RCTs [68].

This was the first explorative study using an impedance-controlled robotic gait trainer in a multi-session training protocol for chronic iSCI individuals. Improvements in functional outcomes and walking quality were similar to improvements found in position-controlled robotic gait-training devices. As mentioned before comparing different studies is difficult because of differences in robotic devices, protocols, patient characteristics, and outcome measures. Therefore, future studies should focus on direct comparisons between both control strategies to determine whether one method is clearly superior.

Patients and therapists will probably benefit the most from robotic gait-training devices during acute stages of recovery [19]. Still, in this study, all participants were chronic individuals. We included only chronic individuals (>12 months) because they typically have reached a stable level of recovery [58]. The average time since onset was 46 months, suggesting that observed improvements can be attributed to the intervention rather than spontaneous recovery. That the participants reached a stable level of recovery was also confirmed by a lack of correlation between the time since onset of the injury and the relative (or absolute) increases in walking speed. Thus, to investigate the true potential of impedance-controlled gait training, acute and sub-acute individuals should also be included in future studies. However, these trials will require larger patient numbers to reach significance due to the potential for underlying spontaneous recovery [58].

Apart from time since injury [19,20,58,71,74], previous studies also showed that ASIA levels [6,19,71,75], LEMS scores [25,75,76] (for recent injuries, for chronic results vary [18,20,22]), sensation [75,77], and age [6,75] are distinguishing factors for the degree of ambulatory capacity after gait rehabilitation. Several of these studies purely focus on increased walking speed, which is considered to be closely related to functional ambulation [78]. Patients who start rehabilitation programs early after injury, have higher ASIA/LEMS/sensory scores, or are younger generally show greater improvements. Factors like ethology, levels of injury, or sex seem to be less predictive [19,75]. Because of the relatively small number of participants in this study, we did not perform an analysis to relate clinical improvement to patient characteristics. Future studies should carefully document these characteristics, or stratify study participants, to determine which iSCI sub-population responds better to robotic gait training. These predictors might be different for robotic gait training where age or sensation, for instance, do not seem to have a clear effect on functional outcomes [19,74].

3.5 Conclusion

This first explorative study using an impedance-controlled robotic gait trainer shows significant improvements in functional and qualitative walking parameters after an eight-week training program in chronic iSCI individuals. The training program did not significantly reduce the amount of assistance/assistive devices during over-ground ambulation. We were able to provide task-specific and intensive training sessions, even for severely affected individuals, with a minimal workload on the therapist. Compared to position-controlled robotic gait-training strategies, the training duration was relatively short, whereas improvements in functional outcomes were similar. Additionally, improvements observed at the end of the training period persisted at the eight-week follow-up. The most impaired ambulators, based on their initial walking speed, benefitted most from the training protocol, showing the greatest relative improvements in walking speed and distance.

Acknowledgments

This study was supported by a grant from the Dutch Ministry of Economic affairs and Province of Overijssel, the Netherlands (grant: PID082004). We would like to thank Martijn Postma, Bram van Gemeren, and Leontien Zonnevijlle, from Het Roessingh, Centre for Rehabilitation, for their assistance during the experiments and their experience in treadmill training.

References

[1] P. R. van Asbeck FW, Post MW, "An epidemiological description of spinal cord injuries in The Netherlands in 1994," *Spinal Cord*, vol. 38, no. 7, pp. 420-4, 2000.

[2] S. Warren, M. Moore, and M. S. Johnson, "Traumatic head and spinal cord injuries in Alaska (1991-1993).," *Alaska Med.*, vol. 37, no. 1, pp. 11-19, 1995.

[3] M. Wyndaele and J.-J. Wyndaele, "Incidence, prevalence and epidemiology of spinal cord injury: what learns a worldwide literature survey?," *Spinal Cord*, vol. 44, no. 9, pp. 523-529, 2006.

[4] K. D. Anderson, "Targeting recovery: priorities of the spinal cord-injured population.," *J. Neurotrauma*, vol. 21, no. 10, pp. 1371-1383, 2004.

[5] P. L. Ditunno, M. Patrick, M. Stineman, and J. F. Ditunno, "Who wants to walk? Preferences for recovery after SCI: a longitudinal and cross-sectional study.," *Spinal Cord,* vol. 47, no. 3, pp. 500-506, 2008.

[6] S. P. Burns, D. G. Golding, W. A. Rolle, V. Graziani, and J. F. Ditunno, "Recovery of ambulation in motor-incomplete tetraplegia.," *Arch. Phys. Med. Rehabil.*, vol. 78, no. 11, pp. 1169-1172, 1997.

[7] A. L. Behrman, M. G. Bowden, and P. M. Nair, "Neuroplasticity after spinal cord injury and training: an emerging paradigm shift in rehabilitation and walking recovery.," *Phys. Ther.*, vol. 86, no. 10, pp. 1406-1425, 2006.

[8] E. T. Harness, N. Yozbatiran, and S. C. Cramer, "Effects of intense exercise in chronic spinal cord injury.," *Spinal Cord*, vol 46, no. 11, pp. 733-737, 2008.

[9] H. J. a van Hedel and V. Dietz, "Rehabilitation of locomotion after spinal cord injury.," *Restor. Neurol. Neurosci.*, vol. 28, no. 1, pp. 123-34, 2010.

[10] M. Hubli and V. Dietz, "The physiological basis of neurorehabilitation - locomotor training after spinal cord injury.," *J. Neuroeng. Rehabil.*, vol. 10, no. 1, pp. 2-8, 2013.

[11] V. Dietz, R. Muller, and G. Colombo, "Locomotor activity in spinal man: significance of afferent input from joint and load receptors," *Brain*, vol. 125, no. Pt 12, pp. 2626-2634, 2002.

[12] V. R. Edgerton, R. D. Leon, S. J. Harkema, J. a Hodgson, N. London, D. J. Reinkensmeyer, R. R. Roy, R. J. Talmadge, N. J. Tillakaratne, W. Timoszyk, and a Tobin, "Retraining the injured spinal cord.," *J. Physiol.*, vol. 533, no. Pt 1, pp. 15-22, 2001.

[13] H. Barbeau, S. Nadeau, and C. Garneau, "Physical Determinants, Emerging Concepts, and Training Approaches in Gait of Individuals with Spinal Cord Injury," vol. 23, no. 3, pp. 571-585, 2006.

[14] P. Winchester, R. McColl, R. Querry, N. Foreman, J. Mosby, K. Tansey, and J. Williamson, "Changes in supraspinal activation patterns following robotic locomotor therapy in motor-incomplete spinal cord injury.," Neurorehabil Neural Repair,vol 19, no. 4, pp. 313-24, 2005

[15] S. Freivogel, D. Schmalohr, and J. Mehrholz, "Improved walking ability and reduced therapeutic stress with an electromechanical gait device.," *J. Rehabil. Med. Off. J. UEMS Eur. Board Phys. Rehabil. Med.*, vol. 41, no. 9, pp. 734-739, 2009.

[16] J. A. Galvez, A. Budovitch, S. J. Harkema, and D. J. Reinkensmeyer, "Trainer variability during step training after spinal cord injury: Implications for robotic gait-training device design.," *J. Rehabil. Res. Dev.*, vol. 48, no. 2, pp. 147-160, 2011.

[17] T. G. Hornby, D. H. Zemon, and D. Campbell, "Robotic-assisted, body-weight-supported treadmill training in individuals following motor incomplete spinal cord injury.," *Phys. Ther.*, vol. 85, no. 1, pp. 52-66, 2005.

[18] M. Wirz, D. H. Zemon, R. Rupp, A. Scheel, G. Colombo, V. Dietz, and T. G. Hornby, "Effectiveness of automated locomotor training in patients with chronic incomplete spinal

cord injury: A multicenter trial," *Arch. Phys. Med. Rehabil.*, vol. 86, no. 4, pp. 672-680, 2005.

[19] J. Benito-Penalva, D. J. Edwards, E. Opisso, M. Cortes, R. Lopez-Blazquez, N. Murillo, U. Costa, J. M. Tormos, J. Vidal-Samsó, J. Valls-Solé, and J. Medina, "Gait training in human spinal cord injury using electromechanical systems: effect of device type and patient characteristics.," *Arch. Phys. Med. Rehabil.*, vol. 93, no. 3, pp. 404-12, 2012.

[20] M. van Nunen, K. H. L. Gerrits, M. Konijnenbelt, T. W. J. Janssen, and A. de Haan, "Recovery of walking ability using a robotic device in subacute stroke patients: a randomized controlled study," *Disabil Rehabil Assist Technol.*, pp. 1-8, 2014.

[21] S. Hesse, C. Werner, and a Bardeleben, "Electromechanical gait training with functional electrical stimulation: case studies in spinal cord injury.," *Spinal Cord*, vol. 42, no. 6, pp. 346-52, 2004.

[22] E. C. Field-Fote and K. E. Roach, "Influence of a locomotor training approach on walking speed and distance in people with chronic spinal cord injury: a randomized clinical trial.," *Phys. Ther.*, vol. 91, no. 1, pp. 48-60, 2011.

[23] C. F. Nooijen, N. Ter Hoeve, and E. C. Field-Fote, "Gait quality is improved by locomotor training in individuals with SCI regardless of training approach," *J. Neuroeng. Rehabil.*, vol. 6, no. 6, pp. 1-11, 2009.

[24] M. Alcobendas-Maestro, A. Esclarín-Ruz, R. M. Casado-López, A. Muñoz-González, G. Pérez-Mateos, E. González-Valdizán, and J. L. R. Martín, "Lokomat robotic-assisted versus overground training within 3 to 6 months of incomplete spinal cord lesion: randomized controlled trial.," *Neurorehabil. Neural Repair*, vol. 26, no. 9, pp. 1058-63, 2012.

[25] T. G. Hornby, D. D. Campbell, D. H. Zemon, and J. H. Kahn, "Clinical and quantitative evaluation of robotic-assisted treadmill walking to retrain ambulation after spinal cord injury," *Top Spinal Cord Inj Rehabil*, vol. 11, pp. 1-17, 2005.

[26] I. Schwartz, A. Sajina, M. Neeb, I. Fisher, M. Katz-Luerer, and Z. Meiner, "Locomotor training using a robotic device in patients with subacute spinal cord injury," *Spinal Cord*, vol. 49, no. 10, pp. 1062-1067, 2011.

[27] C. Tefertiller, B. Pharo, N. Evans, and P. Winchester, "Efficacy of rehabilitation robotics for walking training in neurological disorders: A review," *J. Rehabil. Res. Dev.*, vol. 48, no. 4, pp. 387-416, 2011.

[28] J. Mehrholz, J. Kugler, and M. Pohl, "Locomotor training for walking after spinal cord injury.," *Spine (Phila. Pa. 1976).*, vol. 33, no. 21, pp. E768-E777, 2008.

[29] E. Swinnen, S. Duerinck, J.-P. Baeyens, R. Meeusen, and E. Kerckhofs, "Effectiveness of robot-assisted gait training in persons with spinal cord injury: a systematic review.," *J. Rehabil. Med. Off. J. UEMS Eur. Board Phys. Rehabil. Med.*, vol. 42, no. 6, pp. 520-526, 2010.

[30] D. J. Reinkensmeyer, O. M. Akoner, D. P. Ferris, and K. E. Gordon, "Slacking by the human motor system: Computational models and implications for robotic orthoses", in *Proceedings of the IEEE International Conference of the Eng Med Biol Soc,* pp. 2129-32, 2009

[31] J. L. Emken, R. Benitez, A. Sideris, J. E. Bobrow, and D. J. Reinkensmeyer, "Motor Adaptation as a Greedy Optimization of Error and Effort," *J Neurophysiol*, vol. 97, no. 6, pp. 3997-4006, 2007.

[32] J. F. Israel, D. D. Campbell, J. H. Kahn, and T. G. Hornby, "Metabolic costs and muscle activity patterns during robotic- and therapist-assisted treadmill walking in individuals with incomplete spinal cord injury," *Phys Ther*, vol. 86, no. 11, pp. 1466-1478, 2006.

[33] M. Lotze, C. Braun, N. Birbaumer, S. Anders, and L. G. Cohen, "Motor learning elicited by voluntary drive," *Brain*, vol. 126, no. Pt 4, pp. 866-872, 2003.

[34] A. Kaelin-Lang, A. R. Luft, L. Sawaki, A. H. Burstein, Y. H. Sohn, and L. G. Cohen, "Modulation of human corticomotor excitability by somatosensory input," *J Physiol*, vol. 540, no. Pt 2, pp. 623-633, 2002.

[35] J. M. Hidler and A. E. Wall, "Alterations in muscle activation patterns during robotic-assisted walking. *Clin Biomech (Bristol, Avon)*. vol. 20, no. 2, pp. 184-93, 2005.

[36] J. Hidler, W. Wisman, and N. Neckel, "Kinematic trajectories while walking within the Lokomat robotic," *Clinical biomechanics*, vol. 23, no. 10, pp. 1251-1259, 2008.

[37] J. L. Emken and D. J. Reinkensmeyer, "Robot-enhanced motor learning: accelerating internal model formation during locomotion by transient dynamic amplification," *IEEE Trans Neural Syst Rehabil Eng*, vol. 13, no. 1, pp. 33-39, 2005.

[38] R. A. Scheidt, J. B. Dingwell, and F. A. Mussa-Ivaldi, "Learning to move amid uncertainty.," *J. Neurophysiol.*, vol. 86, no. 2, pp. 971-985, 2001.

[39] S. K. Banala, S. H. Kim, S. K. Agrawal, and J. P. Scholz, "Robot Assisted Gait Training With Active Leg Exoskeleton (ALEX)," *IEEE Trans Neural Syst Rehabil Eng*, vol. 17, no. 1, pp. 1-8, 2009

[40] A. Duschau-Wicke, A. Caprez, and R. Riener, "Patient-cooperative control increases active participation of individuals with SCI during robot-aided gait training," *J. Neuroeng. Rehabil.*, vol. 7, no. 43, pp. 1-13, 2010.

[41] J. L. Emken, S. J. Harkema, J. A. Beres-Jones, C. K. Ferreira, and D. J. Reinkensmeyer, "Feasibility of manual teach-and-replay and continuous impedance shaping for robotic locomotor training following spinal cord injury," *IEEE Trans Biomed Eng*, vol. 55, no. 1, pp. 322-334, 2008.

[42] B. Koopman, E. H. van Asseldonk, and H. van der Kooij, "Selective control of gait subtasks in robotic gait training: foot clearance support in stroke survivors with a powered exoskeleton.," *J. Neuroeng. Rehabil.*, vol. 10, no. 1, pp. 1-21, 2013.

[43] D. Aoyagi, W. E. Ichinose, S. J. Harkema, D. J. Reinkensmeyer, and J. E. Bobrow, "A robot and control algorithm that can synchronously assist in naturalistic motion during body-weight-supported gait training following neurologic injury," *IEEE Trans Neural Syst Rehabil Eng*, vol. 15, no. 3, pp. 387-400, 2007.

[44] J. L. Emken, J. E. Bobrow, and D. J. Reinkensmeyer, "Robotic movement training as an optimization problem: designing a controller that assists only as needed," in *Proceedings of IEEE International Conference on Rehabilitation Robotics*, 2005.

[45] R. Riener, L. Lunenburger, S. Jezernik, M. Anderschitz, G. Colombo, and V. Dietz, "Patient-cooperative strategies for robot-aided treadmill training: first experimental results," *IEEE Trans Neural Syst Rehabil Eng*, vol. 13, no. 3, pp. 380-394, 2005.

[46] A. Duschau-Wicke, J. Von Zitzewitz, A. Caprez, L. Lunenburger, and R. Riener, "Path control: a method for patient-cooperative robot-aided gait rehabilitation.," *IEEE Trans. Neural Rehabil. Syst. Eng.*, vol. 18, no. 1, pp. 38-48, 2010.

[47] S. Jezernik, G. Colombo, and M. Morani, "Automatic Gait-Pattern Adaptation Algorithms for Rehabilitation With a 4-DOF Robotic Orthosis," *IEEE Trans. Robot. Autom.*, vol. 20, no. 3, pp. 574-582, 2004.

[48] L. L. Cai, A. J. Fong, C. K. Otoshi, Y. Q. Liang, J. G. Cham, V. Zhong, R. R. Roy, V. R. Edgerton, and J. W. Burdick, "Effects of consistency vs . variability in robotically controlled training of stepping in adult spinal mice." in *Proceedings of the IEEE International Conference on Rehabilitation Robotics*, 2005

[49] L. L. Cai, A. J. Fong, C. K. Otoshi, Y. Liang, J. W. Burdick, R. R. Roy, and V. R. Edgerton, "Implications of assist-as-needed robotic step training after a complete spinal cord injury on intrinsic strategies of motor learning," *J Neurosci*, vol. 26, no. 41, pp. 10564-10568, 2006.

[50] M. D. Ziegler, H. Zhong, R. R. Roy, and V. R. Edgerton, "Why variability facilitates spinal learning.," *J. Neurosci.*, vol. 30, no. 32, pp. 10720-6, 2010.

[51] P. Sale, M. Franceschini, A. Waldner, and S. Hesse, "Use of the robot assisted gait therapy in rehabilitation of patients with stroke and spinal cord injury," *Eur. J. Phys. Rehabil. Med.*, vol. 48, no. 1, pp. 111-121, 2012.

[52] A. Schück, R. Labruyère, H. Vallery, R. Riener, and A. Duschau-Wicke, "Feasibility and effects of patient-cooperative robot-aided gait training applied in a 4-week pilot trial.," *J. Neuroeng. Rehabil.*, vol. 9, no. 1, pp. 1-14, 2012.

[53] J. F. Veneman, R. Kruidhof, E. E. G. Hekman, R. Ekkelenkamp, E. H. F. Van Asseldonk, and H. Van der Kooij, "Design and Evaluation of the LOPES Exoskeleton Robot for Interactive Gait Rehabilitation," *IEEE Trans Neural Syst Rehabil Eng*, vol. 15, no. 3, pp. 379-386, 2007.

[54] B. Koopman, E. H. van Asseldonk, and H. van der Kooij, "Speed-dependent reference joint trajectory generation for robotic gait support.," *J Biomech.*, vol. 47, no. 6, pp. 1447-58, 2014.

[55] H. J. Van Hedel, M. Wirz, and V. Dietz, "Assessing walking ability in subjects with spinal cord injury: validity and reliability of 3 walking tests.," *Arch. Phys. Med. Rehabil.*, vol. 86, no. 2, pp. 190-196, 2005.

[56] F. M. Maynard, M. B. Bracken, G. Creasey, J. F. Ditunno, W. H. Donovan, B. Ducker, S. L. Garber, R. J. Marino, S. L. Stover, C. H. Tator, R. L. Waters, and J. E. Wilberger, "International standards for neurological and functional classification of spinal cord injury," *Spinal Cord*, vol. 35, pp. 266-274, 1997.

[57] J. C. Dean, N. B. Alexander, and a D. Kuo, "The effect of lateral stabilization on walking in young and old adults.," *IEEE Trans. Biomed. Eng.*, vol. 54, no. 11, pp. 1919-26, 2007.

[58] J. W. Fawcett, a Curt, J. D. Steeves, W. P. Coleman, M. H. Tuszynski, D. Lammertse, P. F. Bartlett, a R. Blight, V. Dietz, J. Ditunno, B. H. Dobkin, L. a Havton, P. H. Ellaway, M. G. Fehlings, a Privat, R. Grossman, J. D. Guest, N. Kleitman, M. Nakamura, M. Gaviria, and D. Short, "Guidelines for the conduct of clinical trials for spinal cord injury as developed by the ICCP panel: spontaneous recovery after spinal cord injury and statistical power needed for therapeutic clinical trials.," *Spinal Cord*, vol. 45, no. 3, pp. 190-205, 2007.

[59] A. B. Jackson, C. T. Carnel, J. F. Ditunno, M. S. Read, M. L. Boninger, M. R. Schmeler, S. R. Williams, and W. H. Donovan, "Outcome measures for gait and ambulation in the spinal cord injury population.," *J. Spinal Cord Med.*, vol. 31, no. 5, pp. 487-499, 2008.

[60] M. Wirz, G. Colombo, and V. Dietz, "Long term effects of locomotor training in spinal humans.," *J. Neurol. Neurosurg. Psychiatry*, vol. 71, no. 1, pp. 93-6, 2001.

[61] A. L. Hicks, M. M. Adams, K. Martin Ginis, L. Giangregorio, a Latimer, S. M. Phillips, and N. McCartney, "Long-term body-weight-supported treadmill training and subsequent follow-up in persons with chronic SCI: effects on functional walking ability and measures of subjective well-being.," *Spinal Cord*, vol. 43, no. 5, pp. 291-8, 2005.

[62] P. W. Duncan, K. J. Sullivan, A. L. Behrman, S. P. Azen, S. S. Wu, S. E. Nadeau, B. H. Dobkin, D. K. Rose, J. K. Tilson, S. Cen, and S. K. Hayden, "Body-weight-supported treadmill rehabilitation after stroke.," *N. Engl. J. Med.*, vol. 364, no. 21, pp. 2026-36, 2011.

[63] G. Stoquart, C. Detrembleur, and T. Lejeune, "Effect of speed on kinematic, kinetic, electromyographic and energetic reference values during treadmill walking.," *Neurophysiol. Clin.*, vol. 38, no. 2, pp. 105-16, 2008.

[64] J. L. Helbostad and R. Moe-Nilssen, "The effect of gait speed on lateral balance control during walking in healthy elderly.," *Gait Posture*, vol. 18, no. 2, pp. 27-36, 2003.

[65] J. L. Lelas, G. J. Merriman, P. O. Riley, and D. C. Kerrigan, "Predicting peak kinematic and kinetic parameters from gait speed," *Gait Posture*, vol. 17, no. 2, pp. 106-112, 2003.

[66] S. J. Harkema, S. L. Hurley, U. K. Patel, P. S. Requejo, B. H. Dobkin, and V. R. Edgerton, "Human lumbosacral spinal cord interprets loading during stepping.," *J. Neurophysiol.*, vol. 77, no. 2, pp. 797-811, 1997.

[67] M. a Guadagnoli and T. D. Lee, "Challenge point: a framework for conceptualizing the effects of various practice conditions in motor learning.," *J. Mot. Behav.*, vol. 36, no. 2, pp. 212-24, Jun. 2004.

[68] B. H. Dobkin, "Progressive Staging of Pilot Studies to Improve Phase III Trials for Motor Interventions.," *Neurorehabil. Neural Repair*, vol. 23, no. 3, pp. 197-206, 2009.

[69] T. G. Hornby, D. J. Reinkensmeyer, and D. Chen, "Manually-assisted versus robotic-assisted body weight-supported treadmill training in spinal cord injury: what is the role of each?," *PM R*, vol. 2, no. 3, pp. 214-21, 2010.

[70] S. Perera, S. H. Mody, R. C. Woodman, and S. A. Studenski, "Meaningful change and responsiveness in common physical performance measures in older adults.," *J. Am. Geriatr. Soc.*, vol. 54, no. 5, pp. 743-749, 2006.

[71] S. J. Harkema, M. Schmidt-Read, D. J. Lorenz, V. R. Edgerton, and A. L. Behrman, "Balance and ambulation improvements in individuals with chronic incomplete spinal cord injury using locomotor training-based rehabilitation.," *Arch. Phys. Med. Rehabil.*, vol. 93, no. 9, pp. 1508-17, 2012.

[72] A. L. Hicks and K. A. M. Ginis, "Treadmill training after spinal cord injury: it's not just about the walking.," *J. Rehabil. Res. Dev.*, vol. 45, no. 2, pp. 241-248, 2008.

[73] M. S. Alexander, K. D. Anderson, F. Biering-Sorensen, A. R. Blight, R. Brannon, T. N. Bryce, G. Creasey, A. Catz, A. Curt, W. Donovan, J. Ditunno, P. Ellaway, N. B. Finnerup, D. E. Graves, B. A. Haynes, A. W. Heinemann, A. B. Jackson, M. V Johnston, C. Z. Kalpakjian, N. Kleitman, A. Krassioukov, K. Krogh, D. Lammertse, S. Magasi, M. J. Mulcahey, B. Schurch, A. Sherwood, J. D. Steeves, S. Stiens, D. S. Tulsky, H. J. A. Van Hedel, and G. Whiteneck, "Outcome measures in spinal cord injury: recent assessments and recommendations for future directions.," *Spinal cord Off. J. Int. Med. Soc. Paraplegia*, vol. 47, no. 8, pp. 582-591, 2009.

[74] P. Winchester, P. Smith, N. Foreman, J. M. Mosby, F. Pacheco, R. Querry, and K. Tansey, "A prediction model for determining over ground walking speed after locomotor training in persons with motor incomplete spinal cord injury," *J. Spinal Cord Med.*, vol. 32, no. 1, pp. 63-71, 2009.

[75] J. J. van Middendorp, A. J. F. Hosman, a R. T. Donders, M. H. Pouw, J. F. Ditunno, A. Curt, A. C. H. Geurts, and H. Van de Meent, "A clinical prediction rule for ambulation outcomes after traumatic spinal cord injury: a longitudinal cohort study.," *Lancet*, vol. 377, no. 9770, pp. 1004-10, 2011.

[76] J. F. Ditunno, H. Barbeau, B. H. Dobkin, R. Elashoff, S. Harkema, R. J. Marino, W. W. Hauck, D. Apple, D. M. Basso, A. Behrman, D. Deforge, L. Fugate, M. Saulino, M. Scott, and J. Chung, "Validity of the walking scale for spinal cord injury and other domains of function in a multicenter clinical trial.," *Neurorehabil. Neural Repair*, vol. 21, no. 6, pp. 539-550, 2007.

[77] C. V Oleson, A. S. Burns, J. F. Ditunno, F. H. Geisler, and W. P. Coleman, "Prognostic value of pinprick preservation in motor complete, sensory incomplete spinal cord injury.," *Arch. Phys. Med. Rehabil.*, vol. 86, no. 5, pp. 988-92, 2005.

[78] H. J. a van Hedel, "Gait speed in relation to categories of functional ambulation after spinal cord injury.," *Neurorehabil. Neural Repair*, vol. 23, no. 4, pp. 343-50, 2009.

Chapter 4

Selective control of gait subtasks in robotic gait training: foot clearance support in stroke survivors with a powered exoskeleton

Published as:
B. Koopman, E. H. F. van Asseldonk, H. van der Kooij, "Selective control of gait subtasks in robotic gait training: foot clearance support in stroke survivors with a powered exoskeleton", *J. Neuroeng. Rehabil.*, vol. 10, pp. 10-31, 2013.

Abstract

Robot-aided gait training is an emerging clinical tool for gait rehabilitation of neurological patients. This paper deals with a novel method of offering gait assistance, using an impedance controlled exoskeleton (LOPES). The provided assistance is based on a recent finding that, in the control of walking, different modules can be discerned that are associated with different subtasks. In this study, a Virtual Model Controller (VMC) for supporting one of these subtasks, namely the foot clearance, is presented and evaluated. The developed VMC provides virtual support at the ankle, to increase foot clearance. Therefore, we first developed a new method to derive reference trajectories of the ankle position. These trajectories consist of splines between key events, which are dependent on walking speed and body height. Subsequently, the VMC was evaluated in twelve healthy subjects and six chronic stroke survivors. The impedance levels, of the support, were altered between trials to investigate whether the controller allowed gradual and selective support. Additionally, an adaptive algorithm was tested, that automatically shaped the amount of support to the subjects' needs. Catch trials were introduced to determine whether the subjects tended to rely on the support. We also assessed the additional value of providing visual feedback. With the VMC, the step height could be selectively and gradually influenced. The adaptive algorithm clearly shaped the support level to the specific needs of every stroke survivor. The provided support did not result in reliance on the support for both groups. All healthy subjects and most patients were able to utilize the visual feedback to increase their active participation. The presented approach can provide selective control on one of the essential subtasks of walking. This module is the first in a set of modules to control all subtasks. This enables the therapist to focus the support on the subtasks that are impaired, and leave the other subtasks up to the patient, encouraging him to participate more actively in the training. Additionally, the speed-dependent reference patterns provide the therapist with the tools to easily adapt the treadmill speed to the capabilities and progress of the patient.

4.1 Introduction

Many patients with neurological injuries, like stroke or spinal cord injury (SCI), suffer from muscle weakness, loss of independent joint control, and spasticity, often resulting in gait disorders. To regain functional mobility, these patients require task-oriented, high-intensity, and repetitive training [1-3]. Robotic gait-training devices are increasingly being used to provide this kind of training. They can provide highly repetitive, more frequent, and intensive training sessions, while reducing the workload of the therapist, compared to more conventional forms of manual-assisted (and body-weight-supported) gait training. Additionally, the assessment of the progress of the patient becomes more objective with the integration of different sensory systems, which can record interaction forces and gait kinematics [4].

Despite the reduction in labor intensity, the therapeutic effect of the different types of gait trainers is inconsistent. Pohl et al. [5] and Mayr et al. [6] reported a significant improvement in gait ability in subacute stroke patients, compared to conventional physiotherapy. Other studies found no significant difference between robotic support and manual treadmill training [7,8], or conventional physiotherapy [9], although robotic gait training did show improvements in gait symmetry [7,9]. Some results even indicate that manual treadmill training is superior to robotic assistance [10]. Recently, a large multicenter randomized clinical trial suggested that the diversity of conventional gait training elicits greater improvements in functional recovery than robotic-assisted gait training [11]. These contradicting results emphasize that robot-aided training needs to be further optimized to increase therapeutic outcome.

One of the most important factors that promotes therapeutic outcome is active participation. Active patient participation has been proven to be beneficial for motor learning in general [12-14] and is suggested to be important for rehabilitation of gait disorders [15]. The “first- generation” devices, like the Lokomat (Hocoma AG, Switzerland) or AutoAmbulator (HealthSouth, USA), were initially developed based on the approach of enforcing gait upon a patient by moving the legs through a prescribed gait pattern. This diminishes the need for the patients to actively contribute to the required motion. Moving the legs in a rigid fashion is known to reduce [16] and affect [17] voluntary muscle activity compared to manual assistance, possibly making the patient reliant on the support. Rigid trajectory control also limits the natural gait variability and the possibility to make small movement errors. These small errors have been suggested to promote motor learning in mice [18] as well as humans [19,20].

To encourage active participation, and allow natural gait variability, more and more robotic devices control the interaction forces by using impedance or admittance control algorithms [21-29]. They guide the leg by applying a force rather than imposing a trajectory. Impedance (or admittance) control can also make the robot’s behavior more flexible and adaptive to the patient’s capabilities, progress, and current participation. Depending on the impedance levels, small errors are still possible, promoting motor

recovery. Patients might also increase their motivation, since additional effort by the patient is reflected in their gait pattern. Controllers based on this principle are referred to as “assist-as-needed” (AAN), “cooperative,” “adaptive,” or “interactive” controllers. In mice, these AAN algorithms have been shown to be more effective than position-controlled training [30].

Using impedance control instead of position control, however, introduces new challenges. First, low impedance levels increase the risk that the subject and robot start to walk out of phase. Consequently, the robot will resist, rather than support, the subject. Different algorithms have been proposed to avoid synchronization problems. To account for alterations in cadence, the reference pattern of the robotic controller can be accelerated or decelerated, based on the difference between the current gait phase of the subject and the state of the robot. This can be done continuously [21] or on a step-by-step basis [27].

Second, the impedance level needs to match the patient’s capabilities and progress, which can vary widely due to different levels of increased muscle tone, muscle weakness, or loss of coordinated control. This makes choosing the appropriate setting a priori a difficult process for the operator. In most applications, the amount of support is set by the operator on a trial-and-error basis. Setting the support levels too low can result in a dangerous situation, whereas too much assistance might reduce active participation of the patient. Roughly two strategies can be distinguished to automate the process of setting the support levels. The support levels can be adjusted based on increased patient effort (detected with force sensors) [24], or based on kinematic errors [27]. Emken et al. [27] developed an error-based controller with a forgetting factor. The algorithm systematically reduces the impedance levels when kinematic errors are small, whereas it increases the impedance when the errors are large. When the subject (unconsciously) reduces his effort, he will experience no support. Only when the subject fails to commit to the reference pattern for a longer duration of time, the support will be increased. This should prevent the patient from becoming reliant on the support. In parallel, it allows normal gait variability by lowering the impedance levels, when possible. Others use a deadband or a non-linear stiffness to allow normal variability, without causing the robot to increase its assistive forces [25,29].

Third, even when the impedance levels are adaptive, the whole movement is still potentially supported. This implies that the patient receives support during gait phases where his performance decreases, making no distinction between the patient’s incapability, reliance, or fatigue. This also limits the possibility to focus the therapy on specific aspects of the walking pattern that require special attention.

Fourth, despite that impedance control does not rigidly impose a fixed reference pattern, it still requires some sort of reference pattern to determine the supportive force. These patterns are mostly based on pre-recorded trajectories from unimpaired volunteers. The major limitation of these patterns is that they are not publically available. Additionally, most patterns are recorded at a limited number of speeds, while the progress of the patients’ preferred walking speed can be as small as 0.1 km/h.

In this paper, we extend the support strategy that we currently use in out gait trainer LOPES [31]. Within this strategy, patients are supported based on the execution of their gait subtasks, rather than their complete leg movement. Recent simulation and experimental studies [32,33] showed that the muscle activity during walking can be decomposed in different "modules." Each of these modules can be associated with a specific subtask of walking (e.g. body weight support, forward propulsion or foot clearance). In stroke survivors, each of these subtasks can be impaired to some degree without automatically affecting others. Selectively supporting these subtasks, based on the capabilities and progress of the patient, can be seen as an extension of the "assist-as-needed" principle. Also, the subtasks of both legs can be regarded separately, since in most stroke survivors the paretic leg will be more affected than the non-paretic leg. Controlling gait subtasks, rather than joint angles, also implies that compensatory strategies, like hip circumduction to create more foot clearance, can still be used. Imposing a symmetrical joint-angular reference pattern also limits the possibility of the non-paretic leg to compensate for the deficiencies of the paretic leg.

For the foot-clearance subtask, we developed a controller based on the Virtual Model Control framework [34]. This kind of control provides an elegant way to prevent synchronization problems by only controlling a specific subtask during the corresponding phase of the gait cycle. Using Virtual Models for different subtasks also allows straightforward adaptation of the support to the subject's specific needs by only turning on the controllers for impaired subtasks. A pilot study on a small number of healthy subjects already showed that this method allows selective control of foot clearance, while leaving the remaining walking pattern largely unaffected [31]. However, also within a specific subtask, the amount of support needs to match the specific needs of the patient. The support should be such that 1) large errors are prevented, 2) safe walking is guaranteed, 3) small errors and variation over steps are allowed and 4) reliance is minimized. In another pilot study we incorporated the adaptive algorithm, that shaped the impedance as a function of tracking performance, and that was introduced by Emken et al. [27]. With that pilot study we showed that the stiffness profile converged to a subject-specific pattern, that varied over the gait cycle and matched the subject's needs [35]. During the varies pilot experiments, we also experienced that visual feedback, based on basic gait parameters like foot clearance, is easier to interpret for patients and therapists than feedback in terms of joint angles or interaction torques.

The main contribution of this paper is to show the effectiveness of selective-subtask-support, in conjunction with adaptive support levels, in stroke survivors. Young healthy subjects will be used as a control group. Secondly, a new method to quantify reliance will be tested. Since reliance, or "slacking," is known to be present in upper-limb robotic support [36], and is considered to be an undesired effect, we try to investigate this phenomena using catch trials. Catch trials are often used in motor learning experiments to evaluate human behavior during prolonged exposure to external stimuli. To our knowledge, this type of methodology, to quantify reliance in lower-limb robotic gait training for stroke survivors, has not been used before. Because reliance is closely related

to the feedback that the patient receives, we also developed a system to provide the patient with visual feedback about his performance. Thirdly, we will investigate the use of compensatory strategies in the robotic gait trainer. Since LOPES [28] allows hip abduction, patients are allowed to employ their compensatory strategies in the device. This puts us in the unique position to evaluate whether patients reduce their compensatory strategies when they receive robotic support. Before testing the VMC framework, we will also present a new method, and results, of constructing reference trajectories for the ankle movement at different speeds. First, the pattern is parameterized by defining different key events (minima, maxima etc.), which are extracted from the individual patterns. Next, the walking speed and body-height dependency of the parameters are determined by regression models. These regression models can be used to reconstruct patient-specific ankle movement patterns at any speed.

4.2 Methods

4.2.1 Reference patterns

Subjects

Eleven healthy elderly subjects (five male, six female, age 57.3 ± 5.9, weight 74.9 kg ± 11.9, length 1.70 m ± 0.11) volunteered to participate in an experiment that was setup to collect the reference patterns that are required for VMC of the step height. All subjects had no symptoms of orthopedic or neurological disorders and gave informed consent before participating in the experiments.

Experimental protocol

Gait kinematics were recorded using an optical tracking system (Vicon Oxford Metrics, Oxford, UK) at a frequency of 120 Hz. To track the motion of the subject, twenty-one passive reflective markers were attached to bony landmarks on the legs and trunk. The subjects were asked to walk on a treadmill at seven different speeds: 0.5, 1, 1.5, 2, 3, 4 and 5 km/h. After a general familiarization period of three minutes, the subjects walked for three more minutes at each selected speed. During each trial, the subjects did not receive any specific instructions about how to walk on the treadmill. After each trial, the subject had a one-minute break.

Data analysis

Different steps were taken to derive the regression models.

Kinematics

Only the last minute of each trial was used for data analysis. The recorded marker positions were processed using custom-written MATLAB software [37]. Since the

proposed VMC approach is end-point based, we do not require the hip and knee angular reference patterns, but only the ankle pattern in Cartesian space.

Key events and predictor variables

The kinematic data was split up into individual strides of the right ankle, based on a phase-detection method developed by Zeni et al. [38], that used the local maxima in the anterior-posterior position of the heel marker. Each individual stride was parameterized by defining points that corresponded to key events in the gait cycle. For the vertical ankle position, from now on referred to as "ankle height," these key events included the ankle height at the heel-contact of the contralateral leg (start of the double stance), and a selection of extreme values in position and velocity data. Each key event was parameterized by an index, representing the percentage of the gait cycle at which the key event occurred, and its position and velocity. The median index, position and velocity of the key events were computed for each subject at each walking speed. Figure 1 shows the selected key events for the reference ankle-height pattern.

Predictor variables

The median index, position, and velocity of the key events were used to construct the regression models. These regression models require a set of predictor variables. We used the following regression formula:

$$Y = \beta_0 + \beta_1 v + \beta_2 v^2 + \beta_3 l \qquad [1]$$

where v represents the walking-speed and l body-height. Y represents the index, position or velocity of a particular key event. Stepwise regression [39] was used to test the statistical significance of the predictor variables, using entrance/exit tolerances of 0.05 on the p-values.

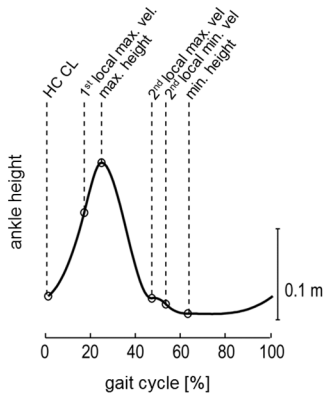

Figure 1: Selection of key events for the reference ankle-height pattern. The key events are a selection of extreme values in position and velocity. HC CL represents the key event that is located at heel contact of the contralateral leg.

Regression coefficients

After selecting the appropriate predictor variables for each regression model, robust regression [40] is used to retrieve the final set of regression coefficients (β_x). Robust regression is an iterative linear regression procedure that uses a tuning function to downweight observations with large residuals. Figure 2 shows an example of how the index, position, and velocity of one key event changes for different walking speeds. The relative position of the key event (the index) decreases at higher walking speeds, whereas the position and velocity of the key event increase. It also shows that these effects are nonlinear. Therefore, the regression models for the index, position, and velocity of this particular key event contain coefficients for the walking speed and walking speed squared. The stepwise regression showed that the body height has no significant contribution to the predictability of the index and position of the key event, whereas for the velocity of this key event it did contribute to the predictability. This indicates that some of the variability in the third figure could be attributed to differences in body height. The lists with the actual values for β_0, β_1, β_2 and β_3, can be found in the results section.

Spline fitting

Now that the regression models for the key events are known, a reference pattern can be reconstructed for each walking speed (in the range of 0.5-5.0 km/h). First, the index, position, and velocity of the key events, for a certain speed and body height, are calculated. Next, a cubic spline is fitted between every pair of consecutive key events, resulting in 6 (3rd order) polynomials describing the ankle-height pattern. By definition the position and velocity of the first key event (at 0 percent of the gait cycle) and the end of the last spline (at 100 percent) are equal. The resulting set of splines are merged to construct the reference pattern over the complete gait cycle.

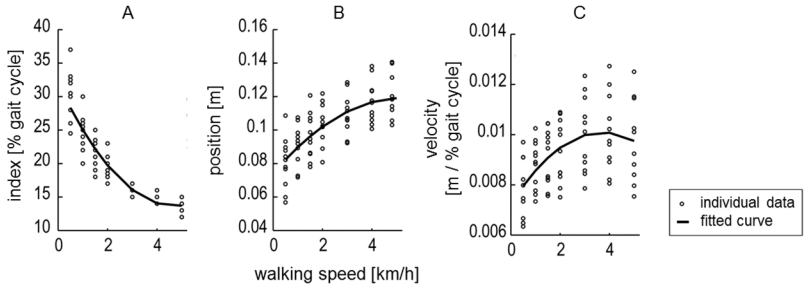

Figure 2: Relation between walking speed and the index, position, and velocity of a particular key event. The figure shows the index (A), position (B), and velocity (C) of the "1st local maximum velocity" key event at different walking speeds. Each circle represents the median value at a specified walking speed for one subject. The timing of the key event (the index) decreases at higher walking speeds, whereas the position and velocity of the key event increase. The solid line represents the fitted regression model. Stepwise regression showed that the velocity (C) of this key event is also dependent on the body height. Here the fitted regression model for the average body height (1,7 m) is shown.

Validation

To determine the accurateness of the spline-fitting procedure, we compared the constructed splines (based on data from the right ankle of all subjects) with the left ankle pattern of each subject. First, we reconstructed the reference patterns for the set of walking speeds (0.5-5 km/h) for each subject, taking into account the subject's individual body height. Next, their average left ankle pattern, during the last minute of walking at the different speeds, was calculated and the Root Mean Square Error (*RMSE*) between both signals was calculated. The resulting *RMSE* was averaged across subjects, for each speed.

Additionally, the correlation coefficient was used to quantify the similarity between the left ankle pattern and the reconstructed pattern. Both comparisons were performed for the ankle-height profile and the ankle-height velocity profile.

4.2.2 Selective support of subtasks

Subjects

Six elderly stroke survivors (five male, one female, age 57.8 ± 6.4, weight 88 kg ± 12.2, length 1.81 m ± 0.05) volunteered to participate in an experiment that was setup to validate the VMC for the step height. Table 1 lists the clinical description of the stroke survivors in more detail. As a control group, twelve healthy young subjects (six male, six female, age 25.8 ± 2.2, weight 70.3 kg ± 10.9, length 1.77 m ± 0.10) also volunteered to participate in the experiments. All healthy subjects had no symptoms of orthopedic or neurological disorders. Both groups gave informed consent before participating in the experiments.

Table 1. Clinical description of patient group.

	Age (years)	Gender	Weight (kg)	Length (m)	Time since stroke (month)	Type of stroke	Paretic side	FAC	DE	TBT	Proprio-ception (P/NP)	MI leg
A1	57	male	89.2	1.79	26	Infarction	left	4	1	4	8/8	14
A2	69	female	71.6	1.74	30	Haemorrhage	right	4	2	4	8/8	33
A3	50	male	96.4	1.89	5.5	Infarction	left	5	2	5	8/8	66
A4	59	male	105.5	1.78	72	Haemorrhage	left	4	1	3	7/8	42
A8	54	male	87.1	1.81	12	Infarction	right	4	3	3	8/8	33
A9	58	male	78.0	1.85	7	Infarction	left	5	3	5	8/8	83

FAC = Functional ambulation categories (max = 5).
DE = Duncan Ely test (min = 0, indicating normal tonus, max = 4, indicating rigidity).
TBT = Timed balance test (max = 5).
Proprioception = Outcome of lower extremity proprioception part of Nottingham sensory assessment, paretic (P) vs. non-paretic (NP) (max = 8).
MI leg = Motricity Index score, of the lower extremity (max = 99).

Figure 3: The LOPES robotic gait trainer.

Experimental apparatus and recordings

For the VMC experiments, the prototype of the gait rehabilitation robot LOPES was used (figure 3). The system is comprised of a bilateral exoskeleton-type rehabilitation robot above an instrumented treadmill. It is lightweight and actuated by Bowden-cable-driven series-elastic actuators [28]. The robot is impedance controlled, which implies that the actuators are used as torque sources [41]. The exoskeleton offers a freely translatable (3D) pelvis, where the sideways and forward/backward motion is actuated. Furthermore, it contains two actuated rotation axes in the hip joints and one at the knee (abduction/adduction of the hip and flexion/extension of hip and knee). A more detailed description of the exoskeleton design is provided in [28].

Linear and rotary potentiometers measured translations and angular rotations of all degrees of freedom. Kinematics were used to detect heel contact (HC) and toe-off (TO) events. HC and TO were used as triggers to switch the robotic support on and off, and used to segment the data into individual strides.

xPC Target was used for real-time control at 1000 Hz. From the measured exoskeleton joint angles, and the human segment lengths, the ankle position is calculated at each instant of time. Data is collected on the target computer in real-time and then transferred to a host machine, where it was sampled at 100 Hz and stored for off-line analysis, using custom software (MATLAB, Mathworks Inc., Natick, MA, USA). For all subjects we measured joint kinematics (angles and Cartesian positions), the torques applied by the LOPES, and the gait phases.

Virtual Model Control

Virtual Model Control was used to selectively support the step-height subtask. The basis of this control method is to define physical interactions with the patient that would assist the gait subtasks. These interactions are then translated into a set of Virtual physical Models (VMs), such as springs and dampers, that can be switched on and off at appropriate times in the gait cycle. The virtual forces, that would be exerted by the VMs, are translated into

joint torque commands for the joint actuators. Here we want to support the foot clearance. Therefore, we define a virtual spring (with stiffness K_z) between the actual ankle height and the reference ankle height (figure 4). If the actual ankle height (z) deviates from the reference ankle height (z_{ref}), a virtual force (F_z) is exerted at the ankle, which mimics a therapist lifting the ankle.

$$F_z = K_z(z_{ref} - z) \quad [2]$$

Initial testing showed that no damping was needed, since the human limbs provide a kind of natural damping to the system. The reconstruction of the reference ankle-height pattern is explained in next section.

The required vertical force is delivered by applying a combination of knee and hip joint torques to the human. The forces of the virtual spring are mapped to joint torques by:

$$\begin{pmatrix} \tau_h \\ \tau_k \end{pmatrix} = {}^{a}_{h}J^{T} \begin{pmatrix} F_x \\ F_z \end{pmatrix} \quad [3]$$

where τ represents the joint torques at the hip and knee, that offers the virtual force in Cartesian coordinates, and ${}^{a}_{h}J^{T}$ is the transpose of the Jacobian that maps the hip ($\dot{\theta_h}$) and knee ($\dot{\theta_k}$) angular velocities to the velocities of the ankle in Cartesian coordinates.

$${}^{a}_{h}J = \begin{bmatrix} L_u\, cos(\theta_h) + L_l\, cos(\theta_h - \theta_k) & -L_l\, cos(\theta_h - \theta_k) \\ L_u\, sin(\theta_h) + L_l\, sin(\theta_h - \theta_k) & -L_l\, sin(\theta_h - \theta_k) \end{bmatrix} \quad [4]$$

For foot-clearance support, only support in vertical direction is required, therefore F_x is zero. The symbols are defined in figure 4.

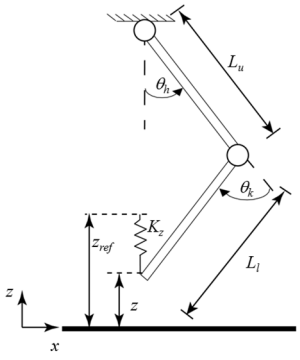

Figure 4: Schematic representation of the VMC approach. z represents the absolute ankle height and z_{ref} the reference ankle height. L_u and L_l represent the upper and lower leg length, and θ_h and θ_k the knee and hip angle. K_z indicates the virtual spring stiffness.

Reference pattern reconstruction

For the patient group, the reference pattern is reconstructed in the way described before, using the obtained regression models (see spline fitting). In order to investigate the effectiveness of the VMC approach for healthy subjects, we chose to increase the reference pattern, since the subjects were expected to already walk according to the pattern. The shape of the reference pattern is calculated similarly as in the patient group, but the obtained pattern was multiplied such that the maximal ankle height of the reference pattern reached a 15-percent increase with respect to their nominal maximum ankle height. The nominal ankle height of each subject was obtained from a walking trial in the LOPES where no support was provided.

Synchronization

To prevent synchronization problems a specific subtask is only supported during the phases in which the subtask should be performed. For the step-height support, this indicates that the controller is only active during the double stance (with the contralateral leg in front) and the swing phase. Heel contact and toe-off events were detected in real time based on a phase-detection method developed by Zeni et al. [38]. To account for alterations in cadence the speed at which the reference trajectory is replayed is scaled to the previous cycle time, and the timer is reset at the contralateral heel contact.

Impedance shaping

To adapt the level of support within the step-height subtask, we adopted the error-driven adaptation algorithm of Emken et al. [27]. The algorithm modifies the virtual spring stiffness, at each percentage of the gait cycle, based on the recorded error in the previous steps:

$$K_z^i(t) = f \cdot K_z^{i-1}(t) + g \cdot \left(z_{ref}(t) - z^{i-1}(t)\right) \quad [5]$$

where the superscript i denotes the i^{th} step cycle, f is a forgetting factor set to 0.9, g is an error-based gain set to 1800, K_z is the resulting stiffness profile for the ankle height, and t indicates the percentage of the gait cycle, which is estimated based on the previous cycle time. The stiffness was constrained to positive values, since the support is intended to lift the ankle, and not push the ankle downwards, when the ankle is above the reference.

4.2.3 Experimental protocol

Before positioning a subject in the LOPES, different anthropometric measurements were taken to adjust the exoskeleton segments lengths. Next, the subject was positioned into the LOPES and the trunk, thigh, and upper- and lower shank were strapped to the exoskeleton.

After a general familiarization period, the preferred walking speed was determined for each stroke survivor individually. During this familiarization period, the LOPES was operated in the zero-impedance mode. In this mode the impedance of every joint is set to zero, so the robot provides minimal resistance/assistance to the stroke survivor [42]. All patient trials were performed at the same predefined preferred walking speed. All healthy control subjects walked at 3 km/h.

Next, the stroke survivors, and healthy control subjects, were exposed to selective control of the step height with a compliant (600 N/m), stiff (1200 N/m) and adaptive virtual spring (see impedance shaping). The stiffest of these springs was chosen as having the maximum stiffness that was comfortable for subjects during pilot experiments. For the healthy control subjects all conditions were tested on the right leg only, while the left leg was operated in zero impedance. The stroke survivors were supported on their impaired side.

For the patient group, we intended to use visual feedback to maximally motivate the subjects in taking higher steps. To investigate if subjects are capable of translating the information from a simple visual feedback system into the appropriate action, the visual feedback system was first tested on the healthy control group. The visual feedback system consisted of a screen, showing bars that represented the maximum ankle height of their most recent step. Also, the target height was displayed. Preliminary results showed that healthy subjects were able to use this visual feedback to reach the target height very accurately. Therefore, it was decided to provide this kind of visual feedback to the patient group in almost all conditions.

All conditions were randomized to minimize the effects of fatigue or motor -learning effects. Table 2 lists the different conditions. To evaluate if the robot is influencing the steps without anticipation of the subject, we decided to use catch blocks, where the subject did not receive any support. 7 catch blocks were randomly interspersed among the first 115 steps of support. Each catch block consisted of three steps. Some patients could not walk for 115 consecutive steps because of the severity of their stroke. For these patients the last 10 steps of their trial are discarded, and only fully accomplished catch blocks and exposure blocks are included in the data analysis. To evaluate the effect of

Table 2: List of the tested conditions

	Stiffness (N/m)	Supported leg	Visual feedback	Abbreviation
Healthy controls	0	-	off	HZ
	600	right	off	HC
	1200	right	off	HS
	1200	right	on	HSV
	Adaptive	right	off	HA
Stroke survivors	0	-	on	PZV
	1200	paretic	on	PSV
	Adaptive	paretic	on	PAV
	Adaptive	paretic	off	PA

prolonged exposure, the trials in the healthy subjects were concluded with 50 steps of continuous exposure.

4.2.4 Data analysis

In general, the effectiveness of the step-height controller was assessed by determining how well the set reference values were attained, and how the support affected other aspects of walking. First, the data was segmented into separate steps based on the heel contact events [38]. Next, different spatiotemporal gait parameters were extracted from the ankle trajectories: the maximal ankle height (step height), the step length, and the cycle time. The maximum ankle height is the maximum vertical displacement of the ankle during swing. The step length is the relative horizontal displacement of one ankle with respect to the opposite ankle at the moment of heel contact. All gait parameters were normalized with respect to their nominal values. This allowed for comparison across subjects and conditions. For the healthy subjects, as well as the stroke survivors, the nominal values were recorded during a trial in which they walked in the zero impedance mode. Additionally, the relative duration of the different gait phases were calculated. All parameters were obtained for the exposure, as well as the catch blocks. Group averages were calculated for the stroke survivor and healthy control group.

To investigate the reduction of compensatory strategies, we also determined the maximum knee flexion, maximum hip abduction, and maximum pelvic height for the stroke survivors during the different conditions. Stroke survivors, with stiff-knee gait, for example, often fail to reach enough toe clearance and use different compensatory strategies to overcome their reduced knee flexion. Common strategies are a circumduction strategy, pelvic hiking, and vaulting. Vaulting is caused by an increase of the plantar flexion of the non-paretic leg, pushing the pelvis upward and creating more foot clearance on the paretic size. We hypothesize that, when stroke survivors experience step-height support, they reduce their compensatory strategies. Thus, assisting one subtask might automatically correct gait kinematics elsewhere.

4.2.5 Statistical analysis

To investigate the selectivity of the VMC support, we first used a one sample t-tests to determine whether the percentage change in the spatiotemporal parameters differed from 0 percent. If the step-height support significantly influenced one of the defined spatiotemporal parameters, we used a paired t-tests to assess whether there was a statistically significant difference between the conditions with the compliant and stiff virtual spring. For each patient an independent two-sample t-test was used to test whether there was a statistically significant difference in maximum hip abduction and maximum pelvic height between 10 steps of zero impedance walking and the last 10 steps of the last exposure block of the condition with the stiff controller. All statistical tests were performed with SPSS Statistics (IBM Corporation , Armonk, NY, USA). The level of significance was defined at 5 percent.

4.3 Results

4.3.1 Regression models for the reference patterns

The timing, position and velocity of the key events were highly dependent on the walking speed (figure 5). Generally, the different subjects showed the same dependencies. However, there was considerable variation between the subjects in the timing, position and velocity of the key events at a specific walking speed (figure 2). The stepwise regression, and subsequent robust regression, showed that most key events were linearly and/or quadratically dependent on speed (table 3). The body height did not influence the timing (index) of the key events. Of all positions it only influenced the "maximal height" key event and it influenced the velocity at three of the six key events. The Root Mean Square Error (*RMSE*), in the prediction of the timing of the key events, was <2 percent of the gait cycle (except for the timing of the "minimal height"). The *RMSE*, in the prediction of the position, was maximally 1.44 cm and was maximally 0.11 cm/%gait cycle for the velocity. Figure 5 also shows that the key events could be predicted well using the regressions equations.

Table 3: Regression equations and RMSE for the parameter values of the key-events.

	Key-event	β_0 (intercept)	β_1 (speed)	β_2 (speed^2)	β_3 (body-height)	*RMSE*
Index	HC CL	0	-	-	-	0
	1st local max vel.	32.0	−7.79	0.826	-	1.92
	max height	34.4	−5.27	0.579	-	1.70
	2nd local max vel.	47.3	−0.609	0.0725	-	1.09
	2nd local min vel.	52.4	-	-	-	1.26
	min height	88.2	−13.3	1.55	-	4.87
		β_0 (intercept)	β_1 (speed)	β_2 (speed^2)	β_3 (body-height)	*RMSE*
Position	HC CL	−0.387 x10^{-2}	0.768 x10^{-2}	-	-	0.572x10^{-2}
	1st local max vel.	7.41 x10^{-2}	1.73 x10^{-2}	−0.165 x10^{-2}	-	1.36 x10^{-2}
	max height	−2.63 x10^{-2}	3.57 x10^{-2}	−0.362 x10^{-2}	6.64 x10^{-2}	1.44 x10^{-2}
	2nd local max vel.	1.49 x10^{-2}	-	0.0221 x10^{-2}	-	0.345x10^{-2}
	2nd local min vel.	1.05 x10^{-2}	-	-	-	0.231x10^{-2}
	min height	0	-	-	-	0
		β_0 (intercept)	β_1 (speed)	β_2 (speed^2)	β_3 (body-height)	*RMSE*
Velocity	HC CL	2.79 x10^{-3}	0.732 x10^{-3}	-	−1.75 x10^{-3}	0.466 x10^{-3}
	1st local max vel.	−6.22 x10^{-3}	1.54 x10^{-3}	−0.207 x10^{-3}	7.95 x10^{-3}	1.08 x10^{-3}
	max height	0	-	-	-	0
	2nd local max vel.	−3.31 x10^{-3}	-	0.0307 x10^{-3}	2.35 x10^{-3}	0.970 x10^{-3}
	2nd local min vel.	−2.57 x10^{-3}	-	-	-	0.628 x10^{-3}
	min height	0	-	-	-	0

Speed is expressed in km/h and body height in m.
HC CL = Heel contact contralateral leg.
"–" indicates that that particular predictor variables does not contribute to the predictability of the key event.

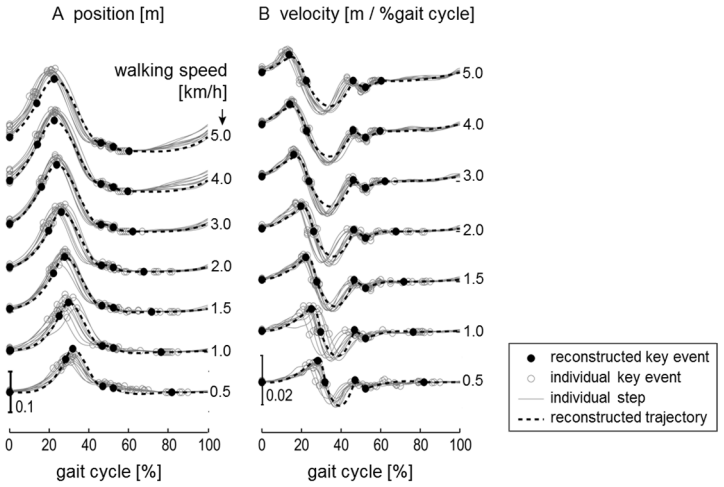

Figure 5: Typical example of the reconstructed ankle-height patterns. Graph A shows the individual steps (gray lines), together with the detected key events (gray circles), at different walking speeds, for a specific subject. The black filled circles represent the predicted key events for this particular subject, based on the obtained regression models. The black line represents the spline, which is fitted through the predicted key events. Graph B shows the velocity profile.

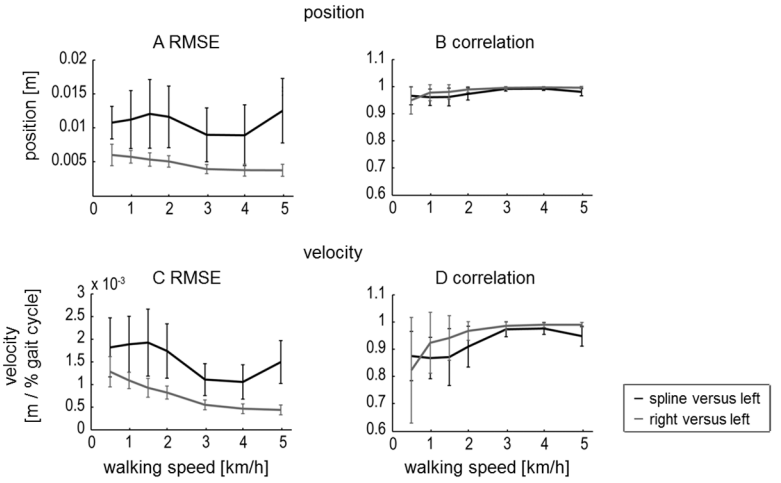

Figure 6: Validation of the reconstructed ankle-height patterns. A: RMSE between the left ankle-height pattern and the reconstructed spline (black line), and the RMSE between the left ankle-height pattern and the right ankle-height pattern (gray). Both measures were averaged across subjects for each walking speed. The error bars indicate the standard deviation. B: Correlation between the left ankle-height pattern and the reconstructed spline (black line), and the correlation between the left ankle-height pattern and the right ankle-height pattern (gray line). Graph C and D show similar figures for the validation of the velocity profile.

From the predicted key events, a reference ankle-height pattern was reconstructed for every subject and walking speed. We validated these patterns by comparing them with the measured patterns of the left leg (NB the regression equations were fitted on data of the right leg). The reconstructed patterns fitted the measured data well (figure 6). The *RMSE*, averaged across subjects, was around 1 cm for all walking speeds and the average correlation coefficient was larger than 0.95, for the low speeds, and showed even larger values for higher walking speeds. Since the error in predicting the key events is reflected in the reconstructed patterns, these *RMSE* values were close to the average *RMSE* in the prediction of the position of the key events (table 3, average position *RMSE* = 0.79 cm). The large correlation coefficients are in line with the small *RMSE* in the prediction of the timing of the key events. Also, the reconstructed velocity profiles matched the measured velocity profiles well (figure 6), though the correlations were a bit lower, especially for the lower velocities.

As a reference, we also calculated the *RMSE* and correlation coefficient between the measured right and left ankle patterns. These values provide an indication of the achievable fitting quality (figure 6). The correlations between the reconstructed spline and left leg data were very close to the correlations between the left and right leg data, whereas the *RMSE* values were approximately twice as large.

4.3.2 Healthy control group

Selective and gradual support

One of the goals of this study was to show the feasibility of selectively and gradually supporting step height during gait training. Providing step-height support resulted in a selective support of this specific subtask. It significantly increased the right step height, whereas it did not significantly affect the other basic gait parameters, like the left step height, step length, cycle time, or the relative duration of the different gait phases (figure 7). Analyzing the gait kinematics showed that the increase in step height was primarily caused by an increase in knee flexion. For the stiff controller, the average knee angle increased with 4.9 degrees at the moment of maximum ankle height, whereas the hip angle at that moment increased with only 1 degree (figure 8). The average maximum joint torques, that causes these changes, were 10 Nm hip extension and 9.6 Nm knee flexion. The support was also gradual, since the use of the stiff controller resulted in a significant increase in step height compared to the compliant controller.

Non-adaptive support does not induce reliance

We did not find any evidence for reliance of the subjects on the provided support, when they are exposed to continuous non-adaptive support. No significant difference between the initial exposure (first steps of the exposure blocks) and prolonged exposure (last steps of the exposure block) was found (figure 9). The step height during the first step of the catch block also revealed no signs of reliance. It shows that the subjects drop back to their

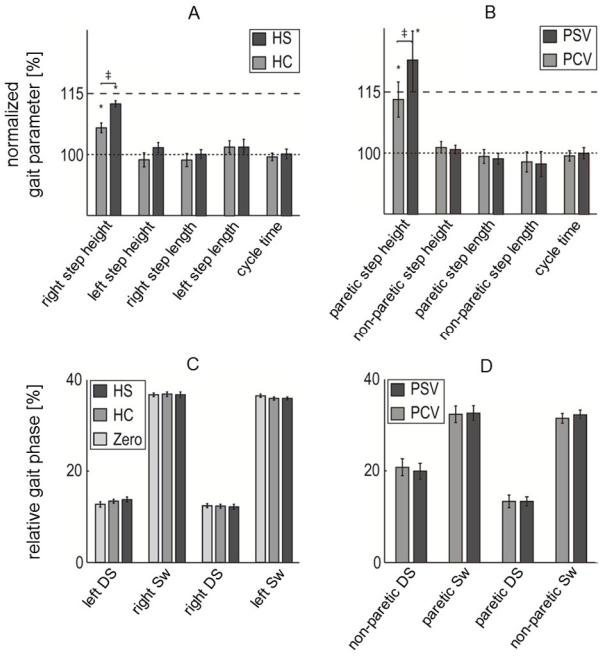

*Figure 7: Selective and gradual foot-clearance support in the healthy control subjects and stroke survivors. A: Mean normalized gait parameters for the trials in which the healthy subjects walked with the compliant (HC) and stiff (HS) step-height VMC. The mean parameters are calculated during the last 10 steps of the last exposure block. C: Mean relative contribution of the different gait phases to the cycle time for both tested conditions. As a reference, also the relative gait phases during walking in the zero impedance mode (HZ) are shown. B: Mean normalized gait parameters for the trials in which stroke survivors walked with the compliant (PCV) and stiff (PSV) step-height VMC, in combination the visual feedback. Mean parameters are calculated during last five steps of the longest exposure block. D: Mean relative gait phases for both tested conditions. The error bars indicate the standard error of the mean. *p < 0.05. ‡ indicates a significant difference between the compliant and stiff VMC.*

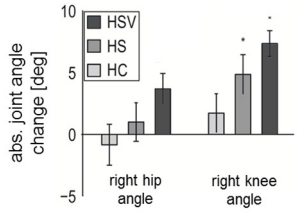

*Figure 8: Increase in hip and knee angle during foot-clearance support for the healthy control subjects. Mean absolute changes in the hip and knee angle for the trials in which the healthy subjects walked with the compliant step-height VMC (HC), stiff VMC (HS), and with the stiff VMC in combination with the visual feedback (HSV). Then mean parameters are calculated during the last 10 steps of the last exposure block. The error bars indicate the standard error of the mean. *p < 0.05.*

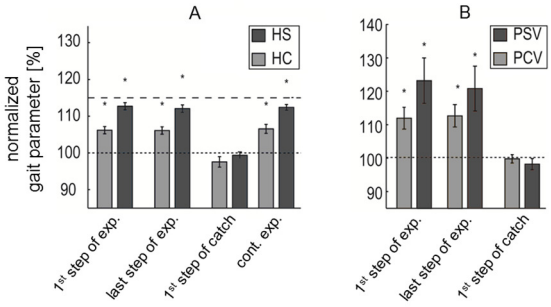

*Figure 9: Effect of non-adaptive support on reliance. A: Mean normalized step height during different steps of the trial in which the healthy subjects walked with the compliant (HC) and stiff (HS) step-height VMC. Mean parameters are calculated during the first step of the exposure block, during the last step of the exposure block, during the first step of the catch block and during continuous exposure. Continuous exposure is based on the last 10 steps of the last exposure block. B: Mean normalized step height during different steps of the trial in which the stroke survivors walked with the compliant (PCV) and stiff (PSV) step-height VMC, in combination with visual feedback. Mean parameters are calculated during the first step of the exposure block, during the last step of the exposure block, and the first step in the catch block. The last exposure block, with 50 steps of continuous exposure, was not included in the protocol of the stroke survivors. The error bars indicate the standard error of the mean. *p < 0.05.*

baseline, without any significant undershoot, which was to be expected when reliance would occur (figure 9). This holds for the compliant as well as the stiff controller. Even when the subjects received continuous support for a longer period of time (50 steps of continuous exposure), the step height did not significantly differ from the initial exposure.

Visual feedback enhances performance and active participation

With visual feedback, the healthy subjects reached an average increase of 14.5 percent in step height during continuous exposure, while the reference was set to 15 percent. This demonstrates that they can easily translate the simple information displayed on the screen into the appropriate hip and knee angular response. The visual feedback resulted in an additional increase in hip and knee flexion compared to the stiff controller (figure 8). The results also demonstrate that the subjects use the feedback to actively increase their step height within one step after the support has switched off (figure 10). After the support is switched on, unexpectedly, they receive additional support, which creates an overshoot. The subjects easily adapt to the additional support and reach the target value again within two steps.

4.3.3 Stroke survivors

Selective and gradual support

Providing step-height support to the stroke survivors resulted in a selective increase in step height, without significantly affecting the other basic gait parameters, including the

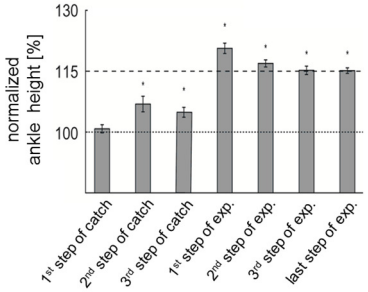

*Figure 10: Influence of adding visual feedback to the support. Mean normalized step height during different steps of the trial in which the healthy subjects walked with the stiff VMC in combination with the visual feedback (HCV). The step height is calculated during the first, second, and third step of the catch block, during the first, second, and third step of the exposure block, and during the last step of the exposure block. The error bars indicate the standard error of the mean. *p < 0.05.*

relative duration of the different gait phases (figure 7). The support was also gradual, since the use of the stiff controller resulted in a significant increase in step height compared to the compliant controller. The stroke survivors show a larger standard error of the mean of the paretic step height, compared to the right step height of the control group. For the compliant controller the increase in nominal step height ranged between 0 and 26 percent, whereas the increase in step height due to the stiff controller ranged between 0 and 44 Percent. For the stiff controller the average maximum joint torques were 21.0 Nm hip extension and 17.4 Nm knee flexion. The stroke survivors also show an asymmetry in stance phase (figure 7), which is often observed in stroke survivors [43].

Impedance shaping

The experiments showed that the impedance-shaping algorithm was effective in adapting the amount of support to the stroke survivor's individual capabilities on a step-by-step basis (figure 11). Starting from the initial stiffness (1200 N/m), the adaptive algorithm causes a gradual increase in stiffness where a kinematic error persists, and a clear reduction in stiffness where the ankle is above the reference (i.e., a negative deviation from the reference in the figure 11B). After ± 30 steps, the stiffness profile reached a steady state, where the forgetting factor and the deviation of the ankle from the reference pattern are in equilibrium. Figure 11B demonstrates that the stiffness can be greatly reduced without automatically compromising the overall kinematic error. That is, the difference between initial stiffness (1200 N/m) and final stiffness is much clearer than the change in kinematic error. With the impedance-shaping algorithm, the spring stiffness was shaped such that it reflected the initial deviation of the ankle from the reference trajectory for all patients (figure 12). Although the stiffness converged to a personal profile for each patient, the highest stiffness occurred at the start of the swing phase for all patients.

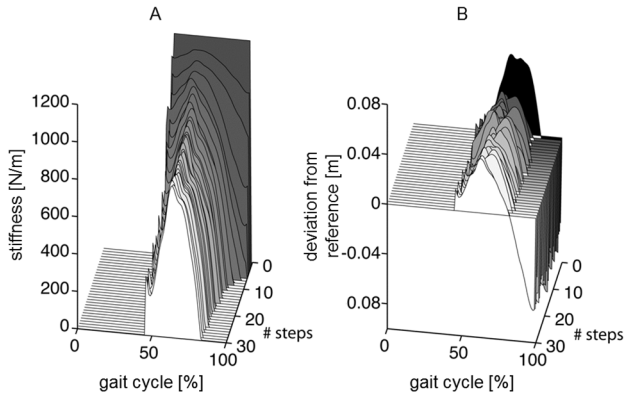

Figure 11: Typical example of the working principle of the impedance-shaping algorithm in a stroke survivor. Graph A demonstrates how the stiffness shapes from a constant stiffness of 1200 N/m to a personal stiffness profile after around 30 steps for stroke survivor A3. Note that the step-height VMC is only active during the double stance, with the non-paretic leg in front, and the paretic swing phase (approximately 50–100 percent of the gait cycle), and that the stiffness has a lower limit of 0. Graph B shows the course of the deviation from the reference pattern over multiple steps. The black area shows the error before the controller is switched on.

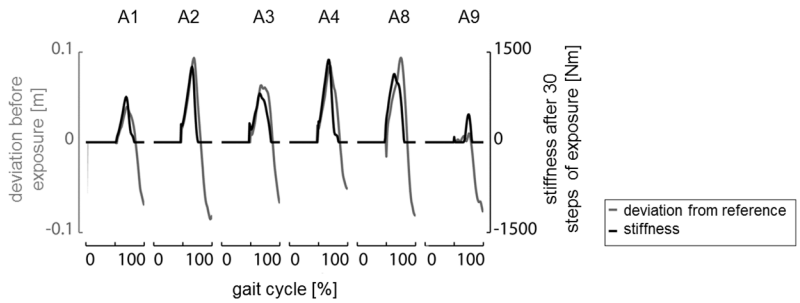

Figure 12: Shape of the stiffness profile after convergence. The figure shows the initial deviation of the ankle from the reference trajectory (gray) together with the converged stiffness profile (black). For all patients, the stiffness shaped according to the initial deviation from the reference.

Non-adaptive support does not induce reliance

Similar to the healthy control group, we did not find any evidence that indicated that the stroke survivors started to rely on the support. We did not find a significant difference between the initial exposure and the end of the exposure blocks (figure 9). This is also confirmed by the catch blocks, which show that during support (with the compliant or stiff VMC) the stroke survivors drop back to their baseline, without any significant undershot.

Visual feedback enhances performance and active participation

To evaluate if stroke survivors can utilize the visual feedback, we compared the trials where the stroke survivors received adaptive support combined with visual feedback

(PAV), with the trials where the stroke survivors received adaptive support only (PA). For this comparison, data from only four patients was available, since the PA condition could not be tested on two patients due to fatigue. In three of the four patients, the mean stiffness over the last five steps of the last exposure block was significantly lower when the patients received visual feedback (figure 13). This indicates that 1) these patients improved their performance with the help of the visual feedback and 2) the impedance-shaping algorithm lowered the impedance when the patients improved their performance.

No reduction of compensatory strategies

During the experiments, the stroke survivors showed different combinations, and degrees, of compensatory strategies to overcome their reduced knee flexion. All patients showed a larger paretic hip abduction range (hip circumduction) and an increased pelvic height during the paretic swing phase (vaulting). Figure 14 shows two typical examples of stroke survivors with stiff-knee gait, who use a vaulting strategy and/or a hip circumduction strategy. None of the patients reduced their compensatory strategies during the assistance of the stiff controller. Although the use of the stiff controller resulted in an average increase of 8.8 degrees in the maximum paretic knee flexion, and all patients reported that they felt the assistance in their paretic leg, we did not find a significant reduction in the hip abduction of the paretic leg, or a decrease in pelvic height during the paretic swing phase.

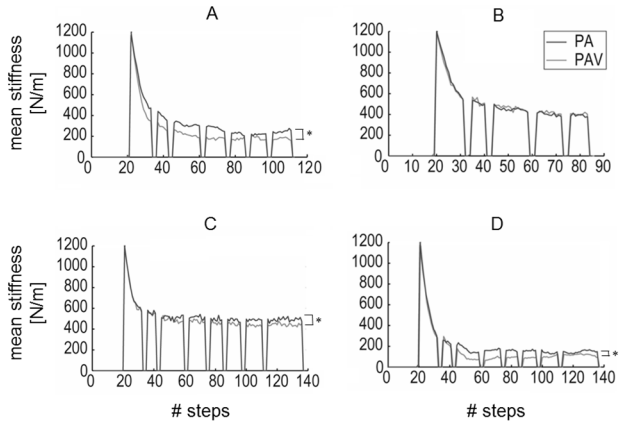

*Figure 13: Adding visual feedback to adaptive support. Mean stiffness over the course of the walking trial in which four stroke survivors (A1, A4, A8, and A9) walked with the impedance-shaping algorithm with (PAV) and without visual feedback (PA). In three patients, the mean stiffness over the last five steps of the last exposure block was significantly lower when the patients received visual feedback. This indicates that 1) these patients improved their performance with the help of the visual feedback and 2) the impedance-shaping algorithm lowered the impedance when the patients improved their performance. *p < 0.05.*

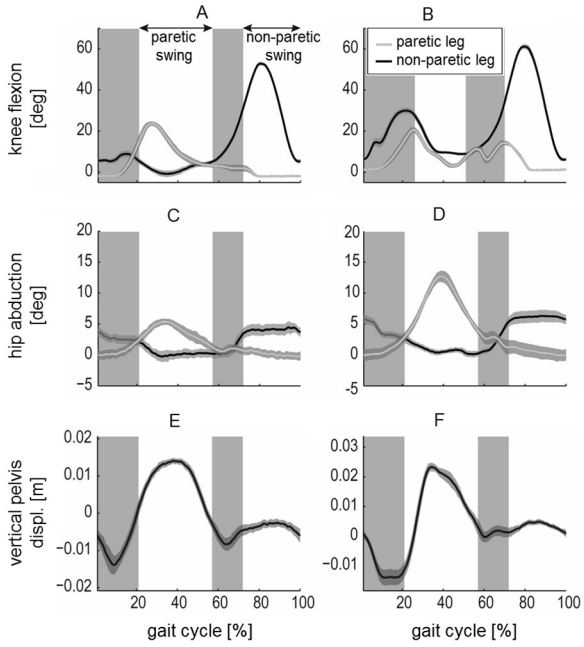

Figure 14: Two typical examples of gait adaptations seen in stroke survivors. Both patients (left: A4, right: A1) show one or more compensatory strategies to overcome a reduced foot clearance due to stiff-knee gait (A and B). They show an increase in hip abduction (D), and an increased pelvic height during the paretic swing phase, compared to the non-paretic swing phase (E and F).

4.4 Discussion

The purpose of this study was to assess the effectiveness of selectively supporting the step height during the swing phase. First, we derived regression models for the key events of the reference ankle-height pattern. These models can be used to reconstruct patient-specific reference patterns at any speed. The proposed step-height VMC was tested on healthy subjects and chronic stroke survivors, and proved effective in selectively influencing the step height. Additionally, the step height could be manipulated easily by changing the impedance levels. Incorporation of an impedance-shaping algorithm resulted in an adaptation of the impedance to the specific needs of every individual stroke survivor. Catch trials were used to investigate whether healthy subjects, or stroke survivors, would start to rely on the robotic support, but revealed no signs of reliance. The step height parameter was used to provide intuitive visual feedback. Both groups were able to utilize this feedback. We did not find evidence that the stroke survivors reduced their compensatory strategies when support was provided.

4.4.1 Reference pattern reconstruction

A large part of this paper concerns the reconstruction of the reference patterns. Throughout the literature, different strategies exist to determine these reference patterns. Most reference patterns are based on pre-recorded trajectories from unimpaired volunteers walking on a treadmill [24,29,44,45], or based on walking in the device while it is operated in a transparent mode [21,27], or with the motors removed [46]. Patient-specific patterns can be obtained by recording the gait trajectories while the patient walks with manual assistance [21,27], or by defining joint patterns based on movements of the unimpaired limb [47]. Most methodologies, however, have certain considerations that limit the use of the recorded trajectories to a specific application.

A major limitation of most of these reference patterns is that it is unknown how to correct for changes in speed. Most pre-recorded trajectories are recorded at a limited number of speeds, while the progress of the patients' preferred walking speed can be as small as 0.1 km/h. The coupling between the right and left leg [47] will change at different speeds and the recorded pattern, obtained during manual assistance [21,27], will only be valid for that specific speed. Scaling algorithms can be used to compensate for changes in speed or cadence [48]. Most scaling algorithms, however, apply scaling in time, amplitude and offset, whereas also the (relative) timing of the maximum joint angles changes at different speeds.

For the patterns recorded in the gait trainer itself, another limitation should be noted. Due to the mass and inertia of the device, and/or imperfections of the transparent mode, these patterns might not match with the ones recorded during free walking. Emken et al. [22] found that the added inertia resulted in a slightly higher stepping pattern compared to free walking, while others found a significant and relevant decrease in knee angular range due to the device [42].

Most pre-recorded trajectories are obtained by rescaling the gait pattern to a percentage of the gait cycle, and taking the mean across subjects. This introduces another issue. Averaging normalized data can result in an underestimation of the extremes in the gait pattern, when the subjects have a different distribution of the gait events throughout the gait cycle [49].

Therefore, we developed a method where the gait pattern is parameterized by defining different key events (minima, maxima etc.), which all have a timing, position, and velocity. Next, the walking speed and body-height dependency of the parameters are determined by regression models. This way, the extreme value in the reconstructed pattern is actually based on the extreme values of the individual patterns, even when the extremes occur at another percentage in the gait cycle.

Another advantage of the proposed method, compared to other available methods, is that it can be used to construct a reference ankle-height pattern at each particular walking speed between 0.5 and 5.0 km/h, for persons with different body heights. This allows the physical therapist to easily increase the training speed, even within a single walking

session. Speed-dependent reference pattern adjustments are also essential when the patient is in control of the walking speed, either manually or with intuitive speed-adaptation algorithms [50].

The proposed method is also generally applicable and can be applied to reconstruct speed-dependent reference patterns for joint angles. Different studies have already shown that peak joint kinematics are dependent in a linear and/or quadratic way on walking speed [51], and that its occurrence (timing) is also speed dependent [52].

There were some limitations in deriving the regression equations, which are related to the relatively low number of subjects (11) in this study. Due to this small number, we did not derive separate equations for male and female subjects, whereas systematic effects of gender of kinematics have been reported [53]. The range of body heights in this group of subjects was limited (1.52 m to 1.86). However, this range is expected to be sufficient for the majority of the elderly population.

4.4.2 Selective and gradual support

The results from the stroke survivors and healthy control group showed that the step-height VMC could selectively influence the step height. Supporting the step height did not significantly affect other spatiotemporal gait parameters, like non-supported step height, step length, or relative gait phase duration. Although the subjects were free to adapt their cadence, no change in cycle time was observed. As expected, the support was also gradual, a higher stiffness resulted in a closer approximation of the target values.

On average, the stroke survivors received more supportive hip and knee torque. At baseline, the stroke survivors walked more below the reference than the healthy subjects, resulting in more supportive torque.

The stroke survivors also showed a larger standard error of the mean of the paretic step height, compared to the right step height of the control group. For the healthy subjects, the reference ankle-height pattern was scaled such that is reached a 15-percent increase with respect to their nominal maximum ankle height. For the stroke survivors, the reference pattern was purely based on the regression formulas. The stroke survivors who were less affected, and almost reached their target value without support, showed a relative smaller increase in step height compared to the patients that performed less without the support.

4.4.3 Impedance shaping

Selective-subtask-support already allowed us to focus the robotic support on the subtasks that are impaired. However, also within a subtask, the amount of support needs to be minimized to the personal needs of the patient. Aoyagi et al. [21] already suggested that by scheduling the impedance as a function of the gait cycle, the assistance can be further personalized. This, however, is impossible for the operator to manually adjust. Therefore,

we chose to adopt an adaptive algorithm, that shaped the impedance based on the tracking performance, that was suggested by Emken et al. [27].

Emken et al. [27] reported that the impedance converged repeatedly over separate trials. Although we only performed one trial with the adaptive algorithm per patient, the impedance profile shaped according to the initial error between ankle and the reference trajectory for all patients. This indicates that the shaped impedance was directly related to the patient's incapabilities.

All stroke survivors converged to a stiffness profile where the stiffness was highest at swing initiation. This is in agreement with the trials where a constant stiffness was used. There, most of the assistive torques were exerted during swing initiation, indicating that that phase requires most of the support. Because of the provided torques during initial swing, the leg was propelled upward with a higher velocity, and required less support during the remainder of the swing phase. Anderson et al. [54] already demonstrated the importance of knee angular velocity at swing initiation in normal gait. They showed that the knee angular velocity at heel off was the main determinant for the maximal knee angle, and foot clearance, during swing. Reduced angular velocity, and foot clearance, in stiff-knee gait is suggested to be caused by an abnormal knee flexion during swing initiation. Kerrigan et al. [55] and Riley et al. [56] found an inappropriate activity in at least one of the quadriceps muscles during the pre-swing or initial swing phase, which inhibit a normal knee flexion. Kerrigan et al. [55] also reported that patients with delayed heel rise achieved less peak knee flexion. The patients included in this study also showed a delayed heel rise. So, providing support during this phase seems like a natural, and the most effective, way to increase the maximum knee angle, and subsequently foot clearance.

Apart from shaping the impedance to the patient's individual needs, minimizing the impedance also allows more variability within the stepping pattern, which has been shown to promote motor learning in mice [18]. Emken et al. [27] reported an increase in variability in maximum step height and step length, but could not verify whether increasing the variability during gait training had a positive effect on EMG activity levels. In our study, we did not investigate the variability within the gait pattern. We did see a clear reduction in the impedance levels where the stroke survivors required less support, which allows them to vary their steps in a more natural way compared to walking with a stiff controller. The possibility to make small gait variation was also promoted by using a unidirectional spring that only provided support in taking a higher step, thus not constraining the ankle when it reached above the reference.

4.4.4 Reliance

Based on previous pilot experiments [35], and computational models of movement training [57], we hypothesized that the stroke survivors and healthy controls would start to rely on the support, such that when assistance is no longer provided, their performance becomes worse. Previous studies, that let subjects adapt to external force fields, already showed that the human motor system can be modeled as a process that greedily

minimizes a cost function, consisting of a weighted sum of kinematic error and effort [58,59]. In these studies, a forgetting factor is introduced in the human effort, which models that the human continuously tries to accomplish the prescribed movement with reduced effort.

In this study, however, we did not find patients, or healthy subjects, who started to rely on the support. A likely explanation for the patient group could be the visual feedback, which we did not use in the pilot experiment [35]. The visual feedback provided them with information about their performance on a step-by-step basis, increasing their motivation and reducing the changes of reliance.

Also in the healthy control group, who did not receive visual feedback in most trials, we did not observe reliance. To evaluate the effects of prolonged exposure, the trials were concluded with 50 steps of continuous exposure. This block might have been too short for the subjects to explore the benefits of the support and start to rely on it. The relative low impedance levels might contribute to this effect.

Also the task instruction and type of support might explain our findings. In most motor learning experiments, a disturbing force field is applied and the subjects are asked to reduce the error. To reduce the error, the subjects have to produce additional effort to overcome the disturbance. During this process, they continuously try to minimize the trade-off between reducing their effort and increasing the error [58,59]. In our experiments, the subjects experience a force field that decreases, rather than increases, the performance error. Here, the subjects are not challenged to provide additional effort, which might not elicit them to reduce their effort.

The fact that a relatively small movement error can cause the subjects to trip might also have contributed to the fact that these subjects did not start to rely on the support. This would indicate that the weight of the error in the cost function increases compared to the reduction in effort. Bays et al. [60] already suggested that humans can change the weighting of different costs, according to the task and type of the movement.

Although the chances that reliance will occur are reduced by minimizing and localizing the support, like we tried to do with the impedance shaping algorithm, there remain two issues. First, the algorithm cannot distinguish between a decrease in effort due to reliance or due to fatigue. In both cases, the algorithm will increase its support. Second, subjects might still, consciously or unconsciously, reduce their effort over time and consequently receive more support. Emken et al. [59] showed that, to effectively assist-as-needed, the robot must reduce its assistance at a rate that is faster than that of the learning human. They stated that reliance can be prevented by setting the forgetting factor to a lower value than the learning rate of the subjects. They also state that determining the learning rate for neurological patients can be difficult because of their impaired motor control due to spasticity, muscle weakness, and synergies. Therefore, we chose to set the forgetting factor based on a stable convergence of the stiffness pattern within approximately 30 steps.

Finally, one might argue that to eliminate reliance one should apply resistive forces rather than supportive forces. In fact, error-enhancing therapy is suggested to be more effective than assistive therapy [20,61]. For some training exercises, where movement errors do not impose serious safety issues, this might be true. For robotic treadmill training, where small movement errors can have large consequences, this strategy may be inappropriate.

4.4.5 Visual feedback

In this study, very simple visual feedback was provided in the form of the step-height parameter. We showed that both the stroke survivors and the healthy controls were capable of utilizing this information effectively. Providing visual feedback to the healthy controls led to a very close approximation of the reference values. Adding visual feedback to the trials, in which the stroke survivors received adaptive support, led to lower impedance levels in three of the four patients, indicating that these patients are additionally motivated by the visual feedback.

The key element of any form of feedback is that it displays the subject's effort in an intuitive manner. Different forms of feedback are available. A review performed by Teasell et al. [62] concluded that there is a positive effect of EMG feedback in patients after stroke. Others use the subject's kinematics to display their performance [25,29] or the interaction force between user and robot, like in the Lokomat [63].

Disadvantage of the latter approach is that it is only applicable to position-controlled gait trainers. In these type of gait trainers, the additional effort of the subject is reflected on the screen, but is not reflected in their gait pattern. This might decrease the motivation of the subject. Thus, to optimize visual feedback, the gait trainer needs to be compliant. In more recent versions of the Lokomat, Duschau-Wicke et al. [25] introduced a more patient-cooperative strategy, effectively making the robot more compliant. In their study, they used body kinematics as visual feedback.

To optimize the feedback, factors like the amount of information and its frequency need to be investigated. Also the complexity of the feedback is important - do we need detailed information from every joint, or combined information from several joints, like the ankle position? Banala et al. [29] only displayed the ankle position in the sagittal plane. Our results suggest that only showing the maximum ankle height of the last step is already sufficient to control the hip and knee joint such that the subject takes a higher step. Also, for the therapist himself, we expect that feedback in the form of basic gait parameters will be easier to interpret, compared to joint angles or ankle trajectories.

The primary goal of visual feedback is, of course, to contribute to the long-term changes in relearned gait kinematics. Kim et al. [26] used the ALEX to induce gait modification in healthy adults. They reported that a combination of visual and force guidance resulted in larger modification in step height that maintained longer, persisting up to two hours, whereas only visual guidance or only force guidance evoked changes that did not last beyond the 10-min retention test. Although we did not investigate retention, our

experience with visual feedback is encouraging, and can serve as a starting point in the investigation about how to optimize gait training in such a way that short-term gait adaptation can become long-lasting gait modification.

4.4.6 Compensatory strategies

The VMC approach, used in this study, is an end-point-based-control strategy. This implies that within a certain subtask there is more freedom to walk, or choose a certain strategy. For example, different patients might choose different strategies to accomplish appropriate foot clearance. With the step-height VMC, the patients are left free in the strategy they use to clear their foot and will only receive support when this task is not executed successfully. This means that compensatory strategies [64,65], like pelvic hiking, hip circumduction, or vaulting [66,67], which are seen in most stroke survivors, can still be employed. Joint control limits the use of these strategies. Additionally, imposing a symmetrical joint-angle pattern limits the possibility of the non-paretic leg to compensate for the deficiencies of the paretic leg. Although these compensatory strategies do not contribute to a more symmetric walking pattern, they do increase basic gait function [68,69]. Some even advocate teaching compensatory strategies because of time and financial limitations [70]. Thus, because it is still largely debated whether the focus of robotic gait training should be on restitution of a normal walking pattern or on these compensatory strategies, they should not be overruled.

The use of these compensatory strategies might even become redundant when support is provided on the impaired subtask that evokes these compensatory strategies. We hypothesized that providing support on one subtask, i.e. foot clearance, would reduce the need for the patient to employ his compensatory strategies. Although all our stroke survivors showed compensatory strategies without support, none of them reduced their compensatory strategies with support. During the experiments, the stroke survivors received no specific instructions about how to walk on the treadmill. Therefore, they might not have been triggered to reduce their compensatory strategies. Also, the limited time that the stroke survivors walked in the LOPES during the experiments, in combination with the amount of time it would take to un-teach their adapted strategies, might be a reason for the unchanged kinematics. In the future, we might even develop special VMC modules that suppress compensatory strategies to promote restitution of a symmetrical walking pattern.

4.4.7 Related work

Different support methods have been suggested to correct the gait pattern of neurological patients. However, none of the compliant, or interactive, support methods has been evaluated in large-scale clinical trials. To guide potential clinical trials, the differences between our and other approaches will be explained. The method presented in this paper can be best compared to the “virtual tunnel” approach. Banala et al. [29] implemented this virtual tunnel approach, which was previously described by Cai et al. [30], and trained

two chronic stroke survivors with the ALEX [29]. Their tunnel consisted of a healthy-control template and the assistance was composed of a normal force, that simulated the virtual walls, and a tangential force that helped the ankle move along the trajectory. A similar virtual tunnel strategy is implemented in the Lokomat to train iSCI patients. Duschau-Wicke et al. also implemented a "moving window" that limits free movement to a region of the tunnel, similar to the tangential force in the ALEX [25]. In contrast to Banala et al. [29] they defined a torque field in joint space rather than a force field in Cartesian space. There are three main differences between the above-mentioned control strategies and the control strategy presented in this study.

First, both the ALEX and the Lokomat use some sort of support that potentially helps the ankle, or joint, move along the trajectory. The tangential force, used by Banala, et al. [29], decreases when the ankle deviates from the trajectory, thus the ankle is only pushed along the path when the ankle is close to the desired trajectory. Duschau-Wicke, et al. [25] use the moving window, that is synchronized with the user's cadence [71], to assist the user. In our study, no tangential force, or moving window, is used. Within the subtask-support strategy, step timing and foot clearance are two separate subtasks. Here, we only supported foot clearance. This allowed the subjects to freely change their timing, if they wished to do so. Still, subjects did not adapt their timing. For bilateral affected iSCI patients, who experience difficulties during swing initiation, or gait initiation in general, gait-timing assistance might be useful. In that case an additional VMC in the horizontal plane can be added. Our experience with stroke survivors suggests that the non-paretic leg can take care of the gait timing and the paretic leg will follow. Second, both studies use a virtual tunnel that lifts the ankle [29], or increases joint angles [25], but can also do the opposite when the subject performs above the reference. In this study, a unidirectional spring was used, because the support is intended to support the subject in taking higher steps, and not push the ankle downwards, when the ankle is above the reference. Third, in contrast to the Lokomat, the support of subtasks is an end-point-based-control strategy, rather than a joint-angle-based-control strategy. As mentioned before, joint-angle-based-control strategies exclude the use of compensatory strategies.

4.4.8 Future applications of selective support

The key goal of future research is to expand the concept of subtask support. Support in taking higher steps is an important part of the rehabilitation process, but other subtasks might also require assistance. A new VMC, that assists patients in taking more symmetric steps, is currently under development, and its interaction with other subtask controllers is being investigated.

For severely affected patients, body weight support systems (BWSS) are often used. Alternatively, VMC can also be used to partially support the body weight by attaching a vertical virtual spring to the hips. In that case, the forces, required to bear your own body weight, are provided in terms of hip and knee torques, rather than lifting the body externally. This allows normal sensory input from the foot soles, which is essential in order

to generate natural gait kinematics [72,73]. VMC for body weight support also allows easy modulation of the amount of support between the different legs, since stroke patients primarily need support during the stance phase of the affected leg. It also enables separate control of body weight support and balance support, which can be considered as two separate subtasks, either of which can be impaired to a certain degree. BWSS, with an overhead harness, not only provide a force in the pure vertical direction, but also in the horizontal plane that stabilizes the body. Pilot experiments have shown the feasibility of body weight support with VMC [74]. The possibilities of VMC for balance support are now being investigated.

Finally, we started preliminary tests with an intuitive speed-adaptation algorithm, in which the patient can move freely over the treadmill and the speed is automatically adapted when the patient deviates from the center of the treadmill. In conjunction with the obtained speed-dependent reference patterns, this will provide the therapist and patient with the tools to easily adapt the treadmill speed to the capabilities and progress of the patient, without the need to manually change the control settings.

4.5 Conclusion

In this study we implemented, and evaluated, a VMC strategy for selective and gradual support of gait subtasks. Here we focused on one specific subtask, i.e. increasing foot clearance. Initially, we derived and provided regression models that can be used to reconstruct patient-specific ankle movement patterns based on body height and walking speed. The *RMSE* between the predicted and actual trajectory was around 1 cm for all walking speeds. The proposed method can also be applied to reconstruct speed-dependent reference patterns for joint angles. Experiments with healthy subjects, and chronic stroke survivors, showed that with the proposed VMC approach, the step height could be selectively and gradually influenced, without affecting other spatiotemporal gait variables. In conjunction, we tested an impedance-shaping algorithm, which shaped the impedance to the patient's individual needs. The provided support did not result in reliance on the support for both the stroke survivors as well as the healthy control groups. Providing visual feedback to the user resulted in an increased active contribution in all healthy subjects and three of the four stroke survivors. The presented VMC approach, and impedance shaping, can be crucial for the development of new rehabilitation strategies and robotic gait trainers. It allows automatic localization and minimization of the support, which increases active patient contribution and promotes functional recovery.

Acknowledgments

This study was supported by a grant from Dutch Ministry of Economic affairs and Province of Overijssel, the Netherlands (grant: PID082004). We would like to thank Jaap Buurke and Martijn Postma, from the Roessingh Research and Development, for their assistance during the patient experiments.

References

[1] G. Kwakkel, R. van Peppen, R. C. Wagenaar, S. Wood Dauphinee, C. Richards, A. Ashburn, K. Miller, N. Lincoln, C. Partridge, I. Wellwood, and P. Langhorne, "Effects of augmented exercise therapy time after stroke: a meta-analysis," *Stroke*, vol. 35, pp. 2529-39, 2004.

[2] G. Kwakkel, R. C. Wagenaar, T. W. Koelman, G. J. Lankhorst, and J. C. Koetsier, "Effects of intensity of rehabilitation after stroke. A research synthesis," *Stroke*, vol. 28, pp. 1550-6, 1997.

[3] R. Teasell, J. Bitensky, K. Salter, and N. A. Bayona, "The role of timing and intensity of rehabilitation therapies," *Top Stroke Rehabil*, vol. 12, pp. 46-57, 2005.

[4] J. Hidler, D. Nichols, M. Pelliccio, and K. Brady, "Advances in the understanding and treatment of stroke impairment using robotic devices," *Top Stroke Rehabil*, vol. 12, pp. 22-35, 2005.

[5] M. Pohl, C. Werner, M. Holzgraefe, G. Kroczek, J. Mehrholz, I. Wingendorf, G. Hoolig, R. Koch, and S. Hesse, "Repetitive locomotor training and physiotherapy improve walking and basic activities of daily living after stroke: a single-blind, randomized multicentre trial (Deutsche GangtrainerStudie, DEGAS)," *Clin Rehabil*, vol. 21, pp. 17-27, 007.

[6] A. Mayr, M. Kofler, E. Quirbach, H. Matzak, K. Frohlich, and L. Saltuari, "Prospective, blinded, randomized crossover study of gait rehabilitation in stroke patients using the Lokomat gait orthosis," *Neurorehabil Neural Repair*, vol. 21, pp. 307-14, 2007.

[7] K. P. Westlake and C. Patten, "Pilot study of Lokomat versus manual-assisted treadmill training for locomotor recovery post-stroke," *J Neuroeng Rehabil*, vol. 6, pp. 1-11, 2009.

[8] C. Werner, S. Von Frankenberg, T. Treig, M. Konrad, and S. Hesse, "Treadmill training with partial body weight support and an electromechanical gait trainer for restoration of gait in subacute stroke patients: a randomized crossover study," *Stroke*, vol. 33, pp. 2895-901, 2002.

[9] B. Husemann, F. Muller, C. Krewer, S. Heller, and E. Koenig, "Effects of locomotion training with assistance of a robot-driven gait orthosis in hemiparetic patients after stroke: a randomized controlled pilot study," *Stroke*, vol. 38, pp. 349-54, 2007.

[10] T. G. Hornby, D. D. Campbell, J. H. Kahn, T. Demott, J. L. Moore, and H. R. Roth, "Enhanced gait-related improvements after therapist- versus robotic-assisted locomotor training in subjects with chronic stroke: a randomized controlled study," *Stroke*, vol. 39, pp. 1786-92, 2008.

[11] J. Hidler, D. Nichols, M. Pelliccio, K. Brady, D. D. Campbell, J. H. Kahn, and T. G. Hornby, "Multicenter randomized clinical trial evaluating the effectiveness of the Lokomat in subacute stroke," *Neurorehabil Neural Repair*, vol. 23, pp. 5-13, 2009.

[12] M. Lotze, C. Braun, N. Birbaumer, S. Anders, and L. G. Cohen, "Motor learning elicited by voluntary drive," *Brain*, vol. 126, pp. 866-72, 2003.

[13] A. Kaelin-Lang, L. Sawaki, and L. G. Cohen, "Role of voluntary drive in encoding an elementary motor memory," *J Neurophysiol*, vol. 93, pp. 1099-103, 2005.

[14] E. Taub, G. Uswatte, and T. Elbert, "New treatments in neurorehabilitation founded on basic research," *Nat Rev Neurosci*, vol. 3, pp. 228-36, 2002.

[15] M. A. Perez, B. K. Lungholt, K. Nyborg, and J. B. Nielsen, "Motor skill training induces changes in the excitability of the leg cortical area in healthy humans," *Exp Brain Res*, vol. 159, pp. 197-205, 2004.

[16] J. F. Israel, D. D. Campbell, J. H. Kahn, and T. G. Hornby, "Metabolic costs and muscle activity patterns during robotic- and therapist-assisted treadmill walking in individuals with incomplete spinal cord injury," *Phys Ther*, vol. 86, pp. 1466-78, 2006.

[17] J. M. Hidler and A. E. Wall, "Alterations in muscle activation patterns during robotic-assisted walking," *Clin Biomech (Bristol, Avon)*, vol. 20, pp. 184-93, 2005.

[18] L. L. Cai, A. J. Fong, C. K. Otoshi, Y. Q. Liang, J. G. Cham, H. Zhong, R. R. Roy, V. R. Edgerton, and J. W. Burdick, "Effects of consistency vs. variability in robotically controlled training of stepping in adult spinal mice.," in *Proceedings IEEE International Conference on Rehabilitation Robotics*, 2005.

[19] S. Jezernik, R. Scharer, G. Colombo, and M. Morari, "Adaptive robotic rehabilitation of locomotion: a clinical study in spinally injured individuals," *Spinal Cord*, vol. 41, pp. 657-66, 2003.

[20] J. L. Emken and D. J. Reinkensmeyer, "Robot-enhanced motor learning: accelerating internal model formation during locomotion by transient dynamic amplification," *IEEE Trans Neural Syst Rehabil Eng*, vol. 13, pp. 33-9, 2005.

[21] D. Aoyagi, W. E. Ichinose, S. J. Harkema, D. J. Reinkensmeyer, and J. E. Bobrow, "A robot and control algorithm that can synchronously assist in naturalistic motion during body-weight-supported gait training following neurologic injury," *IEEE Trans Neural Syst Rehabil Eng*, vol. 15, pp. 387-400, 2007.

[22] J. L. Emken, J. H. Wynne, S. J. Harkema, and D. J. Reinkensmeyer, "A robotic device for manipulating human stepping," *IEEE Transactions on Robotics*, vol. 22, pp. 185-189, 2006.

[23] J. L. Emken, J. E. Bobrow, and D. J. Reinkensmeyer, "Robotic movement training as an optimization problem: designing a controller that assists only as needed," in *Proceedings IEEE International Conference on Rehabilitation Robotics*, 2005.

[24] R. Riener, L. Lunenburger, S. Jezernik, M. Anderschitz, G. Colombo, and V. Dietz, "Patient-cooperative strategies for robot-aided treadmill training: first experimental results," *IEEE Trans Neural Syst Rehabil Eng*, vol. 13, pp. 380-394, 2005.

[25] A. Duschau-Wicke, J. von Zitzewitz, A. Caprez, L. Lunenburger, and R. Riener, "Path control: a method for patient-cooperative robot-aided gait rehabilitation," *IEEE Trans Neural Syst Rehabil Eng*, vol. 18, pp. 38-48, 2010.

[26] S. H. Kim, S. K. Banala, E. A. Brackbill, S. K. Agrawal, V. Krishnamoorthy, and J. P. Scholz, "Robot-assisted modifications of gait in healthy individuals," *Exp Brain Res*, vol. 202, pp. 809-24, 2010.

[27] J. L. Emken, S. J. Harkema, J. A. Beres-Jones, C. K. Ferreira, and D. J. Reinkensmeyer, "Feasibility of manual teach-and-replay and continuous impedance shaping for robotic locomotor training following spinal cord injury," *IEEE Trans Biomed Eng*, vol. 55, pp. 322-34, 2008.

[28] J. F. Veneman, R. Kruidhof, E. E. G. Hekman, R. Ekkelenkamp, E. H. F. Van Asseldonk, and H. Van der Kooij, "Design and Evaluation of the LOPES Exoskeleton Robot for Interactive Gait Rehabilitation," *IEEE Trans Neural Syst Rehabil Eng*, vol. 15, pp. 379-386, 2007.

[29] S. K. Banala, S. H. Kim, S. K. Agrawal, and J. P. Scholz, "Robot assisted gait training with active leg exoskeleton (ALEX)," *IEEE Trans Neural Syst Rehabil Eng*, vol. 17, pp. 2-8, 2009.

[30] L. L. Cai, A. J. Fong, C. K. Otoshi, Y. Liang, J. W. Burdick, R. R. Roy, and V. R. Edgerton, "Implications of assist-as-needed robotic step training after a complete spinal cord injury on intrinsic strategies of motor learning," *J Neurosci*, vol. 26, pp. 10564-8, 2006.

[31] E. H. F. Van Asseldonk, R. Ekkelenkamp, J. F. Veneman, F. C. T. Van der Helm, and H. Van der Kooij, "Selective control of a subtask of walking in a robotic gait trainer(LOPES)," in *Proceedings of the International Conference on Rehabilitation Robotics*, 2007.

[32] R. R. Neptune, D. J. Clark, and S. A. Kautz, "Modular control of human walking: a simulation study," *J Biomech*, vol. 42, pp. 1282-7, 2009.

[33] C. P. McGowan, R. R. Neptune, D. J. Clark, and S. A. Kautz, "Modular control of human walking: Adaptations to altered mechanical demands," *J Biomech*, vol. 43, pp. 412-9, 2010.

[34] J. E. Pratt, P. Dilworth, G. Prat, "Virtual model control of a biped walking robot," in *Proceedings of the 1997 International Conference on Robotics and Automation*, 1997.

[35] E. H. F. van Asseldonk, B. Koopman, J. H. Buurke, C. D. Simons, and H. van der Kooij, "Selective and adaptive robotic support of foot clearance for training stroke survivors with stiff knee gait," in *Proceedings of the IEEE International Conference on Rehabilitation Robotics*, pp. 701-706, 2009,

[36] E. T. Wolbrecht, V. Chan, D. J. Reinkensmeyer, and J. E. Bobrow, "Optimizing compliant, model-based robotic assistance to promote neurorehabilitation," *IEEE Trans Neural Syst Rehabil Eng*, vol. 16, pp. 286-97, 2008.

[37] H. J. F. M. Koopman, "The three-dimensional analysis and prediction of human walking," *Dissertation*, 1989.

[38] J. A. Zeni, Jr., J. G. Richards, and J. S. Higginson, "Two simple methods for determining gait events during treadmill and overground walking using kinematic data," *Gait Posture*, vol. 27, pp. 710-4, 2008.

[39] N. R, Draper, H. Smith, "Applied regression analysis," Hoboken, NJ: Wiley-Interscience; 1998.

[40] J. O. Street, R. J. Carroll, D. Ruppert D: "A note on computing robust regression estimates via iteratively reweighted least squares", Am Stat 1988, 42:152–154.

[41] H. Vallery, R. Ekkelenkamp, H. van der Kooij, and M. Buss, "Passive and Accurate Torque Control of Series Elastic Actuators," in *Proceedings of the IEEE International Conference on Intelligent Robots and Systems*, pp. 3534-3538, 2007

[42] E. H. van Asseldonk, J. F. Veneman, R. Ekkelenkamp, J. H. Buurke, F. C. van der Helm, and H. van der Kooij, "The Effects on Kinematics and Muscle Activity of Walking in a Robotic Gait Trainer During Zero-Force Control," *IEEE Trans Neural Syst Rehabil Eng*, vol. 16, pp. 360-370, 2008.

[43] E. B. Titianova and I. M. Tarkka, "Asymmetry in walking performance and postural sway in patients with chronic unilateral cerebral infarction," *J Rehabil Res Dev*, vol. 32, pp. 236-44, 1995.

[44] H. Yano, K. Kasai, H. Saitou, and H. Iwata, "Development of a gait rehabilitation system using a locomotion interface," *Journal of Visualization and Computer Animation*, vol. 14, pp. 243-252, 2003.

[45] Y. Stauffer, Y. Allemand, M. Bouri, J. Fournier, R. Clavel, P. Metrailler, R. Brodard, and F. Reynard, "The WalkTrainer--a new generation of walking reeducation device combining orthoses and muscle stimulation," *IEEE Trans Neural Syst Rehabil Eng*, vol. 17, pp. 38-45, 2009.

[46] G. Colombo, M. Joerg, R. Schreier, and V. Dietz, "Treadmill training of paraplegic patients using a robotic orthosis," *J Rehabil Res Dev*, vol. 37, pp. 693-700, 2000.

[47] H. Vallery, E. H. van Asseldonk, M. Buss, and H. van der Kooij, "Reference trajectory generation for rehabilitation robots: complementary limb motion estimation," *IEEE Trans Neural Syst Rehabil Eng*, vol. 17, pp. 23-30, 2009.

[48] S. Jezernik, G. Colombo, and M. Morani, "Automatic Gait-Pattern Adaptation Algorithms for Rehabilitation With a 4-DOF Robotic Orthosis," *IEEE Transactions on Robotics and Automation*, vol. 20, pp. 574-582, 2004.

[49] M. Molloy, J. Salazar-Torres, C. Kerr, B. C. McDowell, and A. P. Cosgrove, "The effects of industry standard averaging and filtering techniques in kinematic gait analysis," *Gait Posture*, vol. 28, pp. 559-62, Nov 2008.

[50] J. Von Zitzewitz, M. Bernhardt, and R. Riener, "A novel method for automatic treadmill speed adaptation," *IEEE Trans Neural Syst Rehabil Eng*, vol. 15, pp. 401-409, 2007.

[51] J. L. Lelas, G. J. Merriman, P. O. Riley, and D. C. Kerrigan, "Predicting peak kinematic and kinetic parameters from gait speed," *Gait Posture*, vol. 17, pp. 106-12, 2003.

[52] G. Stoquart, C. Detrembleur, and T. Lejeune, "Effect of speed on kinematic, kinetic, electromyographic and energetic reference values during treadmill walking," *Neurophysiol Clin*, vol. 38, pp. 105-16, 2008.

[53] D. C. Kerrigan, M. K. Todd, and U. Della Croce, "Gender differences in joint biomechanics during walking: normative study in young adults," *Am J Phys Med Rehabil*, vol. 77, pp. 2-7, 1998.

[54] F. C. Anderson, S. R. Goldberg, M. G. Pandy, and S. L. Delp, "Contributions of muscle forces and toe-off kinematics to peak knee flexion during the swing phase of normal gait: an induced position analysis," *J Biomech*, vol. 37, pp. 731-7, 2004.

[55] D. C. Kerrigan, J. Gronley, and J. Perry, "Stiff-legged gait in spastic paresis. A study of quadriceps and hamstrings muscle activity," *Am J Phys Med Rehabil*, vol. 70, pp. 294-300, 1991.

[56] P. O. Riley and D. C. Kerrigan, "Torque action of two-joint muscles in the swing period of stiff-legged gait: a forward dynamic model analysis," *J Biomech*, vol. 31, pp. 835-40, 1998.

[57] D. J. Reinkensmeyer, D. Aoyagi, J. L. Emken, J. A. Galvez, W. Ichinose, G. Kerdanyan, S. Maneekobkunwong, K. Minakata, J. A. Nessler, R. Weber, R. R. Roy, R. de Leon, J. E. Bobrow, S. J. Harkema, and V. R. Edgerton, "Tools for understanding and optimizing robotic gait training," *J Rehabil Res Dev*, vol. 43, pp. 657-70, 2006.

[58] J. L. Emken, R. Benitez, A. Sideris, J. E. Bobrow, and D. J. Reinkensmeyer, "Motor Adaptation as a Greedy Optimization of Error and Effort," J Neurophysiol, Mar 28 2007

[59] J. L. Emken, R. Benitez, and D. J. Reinkensmeyer, "Human-robot cooperative movement training: learning a novel sensory motor transformation during walking with robotic assistance-as-needed," *J Neuroeng Rehabil*, vol. 4, pp. 1-16, 2007.

[60] P. M. Bays and D. M. Wolpert, "Computational principles of sensorimotor control that minimize uncertainty and variability," *J Physiol*, vol. 578, pp. 387-96, 2007.

[61] J. L. Patton, M. E. Stoykov, M. Kovic, and F. A. Mussa-Ivaldi, "Evaluation of robotic training forces that either enhance or reduce error in chronic hemiparetic stroke survivors," *Exp Brain Res*, vol. 168, pp. 368-83, 2006.

[62] R. W. Teasell, S. K. Bhogal, N. C. Foley, and M. R. Speechley, "Gait retraining post stroke," *Top Stroke Rehabil*, vol. 10, pp. 34-65, 2003.

[63] R. Banz, M. Bolliger, G. Colombo, V. Dietz, and L. Lunenburger, "Computerized visual feedback: an adjunct to robotic-assisted gait training," *Phys Ther*, vol. 88, pp. 1135-45, 2008.

[64] I. A. K. DeQuervain, S. R. Simon, S. Leurgans, W. S. Pease, and D. McAllister, "Gait pattern in the early recovery period after stroke," *Journal of Bone and Joint Surgery-American Volume*, vol. 78A, pp. 1506-1514, 1996.

[65] G. Kwakkel, B. Kollen, and E. Lindeman, "Understanding the pattern of functional recovery after stroke: facts and theories," *Restor Neurol Neurosci*, vol. 22, pp. 281-99, 2004.

[66] G. Chen, C. Patten, D. H. Kothari, and F. E. Zajac, "Gait differences between individuals with post-stroke hemiparesis and non-disabled controls at matched speeds," *Gait Posture*, vol. 22, pp. 51-6, 2005.

[67] D. C. Kerrigan, E. P. Frates, S. Rogan, and P. O. Riley, "Hip hiking and circumduction: quantitative definitions," *Am J Phys Med Rehabil*, vol. 79, pp. 247-52, 2000.

[68] M. G. Bowden, C. K. Balasubramanian, R. R. Neptune, and S. A. Kautz, "Anterior-posterior ground reaction forces as a measure of paretic leg contribution in hemiparetic walking," *Stroke*, vol. 37, pp. 872-6, 2006.

[69] J. H. Buurke, A. V. Nene, G. Kwakkel, V. Erren-Wolters, M. J. IJzerman, and H. J. Hermens, "Recovery of Gait After Stroke: What Changes?," *Neurorehabilitation and Neural Repair*, vol. 22, pp. 676-683, 2008.

[70] B. M. Kelly, P. H. Pangilinan, Jr., and G. M. Rodriguez, "The stroke rehabilitation paradigm," *Phys Med Rehabil Clin N Am*, vol. 18, pp. 631-50, 2007.

[71] A. Duschau-Wicke, J. Von Zitzewitz, R. Banz, and R. Riener, "Iterative learning synchronization of robotic rehabilitation tasks," *in Proceedings of the IEEE International Conference on Rehabilitation Robotics*, pp. 335–340, 2007

[72] S. Hesse, B. Helm, J. Krajnik, M. Gregoric, and K. H. Mauritz, "Treadmill training with partial body weight support: Influence of body weight release on the gait of hemiparetic patients," *Journal of Neurologic Rehabilitation*, vol. 11, pp. 15-20, 1997.

[73] V. Dietz, R. Muller, and G. Colombo, "Locomotor activity in spinal man: significance of afferent input from joint and load receptors," *Brain*, vol. 125, pp. 2626-34, 2002.

[74] H. van der kooij, B. Koopman, and E. H. F. Van Asseldonck, "Body weight support by virtual model control of an impedance controlled exoskeleton (LOPES) for gait training.," in *Proceedings of the IEEE International Conference of the Eng Med Biol Soc*, pp. 1969-1972, 2008.

Chapter 5

Improving the transparency of a rehabilitation robot by exploiting the cyclic behaviour of walking

Published as:
B. Koopman†, W. van Dijk†, E. H. F. van Asseldonk, H. van der Kooij, "Improving the transparency of a rehabilitation robot by exploiting the cyclic behaviour of walking", *Proc. IEEE Int. Conf. Rehabil. Robot.*, pp. 1-6, 2013.
† Equal contributors.

Abstract

To promote active participation of neurological patients during robotic gait training, controllers, such as “assist as needed” or “cooperative control”, are suggested. Apart from providing support, these controllers also require that the robot should be capable of resembling natural, unsupported, walking. This means that they should have a transparent mode, where the interaction forces between the human and the robot are minimal. Traditional feedback-control algorithms do not exploit the cyclic nature of walking to improve the transparency of the robot. The purpose of this study was to improve the transparent mode of robotic devices, by developing two controllers that use the rhythmic behavior of gait. Both controllers use adaptive frequency oscillators and kernel-based non-linear filters. Kernel-based non-linear filters can be used to estimate signals and their time derivatives, as a function of the gait phase. The first controller learns the motor angle, associated with a certain joint angle pattern, and acts as a feed-forward controller to improve the torque tracking (including the zero-torque mode). The second controller learns the state of the mechanical system and compensates for the dynamical effects (e.g. the acceleration of robot masses). Both controllers have been tested separately and in combination on a small subject population. Using the feed-forward controller resulted in an improved torque tracking of at least 52 percent at the hip joint, and 61 percent at the knee joint. When both controllers were active simultaneously, the interaction power between the robot and the human leg was reduced by at least 40 percent at the thigh, and 43 percent at the shank. These results indicate that: if a robotic task is cyclic, the torque tracking and transparency can be improved by exploiting the predictions of adaptive frequency oscillator and kernel-based nonlinear filters.

5.1 Introduction

Robot-aided gait training is an emerging clinical tool for gait rehabilitation of neurological patients. These patients benefit form task oriented, high intensity, and repetitive training, to regain functional mobility [1-4]. Due to the repetitive behavior of gait training, rehabilitation robots are introduced. Robots can be used to provide more frequent, and more intensive training sessions, while reducing the workload of the therapist, compared to conventional forms of manual assisted (and body weight supported) gait training.

Despite the mentioned advantages of robotic-assisted gait training a large multicenter randomized clinical trial among stroke survivors suggested that the diversity of conventional gait training results in greater improvements in functional recovery than robotic-assisted gait training [5]. This emphasizes that robotic-assisted training needs to be further optimized in order to improve therapeutic outcome. Active patient participation is thought to be the key in achieving this improvement.

To encourage active participation, more and more robotic devices control the interaction forces with impedance or admittance control algorithms. Control strategies that promote active participation are often referred to as: “assist-as-needed” (AAN), “cooperative”, “adaptive” or “interactive” controllers, and make the robot’s behavior more flexible and adaptive to the patient’s capabilities, progress and current participation. These types of controllers potentially increase the motivation of the patient since additional effort by the patient is reflected in their gait pattern. Additionally, depending on the impedance levels, small errors are still possible, which have been suggested to promote motor learning in mice [6,7] as well as humans [8,9].

A prerequisite of these control strategies is that the robot should have a transparent mode. When the patient does not require any support during specific subtasks or gait phases of walking, or when he increases his capabilities or effort, the robot should reflect normal unassisted walking. Due to the mass and inertia of the device, and/or imperfections in the controller for the transparent mode, unassisted walking is often different from free walking [10,11].

In a perfect transparent mode there are no interaction forces between the subject and the robot. In our gait rehabilitation robot Lopes (figure 1), the transparent mode consists of a zero-torque mode, where torques at the robot joints are controlled to zero. This does however not result in a perfect transparent mode and causes small gait alterations [11]. These imperfections are partly due to sensor noise and friction in the actuation that limit the gains of the PI-controller, resulting in torque tracking errors. Additionally, the forces that occur due to joint friction, gravity, and inertias of the moving segments of the Lopes, are not compensated for in the current implementation. It is possible to compensate for these forces by an additional controller [12].

As mentioned before, the Lopes, like many other rehabilitation robots, is specifically designed to assist a cyclic task, in this case walking. Robotic performance of cyclic tasks

can be improved by repetitive control or adaptive control [13]. The latter has been implemented on the Lokomat rehabilitation robot in order to increase the compliance and transparency of this robot. One of the proposed controllers for this robot minimizes human-robot interaction forces by on-line optimization of a limited number of gait characteristics (angle offset, amplitude, and cycle time) of the reference angle trajectory used by their impedance controller [14]. Thus, the robot motion gets entrained with the desired human motion. In this paper we present a more general framework for improved torque control, and improved transparent control. Therefore we developed two new controllers. Both controllers use a framework of adaptive frequency oscillators and kernel-based non-linear filters to learn a control signal [15,16].

The first controller is intended to improve the limited torque tracking of the currently implemented PI-controller. As suggested by Kuo the control of rhythmic movements can be improved by combining feedback and feed-forward control [17]. In general, feed-forward control requires a precise model of the dynamic system. To establish this model, precise system identification is required which is, for many applications, a limitation to implement feed-forward control strategies. In this special case however we can use the information from previous cycles to learn the feed-forward signal in a model-free manner, and gradually learn the feed-forward signal over multiple cycles.

The second controller compensates for the passive dynamics of the system that exist between the actuator and the user. This includes: gravitational, inertial and frictional forces. Forces that emerge from these effects are not sensed, and therefore not compensated, in the zero-torque mode. Compensation of these forces is achieved by the implementation of an inverse model, which in this case is an inverse dynamical model of the Lopes exoskeleton legs. The forces calculated by the inverse model are opposite to the existing forces. Application of the calculated forces should, theoretically, cancel out the interaction forces between the robot and the human.

Both controllers are tested separately and in combination on a small group of healthy test subjects (N=4). To evaluate the performance of both control strategies the applied torques, the human-robot interaction forces, as well as the joint angles, are tracked. Here the suggested control strategies are specifically applied and tuned for the Lopes gait rehabilitation robot, but both approaches can be applied to other applications as well, as long as it concerns cyclic movement.

5.2 Experimental setup and methodology

5.2.1 Subjects

Four healthy subjects (4 males, age: 28 ± 2 years, height: 1.80 ± 0.03 m, weight: 74.5 ± 11.2 kg) participated in this experiment. All subjects gave written informed consent prior to participation.

5.2.2 Experimental apparatus and recordings

To test both controllers the Lopes was used. The Lopes (figure 1) is a treadmill-based lower-limb exoskeleton type robotic gait trainer. The Lopes is impedance-controlled and has eight actuated degrees of freedom (DoFs) (flexion/extension at the hip and knee, hip abduction/adduction and horizontal pelvis translations). The robot was initially designed to provide supported treadmill training for stroke patients. Torque control was achieved by Bowden-cable-driven, PI-controlled, series-elastic actuators [18]. The actuators themselves were controlled with an inner velocity feedback loop [19]. Every DoF of the Lopes was fitted with potentiometers that record the kinematics, and potentiometers on the springs of the SEA that record the applied torque. Matlab xPC (Mathworks, Natick, Mass., USA) was used to control the applied torques by the exoskeleton joints at 1000 Hz. The performance of the used PI controller is described in [19].

Additionally the interface between the subject's legs and the exoskeleton legs was sensorized using three (six DoFs) force sensors (ATI-Mini45-SI-580-20, ATI Industrial Automation, Apex, N.C., USA, figure 1). The cuffs (Hocoma, Volketswil, Switzerland) used in the Lopes were made of a rigid carbon fiber shell with Velcro straps and secure the subject's legs to the robot. One cuff connected to the upper leg and two cuffs connected to the lower leg of the subject. Only the interface of the right leg was fitted with force sensors. The analog signals coming from the force sensors were sampled at 1000 Hz using a data acquisition system (NI usb-6259, National Instruments, Austin, Texas, USA) and sent to the computer, where the data was stored for further processing. For clarity, the force sensors were only used to quantify the human-robot interaction forces, which were used as a measure for the transparency, and not as an input to the controller.

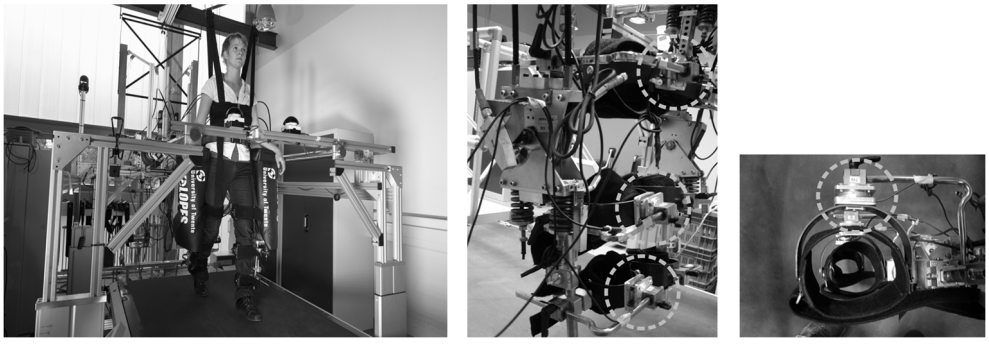

Figure 1: Left: The LOPES robotic gait trainer. The Lopes is a bilateral exoskeleton with eight degrees of freedom. The actuators are detached from the exoskeleton and connected to the joints via Bowden cables and springs. The robot is impedance controlled via series elastic actuation. Right: Six DoF force sensors (encircled). The force sensors are, via carbon shells and Velcro straps, attached to the human at one side and to the robot on the other side. Interaction forces are measured at the thigh (1 connection) and the shank (2 connections, high, and low).

5.2.3 Controller design

For the controllers that are presented in the next sections, an estimate of the position signals and their first and second order derivatives are required. To learn these signals the approach as suggested by [15] was used, which uses adaptive frequency oscillators in combination with kernel-based non-linear filters.

Adaptive frequency oscillator

Positions and their time derivatives can be expressed as a function of the gait phase. To acquire the gait phase, an adaptive frequency oscillator [20] matches a sinusoidal signal to an input signal. The phase of the sinusoidal signal was used as the gait phase (φ) that runs from 0 to 2 π In our application the right and left hip angle were used as input signals, since they show a sinusoidal like profile. The right and left hip angle (θ_{right} and θ_{left}) were estimated with the following sinusoidal functions:

$$\hat{\theta}_{right}(t) = k + a \cdot sin\left(\varphi(t)\right), \quad \hat{\theta}_{left}(t) = k + a \cdot sin\left(\varphi(t) + \pi\right) \qquad [1]$$

Of which k, a and φ are the offset, amplitude and the phase of the signal respectively and t is the time in seconds, the circumflex ($\hat{}$) denotes a signal estimate by the adaptive frequency oscillator. The left and right hip motions were assumed identical, with only a phase shift of π. The signal parameters were continuously updated using two error functions (e).

$$\begin{aligned} e_{right}(t) &= \theta_{right}(t) - \hat{\theta}_{right}(t) \\ e_{left}(t) &= \theta_{left}(t) - \hat{\theta}_{left}(t) \end{aligned} \qquad [2]$$

The following differential equations are governing the update process of the sinusoidal signal parameters:

$$\begin{aligned} \dot{\varphi}(t) &= \omega + \varepsilon(e_{right}(t)cos(\varphi(t)) + e_{left}(t)cos(\varphi(t) + \pi)) \\ \dot{\omega}(t) &= \varepsilon(e_{right}(t)cos(\varphi(t)) + e_{left}(t)cos(\varphi(t) + \pi)) \\ \dot{a}(t) &= \eta(e_{right}(t)sin(\varphi(t)) + e_{left}(t)sin(\varphi(t) + \pi)) \\ \dot{k}(t) &= \eta(e_{right}(t) + e_{left}(t)) \end{aligned} \qquad [3]$$

The parameter ω (rad s^{-1}) estimated the frequency of the stride. Constants η and ε were used to regulate the learning rate of the signal. Pre-trials showed that with a η and ε of respectively 0.4 and 2 the adaptive frequency oscillator was synchronized within approximately ten steps.

Kernel-based non-linear filters

Subsequently, the position signals and their first and second order time-derivatives were estimated. The obtained gait phase of the adaptive frequency oscillator was used to learn the joint angles and the motor angles as a function of the phase. We used kernel-based

non-linear filters as presented by [15] to learn the signal as a sum of n Gaussian functions ($\psi(t)$):

$$\psi_i(t) = exp\left(h\left(cos\left(\varphi(t) - c_i\right) - 1\right)\right) \quad i = 1..n \qquad [4]$$

with

$$c_i = \frac{2\pi i}{n} \qquad [5]$$

where h is a parameter that determines the width of the Gaussian function. Pre-trials showed that with n is 20 and an h of 15 the learned signal matched the angular pattern of the hip and knee well. The learned signal ($\tilde{\theta}$) was estimated on time (t) with:

$$\tilde{\theta}(t) = \frac{\sum_{i=1}^{n} w_i(t)\psi_i(t)}{\sum_{i=1}^{n} \psi_i(t)} \qquad [6]$$

The tilde (~) denotes the signal estimated by the non-linear filter. The weights (w) were adapted according to:

$$\dot{w}(t) = P\psi\left(\theta(t) - \tilde{\theta}(t)\right) \qquad [7]$$

where P had a value of 3 and is the learning gain, determining how fast the filter adapted its prediction. When the non-linear filter had learned the characteristics of the signal the filter can be locked by setting $\dot{w}$ to zero. A nice feature of this filter is that analytical derivatives of the signal estimate can be obtained, which provided the velocity and acceleration estimate that was needed for the improved torque tracking and the improved transparency. The frequency and weights were only changing relatively slow and therefore assumed constant:

$$\dot{\varphi}(t) = \omega \text{ and } \dot{w}(t) = 0 \qquad [8]$$

Additionally it was assumed that:

$$\frac{d}{dt}\left(\sum_{i=1}^{n} \psi_i(t)\right) = 0 \qquad [9]$$

This is approximately true if a sufficient large number of kernels is chosen. The first time derivative is:

$$\dot{\tilde{\theta}} = \frac{\sum_{i=1}^{n} w_i(t)\dot{\psi}_i(t)}{\sum_{i=1}^{n} \psi_i(t)} \qquad [10]$$

with

$$\dot{\psi}_i(t) = -\psi_i(t)h\omega\, sin\left(\varphi(t) - c_i\right) \qquad [11]$$

and the second time derivative is:

$$\tilde{\ddot{\theta}} = \frac{\sum_{i=1}^{n} w_i(t)\ddot{\psi}_i(t)}{\sum_{i=1}^{n} \psi_i(t)} \quad [12]$$

with

$$\ddot{\psi}_i(t) = -\dot{\psi}_i(t)h\omega \sin\left(\varphi(t) - c_i\right) - \psi_i(t)h\omega^2 \cos\left(\varphi(t) - c_i\right) \quad [13]$$

Feed-forward velocity learning controller

In the Lopes the series-elastic actuators were originally PI-controlled. Within this setup sensor noise and friction in the actuation limited the maximal feedback gains that can be used, resulting in tracking errors. The cyclic behavior of walking provides the possibility to estimate a feed-forward signal. The feed-forward signal was obtained with a non-linear filter. This filter learned the motor angles, (θ_{motor}, from the motor encoder) as a function of the phase, according to eq. 0.6. The analytical derivative (eq. 0.10) of the estimated signal ($\tilde{\dot{\theta}}_{motor}$) was used as the feed-forward signal in the Lopes torque control loop (which is velocity controlled). This signal was added to the motor-velocity command ($\dot{\theta}_{PI}$) from the PI-controller and was sent to the actuators. Figure 2 shows this control strategy.

Dynamics compensation controller

In the original transparent mode the joint torques were regulated to zero (zero-torque mode). Even if this control works perfectly this does not mean that the human, who walks in the Lopes, does not experience any interaction forces (F). Friction, gravity and inertia will still result in reaction forces that are felt via the connections with the Lopes. An inverse dynamics module can be used to calculate the torques (τ_{ID}) required to cancel these interaction forces. The inverse dynamics module described two planar double pendulums. Each double pendulum represented one leg of the Lopes in the sagittal plane,

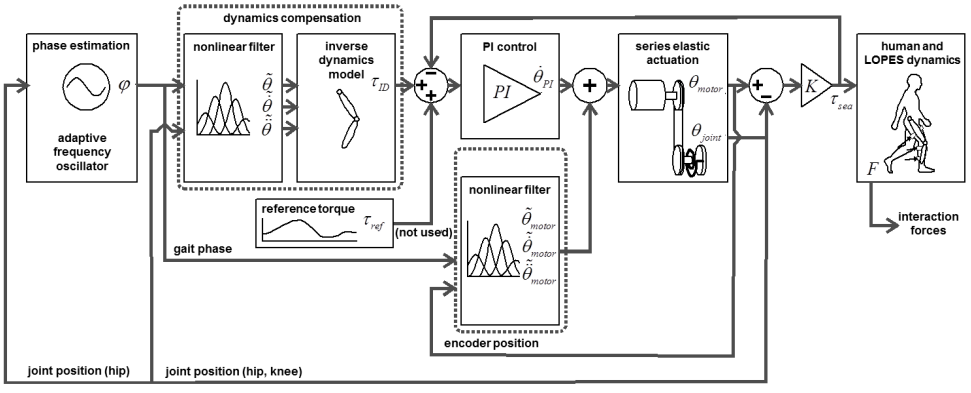

Figure 2: Schematic overview of the implemented controllers on the Lopes rehabilitation robot. The dynamics compensation module and the velocity learning module can be switched off so their output becomes zero. In the experiments described here the transparent mode was evaluated so the reference torque is set to zero.

Table 1: Dynamic properties of the Lopes.

	Thigh	Shank
Mass [kg]	5.9	4.2
Inertia [kg m^2]	0.079	0.044
Length [m]	0.44	--
Centre of mass [m][1]	0.2	0.2
Damping [Nm^{2}s^{-1}]	0.98	0.54
Strap position [m][1]	0.32	0.15 and 0.29

[1]*Measured from the proximal joint.*

consisting of an upper and lower leg segment. Each segment of the pendulums had a mass (located at a certain distance from the proximal joint) and inertia. Additionally, each joint had rotational damping, which represented friction in each joint. The parameters corresponding to the different Lopes segments were estimated using multi-input-multi-output (MIMO) system identification [21]. Table 1 provides an overview of the system parameters. The input of the inverse model consisted of the hip and knee angle, angular velocity, and angular acceleration. The Lopes was not fitted with accelerometers that measure the required signals directly. Therefore, the joint angles and their first and second order derivatives were also obtained with the non-linear filter. Figure 2 shows this control strategy.

5.2.4 Experimental protocol

Before the subject was positioned in the Lopes, different anthropometric measurements were taken to adjust the exoskeleton segment lengths. Additionally, the positions of the cuffs were adjusted to align the subject's knee and hip axis with the exoskeleton joints. Next, the subject was positioned into the Lopes and the trunk, thigh, and upper- and lower shank were strapped to the exoskeleton (figure 1).

After a 5 minute familiarization period, to get used to walking in the Lopes, each subject performed two trials. The trials were performed at a slow walking (0.5 m/s) and fast walking speed (1.0 m/s). First the subjects walked for ninety seconds in the device using only the PI-controller (the conventional zero-torque mode). During this period the subject's cadence was recorded. The interaction forces scale with the cadence and the walking speed. At higher walking speeds the exoskeleton legs are accelerated and decelerated more, resulting in higher interaction forces. To cancel this effect out, the different controllers were tested at a fixed treadmill speed and a fixed cadence. The fixed cadence was achieved by asking the subjects to synchronize their walking tempo with a metronome that was set to the average of the subjects' pre-recorded cadence. This first condition (90 seconds of PI-controller) was also used to learn the signals that were required for the dynamics compensation. After 90 seconds the non-linear filters, that learn the hip and the knee angle (and their derivatives), were locked. Subsequently the different controllers were tested. The non-linear filter for the feed-forward controller was

Table 2: Tested conditions.

Condition	Duration for each speed (s)
PI	90
PI + velocity learning	90
PI + dynamics compensation	90
PI + velocity learning + dynamics compensation	90

not locked. The different walking conditions and their duration are listed in table 2. All conditions (at one speed) were evaluated directly after each other at the same cadence, without interruptions. In the second trial this protocol was repeated for the fast walking speed.

5.2.5 Data analysis

All signal processing was done with custom-written software in Matlab (Natick, Mass., USA). The measured forces from the three force sensors were resampled at 100 Hz and synchronized with the potentiometer data from the Lopes.

Of all the recorded conditions only the last 60 seconds were used for data processing. Performance of the controllers was calculated based on the root mean square (*RMS*) of different signals. The evaluated signals were: 1) the torque tracking error, 2) the interaction force in the sagittal plane (perpendicular to the exoskeleton legs), and 3) the interaction power. The interaction power was calculated by taking the product of the moment of the interaction forces around their proximal joint and the velocity of their proximal joint. Results for the upper and lower shank force were summed. The power provides a measure for the flow of energy between robot and human, that is: it shows how much the robot is supporting, or resisting, the movement of the human.

Average steps were calculated by splitting the data into individual strides, based on the heel-contact event. Next, the different data blocks were normalized as a percentage of the gait cycle and averaged. Paired t-tests were performed to test for significant differences between the conditions. The level of significance was defined at p=0.05.

5.3 Results

5.3.1 Torque tracking

The torque tracking was improved by the feed-forward controller. The *RMS* of the torque tracking error (*RMSE*) significantly reduced (table 3, figure 3). Reductions in tracking error were similar in the zero-torque mode and with the dynamics compensation switched on (table 3). The small standard deviation indicates that all subjects showed similar reductions. In general the knee joint had the largest reduction in *RMSE*. No clear effect of the walking speed on the tracking error was observed. A typical example of the tracking

Table 3: Reductions in RMS torque error.

	Dynamics compensation off		Dynamics compensation on	
	Slow	**Fast**	**Slow**	**Fast**
Hip	52% *(49%-56%)*	59% *(51%-60%)*	56% *(53%-64%)*	58% *(51%-62%)*
Knee	61% *(55%-68%)*	64% *(55%-70%)*	65% *(63%-67%)*	62% *(61%-63%)*

Reductions in RMS of the difference between desired and recorded torque (tracking error), averaged over the subjects. All reductions were significant with $p < 0.01$ (paired t-test). The values between brackets show the range of the data over the different subjects.

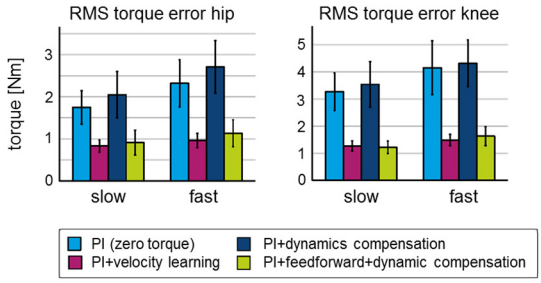

Figure 3: RMS of the tracking error at the hip (left) and knee (right). The bars are the results, averaged over the subjects. The error bars denote the standard deviations.

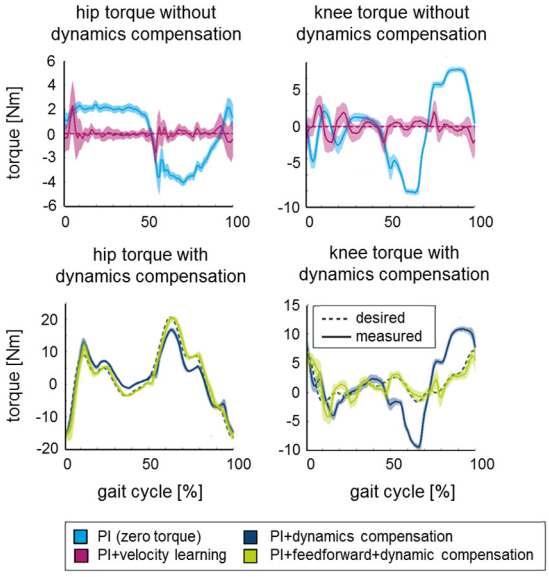

Figure 4: Top: difference between the desired and the measured torque without dynamics compensation (zero-torque mode). Note that the desired torque is zero. Bottom: difference between both signals with dynamics compensation. The figure shows the results for a typical subject. All signals are presented as a function of the gait cycle, starting at heel strike. Left: results for the hip. Right: results for the knee.

error as a function of the gait cycle, with and without the dynamics compensation, is shown in figure 4.

5.3.2 Interaction forces

For the thigh, the interaction forces were reduced when the feed-forward controller was switched on, compared to the zero-torque mode (figure 5). The dynamics compensation also resulted in a reduction in thigh interaction forces compared to the zero-torque mode. An additional decrease was observed when the feed-forward controller was switched on in combination with the dynamics compensation, leading to a total reduction of interaction forces of 39% ($p = 0.001$) for slow walking and 35% ($p = 0.009$) for fast walking. Walking at higher speed showed the same trends. In general: a higher walking speed resulted in higher interaction forces between subjects and robot.

For the interaction forces on the lower leg (shank high and shank low) the dynamics compensation did not result in a reduction of the forces, compared to the zero-torque mode (figure 5). In fact: the interaction forces increased slightly. In contrast, the feed-forward controller did reduce the interaction forces. When it was switched on in the zero-torque mode, as well as in combination with the dynamics compensation, it resulted in reduced interaction forces.

5.3.3 Interaction power

The interaction power (figure 6) showed the same trends as observed in the interaction forces (figure 5). At the thigh the dynamics compensation resulted in a reduction in power compared to the zero-torque mode. An additional decrease was observed when the feed-forward controller was switched on (figure 6). Combining both controllers led to a total reduction of interaction power of 40.9% ($p = 0.002$) for slow walking and 40.2% ($p = 0.007$) for fast walking. Looking solely at the effect of walking speed, walking at higher speeds resulted in larger powers.

For the lower leg the dynamics compensation alone did not result in a clear reduction of the interaction power, compared to the zero-torque mode (figure 6), but the feed-forward controller did reduce the interaction power. In contrast to the interaction force (figure 6), combining both controllers resulted in a large reduction in the power at the shank (slow walking 45.3%, fast walking 43.2%). Figure 6 also shows that the dynamics compensation resulted in a larger reduction in interaction power during the swing phase than during the stance phase.

5.3.4 Kinematics

The recorded joint angles are compared for the different controllers in figure 7. Gait kinematics show only subtle differences. The most prominent difference is the increase in knee flexion angle. If the feed-forward controller and the dynamics compensation are on simultaneously the maximal knee ankle is 5.8 degrees larger than the condition where

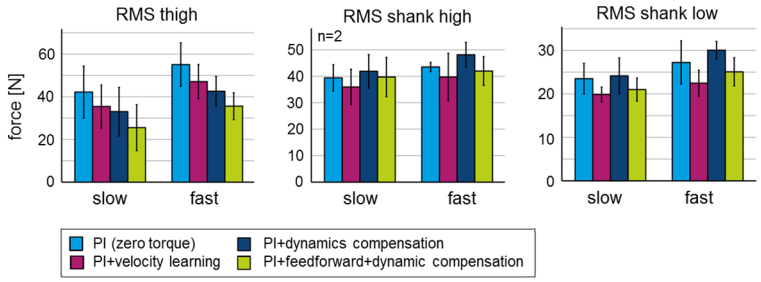

Figure 5: RMS of the interaction forces at the thigh and shank. The bars are the results, averaged over the subjects. The error bars denote the standard deviations.

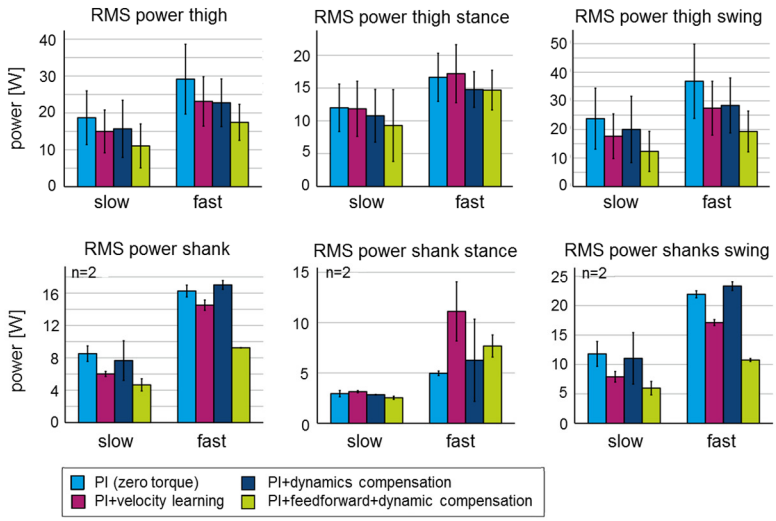

Figure 6: RMS of the power at the thigh (top) and shank (bottom) over the total gait cycle (left) and divided in stance (middle) and swing phase (right). The bars are the results, averaged over the subjects. The error bars denote the standard deviations.

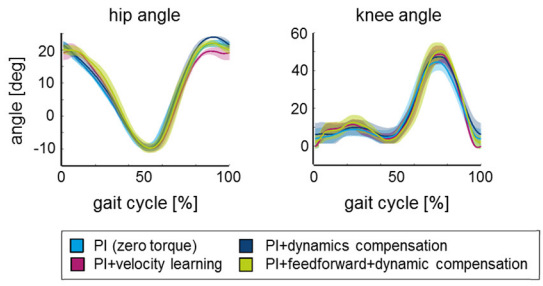

Figure 7: Gait kinematics averaged over the subjects (flexion is positive), and presented as a function of the stride, starting at heel strike. Shaded areas show the standard deviations between the subjects.

both controllers are off ($p = 0.003$).

5.4 Discussion

The purpose of this study was to investigate how the cyclic nature of many rehabilitation tasks could be exploited to improve the control and transparency of rehabilitation robots. The results for the two tested controllers are discussed below.

5.4.1 Feed-forward velocity learning controller

The *RMS* of the torque tracking error showed a large improvement. Still, our approach can only filter out errors that are cyclic, with the same cycle time as the gait cycle (figure 4). Errors that are not a function of the gait phase cannot be captured by the non-linear filter. The remaining error in the torque tracking is partly due to tracking errors that are not cyclic. However, in our study the cyclic effects were dominant and the *RMSE* could be reduced by more than half.

5.4.2 Dynamics compensation

The effect of the dynamics compensation was measured by the interaction power. When the dynamics compensation was switched on the interaction power reduced, especially for the thigh (figure 6). Our results also indicate that the effect of the dynamics compensation controller is larger if the feed-forward velocity controller is active in parallel, which clearly improved the torque tracking (figure 3). This indicates that a good torque tracking is a prerequisite for the dynamics compensation controller to work, especially since the desired torques are relatively small (figure 4).

In general the dynamics compensation controller showed a larger reduction in interaction power during the swing phase than during the stance phase (figure 6). This might be due to larger joint accelerations during the swing phase, than during the stance phase. Larger accelerations correspond to larger forces that can be compensated for with this controller. Indeed, figure 6 shows higher interaction powers during the swing phase compared to the stance phase.

An additional possible explanation is that the interaction forces, during the stance phase, have a source that cannot be compensated for by either one of the controllers. As a safety measure the Lopes has a mechanical end-stop at the knee joint to prevent hyperextension. At initial heel contact, at the beginning of the stance phase, the subject is likely to hit that end-stop and the Lopes cannot reduce the interaction forces by further extending.

Some of the remaining interaction forces might emerge from a misalignment between the human and the robot leg. This cannot be compensated for by the controllers, but can only be solved with a more ergonomic design.

Evaluation of the kinematics showed an increase in maximum knee angle during the swing (figure 7). This suggest that, in our specific case, the previous observed reduction in knee flexion [11] (in de zero-torque mode) was compensated for by our controllers. This might indicate that the subjects have a more natural gait when the controllers are switched on. Up to this point we did not investigate the changes in human performance in terms of the kinematic resemblance of natural walking, energy expenditure or muscle activation. This will be part of further research.

5.5 Conclusion

If a robotic task is cyclic, the performance of this task can be improved by exploiting the predictions of adaptive frequency oscillator and kernel-based nonlinear filters. These filters predict signals for the upcoming steps. This prediction can be used to compose a feed-forward signal to increase robotic control accuracy. We showed that for our rehabilitation robot we improved the torque tracking and reduced the interaction forces between the robot and the human, and thereby improved the transparency of our robot. Still we need to evaluate how the controllers react to sudden gait changes and irregular gait patterns.

References

[1] G. Kwakkel, R. van Peppen, R. C. Wagenaar, S. Wood Dauphinee, C. Richards, A. Ashburn, K. Miller, N. Lincoln, C. Partridge, I. Wellwood, and P. Langhorne, "Effects of augmented exercise therapy time after stroke: a meta-analysis," *Stroke,* vol. 35, pp. 2529-39, 2004.

[2] G. Kwakkel, R. C. Wagenaar, T. W. Koelman, G. J. Lankhorst, and J. C. Koetsier, "Effects of intensity of rehabilitation after stroke. A research synthesis," *Stroke,* vol. 28, pp. 1550-6,1997.

[3] R. Teasell, J. Bitensky, K. Salter, and N. A. Bayona, "The role of timing and intensity of rehabilitation therapies," *Top Stroke Rehabil,* vol. 12, pp. 46-57, 2005.

[4] N. A. Bayona, J. Bitensky, K. Salter, and R. Teasell, "The role of task-specific training in rehabilitation therapies," *Top Stroke Rehabil,* vol. 12, pp. 58-65, 2005.

[5] J. Hidler, D. Nichols, M. Pelliccio, K. Brady, D. D. Campbell, J. H. Kahn, and T. G. Hornby, "Multicenter randomized clinical trial evaluating the effectiveness of the Lokomat in subacute stroke," *Neurorehabil Neural Repair,* vol. 23, pp. 5-13, 2009.

[6] L. L. Cai, A. J. Fong, C. K. Otoshi, Y. Q. Liang, J. G. Cham, H. Zhong, R. R. Roy, V. R. Edgerton, and J. W. Burdick, "Effects of consistency vs. variability in robotically controlled training of stepping in adult spinal mice.," in *Proceeding of IEEE International Conference on Rehabilitation Robotics*, 2005.

[7] M. D. Ziegler, H. Zhong, R. R. Roy, and V. R. Edgerton, "Why variability facilitates spinal learning," *J Neurosci,* vol. 30, pp. 10720-6, 2010.

[8] S. Jezernik, R. Scharer, G. Colombo, and M. Morari, "Adaptive robotic rehabilitation of locomotion: a clinical study in spinally injured individuals," *Spinal Cord,* vol. 41, pp. 657-66, 2003.

[9] J. L. Emken and D. J. Reinkensmeyer, "Robot-enhanced motor learning: accelerating internal model formation during locomotion by transient dynamic amplification," *IEEE Trans Neural Syst Rehabil Eng,* vol. 13, pp. 33-9, 2005.

[10] J. L. Emken, J. H. Wynne, S. J. Harkema, and D. J. Reinkensmeyer, "A robotic device for manipulating human stepping," *IEEE Transactions on Robotics,* vol. 22, pp. 185 - 189, 2006.

[11] E. H. van Asseldonk, J. F. Veneman, R. Ekkelenkamp, J. H. Buurke, F. C. van der Helm, and H. van der Kooij, "The Effects on Kinematics and Muscle Activity of Walking in a Robotic Gait Trainer During Zero-Force Control," *IEEE Trans Neural Syst Rehabil Eng,* vol. 16, pp. 360-370, 2008.

[12] H. Vallery, A. Duschau-Wicke, and R. Riener, "Generalized elasticities improve patient-cooperative control of rehabilitation robots," in *Proceedings of the IEEE International Conference on Rehabilitation Robotics,* pp. 535-541, *2009.*

[13] Y. Wang, F. Gao, and F. J. Doyle Iii, "Survey on iterative learning control, repetitive control, and run-to-run control," *Journal of Process Control,* vol. 19, pp. 1589-1600, 2009.

[14] R. Riener, L. Lunenburger, S. Jezernik, M. Anderschitz, G. Colombo, and V. Dietz, "Patient-cooperative strategies for robot-aided treadmill training: first experimental results," *Neural Systems and Rehabilitation Engineering, IEEE Transactions on,* vol. 13, pp. 380-394, 2005.

[15] A. Gams, A. J. Ijspeert, S. Schaal, and J. Lenarčič, "On-line learning and modulation of periodic movements with nonlinear dynamical systems," *Autonomous robots,* vol. 27, pp. 3-23, 2009.

[16] R. Ronsse, T. Lenzi, N. Vitiello, B. Koopman, E. Van Asseldonk, S. M. M. De Rossi, J. Van Den Kieboom, H. Van Der Kooij, M. C. Carrozza, and A. J. Ijspeert, "Oscillator-based assistance of cyclical movements: model-based and model-free approaches," *Medical and Biological Engineering and Computing,* pp. 1-13, 2011.

[17] A. D. Kuo, "The relative roles of feedforward and feedback in the control of rhythmic movements," *Motor Control,* vol. 6, pp. 129-145, 2002.

[18] J. F. Veneman, R. Kruidhof, E. E. G. Hekman, R. Ekkelenkamp, E. H. F. Van Asseldonk, and H. Van der Kooij, "Design and Evaluation of the LOPES Exoskeleton Robot for Interactive Gait Rehabilitation," *IEEE Trans Neural Syst Rehabil Eng,* vol. 15, pp. 379-386, 2007.

[19] H. Vallery, R. Ekkelenkamp, H. van der Kooij, and M. Buss, "Passive and Accurate Torque Control of Series Elastic Actuators," in *Proceedings of the IEEE International Conference on Intelligent Robots and Systems*, San Diego, USA, 2007, pp. 3534-3538.

[20] L. Righetti, J. Buchli, and A. J. Ijspeert, "Dynamic Hebbian learning in adaptive frequency oscillators," *Physica D: Nonlinear Phenomena,* vol. 216, pp. 269-281, 2006.

[21] B. Koopman, E. van Asseldonk, and H. van der Kooij, "In vivo measurement of human knee and hip dynamics using MIMO system identification," in *Proceedings of the IEEE International Conference of the Eng Med Biol Soc*, pp. 3426-3429, 2010.

Chapter 6

Estimation of human hip and knee multi-joint dynamics using the LOPES gait trainer

Submitted as:
B. Koopman, E. H. F. van Asseldonk, H. van der Kooij, "Estimation of human hip and knee multi-joint dynamics using the lopes gait trainer", *IEEE Trans. Neural Syst. Rehabil. Eng.*

Abstract

In this study we present and evaluate a novel method to estimate multi-joint leg impedance, using a robotic gait training device. The method is based on Multi Input Multi Output (MIMO) system identification techniques and is designed for continuous torque perturbations at the hip and knee joint simultaneously. Eight elderly subjects (age 67-82) performed relax- and position-tasks in three different leg orientations. Multi-joint impedance was estimated non-parametrically and subsequently modelled in terms of inertia and (inter) joint stiffness and damping. The results indicate that all stiffness and damping parameters were significantly higher during the position task compared to the relax task. The majority of the stiffness and damping parameters were not significantly affected by leg orientation. The results also emphasize the importance of considering the visco-elastic coupling between joints when modeling multi-joint dynamics. Measuring joint stiffness with the same device that is used for robotic gait training allows convenient testing of joint properties as part of robotic gait training protocols. These measures might serve as a good basis for quantitative assessment and follow up of patients with abnormal joint stiffness due to neurological disorders and may reveal how changes in these joint properties affect their gait function.

6.1 Introduction

Our ability to resist perturbations during postural control, or coordinated movements like walking, greatly depends on our mechanical joint properties. Joint properties can be characterized by their mechanical impedance, which (in biomechanics) is often defined as the dynamic behavior between joint torque and angular displacement [1]. Experiments to quantify joint impedance typically involve mechanically perturbing the joint in a controlled manner, measuring the motions and torques and applying system identification techniques. These experiments have been performed on a wide variety of joints, including the ankle, wrist, elbow and knee and revealed that, for small displacements, the joint impedance could be described by inertial, viscous and elastic properties [2].

Often, a distinction is made between the impedance measured in a passive joint (passive impedance) or in a joint with a certain level of muscle contraction (active impedance). The passive component is ascribed to the inertia of moving segments and the dynamic properties of anatomical structures like joint capsules, ligaments, connective tissues and inactive muscles. The active impedance is caused by properties of activated muscle groups acting around a joint. Others try to decompose the impedance into an intrinsic and reflexive part. Here the intrinsic part arises from the mechanical properties of passive tissues and active muscles, whereas the reflexive part arises from reflexes, which lead to changes in muscle activation levels and consequently contribute to joint impedance.

Joint perturbation experiments on non-disabled subjects showed that the impedance depends on several factors, such as muscle contraction levels [3-5], joint angle [6,7], movement amplitude [5,8,9] and perturbation bandwidth [10,11]. These dependencies can be explained by several underlying physiological mechanisms. For example, the angular dependency is likely to be related to non-linear behavior of passive structures [12], the change in the overlap between the myosin and actin filaments [13] and changes in muscle moment arm [14]. The increase with contraction level is ascribed to the summation of the stiffness of parallel arranged cross bridges [15]. Cross-bridges are thought to cause a high stiffness during low amplitude perturbations, due to elastic stretch during the initial stages of the stretch, and a lower stiffness during large amplitude perturbations, due to detaching and reconnecting muscle filaments [16]. The bandwidth dependency is related to our capability to modulate our reflexive activity. For low bandwidth perturbations, humans increase their spinal reflexes (muscle spindles and golgi tendon organs) and effectively increase their joint impedance. At higher frequencies this is limited due to instabilities arising from reflexive time-delays [17]. These reflexes have also demonstrated larger gains for small amplitude perturbations, compared to larger perturbations [18].

A thorough understanding of joint stiffness and its variation with posture, muscle activation levels, environmental circumstance or diseases might prove useful for several applications. Knowledge about the way we modulate our joint impedance during different functional tasks like locomotion, running or balance control can benefit the design of

activated prostheses or orthoses [19] and can be used to improve the control of paralyzed limbs using functional electrical stimulation [20]. Additionally, joint impedance measurements can serve as a good basis for quantitative assessment and follow up of patients with ligament injuries [21], or abnormal joint stiffness (spasticity) due to neuromuscular disorders like SCI, stroke, cerebral palsy or Parkinson [22,23]. Quantitative impedance measures were also demonstrated to have an intra-subject reliability which was as good as or better than most clinical measures [24], which makes them also suitable as an objective indicator of the effectiveness of different types of rehabilitational interventions.

As mentioned above, several factors influence joint impedance. Still, the main factor is task instruction [25]. Task instruction is inherently linked to the applied perturbation type; force tasks are used during position perturbations and position tasks during force perturbations [26]. So far, most studies use position perturbations in combination with a torque/force task and focus on the effect of muscle contraction levels on joint stiffness. We believe that torque/force perturbations present a more natural disturbance, since the effort of the subjects is reflected in their performance, whereas during a position perturbation the subject has no influence on the performed movement. Therefore, in this study we will use torque perturbations in combination with relax- and position-tasks to determine the range of joint impedance.

Conventional methods for measuring joint impedance typically have been applied to a single joint. However, due to the presence of bi-articular muscles and heteronymous reflexes [27] the joint impedance of one joint is also influenced by the angular position or movement of the adjacent joint. Several studies have illustrated the effect of bi-articular muscles by the change in the hip-torque versus hip-angles curves, for different orientations of the knee joint and vice versa [28,29]. They are often used to describe how these elastic elements can serve as an energy storage and release mechanism, rather than quantifying the joint mechanics in terms of stiffness and damping [30]. Also, these studies are only performed for passive movements where the joints are slowly moved through its range of motion rather than applying perturbations. For the upper extremities this multi-joint characteristic of joint impedance has been acknowledged, and Multi Input Multi Output (MIMO) techniques have been used for the estimation of multi-joint stiffness (or endpoint stiffness) [31, 32].

The goal of this study is to use similar MIMO techniques to develop and evaluate an approach to assess multi-joint leg impedance using a robotic gait training device. The hip and knee joint will be mechanically perturbed simultaneously and its effect on both hip and knee angular displacement will be measured. Subsequent MIMO system identification techniques in the frequency domain will be used to distinguish between single joint and multi-joint effects. Significant coupling between both joints is expected due to their mechanical connection and the existence of bi-articular muscles and heteronymous reflexes. We used closed-loop identification techniques, which are appropriate when continuous torque disturbances are used. We also investigated the effect of task instruction (relax and positions tasks) and leg posture on the hip and knee stiffness.

6.2 Methods

6.2.1 Subjects

Eight elderly subjects between the age of 67 and 82 (age 74.8 ± 5.3, seven males, one female, weight 81.9 ± 11.6 kg) participated in this study. No subjects had symptoms of neurological or orthopedic dysfunction and all gave informed consent before participating in the experiments. The protocol was in accordance with the Declaration of Helsinki.

6.2.2 Apparatus

To apply hip and knee perturbations, the LOPES (Lower Extremity Powered ExoSkeleton) was used. The LOPES (figure 1) is an exoskeleton type robotic gait trainer with eight actuated Degrees of Freedom (DoF) and was initially designed to provide supported treadmill training for stroke patients. It is torque controlled by means of series elastic actuation (SEA) [33]. Matlab xPC (Mathworks, Natick, Mass., USA) is used to control the applied torques by the exoskeleton joints at 1000Hz. Potentiometers fitted to the LOPES joints record the joint angles. The applied joint torques are calculated from the deflection of the springs of the SEA. The exoskeleton knee and hip angle and exerted joint torques were sampled at 100Hz and stored for later processing.

6.2.3. Electromyography

Muscle activity was recorded (Porti 16-5, supplier: TMS International, Enschede, The Netherlands) from seven muscles acting about the knee and hip joint. We measured EMG levels of the mono-articular, vastus lateralis, gluteus maximus and bi-articular rectus femoris, semitendinosis, biceps femoris, gastrocnemius. Seniam guidelines [34] were followed for skin preparation and placement of the disc-shaped solid-gel Ag/AgCl-electrodes (in a bipolar configuration). The analog signals were sampled at 1024 Hz and

Figure 1: Left: The LOPES robotic gait trainer. It comprises a bilateral exoskeleton series elastic joints, actuated via Bowden cables and capable of applying torque perturbations to the hip and knee joint. Right: Experimental setup. During the perturbation experiments the subjects stood with the non-perturbed leg on a box such that the perturbed leg could move freely.

digitally stored for further processing. A sync signal was used to synchronize the EMG and LOPES data. All recordings were performed on the left leg only. As a reference for the EMG levels maximum voluntary contraction (MVC) levels were collected according to the Seniam guidelines [34]. Some of the cuffs of the LOPES were placed over the electrodes. To account for any changes in EMG levels due to the compression of the skin under the cuffs the MVC levels were recorded in the LOPES. The obtained MVC levels were used to scale the EMG levels during the different conditions.

6.2.4 Experimental protocol

Before positioning the subject in the LOPES, different anthropometric measurements were taken to adjust the exoskeleton segments lengths. Additionally, the position of the cuffs was adjusted in two DoFs to align the subject's knee and hip axis with the exoskeleton joints. Next, the subject was positioned into the LOPES and the trunk, thigh, and upper- and lower shank were strapped to the exoskeleton. To let the subject become familiar with the device, every subject was allowed 5 minutes to freely move in the device while it was operated in zero-impedance mode [35]. During the perturbation experiments the subjects stood with the non-perturbed leg on a box, while holding onto two parallel bars for support (figure 1). The height of the box was 15 cm, which was sufficient to clear the foot of the perturbed leg.

Experimental conditions

Subjects were asked to perform two different tasks: a relax task and a position task. While performing each task, the LOPES applied continuous torque perturbations to the knee and hip. During the position task the hip and knee angles were displayed on a screen in real time and the subject was instructed to keep the deviations as small as possible. During the relax task the subjects were asked not to interfere with the applied perturbations and the screen was turned off to prevent any distraction. To study the effect of leg orientation on the joint impedance, the position and relax tasks were performed at three different leg orientations (hip/knee angles of 5/-55, 25/-35 and 25/-15 degrees). These three leg orientations represent the leg orientation during natural gait, just after toe off, during swing and prior to heel strike. All conditions were randomized, with a resting period of at least two-minutes in between conditions. Since the active impedance does not differ between dominant and non-dominant limbs in healthy subjects [36], all perturbations were applied to the left leg. To obtain the dynamic properties of the exoskeleton, which are required for the estimation of the human dynamical properties, a similar set of experiments was performed without a subject in the LOPES.

Perturbation signal

Quasi random torque perturbations were used to prevent anticipatory muscle contractions. The perturbation signal was composed of multiple sinusoids. This multisine signal had a duration of 20 seconds, and contained power at 35 specified frequencies

(0.05-10 Hz, logarithmically spaced). They were generated off-line and allowed for a well-defined frequency domain analysis. As we used linear system identification techniques large movement amplitudes should be avoided. Therefore the phases of the different sines of the perturbation signal were optimized by using crest optimization [37]. To enable comparison of the different conditions and to justify a linear modeling approach, the amplitude of the multisine torque disturbance was adjusted for every subject and condition so that that the peak-to-peak amplitude of the resulting knee or hip angle did not exceed 15 degrees. These adjustments were made prior to the actual experiments.

A general requirement to identify a MIMO system is that for each degree of freedom an independent perturbation is required. This implies that the system needs to be perturbed in two different manners. In the first trial, the perturbations on the hip and knee had the same sign, whereas in the second trial, the perturbations had opposite signs. For each trial the multisine was repeated 7 times (140 seconds). To minimize the effect of fatigue, each trial during a position task was split up in 2 parts of 80 seconds, with a one minute resting period in between.

During all conditions a bias torque was superimposed on the multisine. The bias torque was used to compensate the gravity of the leg and exoskeleton. This allowed the subject to passively keep the knee and hip joint in the desired testing angle and prevented unwanted muscle contractions (especially during the relax task). The bias torque was set for every subject individually.

6.2.5 Data processing

All signal processing was done with custom-written software in Matlab (Natick, Mass., USA).

Muscle contraction levels

The raw EMG recordings were band-pass filtered (10-400 Hz) with a second-order zero-lag Butterworth filter to remove movement artifacts, full-wave rectified, and low-pass filtered with a low-pass second-order zero-lag Butterworth filter (5 Hz) to smooth the signal. The EMG was resampled to 100 Hz and synchronized to the LOPES data. Mean EMG levels were calculated for all the cycles of the perturbation cycle. Next these mean EMG levels were averaged for every condition to provide a single measure of muscle activity level per condition. Also the standard deviation of the mean EMG levels per condition was calculated to provide a measure for the variability in EMG levels over the different cycles.

Non-parametric MIMO system identification, Frequency Response Functions

The first cycle of the multisine was discarded, to eliminate possible transients at the start of each trial. The data from the remaining six cycles were Fourier transformed, and averaged over the six cycles to reduce the effects of noise. Note that only the Fourier coefficients at the frequencies of the multisine that contained power were used for

further processing. Next, MIMO frequency analysis techniques were used to obtain the non-parametric identification of the overall admittance. Although the admittance, and its inverse, the impedance, technically refers to the relationship between force and velocity, in many studies on joint properties these terms refer to the relationship between force and position [1]. Here the admittance is defined as the causal dynamic relationship with torque as input and angle as output.

The overall admittance of the system is defined according to:

$$\Theta(s) = T(s) \cdot H(s) \qquad [1]$$

where $\Theta(s)$ and $T(s)$ denote the Fourier transforms of the exoskeleton joint angles and applied joint torques respectively and s is the Laplace variable. For the sake of simplicity, (s) is omitted from this point forward. Since the total system (human+LOPES) represents a multivariate system with two inputs and two outputs the admittance Frequency Response Function (FRF) consists of a 2-by-2 matrix with FRFs. The FRFs are calculated according to:

$$H = T^{-1} \cdot \Theta \qquad [2]$$

$$\widehat{H}_{tot} = \begin{bmatrix} H_{\tau_{hip} \rightarrow \theta_{hip}} & H_{\tau_{hip} \rightarrow \theta_{knee}} \\ H_{\tau_{knee} \rightarrow \theta_{hip}} & H_{\tau_{knee} \rightarrow \theta_{knee}} \end{bmatrix} = \begin{bmatrix} \hat{T}_{hip\,1} & \hat{T}_{knee\,1} \\ \hat{T}_{hip\,2} & \hat{T}_{knee\,2} \end{bmatrix}^{-1} \cdot \begin{bmatrix} \widehat{\Theta}_{hip\,1} & \widehat{\Theta}_{knee\,1} \\ \widehat{\Theta}_{hip\,2} & \widehat{\Theta}_{knee\,2} \end{bmatrix} \qquad [3]$$

where T_{hip} and T_{knee} represent the Fourier transforms of the hip and knee torque. Θ_{hip} and Θ_{knee} represent the Fourier transforms of the exoskeleton joint angles. Superscript $^{-1}$ denotes the inverse, subscript $_1$ and $_2$ indicate the Fourier transforms obtained during the first and second trial and the circumflex ^ denotes an estimate. Note that matrix T requires to be invertible. Therefore the hip and knee were excited with the same periodic excitation in the first trial, whereas during the second trial the sign of the second perturbation was changed. $H_{\tau_{hip} \rightarrow \theta_{knee}}$ denotes the calculated FRF between applied hip torque and knee angle etc.

Noise-to-signal ratio

To determine whether it is justified to use time-invariant system-identification methods, we calculated the noise-to-signal ratio (NSR) in the frequency domain [38]. The *NSR* is the ratio of the remnant and the periodic response. Remnant can result from time-variant behavior and/or noise. Consequently a small *NSR* indicates a consistent response of the system to the applied perturbation over the different cycles. It also indicates that the system is appropriately perturbed.

$$NSR_{hip} = \frac{\sigma^2_{\Theta_{hip}}}{\left|\Theta_{hip}\right|^2} \qquad [4]$$

where $\sigma^2_{\Theta hip}$ represents the variance of the remnant (i.e. the variance of the Fourier transforms of the exoskeleton hip angle over the different cycles) and Θ_{hip} the periodic response (i.e. the mean of the Fourier transforms of the exoskeleton hip angle over the different cycles). The *NSR* of the knee angular response is calculated in a similar way. The *NSR* is only calculated for the excited frequencies (that is; the frequencies where the multisine disturbance contained power) and averaged over the frequencies.

Standard deviation

Another measure that reflects the consistency of the response was provided by the standard deviation of the hip and knee angular response. The standard deviation (*std*) was calculated over the different cycles of the perturbation signal. Next, the *std* was averaged over the recorded time instances (20 seconds/2000 samples) to obtain one representative parameter of the variability of the cycles in the time domain.

Model fit

To estimate the hip and knee impedance in terms of physiological relevant parameters, a linear model was constructed. In this model, the mechanical behavior of the complete system is represented by two double pendulums, one representing the exoskeleton/LOPES leg (LOPES pendulum) and one representing the subject's leg (human pendulum) (figure 2A). Both double pendulums are connected by means of parallel spring damper combinations (Kelvin body), which represent the cuffs of the LOPES and the soft tissue of the legs. Each segment of the human pendulum has a mass (located at a certain distance from the joint) and a radius of gyration (figure 2B). Additionally, it has a very simplified muscle model consisting of two mono-articular muscles and one bi-articular muscle (figure 2C), which represent the lumbed behavior of the different mono- and bi-articular muscles of the hip and knee. No attempt was made to discriminate between the individual properties of the different muscles and tendons. In terms of rotational visco-elastic properties the two mono-articular muscles and one bi-articular muscle effectively add rotational stiffness and damping to the hip (K_h, B_h), knee (K_k, B_k) and introduces a symmetric visco-elastic coupling between both joints (K_c, B_c). The definition of the model parameters is listed in table 1. See supplementary material for a detailed description of the model and the parameterized impedance Transfer Function (TF) of the human pendulum model (H_{model}). The best model fit was obtained by minimization of the following criterion function:

$$model\ error = \sum_f \left(\frac{\left| log(\widehat{H}_{human}(f)) - log(H_{model}(f)) \right|}{\left| log(\widehat{H}_{human}(f)) \right|} \right)^2 \quad [5]$$

where H_{model} represents the TF of the human pendulum model. $\widehat{H}_{human}$ represents the impedance FRF of the human leg and is calculated from the total admittance ($\widehat{H}_{tot}$), see supplementary material.

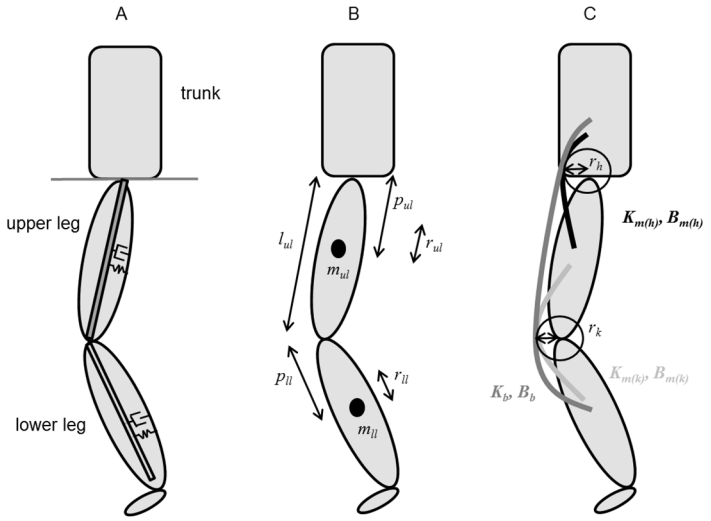

Figure 2: Model representation of the human leg that is attached to the LOPES exoskeleton. A: Schematic presentation of the dynamic model that is used for parameter estimation. It represents the human leg that is attached to the LOPES. Both the LOPES and the human are modelled as a double pendulum, which are connected by means of a parallel spring damper combinations at the thigh and shank. B: Fixed model parameters of the double pendulum that represents the human leg. C: Very simplified muscle model that is added to the double pendulum that represents the human leg. The model consists of two mono-articular muscles and one bi-articular muscle. Each muscle has a linear stiffness (K) and damping component (B). Subscript $_{m(h)}$ refers to the mono-articular muscle around the hip, $_{m(k)}$ to the mono-articular muscle around the knee, and $_b$ to the bi-articular muscle crossing both joints

The optimization was performed with an unconstrained nonlinear optimization routine, and on all 4 FRFs that comprise $\widehat{H}_{human}$ simultaneously. The criterion function is only evaluated for the excited frequencies. Since the *NSR* was relatively high at the frequencies above 3 Hz it was decided to only include all frequencies up to 3 Hz (25 frequencies in total).

To reduce the amount of model parameters that require fitting, the position of the center of mass, the radius of gyration, and the masses of the lower and upper leg were taken from empirical relations found in the literature [39]. To account for some subject variability we introduced a scaling factor (c) that scaled the mass of the upper and lower leg equally (assuming that subjects with an above-average lower leg mass also exhibit equally enlarged upper legs).

For each subject a total of seven parameters (K_h, B_h, K_k, B_k, K_c, B_c and c) had to be estimated for each condition. The most reliable estimates for the inertia are obtained at rest, when the contribution of joint stiffness and damping is small [31]. Therefore the scaling factor for the segment masses was first estimated for the three passive conditions (relax tasks) simultaneously. During the optimization, the stiffness and damping

Table 1: Model parameters.

	Description	Unit	Parameterization
K_h	Hip stiffness	Nm/rad	Optimized
K_k	Knee stiffness	Nm/rad	Optimized
K_c	Multi-joint stiffness due to bi-articular effect	Nm/rad	Optimized
B_h	Hip damping	Nms/rad	Optimized
B_k	Knee damping	Nms/rad	Optimized
B_c	Multi-joint damping due to bi-articular effect	Nms/rad	Optimized
c	Scaling factor for m_{ul} and m_{ll}	dimensionless	Optimized
l_{ul}	Length of the upper leg	m	Fixed (True value)
m_{ul}	Mass of the upper leg	kg	Fixed (0.115·body mass)[4]
p_{ul}	Position of the center of mass of the upper leg[2]	m	Fixed (0.425· upper leg length)[4]
r_{ul}	Radius of gyration of the upper leg	m	Fixed (0.29· upper leg length)[4]
l_{ll}	Length of the lower leg[1]	m	Fixed (True value)
m_{ll}	Mass of the lower leg[1]	kg	Fixed (0.061·body mass)[4]
p_{ll}	Position of the center of mass of the lower leg[1,3]	m	Fixed (0.525· lower leg length)[4]
r_{ll}	Radius of gyration of the lower leg[1]	m	Fixed (0.365· lower leg length)[4]

[1] *The parameters for the lower leg included the shank and foot.*
[2] *With respect to hip joint.*
[3] *With respect to knee joint.*
[4] *Parameters according to the list compiled by Stein et al.* [39] *(table II.For some parameters they reported a range, in those cases we used the mean.*

parameters were free for all three conditions, whereas the scaling factor was taken equally across the conditions. Also, for all three active conditions (position tasks) the model parameters were optimized simultaneously. Here the previously determined scaling factor was used for all conditions. This resulted in a total set of 37 parameters.

Model validation

To obtain a measure for the estimated model prediction we calculated the "goodness of fit" (*GOF*) in the frequency domain, where 100% reflects a perfect model fit.

$$GOF = \left(1 - \frac{\sum_f \left| \log(\widehat{H}_{human}(f)) - \log(H_{model}(f)) \right|^2}{\sum_f \left| \log(\widehat{H}_{human}(f)) \right|^2} \right) \cdot 100 \qquad [6]$$

The *GOF* was calculated for all 4 FRFs that comprise $\widehat{H}_{human}$ separately. Since we used a logarithmic criterion function we also calculated a logarithmic based *GOF*.

Perturbation evoked reflex mechanisms

In our model we do not attempt to decompose the stiffness into its reflexive and non-reflexive components. To determine the possible contribution of reflexive behavior to the joint stiffness we calculated the *NSR* (in the frequency domain) of the EMG signal at the

perturbed frequencies. This provides a measure for the consistency of the muscle activation levels at the perturbed frequencies. The raw EMG recordings were band-pass filtered (30-400 Hz) with a second-order zero-lag Butterworth filter, full-wave rectified, and synchronized with the LOPES data. The lower bound of the filter was set at 30Hz to ensure that all movement artefacts, due to the perturbation (which has frequencies up to 10Hz) are removed. Since this is done before rectifying the EMG signal this does not remove the actual muscle activation at the lower frequencies. The first cycle of the perturbation signal was discarded, to eliminate possible transients at the start of each trial. The EMG data from the remaining six cycles were Fourier transformed and the *NSR* was calculated for each muscle (in a similar way as described in eq.4).

6.2.6 Statistics

Stiffness and damping parameters were estimated in different leg postures. A Mixed Model Analysis of repeated measures was used for every model parameter to test the effect of leg orientation (3 levels) and task instruction (2 levels) on the estimated model parameters, at an alpha of 0.05. Post-hoc pairwise comparisons were performed with a Bonferroni correction to account for multiple comparisons. All statistical tests were performed with SPSS Statistics (IBM Corp., Armonk, NY, USA).

6.3 Results

6.3.1 Relax task

The angular response of the hip and knee joint to the 6 cycles of the perturbation signals were very consistent when subjects were instructed to relax (see figure 3 for a representative example). The consistent response of the subjects to the perturbation was also reflected in a low standard deviation and low *NSR* (figure 3). It also shows that the noise levels are low and that there is no time-variant behavior. Generally the *NSR* remains well below one and increases at the higher frequencies and lower frequency range (figure 3). Similar results were observed during the second perturbation round (with a knee perturbation with revered sign, figure 3) and during the perturbation for the other leg configurations. The average *NSR* levels (averaged over all frequencies, perturbation cycles, subjects and leg configurations) were 0.10 for the knee angle and 0.21 for the hip angle. The similarity in the response to the different cycles of the perturbation signal was also confirmed by the low standard deviation over the 6 cycles (figure 3). The average standard deviations (averaged over all perturbation rounds, subjects and leg configurations) were 0.6 and 1.3 degrees for the hip and knee respectively (table 2). For the relax tasks the average peak-to-peak torque amplitudes (averaged over all perturbation cycles, subjects and leg configurations) was 13.4 Nm for the hip, and 6.3 Nm for the knee, resulting in peak to peak angular displacement of 15.0 and 8.9 degrees (table 2). During the relax tasks the average EMG levels were 3% of the MVC (figure 4). We excluded two subjects from the analysis as they were not able to properly relax (EMG levels>10%MVC).

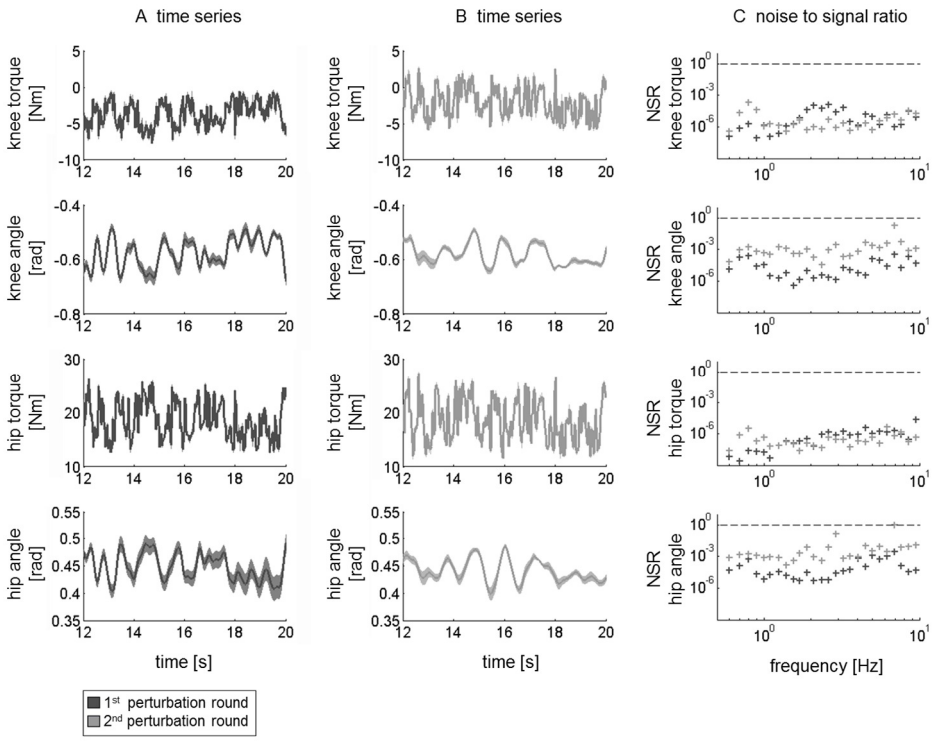

Figure 3: Time series and NSR during a relax task. Eight-second time series and NSR of one representative participant during a relax task (subject 5, leg orientation: hip=25°, knee=-35°). A: time series for the first perturbation round. B: time series for the second perturbation round. From top to bottom: knee torque perturbation, knee angular response, hip torque perturbation and hip angular response. For the time series the mean is depicted by the solid line and the standard deviation over the 6 cycles by the shaded area. C: NSR of the different signals, the dashed line depicts NSR=1. The responses of the participant were consistent, as evidenced by small standard deviations over the different cycles of the perturbations and low NSRs.

6.3.2 Position task

Generally, during the position task the variability in the response to the 6 cycles of the perturbation signal was larger than during the relax task (figure 5 for a representative example). This is also reflected in higher *NSR* levels and higher standard deviations over the cycles, especially for the hip joint (table 2). This is very likely due to some drift that occurs when the subjects co-contract. With the help of the visual feedback subjects tried to compensate for this drift by small, low frequency, angular corrections. These low frequency angular corrections also explain the larger *NSR* at the lower frequencies (figure 5). Subjects also indicated that it was easier to maintain a certain knee angle, opposed to keeping their hip joint in the required testing position. No consistent increase in the movement amplitude during the position task was found, which indicated that 1) fatigue was avoided and 2) a relatively constant co-contraction level was maintained. For the

Table 2: Experimental parameters.

	Relax task		Position task	
	Hip	**Knee**	**Hip**	**Knee**
Peak to peak angular displacement [deg]	8.9±1.5	15.0±2.9	9.2±1.0	13.5±2.0
Peak to peak angular torque [Nm]	13.4±1.2	6.3±1.0	19.9±0.2	10.6±0.9
NSR	0.21±0.23	0.10±0.04	0.54±0.26	0.21±0.10
***STD* [deg]**	0.6±0.1	1.3±0.8	1.9±0.5	2.3±0.7
***GOF* (with bi-articular effect)**	**Relax task**		**Position task**	
$H_{\theta_{hip}\rightarrow\tau_{hip}}$	99±0.23		99±0.95	
$H_{\theta_{hip}\rightarrow\tau_{knee}}$	85±20		88±12	
$H_{\theta_{knee}\rightarrow\tau_{hip}}$	78±13		94±5.0	
$H_{\theta_{knee}\rightarrow\tau_{knee}}$	84±27		94±7.3	
***GOF* (without bi-articular effect)**	**Relax task**		**Position task**	
$H_{\theta_{hip}\rightarrow\tau_{hip}}$	99±0.23		99±0.95	
$H_{\theta_{hip}\rightarrow\tau_{knee}}$	74±22		62±16	
$H_{\theta_{knee}\rightarrow\tau_{hip}}$	68±17		72±7.4	
$H_{\theta_{knee}\rightarrow\tau_{knee}}$	84±27		94±7.3	

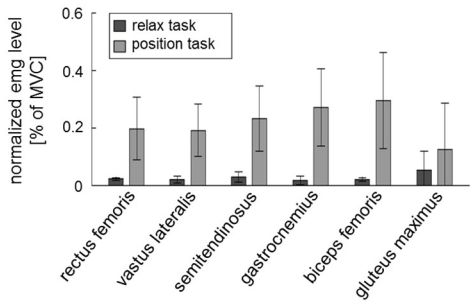

Figure 4: EMG levels. Normalized EMG levels for the recorded muscles during the relax (dark gray) and position (light gray) tasks. The EMG levels are averaged over all perturbation rounds, subjects and leg configurations. The error bars indicate the standard deviation.

position tasks the average peak-to-peak, angular response was similar to the relax task, whereas a higher peak-to-peak torque perturbation was required to evoke the displacement (table 2) due to the co-contraction. During the relax tasks the average EMG levels were 22% of the MVC levels (figure 4).During the position task, where the subjects were asked to keep a constant level of co-contraction, they were able to keep their co-contraction level relatively constant. Although they did not receive any EMG feedback, the average variation (i.e., standard deviation) of the mean EMG levels over the different cycles of the perturbation signal was only 4% of the MVC levels.

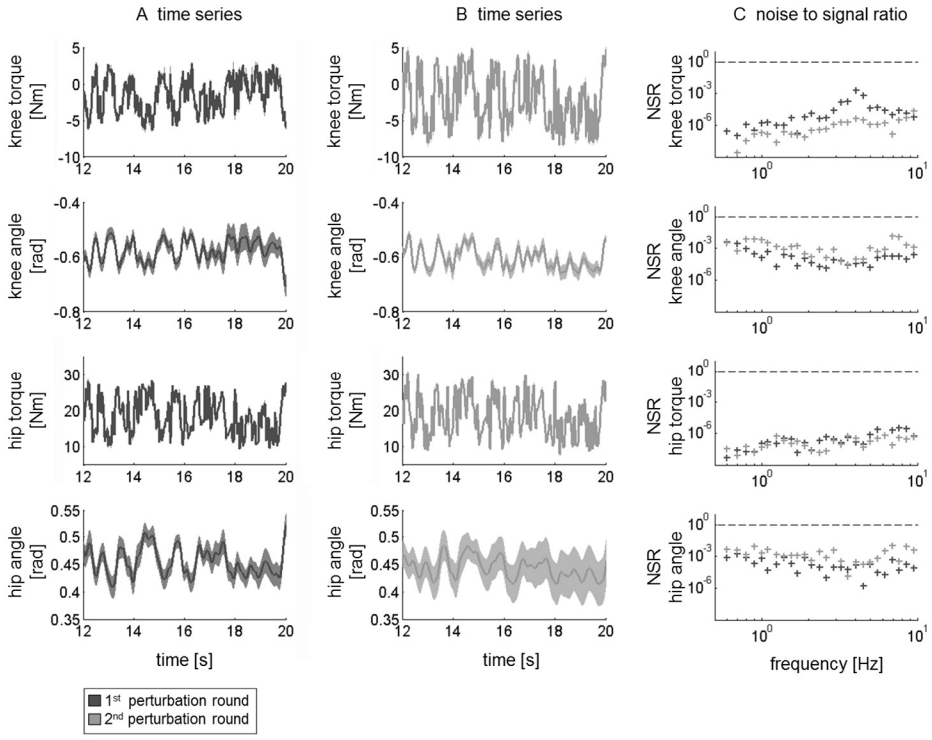

Figure 5: Time series and NSR during a position task. Eight-second time series and NSR of one representative participant during a position task (subject 5, leg orientation: hip=25°, knee=-35°). A: time series for the first perturbation round. B: time series for the second perturbation round. From top to bottom: knee torque perturbation, knee angular response, hip torque perturbation and hip angular response. For the time series the mean is depicted by the solid line and the standard deviation over the 6 cycles by the shaded area. C: NSR of the different signals, the dashed line depicts NSR=1. The responses of the participant were consistent, as evidenced by small standard deviations over the different cycles of the perturbations and low NSRs.

6.3.3 Non-parametric Frequency Response Functions

From the 2 perturbation trials we calculated the FRF of the total system (human and exoskeleton) (eq. 2) and subsequently the impedance FRF of the human leg. As expected (see supplementary material), each of the four impedance FRFs resembles a second-order system (see figure 6 for representative example). The relatively constant gain at the lower frequency range is due to the stiffness, whereas the reduced gain in the mid-frequency range is due to the viscous properties. The increasing gain with higher frequencies is due to the legs' inertia. Generally, the task instruction had a clear effect on the estimated FRF. The position task resulted in higher gains for the lower and mid frequency range. The task instruction did not affect the high frequency part of the FRFs, which is dominated by the leg's inertia.

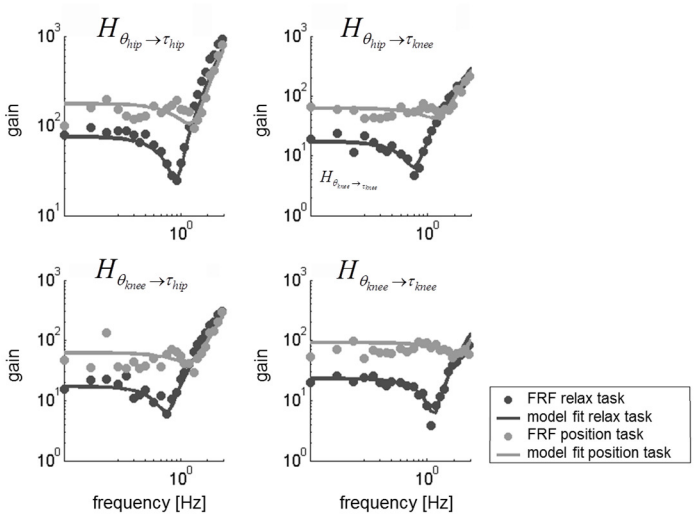

Figure 6: Model fit during relax and position task. Multiple-Input-Multiple-Output Frequency Response Functions (FRFs) of one representative participant during a relax task (dark gray) and position task (light gray) (subject 6, leg orientation: hip=25°, knee=-15°). $H_{\theta_{hip}\rightarrow\tau_{knee}}$ indicates the impedance FRF from hip angle to knee torque etc. The solid lines represent the TF of the optimized human leg model. The FRFs and model fit are only shown for the frequency range that is used for the parameter optimization (0.5-3 Hz).

6.3.4 Parametric identification, model fit

The estimated FRFs of the human leg could be described very well with the human leg model, for the relax as well as the position task (figure 6 for representative example). That the model accurately captured the dynamics of the system is also reflected in a generally high *GOF* for each of the four TFs of the pendulum model (table 2).

Adding the stiffness and damping parameters that represent the effect of bi-articular muscles, clearly improved the model fit. To illustrate this we also show the best model fit, not taking into account this bi-articular effect. If this bi-articular behavior is neglected the 2 FRFs: $H_{\theta_{hip}\rightarrow\tau_{knee}}$ and $H_{\theta_{knee}\rightarrow\tau_{hip}}$ are not properly fitted by the TFs of the model (figure 7 for representative example during a relax task). This is also illustrated by a clear reduction of the *GOF* for both TFs when the bi-articular effect was included (table 2).

6.3.5 Parametric identification, estimated model parameters

To avoid convergence of the fitting procedure to local minima we performed the optimization routine with different initial parameters. Still, all optimizations resulted in the same set of estimated parameters. Generally, the scaling factors, which were used to scale the masses of the upper and lower leg, were below 1 (0.88±0.11), indicating that the estimated masses are lower than reported in the literature [39].

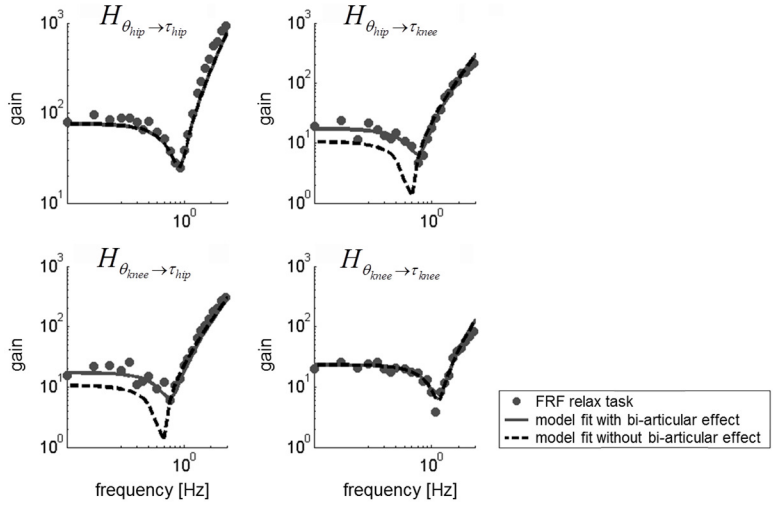

Figure 7: Model fit without bi-articular stiffness and damping. MIMO FRF of one representative participant during a relax task (subject 6, leg orientation: hip=25°, knee=-15°). $H_{\theta_{hip}\to\tau_{knee}}$ indicates the impedance FRF from hip angle to knee torque etc. The solid lines represent the TF of the optimized human leg model that includes the bi-articular stiffness and damping, whereas the dotted line shows the results from an optimized model without bi-articular stiffness and damping.

Task instruction significantly affected all the stiffness and damping parameters. During the position task all stiffness and damping parameters were significantly higher than during the relax task (table 3). The stiffness and damping parameters were less clearly affected by leg orientation. Leg orientation only significantly affected the K_k and B_c parameter. Post hoc pairwise comparison showed that K_k was significantly lower in the second position (hip at 5° an knee at -55°), compared to the first position (hip at 25° an knee at -15°) and B_c was significantly lower in the second position, compared to the third position (hip at 25° and knee at -35°). For the K_h and K_c parameters there was an interaction between task instruction and leg orientation. Post hoc tests showed there were significant differences in parameter stiffness levels (especially between the second and third position), whereas there were no differences during the relax task (figure 8).

6.3.6 Perturbation evoked reflex mechanisms

The model presented in this study only considers intrinsic muscle stiffness, but some of this stiffness may have been caused by reflex pathways excited by the perturbation. During the relax tasks there did not seem to be a difference in *NSR* at the perturbed frequencies compared to the non-perturbed frequencies. During the position task there was a reduced *NSR* at the higher perturbed frequencies (see figure 9 for a representative example). Although there seems to be a difference in EMG response during the relax and position task, the *NSR* is high, suggesting that the contribution of the reflex pathways to the stiffness is limited. In an effort to quantify this difference we calculated the mean *NSR*

Table 3: Statistical results.

	Task	Position	Task * Position
K_h	F(1, 29.927) = 158.834 p < 0.01	F(2, 28.788) = 4.814 p = 0.016	F(2, 28.788) = 5.923 p < 0.01
K_k	F(1, 29.671) =77.840 p < 0.01	F(2, 27.540) = 2.827 p = 0.076	F(2, 27.540) = 5.097 p = 0.013
K_c	F(1, 29.324) = 157.418 p < 0.01	F(2, 28.293) = 2.842 p = 0.075	F(2, 28.293) = 2.6234 p = 0.089
B_h	F(1, 30.307) = 205.394 p < 0.01	F(2, 29.242) = 2.661 p = 0.087	F(2, 29.424) = 0.103 p = 0.903
B_k	F(1, 33.473) = 80.814 p < 0.01	F(2, 29.988) = 8.375 p < 0.01	F(2, 29.988) = 0.510 p = 0.606
B_c	F(1, 31.489) = 22.081 p < 0.01	F(2, 25.851) = 3.444 p = 0.047	F(2, 25.851) = 0.112 p = 0.895

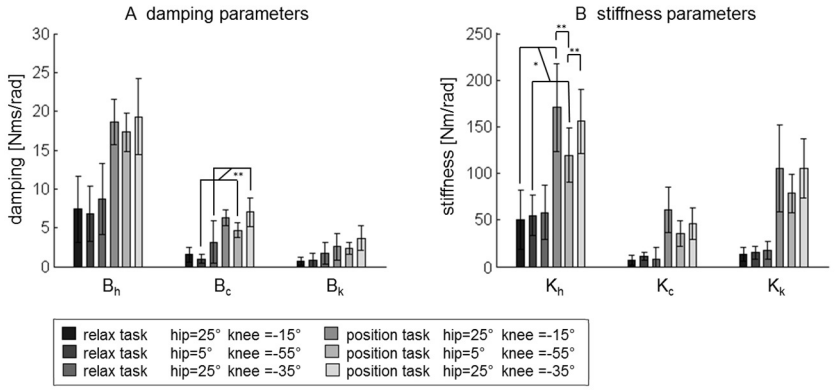

*Figure 8: Stiffness and damping parameters. Estimated stiffness and damping parameters for the relax and position tasks in the different leg orientations. The error bars indicate the standard deviation over the subjects. For all parameters there was also a significant main effect of task instruction (p < 0.01). Other significant main effects and interaction effects are indicated with a * for p < 0.05 and ** for P < 0.01.*

over the 10 highest perturbed frequencies (3.2-10 Hz) and the non-perturbed frequencies 27.9±155.0 (averaged over all muscles, subjects and leg configurations) and 33.5±30.9 at the non-perturbed frequencies. For the position task the mean *NSR* at the perturbed frequencies was 6.07±19.2 and 30.1±37.0 at then non-perturbed frequencies.

6.4 Discussion and conclusion

In this study we present a method to estimate hip and knee dynamic properties during multi-joint leg movements, using a robotic gait trainer. The LOPES was successfully used to apply continuous multisine force perturbations to the hip and knee joint simultaneously.

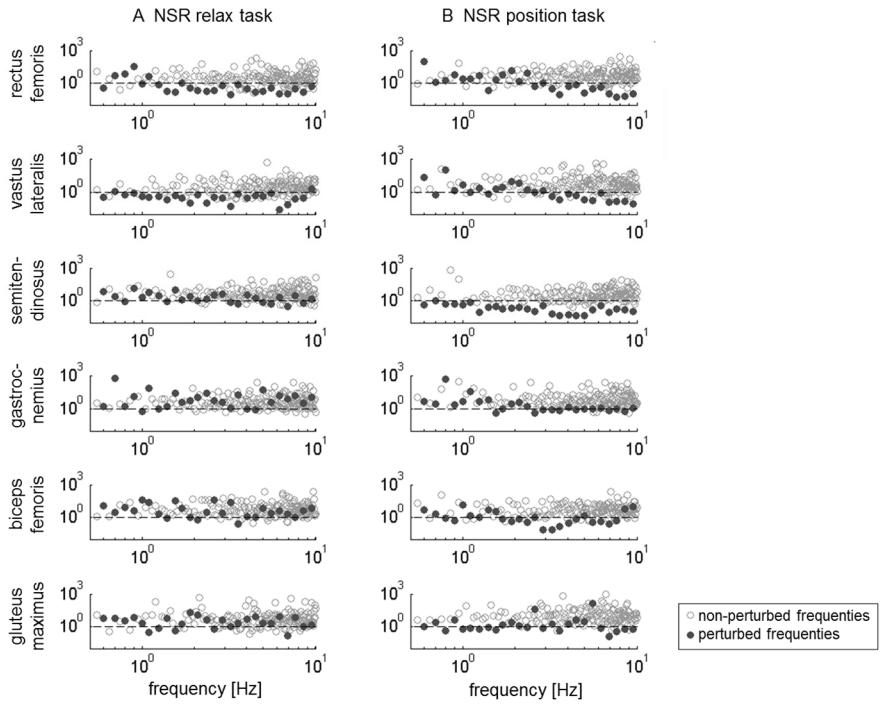

Figure 9: NSR of the EMG activity. NSR of the EMG activity for the 6 recorded muscles of one representative participant (subject 5) during a relax task and during a position task (leg orientation: hip=25°, knee=-35°). The solid dark gray circles represent the NSR at the perturbed frequencies, the dashed line depicts NSR=1.

Frequency-domain MIMO linear system identification techniques were used to quantify the hip and knee dynamic (inter) joint stiffness, damping, and limb inertia. The results indicate that 1) all stiffness and damping parameters were significantly higher during the position task compared to the relax task, 2) the majority of the stiffness and damping parameters were not significantly affected by leg orientation and 3) including the effect of bi-articular muscles clearly improves the predictability of the multi-joint leg model. This section discusses these findings in further detail.

6.4.1 Estimated segment masses

In this study we scaled segment masses found in the literature to fit the estimated FRFs. The scaling factor ranged between 0.74 and 1.0, with an average of 0.88, indicating that the estimated masses for most subjects were slightly lower than reported in the literature [39]. This may be related to the elderly population that we included, who may have relatively low upper- and lower-leg masses due to reduction in muscle mass. Preliminary data (not shown) on 9 young subjects (age 24.8±2.1), using the same protocol, resulted in an average scaling factor of 0.99±0.08.

6.4.2 Effect of task instruction

All stiffness and damping parameters that were used to model the multi-joint leg dynamics were significantly higher during the position task compared to the relax task. During the position task subjects used co-contraction to reduce the displacement amplitude. Stiffness and damping are strongly related to muscle activation levels, due to a larger number of active cross bridges. Overall, the stiffness and damping parameters increased with 273% and 157% when the subjects were asked to minimize joint displacements.

Knee Stiffness

For the relax task we found an average stiffness of 15.3 Nm/rad, which seems reasonable taking into account the perturbation amplitude. It is known that estimates for joint stiffness decrease with perturbation amplitude, due to cross-bridges dynamics. Although these amplitude dependencies are often associated with active muscles, they are also observed in passive isolated muscles [40]. More recently, amplitude dependencies have also been reported for the human knee joint [5,9]. In the current study we evoked angular displacements with a peak-to-peak amplitude of 15°. Studies that used small amplitude perturbations reported larger stiffness levels [4,5,9]. Reversely, studies that applied pull or drop tests, and consequently evoked larger movement, reported lower stiffness levels [39].

Only a few studies tried to measure knee stiffness during co-contraction. Pfeifer et al. [5] applied small amplitude position perturbations at different co-contraction levels. Their highest level of co-contraction corresponded to 10% MVC and resulted in a measured active stiffness ranging between 50 and 130 Nm/rad. In our study the estimated stiffness during the position task ranged between 50 and 190Nm/rad, but corresponded to higher co-contraction levels (22% MVC). Note also that this included the passive stiffness, whereas the active stiffness reported by Pfeifer et al. is defined as the total stiffness minus the stiffness measured in relax condition. Tai et al. [9] performed one of the few studies studying stiffness during a position task as we did. They reported knee stiffness levels similar to ours, ranging between 130 Nm/rad (at low amplitude perturbations) to 60 Nm/rad (for large amplitude perturbations). Regretfully they did not record the amount of muscle contraction. The fact that the above mentioned studies report similar stiffness levels, while using a wide variety of perturbation amplitudes also suggests that the amplitude-dependent change in knee stiffness primarily arises from passive properties of the joint. This has also been confirmed experimentally by Pfeifer et al. [5] who showed a drastic reduction in passive stiffness with increasing perturbation amplitude, whereas the active part of the total stiffness remained relatively constant. Similarly, Tai et al. [9] showed a reduction in active stiffness at larger amplitudes, which can predominantly be attributed to a reduction of the passive stiffness .

Knee damping

Knee damping has only been determined in a limited number of studies. The passive knee damping found in our study (1.1 Nms/rad) is in agreement with these studies. Tai et al. [41] and Zhang et al. [4] and, who used small amplitude position perturbations, reported a passive damping parameters of around 1 and 2 respectively. During the position task we found a damping of 2 Nms/rad, similar as reported by Tai et al. [41]. They also showed that the damping parameter is not affected by perturbation amplitude (during passive conditions as well as co-contraction). This may explain why we found similar damping levels, even though we used perturbations with larger amplitudes.

Hip stiffness and damping

Hip dynamics were not studied as extensively as knee dynamics, and there are no studies where the hip joint was mechanically perturbed to estimate its stiffness and damping parameters. Torque-angle curves have been obtained while slowly moving the hip through its range of motion, but the stiffness based on the derivative of these curves is much lower than the stiffness during the relax task found in our study. As suggested before this may be related to different mechanisms, that are active when the amplitude of the movement increases. In this study we found that the passive hip stiffness was much larger than the passive knee stiffness, possibly due to a larger amount of ligaments and muscle mass surrounding the hip joint.

6.4.3 Effect of leg orientation on knee stiffness

In this study we did not find a significant effect of leg orientation on knee stiffness. For the knee stiffness during a relax task Zhang et al. [4] and Tai et al. [9] report that the highest stiffness levels are recorded in the most extended positions (<10° flexion). That we did not find such a dependency is most likely due to the relatively high flexion angles that we tested (15°, 35 and 55°). Note also that, in order to make a fair comparison between passive knee stiffness levels the hip angle should be taken into account, as this angle effects the pretention of bi-articular muscles and consequently the knee stiffness [29].

For the knee stiffness during a position task Tai et al. [9] found that the stiffness was largest for the most extended positions, even after subtraction of the passive part. Although we did not find a significant effect of leg orientation on knee stiffness the largest average knee stiffness (after subtraction of the passive part) was found in the most extended position. The relatively large moment arm of the knee flexor muscles around 15° [14] might explain the increase in stiffness in the extended position.

6.4.4 Estimating inter-joint stiffness and damping

All previous studies that assessed joint stiffness and damping in the lower extremities focused on a single joint. In the current study we perturbed the hip and knee joint simultaneously to assess multi-joint leg impedance. To model the recorded multi-joint leg

impedance a simple muscle model was constructed that also included the visco-elastic coupling between both joints, caused by bi-articular muscles. This model simulated the combined effect of bi-articular muscles like the hamstrings and the rectus femoris. The results show that these muscles create a substantial coupling between both joints, as reflected in the K_c and B_c parameter.

Hogan et al. [42] showed that for arm movements the presence of bi-articular muscles around the shoulder and elbow dramatically increases the ability of the central nervous system to modulate the so called end-point stiffness (stiffness of the hand in Cartesian space), through coordinated muscle activation of mono and bi-articular muscles. He showed that without coupling between the joints it is not possible to achieve an isotropic end-point stiffness (meaning that an input displacement in any direction would produce a proportional restoring force in exactly the opposite direction). In other words, without bi-articular muscles the end-point stiffness cannot be modulated in all directions, whereas humans have shown to be capable of modulating their endpoint stiffness such that it specifically increases in the direction of the instability in the environment [43].

A similar mechanism might also be present in the lower extremities, to modulate the stiffness of the total leg. Simple bipedal spring damper-mass models have already shown that the basic dynamics of walking and running can be explained by modelling the leg as one compliant element [44,45], whose properties can be adjusted to cope with different environmental condition or disturbance [46]. As with the upper extremities, the existence of a bi-articular coupling between the different joints increases the possibilities to modulate the compliance of the total leg. In fact, biped robot that are fitted with springs that correspond to bi-articular muscles have shown to improve the self-stabilizing characteristics for both walking and running gaits, compared to a setup where only mono-articular springs are used [47]. Thus, besides the ability to transfer energy between different joints [48], which is often regarded as their main task, bi-articular muscles might also contribute to a more stable gait.

6.4.5 Limitations

In this study we performed perturbations during relaxed state and during co-contracted states. The co-contracted state was used to determine the maximum joint impedance. Still, this resulted in relatively low co-contraction levels (22% MVC). This is probably related to the duration of the experiments. Subjects had to maintain a constant level of co-contraction throughout the trials. Since they are aware of the 1-minute duration of the position tasks they may choose a relatively low co-contraction level. Still, the contraction levels are much higher than during the relax task (3% MVC) and have a clear effect on the stiffness. We also observed quite some variability in the EMG levels during the position task. The large inter-subject variability in the active stiffness (figure 8) could be a reflection of the differences caused by different co-contraction levels. During the passive trials the inter-subject variability in parameters was smaller.

In our study we did not model reflexes that may have been evoked by the perturbation. Several studies showed that reflex activation contributes to joint stiffness for the ankle [49,50]. For the knee joint Pfeifer et al. [5] reported that there was no substantial relationship between perturbation and EMG during the passive trials, suggesting little reflex contribution, whereas during the active trials it was possible to predict 15-30% of the EMG variance. In our study we did observe a reduced *NSR* of the EMG at the perturbed frequencies compared to the non-perturbed frequencies during the position task (figure 9). However, the *NSR* was high, suggesting that the contribution of the reflex pathways to the stiffness is limited. Since we used perturbation with much larger amplitudes, and reflex response have been shown to decrease with amplitude [18] and at high levels of muscle contraction [49,50], we did not expect a large contribution of reflex activation to the measured knee stiffness. Additionally, these reflexes have a decreased effect during sustained voluntary contractions [51] and have greater contributions for lower frequency bandwidth perturbations [52], whereas we also included higher frequencies.

6.4.6 Future directions

This study shows that the LOPES can be used to estimate multi-joint stiffness, as long as the equilibrium position of the joint and the levels of co-contraction remain constant. Measuring joint stiffness with the same device that is used for robotic gait training allows convenient testing of joint properties as part of robotic gait training protocols, and can provide direct insight into how changes in joint properties affect gait function. In order to gain direct insight into how humans modulate their limb stiffness during different gait-related tasks, it would be of great benefit to estimate the joint stiffness during locomotion itself. Such knowledge may allow the adaptability and complexity of unimpaired gait to be implemented in activated prostheses or orthoses. Also, increased stiffness is reported in neurological patients during relax conditions, but little is known about its consequences and even its occurrence during gait. Finally, estimates of the joint stiffness of neurological patients during locomotion might be used to create a patient specific leg model and optimize the amount of applied torques by rehabilitation devices like the LOPES.

Acknowledgments

This study was supported by a grant from Dutch Ministry of Economic affairs and Province of Overijssel, the Netherlands (grant: PID082004), and the EU, within the EVRYON Collaborative Project (Evolving Morphologies for Human-Robot Symbiotic Interaction, Project FP7-ICT-2007-3-231451).

References

[1] D. T. Westwick and E. J. Perreault, "Estimates of acausal joint impedance models.," *IEEE Trans. Biomed. Eng.*, vol. 59, no. 10, pp. 2913-21, 2012.

[2] R. E. Kearney and I. W. Hunter, "System identification of human joint dynamics," *Crit Rev Biomed Eng*, vol. 18, no. 1, pp. 55-87, 1990.

[3] P. L. Weiss, I. W. Hunter, and R. E. Kearney, "Human ankle joint stiffness over the full range of muscle activation levels," *J. Biomech.*, vol. 21, no. 7, pp. 539-544, 1988.

[4] L. Q. Zhang, G. Nuber, J. Butler, M. Bowen, and W. Z. Rymer, "In vivo human knee joint dynamic properties as functions of muscle contraction and joint position," *J Biomech*, vol. 31, no. 1, pp. 71-76, 1998.

[5] S. Pfeifer, H. Vallery, M. Hardegger, R. Riener, and E. J. Perreault, "Model-based estimation of knee stiffness.," *IEEE Trans. Biomed. Eng.*, vol. 59, no. 9, pp. 2604-12, 2012.

[6] G. L. Gottlieb and G. C. Agarwal, "Dependence of human ankle compliance on joint angle," *J. Biomech.*, vol. 11, no. 4, pp. 177-181, 1978.

[7] P. L. Weiss, R. E. Kearney, and I. W. Hunter, "Position dependence of ankle joint dynamics--II. Active mechanics," *J Biomech*, vol. 19, no. 9, pp. 737-751, 1986.

[8] R. E. Kearney and I. W. Hunter, "Dynamics of human ankle stiffness: Variation with displacement amplitude," *J. Biomech.*, vol. 15, no. 10, pp. 753-756, 1982.

[9] C. Tai and C. J. Robinson, "Knee elasticity influenced by joint angle and perturbation intensity.," *IEEE Trans. Rehabil. Eng.*, vol. 7, no. 1, pp. 111-5, 1999.

[10] F. C. van der Helm, A. C. Schouten, E. de Vlugt, and G. G. Brouwn, "Identification of intrinsic and reflexive components of human arm dynamics during postural control," *J Neurosci Methods*, vol. 119, no. 1, pp. 1-14, 2002.

[11] W. Mugge, D. A. Abbink, and C. T. Helm, "Reduced Power Method: how to evoke low-bandwidth behaviour while estimating full-bandwidth dynamics," in *Proceeding of the IEEE International Conference on Rehabilitation Robotics,* pp. 575-581, 2007

[12] P. L. Weiss, R. E. Kearney, and I. W. Hunter, "Position dependence of ankle joint dynamics--I. Passive mechanics.," *J. Biomech.*, vol. 19, no. 9, pp. 727-35, 1986.

[13] P. M. H. Rack and D. R. Westbury, "The effect of length and stimulus rate on tension in the isometric cat soleus muscle," *J. Physiol.* , pp. 443-460, 1969.

[14] M. D. Klein Horsman, H. F. J. M. Koopman, F. C. T. van der Helm, and H. E. J. Veeger, "The Twente Lower Extremity Model: a comparison of muscle moment arms with the literature," *Dissertation*, 2007.

[15] D. L. Morgan, "Separation of active and passive components of short-range stiffness of muscle.," *Am. J. Physiol.*, vol. 232, no. 1, pp. C45-C49, 1977.

[16] P. M. Rack and D. R. Westbury, "The short range stiffness of active mammalian muscle and its effect on mechanical properties.," *J. Physiol.*, vol. 240, no. 2, pp. 331-350, 1974.

[17] E. de Vlugt, F. C. van der Helm, a C. Schouten, and G. G. Brouwn, "Analysis of the reflexive feedback control loop during posture maintenance.," *Biol. Cybern.*, vol. 84, no. 2, pp. 133-41, 2001.

[18] A. Klomp, J. H. De Groot, E. De Vlugt, C. G. M. Meskers, J. H. Arendzen, and F. C. T. Van Der Helm, "Perturbation Amplitude Affects Linearly Estimated Neuromechanical Wrist Joint Properties," *IEEE Trans Biomed Eng*, vol. 61, no. 4, pp. 1005-1014, 2014.

[19] A. H. Hansen, D. S. Childress, S. C. Miff, S. a Gard, and K. P. Mesplay, "The human ankle during walking: implications for design of biomimetic ankle prostheses.," *J. Biomech.*, vol. 37, no. 10, pp. 1467-74, 2004.

[20] E. J. Perreault, A. M. Acosta, R. F. Kirsch, P. E. Crago, C. Western, and E. Ave, "Using Estimates of Dynamic Endpoint Stiffness to Quantify the Effects of Triceps Functional

Neuromuscular Stimulation," in *Proceedings of the 2nd Annual Conference of the International Functional Electrical Stimulation Society*, pp. 2-4, 2011

[21] J. T. Blackburn, D. A. Padua, B. L. Riemann, and K. M. Guskiewicz, "The relationships between active extensibility, and passive and active stiffness of the knee flexors," *J. Electromyogr. Kinesiol.*, vol. 14, no. 6, pp. 683-691, 2004.

[22] M. M. Mirbagheri, H. Barbeau, M. Ladouceur, and R. E. Kearney, "Intrinsic and reflex stiffness in normal and spastic, spinal cord injured subjects.," *Exp. Brain Res.*, vol. 141, no. 4, pp. 446-59, 2001.

[23] L. Galiana, J. Fung, and R. Kearney, "Identification of intrinsic and reflex ankle stiffness components in stroke patients," *Exp Brain Res*, vol. 165, no. 4, pp. 422-434, 2005.

[24] R. E. Kearney, P. L. Weiss, and R. Morier, "System identification of human ankle dynamics: intersubject variability and intrasubject reliability.," *Clin. Biomech. (Bristol, Avon)*, vol. 5, no. 4, pp. 205-17, 1990.

[25] D. A. Abbink, "Task instruction: The largest influence on human operator motion control dynamics," in *Proceedings of the Second Joint EuroHaptics Conference and Symposium on Haptic Interfaces for Virtual Environment and Teleoperator Systems,* pp. 206-211, 2007

[26] P. A Forbes, R. Happee, F. C. T. van der Helm, and A. C. Schouten, "EMG feedback tasks reduce reflexive stiffness during force and position perturbations.," *Exp. brain Res.*, vol. 213, no. 1, pp. 49-61, 2011.

[27] R. J. H. Wilmink and T. R. Nichols, "Distribution of heterogenic reflexes among the quadriceps and triceps surae muscles of the cat hind limb.," *J. Neurophysiol.*, vol. 90, no. 4, pp. 2310-2324, 2003.

[28] A. Silder, B. Whittington, B. Heiderscheit, and D. G. Thelen, "Identification of passive elastic joint moment-angle relationships in the lower extremity.," *J. Biomech.*, vol. 40, no. 12, pp. 2628-35, 2007.

[29] R. Riener and T. Edrich, "Identification of passive elastic joint moments in the lower extremities," *J. Biomech.*, vol. 32, no. 5, pp. 539-544, 1999.

[30] B. Whittington, A. Silder, B. Heiderscheit, and D. G. Thelen, "The contribution of passive-elastic mechanisms to lower extremity joint kinetics during human walking.," *Gait Posture*, vol. 27, no. 4, pp. 628-34, 2008.

[31] E. J. Perreault, R. F. Kirsch, and P. E. Crago, "Multijoint dynamics and postural stability of the human arm.," *Exp. brain Res.*, vol. 157, no. 4, pp. 507-17, 2004.

[32] E. De Vlugt, A. C. Schouten, and F. C. Van der Helm, "Closed-loop multivariable system identification for the characterization of the dynamic arm compliance using continuous force disturbances: a model study," *J Neurosci Methods*, vol. 122, no. 2, pp. 123-140, 2003.

[33] J. Veneman, "Design and evaluation of the gait rehabilitation robot lopes," *Dissertation*, 2007.

[34] H. J. Hermens, B. Freriks, R. Merletti, D. Stegeman, J. Blok, G. Rau, C. Disselhorst-Klug, and G. Hägg, *European recommendations for surface electromyography, results of the SENIAM project*. Enschede: Roessingh Research and Development B.V, 1999.

[35] E. H. F. van Asseldonk, J. F. Veneman, R. Ekkelenkamp, J. H. Buurke, F. C. T. van der Helm, and H. van der Kooij, "The Effects on Kinematics and Muscle Activity of Walking in a Robotic Gait Trainer During Zero-Force Control.," *IEEE Trans. Neural Syst. Rehabil. Eng.*, vol. 16, no. 4, pp. 360-370, 2008.

[36] A. G. Jennings and B. B. Seedhom, "The measurement of muscle stiffness in anterior cruciate injuries -- an experiment revisited," *Clin Biomech (Bristol, Avon)*, vol. 13, no. 2, pp. 138-140, 1998.

[37] R. Pintelon and J. Schoukens, *System identification: a frequency domain approach*. New York, USA: IEEE Press, 2001.

[38] T. A. Boonstra, A. C. Schouten, and H. van der Kooij, "Identification of the contribution of the ankle and hip joints to multi-segmental balance control.," *J. Neuroeng. Rehabil.*, vol. 10, no. 1, pp. 1-18, 2013.

[39] R. B. Stein, E. P. Zehr, M. K. Lebiedowska, D. B. Popovic, A. Scheiner, and H. J. Chizeck, "Estimating mechanical parameters of leg segments in individuals with and without physical disabilities," *IEEE Trans Rehabil Eng*, vol. 4, no. 3, pp. 201-211, 1996.

[40] U. Proske and D. L. Morgan, "Do cross-bridges contribute to the tension during stretch of passive muscle?," *J. Muscle Res. Cell Motil.*, vol. 20, no. 5-6, pp. 433-42, 1999.

[41] C. Tai and C. J. Robinson, "Variation of human knee stiffness with angular perturbation intensity," in *Proc. 17th Int. Conf. Eng. Med. Biol. Soc.*, 1995.

[42] N. Hogan, "The Mechanics of Multi-Joint Posture and Movement Control," *Biol Cybern*, vol. 331, pp. 315-331, 1985.

[43] D. W. Franklin, G. Liaw, T. E. Milner, R. Osu, E. Burdet, and M. Kawato, "Endpoint stiffness of the arm is directionally tuned to instability in the environment.," *J. Neurosci.*, vol. 27, no. 29, pp. 7705-16, 2007.

[44] H. Geyer, A. Seyfarth, and R. Blickhan, "Compliant leg behaviour explains basic dynamics of walking and running.," in *Proc. Biol. Sci.*, vol. 273, no. 1603, pp. 2861-7, 2006.

[45] E. Etenzi, S. Micera, and S. S. S. Anna, "Model of a stable passive bipedal walker provided with spring-damping legs .," pp. 5-6.

[46] M. Ernst, H. Geyer, and R. Blickhan, "Extension and customization of self-stability control in compliant legged systems.," *Bioinspir. Biomim.*, vol. 7, no. 4, pp. 1-10,2012.

[47] F. Iida, J. Rummel, and A. Seyfarth, "Bipedal walking and running with spring-like biarticular muscles.," *J. Biomech.*, vol. 41, no. 3, pp. 656-67, 2008.

[48] J. V. A. N. Ingen, "From rotation to translation : constraints on multi-joint movements and the unique action," *Hum. Mov. Sci.*, vol. 8, pp. 301-337, 1989.

[49] T. Sinkjaer, E. Toft, S. Andreassen, and B. C. Hornemann, "Muscle stiffness in human ankle dorsiflexors: intrinsic and reflex components.," *J. Neurophysiol.*, vol. 60, no. 3, pp. 1110-1121, 1988.

[50] M. M. Mirbagheri, H. Barbeau, and R. E. Kearney, "Intrinsic and reflex contributions to human ankle stiffness: variation with activation level and position," *Exp Brain Res*, vol. 135, no. 4, pp. 423-436, 2000.

[51] G. Macefield, K. E. Hagbarth, R. Gorman, S. C. Gandevia, and D. Burke, "Decline in spindle support to alpha-motoneurones during sustained voluntary contractions.," *J. Physiol.*, vol. 440, pp. 497-512, 1991.

[52] F. C. T. van der Helm, A. C. Schouten, E. de Vlugt, and G. G. Brouwn, "Identification of intrinsic and reflexive components of human arm dynamics during postural control.," *J. Neurosci. Methods*, vol. 119, no. 1, pp. 1-14, 2002.

Supplementary material

This appendix summarized the model that is used to describe the dynamics of the human that is connected to the LOPES.

Figure 10 shows the linear system approximation of the non-linear model shown in figure 2A, expressed in the frequency domain.

The input consists of the applied knee and hip torque (T) and the output is formed by the exoskeleton hip and knee angle (Θ). The exoskeleton dynamics (H_{exo}) describe the dynamic behavior of the exoskeleton in terms of the admittance and the human dynamics (H_{human}) describe the dynamic behavior of the human (admittance). The strap dynamics (H_{strap}) describe the dynamic behavior of the connection between exoskeleton and human (impedance). The strap dynamics is used to model the dynamic behavior that arises from the fact that the LOPES cannot be rigidly connected to the human (due to soft tissue surrounding the legs). The admittance of the total system (H_{tot}) becomes:

$$H_{tot} = \left[I + H_{exo} \left[I + H_{strap} \cdot H_{human} \right]^{-1} \cdot H_{strap} \right]^{-1} \cdot H_{exo} \qquad [7]$$

where I is a 2-by-2 unit matrix. Rewriting equation 4 yields the equation used to estimate the admittance FRF or the human leg ($\hat{H}_{human}$).

$$\hat{H}_{human} = \left[\hat{H}_{tot}^{-1} - \hat{H}_{exo}^{-1} \right]^{-1} - \hat{H}_{strap}^{-1} \qquad [8]$$

Each part of the equation represents a 2by2 matrix with Transfer Functions (TFs) or Frequency Response Functions (FRFs). $\hat{H}_{tot}$ refers to FRFs of the estimated admittance of the total system, calculated according to:

$$\hat{H}_{tot} = \begin{bmatrix} H_{\tau_{hip} \to \theta_{hip}} & H_{\tau_{hip} \to \theta_{knee}} \\ H_{\tau_{knee} \to \theta_{hip}} & H_{\tau_{knee} \to \theta_{knee}} \end{bmatrix} = \begin{bmatrix} \hat{T}_{hip\,1} & \hat{T}_{knee\,1} \\ \hat{T}_{hip\,2} & \hat{T}_{knee\,2} \end{bmatrix}^{-1} \cdot \begin{bmatrix} \hat{\Theta}_{hip\,1} & \hat{\Theta}_{knee\,1} \\ \hat{\Theta}_{hip\,2} & \hat{\Theta}_{knee\,2} \end{bmatrix} \qquad [9]$$

The strap dynamics (H_{strap}) was modeled as a 2-by-2 matrix with the TFs of the two Kelvin bodies on its diagonal. The strap viscosity and stiffness were set at 500 Nm/rad and

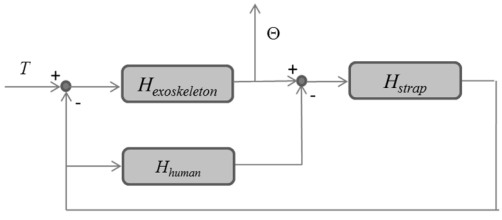

Figure 10: Linear system approximation of the nonlinear system (figure 2A), relating input joint torque disturbances (T) output exoskeleton segment angles (Θ).

2Ns/rad (based on pilot experiments), and equal for hip and knee joint. These parameters were kept constant for all subjects and conditions. $\widehat{H}_{exo}$ refers to the estimated FRFs of the admittance of the exoskeleton. These are obtained by performing the same perturbation experiments (and applying eq. 9), but without a subject in the LOPES.

To obtain the 4 parameterized TFs (H_{human}), that can be fitted on the $\widehat{H}_{human}$, the equations of motions of a double pendulum are derived using Kane's method (TMT method). Each segment of the double pendulum has a mass (located at a certain distance from the joint), a radius of gyration (figure 2B). It also contains a very simplified muscle model consisting of two mono articular muscles and one bi-articular muscle (figure 2C), which represent the lumbed behavior of the different mono- and bi-articular muscles of the hip and knee. In terms of rotational visco-elastic properties the two mono articular muscles and one bi-articular muscle effectively add rotational stiffness and damping to the hip and knee and introduces a visco-elastic coupling between both joint according to:

$$\begin{aligned}
\Delta\tau_{hip} &= \Delta l_{m(h)} \cdot K_{m(h)} \cdot r_{hip} + \Delta l_b \cdot K_b \cdot r_{hip} \\
\Delta l_{m(h)} &= \Delta\theta_{hip} \cdot r_{hip}, \\
\Delta l_b &= \Delta\theta_{hip} \cdot r_{hip} + \Delta\theta_{knee} \cdot r_{knee} \\
\Delta\tau_{hip} &= \Delta\theta_{hip} \cdot r_{hip}{}^2 \cdot K_{m(h)} + \Delta\theta_{hip} \cdot r_{hip}{}^2 \cdot K_b + \Delta\theta_{knee} \cdot r_{knee} \cdot r_{hip} \cdot K_b
\end{aligned}$$

$$\begin{aligned}
\frac{\Delta\tau_{hip}}{\Delta\theta_{hip}} &= r_{hip}{}^2 \cdot K_{m(h)} + r_{hip}{}^2 \cdot K_b = K_h \\
\frac{\Delta\tau_{hip}}{\Delta\theta_{knee}} &= r_{knee} \cdot r_{hip} \cdot K_b = K_c \\
\Delta\tau_{knee} &= \Delta\theta_{knee} \cdot r_{knee}{}^2 \cdot K_{m(k)} + \Delta\theta_{knee} \cdot r_{knee}{}^2 \cdot K_b + \Delta\theta_{hip} \cdot r_{hip} \cdot r_{knee} \cdot K_b \\
\frac{\Delta\tau_{knee}}{\Delta\theta_{knee}} &= r_{knee}{}^2 \cdot K_{m(k)} + r_{knee}{}^2 \cdot K_b = K_h \\
\frac{\Delta\tau_{hip}}{\Delta\theta_{knee}} &= r_{knee} \cdot r_{hip} \cdot K_b = \frac{\Delta\tau_{knee}}{\Delta\theta_{hip}} = K_c
\end{aligned} \qquad [10]$$

where subscript $_{m(h)}$ refers to the mono-articular muscle around the hip (figure 2C), $_{m(k)}$ to the mono-articular muscle around the knee, and $_b$ to the bi-articular muscle crossing both joints. K represents the linear stiffness and l the muscle length. r_{hip} and r_{hip} represent the moment arm of the muscles around the hip and knee respectively. For simplicity the moment arms will be assumed constant, which is a valid assumption when joint movements are small. Parameter K_h describe the rotational stiffness around the hip joint, K_k the stiffness around the knee joint. K_c relates the hip torque to knee displacement (and knee torque to hip displacement).

The derivation above shows that this coupling (K_c) is symmetric. It is important to keep in mind that some of the visco-elastic behavior of the modelled muscle may be due to feedback action. In addition, multijoint reflexes (heteronymous reflexes) could allow the CNS to produce asymmetric stiffness. However, in this study we did not observe a large

contribution of reflexes to the stiffness (see section 3.6), therefore we did not try to model the reflex contribution separately.

A similar set of relations as derived for the muscular stiffness can be derived for the muscular damping (B_h, B_k, and c). Thus, adding the mono- and bi-articular muscles to the double pendulum model effectively adds 6 parameters to the model.

Next the equation of motions of the double pendulum model (with the muscle model), are linearized, written in state space notation, and transformed to the frequency domain (H_{model}, figure 11). Next, the model admittance is converted into impedance (by taking the inverse of the 2-by-two matrix at every frequency). This transformation is performed because it yields 4 relatively simple TF's (figure 12). Each TF now basically consists of a simple mass-spring-damper system (eq. 11), which facilitates the fitting procedure.

$$H_{ij} = I_{ij}s^2 + B_{ij}s + K_{ij} \quad \text{with } s = j\omega$$

$$\begin{aligned}
I(1,1) &= (p_{ul}{}^2 + r_{ul}{}^2)\cdot m_{ul}\cdot c + (l_{ul}{}^2 + 2\cdot cos(\theta_{knee})\cdot l_{ul}\cdot p_{ll} + p_{ll}{}^2 + r_{ll}{}^2)\cdot m_{ll}\cdot c \\
I(1,2) &= (p_{ll}{}^2 + l_{ul}\cdot cos(\theta_{knee})\cdot p_{ll} + r_{ll}{}^2)\cdot m_{ll}\cdot c \\
I(2,1) &= (p_{ll}{}^2 + l_{ul}\cdot cos(\theta_{knee})\cdot p_{ll} + r_{ll}{}^2)\cdot m_{ll}\cdot c \\
I(2,2) &= (p_{ll}{}^2 + r_{ll}{}^2)\cdot m_{ll}\cdot c
\end{aligned}$$

$$\begin{aligned}
K(1,1) &= K_h + g\cdot m_{ll}\cdot c\cdot(p_{ll}\cdot cos(\theta_{hip}+\theta_{knee}) + l_{ul}\cdot cos(\theta_{hip})) + g\cdot m_{ul}\cdot p_{ul}\cdot cos(\theta_{hip}) \\
K(1,2) &= K_c + g\cdot m_{ll}\cdot c\cdot p_{ll}\cdot cos(\theta_{hip}+\theta_{knee}) \\
K(2,1) &= K_c + g\cdot m_{ll}\cdot c\cdot p_{ll}\cdot cos(\theta_{hip}+\theta_{knee}) \\
K(2,2) &= K_k + g\cdot m_{ll}\cdot c\cdot p_{ll}\cdot cos(\theta_{hip}+\theta_{knee})
\end{aligned} \qquad [11]$$

$$B = \begin{bmatrix} B_h & B_c \\ B_c & B_k \end{bmatrix}$$

where subscript $_{ul}$ refers to the upper leg and $_{ll}$ to the lower leg. m represent the segment mass, l the segment length, p the position of the centre of mass, r the radius of gyration, c the scaling factor for the segment masses and g the gravitational acceleration (9.81m/s^2). In principle, the inertia matrix I could be used to estimate the mass of the upper leg and lower leg separately. However, the largest component of the total inertia of the whole leg ($I(1,1)$) actually originates from the mass of the lower leg (second term of $I(1,1)$). Consequently a small error in the estimation of parameters like l_{ul}, p_{ul}, *or* p_{ll} can lead to large errors in the estimating of the mass of the upper leg. For example; a 10% overestimation of the length of the upper leg results in a 38% underestimation of the mass of the upper leg, whereas the mass of the lower leg is only 5% overestimated. Therefore, it is recommended to use standard estimates of the mass of the upper leg, relative to total body estimates [39]. Here, in order to account for some subjects variability we still introduced a scaling factor (c) that scaled the mass of the upper and

lower leg equally (assuming that subjects with an above-average lower leg mass also exhibit equally enlarged upper legs).

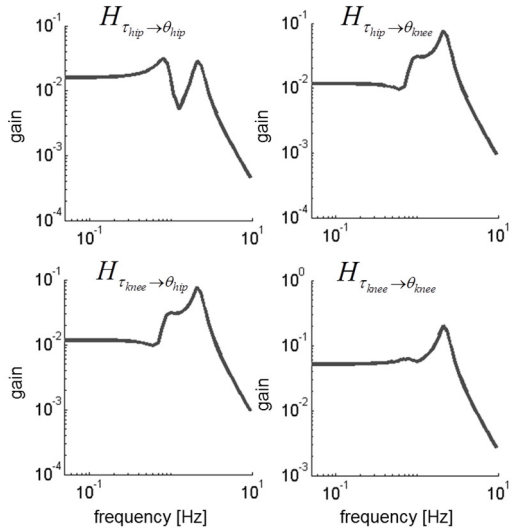

Figure 11: Admittance TFs of the double pendulum model. Multiple-Input-Multiple-Output (MIMO) admittance transfer function (TF) of the double pendulum model. $H_{\tau_{hip}\rightarrow\theta_{knee}}$ indicates the admittance TF from hip torque to knee angle etc.

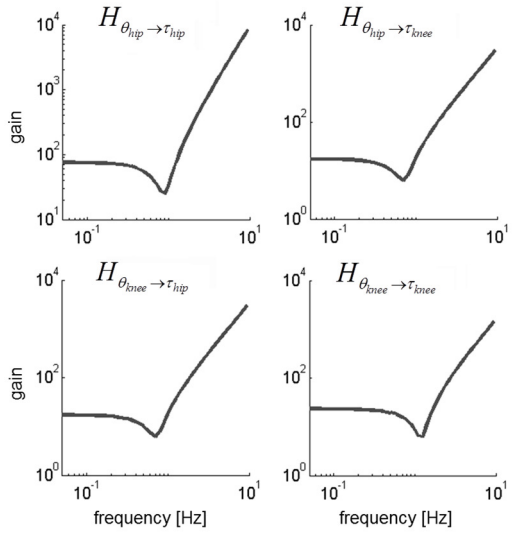

Figure 12: Impedance TFs of the double pendulum model. MIMO impedance TF of the double pendulum model. Taking the inverse of the admittance yields the impedance TFs, which consist of 4 relatively simple TF's. $H_{\theta_{hip}\rightarrow\tau_{knee}}$ indicates the impedance TF from hip angle to knee torque etc.

Chapter 7

General discussion

7.1 Introduction

The overall goal of this thesis was twofold. The first goal was to develop and evaluate the effectiveness of different controllers based on the Assist-As-Needed (AAN) principle. Such controllers enable the magnitude of the provided assistance to be gradually reduced, depending on the recovery stage of the patient. Such a gradual reduction in support will continuously challenge the patient to his maximum capacity, and will reduce the likelihood of the patient becoming reliant on the support. In most support strategies the amount of support is proportional to the deviation from a "healthy" reference trajectory. In Chapter 2 we developed and evaluated a novel method to reconstruct such reference trajectories, taking into account the subject's body-height and current walking speed. Robotic support is often provided on a joint level, which aims at improving motor function through restoration of original movement patterns. In Chapter 3 we evaluated the effectiveness of an impedance controller on joint level in a group of SCI patients. In Chapter 4 we used an alternative approach, called "selective subtask support". Here virtual mechanical components (like springs) are defined to assist specific subtasks of walking, and simulate any interaction that a therapist would normally have with a patient. To effectively increase the required active contribution from the patient when the support levels are decreased, it is essential that robotic gait trainers are sufficiently transparent. Therefore, we developed two new controllers that exploit the cyclic behavior of walking to improve the transparency of the LOPES (Chapter 5). The second goal of this thesis was to assess the feasibility of using the LOPES as a measurement tool to quantify joint properties. Hence, we evaluated a new method to quantify passive and active multi-joint-impedance using Multi Input Multi Output (MIMO) system identification techniques (Chapter 6).

These two topics will be discussed separately. First, we will discuss several control considerations with respect to active participation, motivation and movement variability, followed by a section in which we discuss the role of compensatory movement strategies in robot-aided gait training. In the next sections the importance of properly estimating reference trajectories, and the importance of robotic transparency, will be substantiated and the clinical effectiveness of different types of AAN control strategies will be reviewed. In the second part of this chapter we discuss how robotic gait trainers can be employed to quantify joint properties. We will conclude with some remarks and recommendations for future developments.

7.2 Robotic control strategies

Robotic gait trainers are gaining popularity in the rehabilitation of individuals who suffered a SCI or stroke. These robots provide promising opportunities, as they allow high dosage gait training, while reducing the physical demands on the therapists. Despite these potential benefits, superiority of robotic gait trainers over conventional gait-training approaches has not been demonstrated [1-4]. It is believed that this is related to the fact

that most robotic gait trainers were initially designed to move the patient's legs through a prescribed gait pattern, irrespective of the patient's self-generated activity. New insights in neural plasticity, motor learning and motor recovery, however, have resulted in a paradigm shift towards support strategies that encourage active participation and allow movement variability.

7.2.1 Active participation

To promote active participation, a patient should receive the minimal amount of assistance possible. In both controllers that were tested in this thesis, the required active participation can be increased by lowering the impedance level (Chapter 3), or by reducing the stiffness of the virtual model (Chapter 4). Although we did not explicitly study active participation in terms of muscle activation levels, or self-generated torque, we showed that both controllers were able to provide support in a gradual manner. That is; by increasing the support levels, the subjects were attracted more towards the reference trajectory and, reversely, by lowering the support levels the subjects were forced to contribute more actively to the prescribed movement. The possibility to modify the support levels raises an important question: what are the proper support levels? In Chapter 3 the reduction in impedance levels was based on: 1) visual inspection of the quality of walking (adequate step height during the swing phase and adequate knee stability during the stance phase), 2) the current physical condition of the patient (observation of breathing rate and degree of transpiration), and 3) his motivation (as verbally communicated). As discussed in Chapter 3, some participants, especially the slowest walkers, could not train for the same duration as reported in position-controlled gait training studies. This could be an indirect sign that training in the LOPES requires more active participation.

It seems there is an inherent trade-off between increasing active participation and maintaining the duration of training. A similar trade-off with training duration will likely exist for the body weight support (BWS) level and walking speed. The progressive reduction in BWS level, or increase in treadmill speed, required more active participation from the patient but might also have contributed to the relative short training time observed in Chapter 3. Therefore, it is important that future research will further explore the interrelationships between these training parameters and training intensity. For example, a very recent study by Van Kammen et al. [5] showed that the typical effects of treadmill speed on muscle activity, and temporal gait parameters, are attenuated at high levels of BWS. This suggests that, when the goal is to increase training intensity, the first step should be to reduce the amount of BWS, as opposed to increasing treadmill speed. They also showed that high levels of BWS affect the temporal gait parameters, which also stresses that, when possible, BWS should be reduced, before increasing treadmill speed.

7.2.2 Adaptive support

Manually setting the support levels, like we did in Chapter 3, requires the therapist to continuously monitor the patient's capabilities and progress. Also, different joints (or subtasks) may require a different amount of support. Some therapists may appreciate the various support options, but others may find it difficult to choose the appropriate settings. If the support levels are set too low, dangerous situations can occur, whereas too much assistance possibly evokes reliance on the provided support. Consequently, some therapists may use relatively high support levels to assure safety, whereas others encourage active patient participation by using low support levels. To eliminate such variability in training setting we incorporated an error-driven adaptation algorithm developed by Emken et al. [6] (Chapter 4). The algorithm modified the virtual spring stiffness (at each percentage of the gait cycle) based on the experienced error in the previous step. In line with the findings from Emken et al. [6], the stiffness converged to a unique profile for every patient, with a large stiffness in the problematic areas. All stroke survivors reached a profile where the stiffness was highest at swing initiation. This helped the patients to overcome their reduced knee flexion and create enough toe clearance during the swing phase. Such adaptive algorithms greatly reduce the number of parameters that have to be set by the therapist. They also continuously challenge the patient, since the amount of support no longer relies on the fixed predefined setting from the therapist, but instead adapts to the current needs of the patient. Although we implemented the adaptive algorithm in our subtask support controller they can also easily be implemented in control strategies that provide support on a joint level.

Still, there are some considerations when using these algorithms. Firstly, the learning gain and the forgetting factor determine the speed of convergence and the kinematic error that persists after convergence. Thus, it may still be necessary to define the model parameters on a subject-specific basis to allow the assistance to be more precisely tailored to the needs of the patient. Secondly, we did not take into account the fact that human movement is inherently variable. The controller responded to this variability on a step-by-step basis, by increasing and decreasing the support level. Although these corrections were really small and probably went unnoticed by the patient, introduction of a deadband [7,8] around the reference trajectory (in which the controller does not respond to movement errors) can easily solve this in future applications. Finally, the algorithm does not dissociate between a decrease in effort due to reliance or fatigue. In both cases the algorithm will increase the support level. This issue is not restricted to control algorithms that adapt the support based on kinematic errors, but also holds for algorithms that modify the support levels based on estimations of the self-generated joint torques [9], [10]. Emken et al. [11] showed that, to prevent reliance, the robot must relax its assistance at a faster rate than the human motor system learns to decrement its own contributing. Yet, this rate is probably patient-dependent and will be difficult to measure in neurological patients with impaired motor control due to spasticity, muscle weakness and synergies. Furthermore, the occurrence of fatigue will also interfere with the determination of this

learning rate. Therefore, the settings of the adaptive algorithm are currently not based on the learning rate, but on a stable convergence of the stiffness pattern within approximately 20 steps.

7.2.3 Performance feedback

To further enhance active participation, it is important to provide patients with some sort of external feedback on their performance. Especially patients with neurological disorders, that exhibit sensory impairments (in addition to motor impairments), may benefit from external information. In a regular therapeutic setting, this information comes from the therapist, who verbally tries to motivate the patient to actively participate and perform the correct movements. This feedback can be based on visual observations and/or the amount of assistance that the therapist provides. The introduction of robotic gait trainers, which are generally equipped with various sensors that measure joint angles and interaction forces, provides new possibilities to offer both the patient and the therapist performance-related feedback. Several research groups have already built robots that display information about the kinematics of a single joint [7,12], multiple joints [8] or self-generated joint torques [13,14]. The added value of visual feedback has been demonstrated in healthy subjects, where participants who trained with an assistive controller and visual guidance retained the evoked gait adaptations for a longer period of time than those who trained with either visual guidance or support alone [15].

The key element of any form of feedback is displaying the subject's effort in an intuitive manner, without overloading him with information. To our experience not every patient prefers real time information about the predefined reference trajectories and their actual performance. In Chapter 4 we demonstrated that very basic visual feedback (consisting of the maximum step height of the last step) provides stroke patients with sufficient information to motivate and guide them in taking higher steps. Others use weighting functions to reduce the number of parameters that are presented to the patient [13]. Although all these strategies were demonstrated to lead to an instantaneous increase in activity (or reduced errors), so far, there is no clinical evidence that adding visual feedback results in better functional outcomes. Also, the impact of many characteristics of feedback systems remains unclear. Factors like the timing, frequency, type (auditory, sensory and visual) and measured parameters of the feedback require further investigation. Furthermore, the feedback will have to be adjusted to the patient's type of impairments (cognition, vision etc.). In addition, recent developments like virtual reality [16,17] and computer games [18,19] also provide new opportunities to promote active participation. With all these different options to increase patient motivation, the type of feedback provided during robot-assisted training may ultimately be equally important as the support strategy.

7.2.4 Kinematic movement variability

As outlined in the introduction, it is thought that training with a certain amount of movement variability (in terms of both joint kinematics and timing) contributes to learning a new task, or relearning a lost task. In the controllers tested in this thesis, the amount of movement variability can be increased by lowering the impedance level (Chapter 3), or by reducing the stiffness of the virtual model (Chapter 4). Although we did not explicitly measure the variability allowed by the controllers, in Chapter 3 we showed that for a healthy subject, increasing the impedance levels results in a closer approximation of the reference trajectory and a reduction in the movement variability between steps, and vice versa. In Chapter 4, where we implemented the impedance-shaping algorithm, we demonstrated that for the gait phases where the patient required little support, the stiffness of the virtual spring was decreased, thus allowing more movement variability.

With most control strategies, the patient is attracted to a reference trajectory, regardless whether he/she is above or below the reference. This implies that, for example, walking with more knee flexion is corrected, while this does not necessarily have a negative impact on gait performance. In Chapter 4 we used a unidirectional spring that only assisted the patient in creating more toe clearance, but did not intervene when the patient reached more toe clearance. This also allowed for additional variability in gait kinematics.

7.2.5 Temporal movement variability

Allowing variability in timing (taking steps with different cycle times) requires synchronization of the reference trajectories with the movements of the subject. Especially when the support levels are low, there is a risk that the subject and robot start to walk out of phase. As a result, the robot is going to resist, rather than support, the subject. In Chapter 4 we adopted a controller developed by Aoyagi et al. [20], that continuously compares the current state of the subject to the desired state (a known pattern), and subsequently increases or reduces the replay speed of the reference trajectories, in order to align the two. In contrast to Aoyagi et al., who used a state consisting of 18 dimensions (9 DoFs, position and velocity), we only used 8 dimensions (left and right hip and knee angle and velocity), but still the controller was able to sufficiently estimate the state of the user and synchronize the reference trajectory with its motions.

For the support of gait subtasks (Chapter 4) continuous synchronization was not required, since the support was gait phase dependent. The subtask was only supported during the swing phase, and the replay timer was reset after detection of the next foot-off event. The use of discrete gait events to synchronize the robot and the subject requires an accurate online detection of these gait events. For the LOPES we implemented two types of discrete phase detection algorithms; one based on the forward-backward position of the ankle [21] and the other based on the movement of the Center of Pressure (CoP) [22]. We experienced that the phase detection algorithm based on the position of the ankle was

more accurate, especially at lower walking speeds. The CoP signal required significant filtering to obtain its characteristic “butterfly pattern” [22], and prevent the detection of local extremes in the CoP. Filtering such signals creates a temporal delay between peak identification and the true gait events.

7.2.6 Trade-off between support levels and learning rate

In this thesis we showed that both controllers are capable of providing support in a gradual manner. Kinematic errors can be reduced by increasing the impedance levels (Chapter 3), or by increasing the stiffness of the virtual spring (Chapter 4). Note, however, that reducing these errors may also slow down the learning process, since these movement errors are considered the key component for motor learning [23,24]. So far, this trade-off between learning rate and the amount of robotic support is unknown [25]. Consequently, future research will have to reveal the optimum between providing support, such that the task can be accomplished, and reducing support level to allow movement errors.

7.3 The role of compensatory movement strategies in robot-aided gait training

As discussed in detail in the introduction of this thesis, there is an ongoing discussion in rehabilitation science whether gait therapy should focus on “restitution” (reappearance of pre-injury movement patterns) or “compensation” (appearance of compensatory movement strategies). To date, no solid scientific evidence favors one mechanism over the other. Whether a therapist will focus his therapy on restitution or compensation will probably depend on the severity of, and the time since, the injury. In acute patients therapy will likely be focused on restitution, as this might also increase the performance of other functional tasks. For example, retraining knee function will probably also benefit other gait related tasks like stair walking or stepping over obstacles, whereas adopting a hip circumduction strategy to overcome reduced knee flexion will probably not. For patients in the chronic stage of their injury, additional improvements in knee flexion will probably be small and in this case, a hip circumduction strategy will likely allow them to walk at a faster pace.

A fundamental difference between the two controllers that were tested in this thesis is whether they allow the use of these compensatory strategies. Support on a joint level (Chapter 3) is purely focused on restitution, as the support is directed towards restoring a “normal” walking pattern. In contrast, the Virtual Model approach (Chapter 4) does not intervene when the patient create sufficient toe clearance, regardless of the strategy they use. Without the support the majority of the stroke survivors showed a marked lower knee flexion range in the paretic leg, compared to the non-paretic leg, resulting in a reduced toe clearance. Most patients compensated for this with different combinations, and degrees, of compensatory strategies. All patients showed a larger paretic hip

abduction range (hip circumduction) and an increased pelvic height during the paretic swing phase (vaulting).

We hypothesized that providing support on one subtask, i.e. toe clearance, would reduce the need for these compensatory strategies. However, despite a clear increase in knee flexion due to the support, none of the stroke survivors reduced their compensatory strategies. Similar findings have been reported by others. For example, Neckel et al. [26] reported that stroke patients who trained in the Lokomat still generated considerable hip abduction torques (hip circumduction) and hip hiking strategies, even though the Lokomat provided a physiological kinematic pattern that would make the use of these strategies unnecessary. More specifically, Sulzer et al. [27] used a robotic knee orthosis to study stiff knee gait in chronic stroke patients. They provided knee flexion assistance during foot-off and reported a small but significant increase, rather than decrease, in hip abduction.

Such findings stand in contrast with the theory that stroke patients use hip abduction as a compensatory mechanism for reduced knee flexion. Possible explanations may be found in an abnormal torque coupling between joints, which is reported for stroke survivors [28], [29], or an altered stretch reflex coupling between the hip and the knee [30]. On the other hand it has to be noted that in the studies that did not find a reduction in compensatory strategies [26,27] (including ours) the patients were not given any specific instructions about how to walk. If the training was directed at reducing the use of compensatory strategies, the patient would probably require clear instructions from the therapist. In our study we used visual feedback, but we only showed the maximum step height, regardless of the employed strategy. Consequently, the patients may not have been triggered to reduce their compensatory strategies. In addition, these results were obtained in chronic stroke patients during single trial experiments. For these patients the training sessions may have been too short for them to alter their stereotypical compensatory strategies. Longer training sessions, in combination with (visual) feedback on the amount of compensation that is used, might reveal whether patients are truly incapable of reducing their compensatory strategies. Such information is valuable for further development of robotic support regimes. For example, when a therapist believes that regaining an appropriate knee flexion is not feasible (e.g. due to significant joint contractures), controllers can be designed that support learning a hip circumduction strategy.

7.4 Future applications and considerations for selective support of subtasks

The key goal of future research is to expand the concept of subtask support. Body weight support can also be regarded as one of these subtasks. Most robotic gait trainers use body weight support systems (BWSS) that consist of an overhead suspension system in combination with a harness to unload the patient. By removing a percentage of their body weight, patients with excessive weakness can start gait rehabilitation in the very early stages after their injury. However, using these overhead suspension systems has some

disadvantages. First, BWSS that use a counterweight or spring mechanism not only provide a force in the vertical direction but also in the horizontal direction, which helps to stabilize the human body [31]. This implies that the amount of support on weight bearing and balance control cannot be controlled independently. Although, in many cases, both balance and weight bearing have to be supported, the amount of required support for each of these tasks can vary widely within patients. Second, in case of a counterweight mechanism, the supportive forces vary because of the acceleration and deceleration of the counterweight during the movements of the human body [32]. Third, most systems provide an equal amount of BWS for the paretic and non-paretic leg, while in many cases hemiplegic subjects only need support during the stance phase of the affected leg. Fourth, reducing the body load affects spatial, temporal, and kinematic gait parameters [5],33]-35]. Although more complex BWSS allow the support to be gait cycle (or leg) dependent [32], the body is still unloaded. To overcome the aforementioned disadvantages, we assessed the feasibility of a Virtual Model (VM) that (partially) counteracts the gravitational force and prevents knee buckling [36]. Similar to the VM that supported toe clearance (Chapter 4), the virtual force is translated into joint torques that are applied to the hip and knee joint. The presented approach enables selective control of BWS for the paretic leg, and is only active during the stance phase. The VM was tested on a single healthy subject. The results showed a reduction in muscle activity during initial stance, indicating that the algorithm was effectively providing weight support, while the kinematics remained close to normal. Future experiments will have to show the effectiveness of the proposed VM in neurological patients.

Shifting weight from one leg to the other is also an important subtask of gait, and is essential in order to maintain balance. In fact, during manually assisted treadmill training a dedicated therapist often supports this subtask [37]. So far, the need for active balance control has been limited in most robotic gait trainers. It has even been suggested that "training stereotypical leg motions without challenging balance control may squander training time by focusing training on the impairment that is not the bottleneck for achieving a greater walking speed" [38]. Thus, adding active practice of balance to robot-aided gait training may seem like a logical next step. In the LOPES we incorporated actuated pelvis translations to allow the training of balance tasks, but also other gait trainers like the PAM and POGO [20] and ALEX III [39] were designed to assist pelvic motions during stepping. Also, for the Lokomat, a separate module has been developed which incorporates additional degrees of freedom (DoFs) at the hip and pelvis [40]. However, the control strategies for these additional DoFs have not yet received a lot of attention. For the LOPES we developed a VM that was designed to assist weight shift and support balance. It consisted of a virtual spring and damper, of which the equilibrium position moved along a reference lateral pelvis trajectory. To specifically examine its effectiveness, we tested it in an experimental set-up, designed to study lateral balance [41]. The results indicated that the controller was able to gradually support weight shift. In other words, a larger stiffness resulted in a closer approximation of the reference trajectory. The balance controller was also selective, as the effects were mainly restricted

to the frontal plane. When the external stabilization was switched on, the step width and step width variability decreased and the "stability margin" [42] increased. The changes in these parameters indicate that the provided external stabilization reduced the need for active lateral balance control by the subject. Although we used a dedicated experimental setup to test the support algorithm it can easily be implemented in the LOPES or other robotic gait trainers.

The rationale for the use of selective support of subtasks is that the affected subtasks can be supported without affecting, or supporting, the unimpaired subtasks. By selecting subtasks that require support, and selecting the proper support level, the robotic assistance can be tailored to the needs of the patient. In Chapter 4 we showed that we could selectively and gradually influence the step height (toe clearance), without affecting other spatiotemporal gait parameters like the non-supported step height, step length or cycle time. As expected, a higher stiffness resulted in a closer approximation of the target values. In another study we combined the step height VM with a VM that assisted in taking longer steps [43]. Providing step-length support resulted in a less selective effect. Here, the increase in step length was accompanied by a reduction in step height. The decrease in step height can be explained by the exerted hip flexion and knee extension torques that are applied to support the step length. These torques inhibit a normal knee flexion during the initial swing phase, resulting in a reduced step height. Although this can (partially) be compensated for by switching on the step height VM in parallel, it demonstrates that not every subtask can be supported without affecting the execution of other subtasks.

7.5 Reference trajectories

The two control strategies that are used in this thesis (Chapter 3 and 4), as well as many other control strategies [7,9,10,20,44,45], require the use of reference trajectories to determine the amount of support. As described in Chapter 1, these trajectories are generally based on pre-recorded trajectories from healthy individuals. In most cases they are obtained at a limited number of speeds. As a consequence, the gait trajectories have to be modified when the training speed of the patient does not match the speed of one of the pre-recorded patterns. In Chapter 2 we presented and evaluated a novel method to reconstruct speed-dependent joint trajectories, based on regression models for certain key events in the joint trajectories. In Chapter 4 we used the same methodology to reconstruct reference trajectories for the ankle. This method eliminates the need to pre-record joint trajectories at numerous walking speeds, and allows the patient to transition between different training speeds, without manual adjustment of the reference trajectories. Still, for some patients it may be necessary to modify the reconstructed trajectories. For example, patients with severe joint pain may prefer training with reduced knee flexion. With the proposed method the key event that represents the maximum knee angle can simply be reduced and a new trajectory can be generated.

As discussed in Chapter 4, therapists greatly appreciate the possibility to set training goals in terms of parameters like step height or step length, as opposed to defining target values in terms of joint angles. Therefore, in the new LOPES (LOPES II) we implemented an algorithm that connects the key events in joint trajectories to gait parameters like step height or step length. This way, the therapist can define the desired step height and/or step length and the algorithm will generate the appropriate joint angular trajectories.

The predefined joint trajectories essentially focus on restitution. Compensatory strategies can only be used if these movements are defined in the reference trajectories. Although the number of observed compensatory strategies is limited, there is still considerable variation between patients, which complicates a proper definition of the reference trajectories for alternative movement strategies. A possible solution would be to use teach-and-replay algorithms [6]. Here, the robot first records the movements of an alternative pattern, which is obtained when the therapist manually moves the leg through the desired pattern. Then, these alternative patterns can be replayed to assist the patient in adopting an alternative movement strategy. In Chapter 5 we used adaptive frequency oscillators (AFOs) and kernel-based non-linear filters (NFLs) [46,47] to learn and replay the joint angles of the exoskeleton during walking in the LOPES. The AFOs are used to acquire the gait phase, based on a sinusoidal input signal (in our case the hip angles). Subsequently, the NFLs learn the joint angles as a function of the phase. Such algorithms can also be adapted for the purpose of learning and replaying gait trajectories. It is expected that gait training with a personalized gait pattern, as opposed to a normative gait pattern, facilitates the transfer of relearned capabilities in the robot to overground walking. However, so far, there is no evidence that supports this hypothesis. Implementation of teach-and-replay algorithms provides a way to test this hypothesis.

7.6 Transparency

AAN can only be effectively implemented in robotic gait training if the robot is sufficiently transparent. In a perfect transparent mode, the robot does not hinder the motion of the subject when assistance is not required. This is especially important at the final stages of recovery. Here walking in the robot should resemble walking without the robot, to promote the transfer of the relearned capabilities to overground walking. For example, when the robot produces resistance in a certain joint, the patient will have to learn to overcome this resistance during training. Subsequently, during free walking, the learned extra muscular activity to overcome the resistance will result in unwanted movements. Transparency is also important when the therapist wants to focus the support on the impaired subtasks of gait, while leaving the execution of the unaffected subtasks up to the patient.

In the introduction we stated that the overall transparency of the robot depends on: 1) the amount of DoFs, 2) the weight of the robot and 3) the used control strategies. In the LOPES, a lightweight frame (with 9 DOFs) [48] is combined with closed-loop force control

[49], which allows the robot to be controlled in zero-force control. Still, previous experiments showed that the amount of knee flexion decreases, and muscle activation levels increase, due to the inertia of the exoskeleton leg. In Chapter 5 we tested two controllers that utilize the cyclic nature of locomotion to improve the transparency of the current LOPES setup. Both controllers are based on a combination of AFOs and NLFs. The first consisted of a feed-forward controller to improve the torque tracking (including the zero-torque mode). The second controller learned the state of the exoskeleton and subsequently compensated for its dynamical effects (e.g. its inertia). When both controllers were active simultaneously, the interaction power between the robot and the human leg was reduced by at least 40 percent at the thigh and 43 percent at the shank. It also resulted in an increased amount of knee flexion. Although these results are promising, future experiments will have to demonstrate if walking with these controllers truly reflects free walking in terms of muscle activation levels and gait kinematics. Also, since both controllers rely on AFOs, they require thorough testing for their stability during transitions in walking velocity and/or cadence. This is particularly important for neurological patients, as they tend to walk with increased spatiotemporal variability [50], [51]. In addition, the performance of the feed-forward controller needs to be assessed during unpredicted movements like balance corrections. Finally, since transparency is the basis, on top of which any form of assistance will be added, it has to be determined how the proposed controllers interact with assistive controllers, such as the ones presented in Chapter 3 and 4.

7.7 Recovery of walking ability using AAN strategies

For people with chronic incomplete SCI, we studied the effectiveness of gait training using the impedance controller on joint level. Ten participants received gait training with the LOPES, three times a week for eight weeks. We found significant improvements in all gait related parameters. In Chapter 3 we concluded that training with the impedance control regime is as effective as position controlled gait training, taking into account the state of the patient (acute/chronic) and their initial level of ambulation. Here we discuss our results in relation to other studies that use AAN control regimes.

To date, only a limited number of studies have assessed the effectiveness of AAN controllers in multisession training protocols. Schück et al. [52] used the Lokomat to test the combined effect of their “patient-cooperative” and “Generalized Elastic Path Control” approach. They trained two chronic incomplete SCI patients and two stroke survivors, with initial walking speeds comparable to our study (± 0.6 m/s). Over the course of four weeks their patients participated in 16 (45 min.) training sessions. Only one stroke patient showed a significant increase in walking speed. In line with what we already stressed before, the lack of improvement was suggested to be due to deeply engrained compensation strategies. These compensation strategies most likely reduce the effectiveness of robotic gait training with physiological gait pattern. In contrast, Krishnan et al. [53], who used the same control regimes to train a single chronic stroke survivor, did

find a substantial increase in walking speed. Their training protocol consisted of 12 (45-60 min.) training sessions (three times per week for four weeks). Noteworthy, the same patient also participated in four weeks of conventional Lokomat training, which did not produce any meaningful changes in the measured clinical outcomes. Although the increase in walking speed (± 0.3 m/s), obtained with their cooperative control approach, far exceeds the mean increase in walking speed reported in Chapter 3 (± 0.06 m/s), it should be noted that their results are only from a single subject. Also they tested the effectiveness of their approach in a stroke survivor, whereas we included SCI patients.

In another study, Banala et al. [7] used the ALEX to test their "tunnel" approach in combination with a "moving back wall" on two chronic stroke survivors. Over the course of six weeks their patients participated in 15 training sessions. They reported that, at the end of the training program, the patients' gait pattern was closer to a "healthy" gait pattern. In addition, the tolerable treadmill speeds increased from 0.45 to 0.72 m/s and 0.63 to 0.85 m/s. Their tunnel approach is similar to the subtask approach that we used in Chapter 4. They applied tangential and normal forces to the ankle path, whereas we only applied vertical forces to the ankle. Furthermore, Banala et al. [7] used constant stiffness levels, whereas we used an adaptive stiffness algorithm. In additional to the single-session experiments discussed in Chapter 4, our subtask approach has also been tested in a multiple-session experiment. Five chronic stroke survivors participated in 18 (45 min) training sessions, during a 6-week training program [43]. All subjects showed a marked increase in training speed (0,292 m/s). Yet, there was only limited transfer of increase in walking speed to overground walking (0.025 m/s). A similar effect was found in the study described in Chapter 3. Here, the average treadmill speed increased with 0.15 m/s, whereas overground walking speed increased with only 0.06 m/s. This demonstrates that the effectiveness of the support strategies cannot simply be determined purely based on the increase of walking speed on the treadmill.

On the one hand, the relatively small improvements obtained with AAN controllers have to be placed within the context of the included patient population. In all the studies discussed above, the effectiveness of the control methodology was tested in chronic SCI or stroke patients. Chronic patients are attractive for pilot trials, because improvements can be attributed to the intervention rather than spontaneous recovery. However, they may not be the ideal candidates to evaluate the true potential of AAN controllers. The chronic patients included in most studies have relatively high initial walking speeds, whereas patients with a lower level of ambulation are more likely to benefit from robotic gait training [3].

On the other hand, we may have to conclude that, even though AAN controllers are designed to benefit less severely affected patient, their effect is limited. A possible negative consequence of all AAN strategies is that they are designed to provide support and reduce movement errors. Several studies have shown that increasing movement errors [25,54-56], or applying resistive forces [57,58], can increase the learning process or induce potentially useful aftereffects. However, the extent to which these temporary

improvements, or aftereffects, may contribute to clinical improvement remains unknown. Also, for gait related tasks, where large kinematic errors can have serious consequences, the use of error augmentation or resistive forces may be limited.

7.8 Assessment of joint properties with the LOPES

Robotic gait trainers can be used in a wider sense than just providing support during gait training. Implementation of standardized assessment tools provide valuable information about the clinical state of the patient throughout the therapy and may also provide an objective measure for the effectiveness of different robotic gait training regimes. In Chapter 6 we used a novel method to estimate multi-joint leg impedance in elderly, using Multi-Input Multi-Output (MIMO) system identification techniques. Although the results were promising there are some limitations. Since we only performed the measurements in each subject once, the results do not allow conclusions about the repeatability of the measure. Furthermore, subsequent testing on neurological patients has to confirm its validity for measuring spasticity or abnormal muscle tone. Another potential limitation of the presented method is that we used a relatively simple model to describe the joint dynamics, in which we lumped the effect of the intrinsic and reflexive stiffness. As it is known that spasticity is caused by increased reflex gains [59,60], the proposed model may have to be modified to determine the separate contributions of the intrinsic and reflexive mechanisms in neurological patients. Also, the joint stiffness is measured under semi-static conditions (i.e. around a certain equilibrium position). So far, it is unknown whether the identified abnormal stiffness measured under these conditions also hinders walking capacity. This information is critical in order to understand if, and how, their impairment affects walking ability.

Several methods have been proposed to estimate hip, knee and ankle stiffness during locomotion. Some are based on the slope of the torque-angle curve [61]. These estimates, however, should be distinguished from the intrinsic (and reflexive) stiffness, as they do not represent the instantaneous mechanical properties of the joint [62]. Also, these approaches are based on the net forces and, consequently, ignore possible co-contraction. Ideally, the joint impedance should be estimated by during gait, through the application of force or position perturbations. However, direct measurement of the joint stiffness is complex requires a device that is: 1) lightweight, 2) attaches rigidly to the limb so that accurate perturbations can be applied and 3) is transparent when not applying the perturbations. Although the LOPES fulfills these requirements to a certain extent, joint impedance measurement during gait will probably start at a single joint level, requiring a more modular approach. Examples of such modular devices that can serve this purpose are the Bowden-cable-driven knee actuator used by Tucker et al. [63], or the pneumatically actuated AnkleBot presented by Lee et al. [64]. At our department we are now developing a modular device, specifically dedicated to apply perturbations at the hip and knee, which can be used to estimate joint properties.

During walking the time is limited to apply stochastic perturbations. Also, the joint impedance varies continuously due to: 1) variations in activation levels throughout the different gait phases and 2) a constant change in joint angle. Consequently, different system identification will be required, such as the ones used by Ludvig et al. [65,66], which allow the estimation of time varying joint stiffness. We intent to further develop such methods and combine them with our method to estimate multi-joint impedance. Preferably small scale perturbations are used that minimally interfere with normal walking. Such experiments will allow us to study to what extent neurological patients also show increased joint impedance during gait and how it affects their walking ability.

The results from impedance measurements during gait can also be used to validate models that predict joint stiffness based on EMG measurements. For example, Pfeifer et al. [67] developed a method to estimate knee stiffness based on EMG-to-force functions which are obtained from isometric tests. The estimated muscle forces are used to estimate the overall stiffness using a musculoskeletal model of the leg and a model for activation-dependent short-range muscle stiffness. Their model is capable of estimating joint impedance during gait, but was only validated with experimental measurements during isometric force-tasks. Impedance measurements during gait can provide the means to validate such models.

7.9 Recommendations for future developments

The experience gained with the LOPES has led to the development of the LOPES II [68] (figure 1). The LOPES II differs from the LOPES on several aspects. The LOPES II has additional passive DoFs at the hip and pelvis which increase its transparency. Furthermore, it has a non-exoskeleton structure, which attaches to the backside of the shank and the pelvis. This setup does not require precise joint alignment, thus minimizing donning and doffing time, and allows free arm swing. In addition, the LOPES II is equipped with ankle actuation to assist push-off and prevent drop-foot. In contrast to the LOPES,

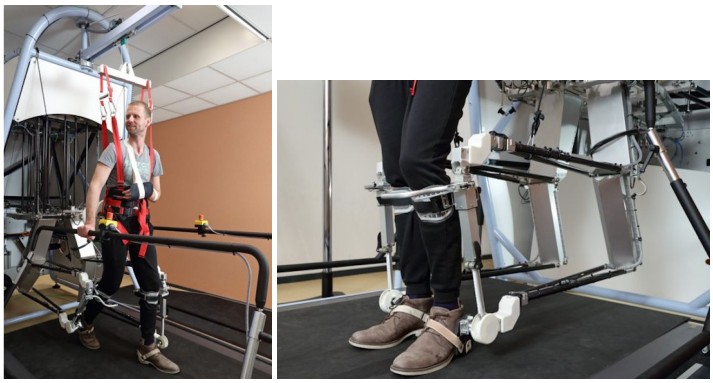

Figure 1: The LOPES II robotic gait trainer.

which is impedance controlled, the LOPES II is admittance controlled. Still, it will be controlled using the same AAN approaches as used in this thesis.

With the introduction of the LOPES II in several rehabilitation centers in The Netherlands, large randomized controlled trials on the effectiveness of the different controllers will become feasible. If the LOPES II becomes more widely available, it may also be possible to tests its effectiveness in acute, and non-ambulatory patients, which are expected to benefit more from robotic gait training than chronic patients. Future clinical evaluations can also be directed at other patient groups that may benefit from robot-aided gait training, such as patients with multiple sclerosis, cerebral palsy, or Parkinson's disease.

Regarding future studies on therapy effectiveness, we recommend that these include long-term follow up. Reaching a certain level of ambulation at the end of the training regime will likely promote the continuous use of relearned capabilities after training, whereas reaching a level of ambulation that has no functional benefit to the patient will probably not. Consequently these patients might not attain their relearned capabilities. Thus, the recovery level at the final stages of therapy may be an indicator for the long-term effect of the intervention. The only way to identify these levels is by long-term follow up. Follow up is also essential to determine the therapeutic effect in patients in the acute stage of their injury. For example, Duncan et al. [69] compared three different interventions in acute stroke survivors and found that at six months, a specific intervention seemed superior. However, one year after the stroke, all participants had reached the same ambulatory level. This may indicate that the intervention temporarily accelerated the recovery process, but had no added value in terms of overall effect.

For the LOPES II we will continue the development of new assessment modules to quantify neurological impairment. So far we focused on joint impedance measurements, which allow the quantification of increased joint impedance due to spasticity and abnormal muscle tone. However, a properly instrumented robotic gait trainer also allows assessment of muscle weakness or abnormal synergies. As mentioned above, these measures can be used for intra- and inter-subject comparisons, which are required to determine the effectiveness of different types of robotic assistance. Also, this information might reveal which patients are more likely to benefit from a certain type of robotic assistance. To obtain such information from a large population of different patient groups, collaboration between several rehabilitation institutes is essential. This will result in a rich stream of objective data that can be added to a large database, which can be used to detect possible correlations. Since time is a limiting factor in most rehabilitation programs, it is critical that these measurements are performed in an efficient way and do not go at the expense of the training time of the patient.

7.10 Final statement

In this thesis the feasibility of different types of robotic assistance that are based on the AAN principle is demonstrated. Combining sensors and complex control regimes provides

an endless amount of possibilities to modify the support to the individual needs of the patient, but also introduces many new questions and challenges, as discussed in this final chapter. Further research, involving large trials, is needed to address these challenges and has to reveal the key elements in facilitating functional improvement. Such trials will also have to prove that the use of robotic gait trainers can exceed (or accelerate) the functional improvements obtained with more conventional forms of therapy.

References

[1] B. H. Dobkin and P. W. Duncan, "Should body weight-supported treadmill training and robotic-assistive steppers for locomotor training trot back to the starting gate?," *Neurorehabil. Neural Repair*, vol. 26, no. 4, pp. 308-17, 2012.

[2] A. Wernig, "'Ineffectiveness' of automated locomotor training.," *Arch. Phys. Med. Rehabil.*, vol. 86, no. 12, pp. 2385-6; 2005.

[3] J. Mehrholz, B. Elsner, C. Werner, J. Kugler, and M. Pohl, "Electromechanical-assisted training for walking after stroke (Review)," Cochrane Database Syst Rev., 2013

[4] J. Mehrholz, J. Kugler, and M. Pohl, "Locomotor training for walking after spinal cord injury (Review)," *Cochrane Database Syst Rev*, 2012.

[5] K. Van Kammen, A. Boonstra, H. Reinders-Messelink, and R. den Otter, "The Combined Effects of Body Weight Support and Gait Speed on Gait Related Muscle Activity: A Comparison between Walking in the Lokomat Exoskeleton and Regular Treadmill Walking.," *PLoS One*, vol. 9, no. 9, p. e107323, 2014.

[6] J. L. Emken, S. J. Harkema, J. A. Beres-Jones, C. K. Ferreira, and D. J. Reinkensmeyer, "Feasibility of manual teach-and-replay and continuous impedance shaping for robotic locomotor training following spinal cord injury," *IEEE Trans Biomed Eng*, vol. 55, no. 1, pp. 322-334, 2008.

[7] S. K. Banala, S. H. Kim, S. K. Agrawal, and J. P. Scholz, "Robot Assisted Gait Training With Active Leg Exoskeleton (ALEX)," IEEE Trans Neural Syst Rehabil Eng, vol. 17, no. 1, pp. 1-8, 2009

[8] A. Duschau-Wicke, J. von Zitzewitz, A. Caprez, L. Lunenburger, and R. Riener, "Path control: a method for patient-cooperative robot-aided gait rehabilitation," *IEEE Trans Neural Syst Rehabil Eng*, vol. 18, no. 1, pp. 38-48, 2010.

[9] R. Riener, L. Lunenburger, S. Jezernik, M. Anderschitz, G. Colombo, and V. Dietz, "Patient-cooperative strategies for robot-aided treadmill training: first experimental results," *IEEE Trans Neural Syst Rehabil Eng*, vol. 13, no. 3, pp. 380-394, 2005.

[10] S. Hussain, S. Q. Xie, and P. K. Jamwal, "Adaptive impedance control of a robotic orthosis for gait rehabilitation.," *IEEE Trans. Cybern.*, vol. 43, no. 3, pp. 1025-34, 2013.

[11] J. L. Emken, R. Benitez, and D. J. Reinkensmeyer, "Human-robot cooperative movement training: learning a novel sensory motor transformation during walking with robotic assistance-as-needed," *J Neuroeng Rehabil*, vol. 4, pp. 1-16, 2007.

[12] C. Krishnan, R. Ranganathan, Y. Y. Dhaher, and W. Z. Rymer, "A pilot study on the feasibility of robot-aided leg motor training to facilitate active participation.," *PLoS One*, vol. 8, no. 10, p. e77370, 2013.

[13] R. Banz, M. Bolliger, G. Colombo, V. Dietz, and L. Lünenburger, "Computerized visual feedback: an adjunct to robotic-assisted gait training.," *Phys Ther*, vol. 88, no. 10, pp. 1135-1145, 2008.

[14] A. Koenig, X. Omlin, J. Bergmann, L. Zimmerli, M. Bolliger, F. Müller, and R. Riener, "Controlling patient participation during robot-assisted gait training.," *J. Neuroeng. Rehabil.*, vol. 8, no. 1, p. 14, 2011.

[15] S. H. Kim, S. K. Banala, E. A. Brackbill, S. K. Agrawal, V. Krishnamoorthy, and J. P. Scholz, "Robot-assisted modifications of gait in healthy individuals," *Exp Brain Res*, vol. 202, no. 4, pp. 809-824, 2010.

[16] L. Lilnenburger, M. Wellner, R. Banz, G. Colombo, and R. Riener, "Combining Immersive Virtual Environments with Robot-Aided Gait Training," in *Proceedings of the IEEE International Conference on Rehabilitation Robotics*, pp. 421-424, 2007.

[17] A. Mirelman, B. L. Patritti, P. Bonato, and J. E. Deutsch, "Effects of virtual reality training on gait biomechanics of individuals post-stroke," *Gait Posture*, vol. 31, no. 4, pp. 433-437, 2010.

[18] K. Brütsch, A. Koenig, L. Zimmerli, S. Mérillat-Koeneke, R. Riener, L. Jäncke, H. J. a van Hedel, and A. Meyer-Heim, "Virtual reality for enhancement of robot-assisted gait training in children with central gait disorders.," *J. Rehabil. Med.*, vol. 43, no. 6, pp. 493-9, 2011.

[19] U. Götz, K. Brütsch, R. Bauer, F. Faller, R. Spoerri, A. Meyer-heim, R. Riener, A. Koenig, and B. Hardware, "A Virtual Reality System for Robot-Assisted Gait Training Based on Game Design Principles," in *Proceedings of the International Conference on Virtual Rehabilitation*, pp. 1-2, 2011.

[20] D. Aoyagi, W. E. Ichinose, S. J. Harkema, D. J. Reinkensmeyer, and J. E. Bobrow, "A robot and control algorithm that can synchronously assist in naturalistic motion during body-weight-supported gait training following neurologic injury," *IEEE Trans Neural Syst Rehabil Eng*, vol. 15, no. 3, pp. 387-400, 2007.

[21] J. A. Zeni Jr., J. G. Richards, and J. S. Higginson, "Two simple methods for determining gait events during treadmill and overground walking using kinematic data," *Gait Posture*, vol. 27, no. 4, pp. 710-714, 2008.

[22] M. Roerdink, B. H. Coolen, B. H. E. Clairbois, C. J. C. Lamoth, and P. J. Beek, "Online gait event detection using a large force platform embedded in a treadmill.," *J. Biomech.*, vol. 41, no. 12, pp. 2628-32, 2008.

[23] J. L. Emken, R. Benitez, A. Sideris, J. E. Bobrow, and D. J. Reinkensmeyer, "Motor Adaptation as a Greedy Optimization of Error and Effort," *J Neurophysiol*, vol. 97, no. 6, pp. 3997-4006, 2007.

[24] R. A. Scheidt, J. B. Dingwell, and F. A. Mussa-Ivaldi, "Learning to move amid uncertainty," *J Neurophysiol*, vol. 86, no. 2, pp. 971-985, 2001.

[25] D. J. Reinkensmeyer and J. L. Patton, "Can robots help the learning of skilled actions?," *Exerc. Sport Sci. Rev.*, vol. 37, no. 1, pp. 43-51, Jan. 2009.

[26] N. D. Neckel, N. Blonien, D. Nichols, and J. Hidler, "Abnormal joint torque patterns exhibited by chronic stroke subjects while walking with a prescribed physiological gait pattern.," *J. Neuroeng. Rehabil.*, vol. 5, p. 19, 2008.

[27] J. S. Sulzer, K. E. Gordon, Y. Y. Dhaher, M. A. Peshkin, and J. L. Patton, "Preswing knee flexion assistance is coupled with hip abduction in people with stiff-knee gait after stroke," *Stroke*, vol. 41, no. 8, pp. 1709-1714, 2010.

[28] T. H. Cruz and Y. Y. Dhaher, "Evidence of Abnormal Lower-Limb Torque Coupling After Stroke; An Isometric Study," *Stroke*, vol. 39, no. 1, pp. 139-47, 2008.

[29] N. Neckel, M. Pelliccio, D. Nichols, and J. Hidler, "Quantification of functional weakness and abnormal synergy patterns in the lower limb of individuals with chronic stroke," *J Neuroengineering Rehabil*, vol. 3, no. 17, pp.1-11, 2006.

[30] J. M. Finley, E. J. Perreault, and Y. Y. Dhaher, "Stretch reflex coupling between the hip and knee: Implications for impaired gait following stroke," *Exp. Brain Res.*, vol. 188, no. 4, pp. 529-540, 2008.

[31] A. Pennycott, D. Wyss, H. Vallery, and R. Riener, "Effects of added inertia and body weight support on lateral balance control during walking.," in in Proceedings of the IEEE International Conference on Rehabilitation Robotics, 2011.

[32] M. Frey, G. Colombo, M. Vaglio, R. Bucher, M. Jorg, and R. Riener, "A novel mechatronic body weight support system," *IEEE Trans Neural Syst Rehabil Eng*, vol. 14, no. 3, pp. 311-321, 2006.

[33] H. J. Van Hedel, L. Tomatis, and R. Muller, "Modulation of leg muscle activity and gait kinematics by walking speed and bodyweight unloading," *Gait Posture*, vol. 24, no. 1, pp. 35-45, 2006.

[34] A. J. Threlkeld, L. D. Cooper, B. P. Monger, A. N. Craven, and H. G. Haupt, "Temporospatial and kinematic gait alterations during treadmill walking with body weight suspension.," *Gait Posture*, vol. 17, no. 3, pp. 235-45, 2003.

[35] L. Finch, H. Barbeau, and B. Arsenault, "Influence of Body Weight Support on Normal Human Gait : Development of a Gait Retraining Strategy," *Phys Ther*, vol. 71, no. 11, pp. 842-855, 1991.

[36] H. van der Kooij, B. Koopman, and E. H. F. van Asseldonk, "Body weight support by virtual model control of an impedance controlled exoskeleton (LOPES) for gait training.," in *Proceedings of the IEEE International Conference of the Eng Med Biol Soc*, pp. 1969-72, 2008.

[37] A. L. Behrman and S. J. Harkema, "Locomotor training after human spinal cord injury: a series of case studies," *Phys Ther*, vol. 80, no. 7, pp. 688-700, 2000.

[38] T. G. Hornby, D. J. Reinkensmeyer, and D. Chen, "Manually-assisted versus robotic-assisted body weight-supported treadmill training in spinal cord injury: what is the role of each?," *PM R*, vol. 2, no. 3, pp. 214-21, 2010.

[39] D. Zanotto, P. Setgal, and S. K. Agrawal, "Adaptive Assist-As-Needed Controller to Improve Gait Symmetryin Robot-Assisted Gait Training," in *Proceedings of the IEEE International Conference on Robotics & Automation*, pp. 724-729, 2014

[40] Hocoma, "Lokomat® Pro with FreeD." [Online]. Available: http://www.hocoma.com/fileadmin/user/Dokumente/Lokomat/fly_L6freeD_140128_en.pdf. [Accessed: 10-Sep-2014].

[41] B. Koopman, J. H. Meuleman, E. H. F. van Asseldonk, and H. van der Kooij, "Lateral balance control for robotic gait training.," in P*roceedings of the IEEE International Conference on Rehabilitation Robotic*s, 2013.

[42] A. L. Hof, M. G. J. Gazendam, and W. E. Sinke, "The condition for dynamic stability.," *J. Biomech.*, vol. 38, no. 1, pp. 1-8, 2005.

[43] E. H. F. van Asseldonck and H. van der Kooij, *Neurorehabilitation Technology*. Springer, 2012, pp. 379-396.

[44] M. Wu, T. G. Hornby, J. M. Landry, H. Roth, and B. D. Schmit, "A cable-driven locomotor training system for restoration of gait in human SCI.," *Gait Posture*, vol. 33, no. 2, pp. 256-60, 2011.

[45] J. L. Emken, J. E. Bobrow, and D. J. Reinkensmeyer, "Robotic movement training as an optimization problem: designing a controller that assists only as needed," in *Proceedings of IEEE International Conference on Rehabilitation Robotics*, 2005.

[46] I. Righetti, J. Buchli, and A. J. Ijspeert, "Dynamic hebbian learning in adaptive frequency oscillators," *Phys. D*, vol. 216, pp. 269-281, 2006.

[47] A. Gams, A. J. Ijspeert, S. Schaal, and L. J., "On-line learning and modulation of periodic movements with nonlinear dynamical systems," *Aut. Robot*, vol. 27, pp. 3-23, 2009.

[48] J. F. Veneman, R. Kruidhof, E. E. G. Hekman, R. Ekkelenkamp, E. H. F. Van Asseldonk, and H. Van der Kooij, "Design and Evaluation of the LOPES Exoskeleton Robot for Interactive Gait Rehabilitation," *IEEE Trans Neural Syst Rehabil Eng*, vol. 15, no. 3, pp. 379-386, 2007.

[49] Vallery H., Veneman J., Asseldonk E.H.F., Ekkelenkamp R., and H. van der Kooij, "Compliant Actuation of Rehabilitation Robots: Advantages and Limitations," *RAM,*, vol. 6, no. 1, pp. 60-69, 2007.

[50] C. K. Balasubramanian, R. R. Neptune, and S. A. Kautz, "Variability in spatiotemporal step characteristics and its relationship to walking performance post-stroke," *Gait Posture*, vol. 29, no. 3, pp. 408-414, 2010.

[51] J. M. Hausdorff, M. E. Cudkowicz, and R. Firtion, "Gait Variability and Basal Ganglia Disorders : Stride-to-S tride Variations of Gait Cycle Timing in Parkinson ' s Disease and Huntington' s Disease," vol. 13, no. 3, pp. 428-437, 1998.

[52] A. Schück, R. Labruyère, H. Vallery, R. Riener, and A. Duschau-Wicke, "Feasibility and effects of patient-cooperative robot-aided gait training applied in a 4-week pilot trial.," *J. Neuroeng. Rehabil.*, vol. 9, no. 1, p. 31, 2012.

[53] C. Krishnan, D. Kotsapouikis, Y. Y. Dhaher, and W. Z. Rymer, "Reducing robotic guidance during robot-assisted gait training improves gait function: a case report on a stroke survivor.," *Arch. Phys. Med. Rehabil.*, vol. 94, no. 6, pp. 1202-6, 2013.

[54] J. L. Emken and D. J. Reinkensmeyer, "Robot-enhanced motor learning: accelerating internal model formation during locomotion by transient dynamic amplification," *IEEE Trans Neural Syst Rehabil Eng*, vol. 13, no. 1, pp. 33-39, 2005

[55] D. S. Reisman, R. Wityk, K. Silver, and A. J. Bastian, "Locomotor adaptation on a split-belt treadmill can improve walking symmetry post-stroke," *Brain*, vol. 130, no. Pt 7, pp. 1861-1872, 2007.

[56] P. C. Kao, S. Srivastava, S. K. Agrawal, and J. P. Scholz, "Effect of robotic performance-based error-augmentation versus error-reduction training on the gait of healthy individuals," *Gait Posture*, vol. 37, no. 1, pp. 113-120, 2013.

[57] T. Lam, M. Wirz, L. Lunenburger, and V. Dietz, "Swing phase resistance enhances flexor muscle activity during treadmill locomotion in incomplete spinal cord injury," *Neurorehabil. Neural Repair*, vol. 22, no. 5, pp. 438-446, 2008.

[58] E. H. F. Van Asseldonk, B. Koopman, and H. Van Der Kooij, "Locomotor adaptation and retention to gradual and sudden dynamic perturbations," in *Proceedings of the IEEE International Conference on Rehabilitation Robotics*, 2011.

[59] M. M. Mirbagheri, L. Alibiglou, M. Thajchayapong, and W. Z. Rymer, "Muscle and reflex changes with varying joint angle in hemiparetic stroke.," *J. Neuroeng. Rehabil.*, vol. 5, no. 6, pp. 1-15, 2008.

[60] M. M. Mirbagheri, "Reflex stiffness gain and dynamics in spinal cord injury: Abnormalities and underlying mechanisms," in *Proceedings of the IEEE/EMBS International Conference on Neural Engineering*, pp. 798-801, Nov. 2013.

[61] A. H. Hansen, D. S. Childress, S. C. Miff, S. a Gard, and K. P. Mesplay, "The human ankle during walking: implications for design of biomimetic ankle prostheses.," *J. Biomech.*, vol. 37, no. 10, pp. 1467-74, 2004.

[62] M. L. Latash and V. M. Zatsiorsky, "Joint stiffness: Myth or reality?," *Hum. Mov. Sci.*, vol. 12, no. 6, pp. 653-692, 1993.

[63] M. R. Tucker, A. Moser, O. Lambercy, J. Sulzer, and R. Gassert, "Design of a wearable perturbator for human knee impedance estimation during gait.," in *Proceeding of the IEEE International Conference on Rehabilitation Robotics*, 2013.

[64] H. Lee, S. Member, and N. Hogan, "Investigation of Human Ankle Mechanical Impedance during Locomotion using a Wearable Ankle Robot.," in *Proceedings of the IEEE International Conference on Robotics and Automation*, pp. 2651-2656, 2013.

[65] D. Ludvig, T. S. Visser, H. Giesbrecht, and R. E. Kearney, "Identification of time-varying intrinsic and reflex joint stiffness.," *IEEE Trans. Biomed. Eng.*, vol. 58, no. 6, pp. 1715-23, 2011.

[66] D. Ludvig and E. J. Perreault, "Estimation of joint impedance using short data segments.," in *Proceedings of the IEEE International Conference of the Eng Med Biol Soc*, pp. 4120-3, 2011.

[67] S. Pfeifer, H. Vallery, M. Hardegger, R. Riener, and E. J. Perreault, "Model-based estimation of knee stiffness.," *IEEE Trans. Biomed. Eng.*, vol. 59, no. 9, pp. 2604-12, 2012.

[68] J. Meuleman, E. H. F. Van Asseldonk, and H. Van Der Kooij, "Novel actuation design of a gait trainer with shadow leg approach," in *Proceedings of the IEEE International Conference on Rehabilitation Robotics*, 2013.

[69] P. W. Duncan, K. J. Sullivan, A. L. Behrman, S. P. Azen, S. S. Wu, S. E. Nadeau, B. H. Dobkin, D. K. Rose, J. K. Tilson, S. Cen, and S. K. Hayden, "Body-weight-supported treadmill rehabilitation after stroke.," *N. Engl. J. Med.*, vol. 364, no. 21, pp. 2026-36, May 2011.

Summary

Summary

Many patients with neurological injuries like stroke or spinal cord injury (SCI) suffer from reduced walking ability. The ability to walk is a key component of independent functioning, and as such it represents an important rehabilitation goal for these patients. Repetitive practice of stepping movements has been shown to increase the effectiveness of the rehabilitation process. To aid the therapist in providing such training sessions, robotic gait trainers were introduced. These robots have the potential to deliver longer, and more intensive, locomotor training, compared to conventional (manually assisted) gait training, while relieving the therapists from physically demanding work.

Chapter 1 provides an overview of the different types of robotic gait trainers and their control strategies, and summarizes the clinical results obtained with these gait trainers so far. Despite their potential to increase training intensity, these robotic gait trainers are not proven to be superior to conventional gait training approaches in terms of clinical effectiveness. A key factor for this may be the used control strategies. Initially, most robotic gait trainers used "position control" to ensure that the patient followed a pre-specified movement as closely as possible. Position controlled gait training did not allow the support levels to be adapted to the activity of the patient. Guiding movement in this manner appeared to promote a "slacking" phenomenon, where patients start to rely on the robotic support instead of actively initiating and performing the movements themselves. Based on modern insights in neural plasticity, motor learning and motor recovery, it is suggested that the therapeutic benefit of robot-aided gait training can be increased by providing 'assist-as-needed' (AAN). The basic idea behind these AAN strategies is that the patient is supported only as much as is needed to accomplish the task. This way, each patient can be challenged to his maximum capacity, and reliance upon the assistance is prevented. While these AAN strategies require more active patient participation, evidence for better functional outcomes is still limited. Therefore, the first goal of this thesis was to develop different controllers, based on the assist-as-needed (AAN) principle, and evaluate their effectiveness.

Although AAN strategies apply supportive forces rather than enforcing a pre-specified gait pattern, they still require a predefined reference trajectory to determine the amount of support. That is; the more the patients gait pattern deviates from the reference, the more support is provided. To support neurological patients towards a healthy gait pattern it is important to consider that these patterns are dependent on walking speed. Especially since these patients typically walk at much lower speeds, compared to healthy individuals. In chapter 2 we confirmed that the amplitude and relative timing of these patterns are highly dependent on walking speed (and body-height) and we evaluated a novel method to create reference trajectories for robotic gait applications. Regression-models were constructed that can predict the timing, angle, angular velocity and acceleration of specific key events in the gait pattern. Subsequently quintic splines were fitted between the predicted key events to reconstruct a full gait cycle. These patterns can be implemented in

robotic gait trainers, but can also facilitate the assessment of pathological gait, where they can serve as a reference for 'normal' gait.

In chapter 3 we implemented a robotic support strategy based on impedance-control, using the derived reference angular trajectories. Its effectiveness on walking ability and walking quality was tested in 10 individuals with chronic incomplete spinal cord injury, who trained three times a week, for eight weeks. The LOPES (Lower Extremity Powered Exoskeleton) was used to provide the gait training. During the robot-aided gait training the device only intervened when the patients deviated from the specified angular trajectory. By reducing the impedance levels, the therapist could progressively reduce the support levels, depending on the capabilities and progress of the patient. At the end of the training period the participants significantly improved on functional outcomes, muscle strength, kinematics, and spatiotemporal measures. These improvements persisted at the eight-week follow-up. We also demonstrated that the most impaired ambulators, based on their initial walking speed and distance, benefitted the most from the training protocol (showing the greatest relative improvements in walking speed and distance).

Robotic support on joint level, as used in chapter 3, supports the complete gait pattern. In chapter 4 we used an alternative approach. Here we divided the control of human gait into different functional subtasks such as: creating sufficient foot clearance during swing, making a forward step, weight bearing or balance control. In neurologically impaired patients, each of these subtasks may be impaired to some degree without automatically affecting other subtasks. Partially and selectively supporting these subtasks, based on the patient's individual needs, can be seen as an extension of the 'assist-as-needed' principle. Support on subtask level also leaves room for the use of 'compensatory strategies'. Although these alternative movement strategies do not contribute to a more symmetric walking pattern, they can increase walking ability. Consequently, larger gains in motor function might be obtained when patients can still employ there compensatory movements in the robot. In chapter 4 we tested this subtask-support-strategy for one specific subtask: foot clearance. The foot clearance support was tested on 12 healthy subjects and 6 chronic stroke survivors, and proved effective in gradually and selectively influencing the foot clearance. That is; the foot clearance could easily be manipulated by changing the impedance levels, and supporting the foot clearance did not affect other basic gait parameters. Furthermore, we incorporated a stiffness-shaping algorithm that automatically shaped the amount of support to the subjects' needs, based on the deviation from the reference trajectory. This algorithm clearly shaped the support level to the specific needs of every stroke survivor and eliminated the need for the therapist to set the support levels based on trial and error.

A prerequisite for any support strategy that tries to enhance active patient participation is that the device can be sufficiently transparent, and thus does not hinder the motion of the subject when assistance is not provided. A high degree of transparency is thus needed for less impaired patients, who only require little support. Although the LOPES is force controlled, which allows the applied robotic forces to be controlled to zero when support

is not needed, previous experiments have shown that the amount of knee flexion decreases and muscle activation levels increase, due to the inertia of the exoskeleton leg. In chapter 5 we tried to increase the transparency with two different controllers that both exploit the cyclic nature of locomotion. Both controllers are based on a combination of Adaptive Frequency Oscillators (AFOs) and kernel-based Non-Linear Filters (NLFs), which can be used to learn and replay signals of cyclical movements. The first consisted of a feed-forward controller to improve the torque tracking (including the zero-torque mode). The second controller learned the state of the exoskeleton and used an inverse model of the LOPES to compensate for its dynamical effects (e.g. its inertia and friction). As a first step we evaluated the effectiveness of both controllers on 4 healthy subjects during slow and fast walking. Using the feed-forward controller resulted in an improved torque tracking of at least 52 percent at the hip joint and 61 percent at the knee joint. When both controllers were active simultaneously, the interaction power between the robot and the human leg was reduced by at least 40 percent at the thigh and 43 percent at the shank. These findings indicate that if a robotic task is rhythmic, the torque tracking and transparency can be improved by exploiting the predictions of AFOs and NFLs. Future experiments will have to demonstrate the effectiveness of both controllers when they are combined with assistive strategies, such as the ones presented in chapter 3 and 4.

Because the majority of the robotic gait trainers are instrumented with sensors that can measure joint angles and forces, these variables can be used to objectively assess the patient's performance and monitor their recovery. The patient's performance throughout the training sessions is often monitored by recording gait parameters like stride length, cadence, gait symmetry, joint range of motion or joint moments. However, gait kinematics and kinetics are not the only important measures in rehabilitation. Often stroke survivors and individuals with spinal cord injury show increased joint impedance, resulting from spasticity or abnormal muscle tone, which affects their walking ability. The second aim of this thesis was to assess the feasibility of using the LOPES as a measurement tool to quantify such joint properties. In chapter 6 we developed a novel method to estimate multi-joint leg impedance in a group of 8 elderly healthy individuals. Continuous torque perturbations were applied to the hip and knee joint simultaneously, while the subject's leg was suspended in the air. Multi-joint impedance was estimated non-parametrically using Multi-Input Multi-Output (MIMO) system identification techniques. Subsequently, it was modelled in terms of stiffness and damping around the hip and knee joint, but also with a visco-elastic coupling between both joints. Impedance measurements were performed during relax- and position-tasks. During the positon task the subjects were instructed to keep the deviations as small as possible, which resulted in a significant increase in estimated stiffness and damping parameters. The results also emphasized the importance of considering the visco-elastic coupling between joints when modeling multi-joint dynamics. Further tests with neurological patients have to confirm if this method can be used to discriminate between different impairment levels and if such measures can explain improvements in walking ability.

Finally, implications of the presented results and areas for further study are discussed in chapter 8. In this thesis the feasibility of different types of robotic assistance that are based on the AAN principle is demonstrated. In our experiments we demonstrated how active participation, movement variability and motivation, which are important preconditions for motor (re)learning, are promoted by such controllers. Combining sensors and complex control regimes creates an endless amount of possibilities to provide support, but also introduces many new questions and challenges. For example, in all implementations of interactive control schemes it has to be decided how much support should be provided. A decrease in support requires a larger effort from the patient. Given that the physical endurance of the patient is limited this results in a decrease in training time, and thus the amount of step repetitions (see chapter 3). Therefore, it is important that future research will further explore if there exists an optimum in this tradeoff between training intensity and the amount of step repetitions. A similar tradeoff exists between the amount of provided support and the movement variability that is allowed. Movement variability enables the patient to make and correct small movement errors, which can strongly enhance the effect of locomotor rehabilitation. However, the optimal level of required kinematic variability remains to be elucidated. Also questions like, what is the most effective robotic rehabilitation strategy?, can robotic gait training be combined with other neurorehabilitation methods (functional electrical stimulation, epidural electrical stimulation, pharmacological interventions) to increase its effectiveness?, who might benefit the most from a certain type of intervention?, require answers before the field can effectively advance. Robotic gait trainers make it possible to test these different therapeutic approaches in a well-controlled and reproducible manner. At the same time they enable standardized and objective assessment methods (like the one presented in chapter 6) to evaluate the effectiveness of the different robotic gait training regimes. In the future, large multicenter trials have to reveal the key elements that facilitate functional improvement, and need to prove that the use of robotic gait trainers can exceed (or accelerate) the functional improvements obtained with more conventional forms of therapy.

Samenvatting

Samenvatting

Veel patiënten met neurologische aandoeningen, zoals een beroerte (CVA) of een (gedeeltelijke) dwarslaesie, hebben last van een verminderd loopvermogen. Zelfstandig kunnen lopen is belangrijk voor het onafhankelijk functioneren, en vormt daarom een belangrijk doel bij de revalidatie van deze patiënten. Tijdens het revalidatietraject is het van belang dat de patiënt de loopbeweging op en intensieve manier kan oefenen. Om de fysiotherapeut te ondersteunen tijdens het begeleiden van looptraining zijn looprobots ontwikkeld. Looprobots maken het mogelijk om de patiënt langer en intensiever te laten trainen. Daarnaast zorgen deze robots ervoor dat de fysiotherapeut fysiek minder wordt belast bij het ondersteunen van de patiënt.

In hoofdstuk 1 wordt een overzicht gegeven van de verschillende looprobots en hun manier van aansturing, en worden de klinische resultaten die tot dusverre met deze robots zijn behaald beschreven. Hoewel de trainingsintensiteit kan worden verhoogd door het gebruik van looprobots, moet worden geconcludeerd dat ze, klinisch gezien, niet superieur zijn t.o.v conventionele looptraining. Een belangrijke factor hierin is mogelijk de manier van aansturen. Aanvankelijk werd voor de meeste looprobots gebruik gemaakt van “positie-aansturing”, waarbij een specifiek looppatroon aan de patiënt wordt opgelegd. Met deze vorm van aansturing kan de hoeveelheid ondersteuning niet worden aangepast aan de eigen activiteit van de patiënt. Dit lijkt te resulteren in “slacking" (ondersteuningsafhankelijkheid), wat betekent dat de patiënt afhankelijk wordt van de robot en een steeds kleinere bijdrage levert aan de beweging. Op basis van nieuwe inzichten op het gebied van neurale plasticiteit, bewegingsleer en bewegingsherstel, wordt nu gedacht dat het therapeutische voordeel van robot-ondersteunende looptraining kan worden vergroot, door het toepassen van “assist-as-needed” (AAN) principes. In tegenstelling tot de positie-aansturing, wordt in dit geval minimale ondersteuning geboden; net voldoende voor het uitvoeren van de beweging. Op deze manier wordt van de patiënt gevraagd dat hij zijn eigen capaciteiten volledig benut, wat het risico op slacking verkleint. Hoewel deze AAN strategieën resulteren in een grotere actieve bijdrage van de patiënt, is er nog weinig bewijs dat ze ook daadwerkelijk leiden tot een verhoogde mate van herstel. Het eerste doel van dit proefschrift was dan ook het ontwikkelen van verschillende aansturingsprincipes (gebaseerd op de AAN gedachte) en het testen van hun effectiviteit.

Hoewel met AAN-strategieën ondersteunende krachten worden aangeboden, in plaats van dat een voorgeschreven looppatroon wordt opgelegd, wordt nog steeds gebruik gemaakt van referentie looppatronen. Hoe meer de patiënt afwijkt van het voorgeschreven looppatroon, des te groter de geleverde ondersteuning. Deze looppatronen zijn sterk afhankelijk van de loopsnelheid. Dit is vooral van belang bij de revalidatie van neurologisch-aangedane patiënten, omdat zij vaak langzamer lopen dan niet-aangedane individuen. In hoofdstuk 2 laten we zien dat de amplitude en de timing van het looppatroon inderdaad sterk afhankelijk zijn van de loopsnelheid (en de

lichaamslengte). Op basis hiervan hebben we een nieuwe methode ontwikkeld en geëvalueerd, die gebruikt kan worden om referentiepatronen te reconstrueren. Hiervoor zijn regressie modellen opgesteld, die de timing, hoek, hoeksnelheid en versnelling van bepaalde “key events” in het looppatroon kunnen voorspellen. Tussen de voorspelde key events kunnen vervolgens 5de graads polynomen worden gefit. De gereconstrueerde referentiepatronen kunnen worden geïmplementeerd in looprobots, maar kunnen ook dienen als normaal referentiepatroon, op basis waarvan afwijkende looppatronen kunnen worden beoordeeld.

In hoofdstuk 3 is een manier van robotische ondersteuning getest, die is gebaseerd op “impedantie control”, en waarbij bovenstaande referentiepatronen zijn gebruikt. De effectiviteit van de ontworpen impedantie controller is vervolgens getest bij 10 patiënten met chronische, incomplete dwarslaesie die gedurende 8 weken drie trainingssessies per week volgden. Hierbij werd gebruik gemaakt van de LOPES (Lower Extremity Powered Exoskeloton). Tijdens de training bood de LOPES alleen ondersteuning wanneer patiënten afweken van het vooraf gedefinieerde looppatroon. Door de impedantie van de LOPES te verlagen kon de fysiotherapeut, op basis van de capaciteiten en de progressie van de patiënt, de ondersteuning steeds verder afbouwen. Aan het eind van de training werd een significante verbetering gezien in loopfunctie, spierkracht, kinematica en spatiotemporele parameters. Bij “follow-up", 8 weken na beëindigen van de training, waren deze verbeteringen nog steeds zichtbaar. Daarnaast toonde dit experiment aan dat de meest-aangedane patiënten de grootste relatieve verbetering lieten zien in loopsnelheid en afstand.

Robotische ondersteuning op gewrichtsniveau, zoals gebruikt in hoofdstuk 3, ondersteunt de hele loopbeweging. In hoofdstuk 4 hebben we een alternatieve aanpak gekozen, waarbij de loopbeweging in verschillende onderdelen (subtaken) werd gesplitst. Voorbeelden van deze subtaken zijn: het creëren van voldoende ruimte tussen de teen en de grond tijdens de zwaai van het been (“foot clearance”), het maken van een voorwaartse stap, het dragen van het lichaamsgewicht of het controleren van de balans. Bij neurologisch-aangedane patiënten kan elk van deze onderdelen afzonderlijk zijn aangedaan, zonder dat de andere onderdelen worden beïnvloedt. Het partieel en selectief ondersteunen van deze subtaken, op basis van de behoefte van de individuele patiënt, kan worden gezien als een uitbreiding van het eerder beschreven AAN principe. Met deze vorm van ondersteuning behoudt de patiënt ook de mogelijkheid om zelf-aangeleerde “compensatie strategieën” te gebruiken. Hoewel deze compensatie strategieën niet leiden tot een meer symmetrisch looppatroon, kunnen ze wel bijdragen aan een verbetering van het algemene loopvermogen. Dus, wanneer patiënten ook tijdens de training in een looprobot gebruik kunnen blijven maken van hun compensatie strategieën, zou de training uiteindelijk kunnen resulteren in een grotere verbetering van de loopfunctie. In hoofdstuk 4 hebben we deze selectieve ondersteuning van subtaken getest voor één specifieke subtaak; foot clearance. Hieraan hebben 12 gezonde vrijwilligers en 6 chronische CVA patiënten meegewerkt. Uit de resultaten bleek dat de staphoogte gradueel en selectief kon worden ondersteund. Met andere woorden; de staphoogte kon

gemakkelijk worden beïnvloedt door de impedantie van de robot bij te stellen, en ondersteuning van de staphoogte had geen effect op de uitvoering van andere subtaken. Ook werd een algoritme geïmplementeerd dat de mate van ondersteuning automatisch aanpast, op basis van de afwijking van de patiënt ten opzichte van het referentiepatroon. Op deze manier krijgt elke patiënt automatisch de juiste hoeveelheid ondersteuning, waar dit voorheen door de fysiotherapeut handmatig moest worden ingesteld, op basis van trial-and-error.

Een voorwaarde voor het gebruik van AAN strategieën is dat de robot voldoende transparant is. Dat houdt in dat de robot de beweging van de patiënt niet mag hinderen of remmen, wanneer deze geen ondersteuning biedt. Vooral voor relatief zelfstandige patiënten, die weinig ondersteuning nodig hebben, is dus een hoge transparantie vereist. De LOPES is kracht gestuurd, en daarmee is het mogelijk de krachten tot nul te reduceren wanneer geen ondersteuning nodig is. Eerdere experimenten hebben echter aangetoond dat de inertia van het exoskelet toch leidt tot een afname van de maximale knieflexie en een toename van de spieractivatie. In hoofdstuk 5 hebben we daarom geprobeerd de transparantie van de robot te verhogen. Hiervoor zijn twee controllers ontwikkelt, die beide gebruik maken van het feit dat lopen een cyclische beweging is. Beide controllers zijn gebaseerd op een combinatie van Adaptive Frequency Oscillators (AFOs) en kernel-based Non-Linear Filters (NLFs). De eerste controller bestaat uit een feed-forward controller, gericht op het verbeteren van de kracht-aansturing (dus ook wanneer er geen kracht moet worden aangeboden). De tweede controller leert de beweging van het exoskelet en maakt gebruik van een invers model om de dynamica van het exoskelet (zoals inertia en wrijving) te compenseren. De effectiviteit van beide controllers is getest op vier gezonde proefpersonen, tijdens langzaam en snel lopen. Het gebruik van de feed-forward controller resulteerde in een toename van de nauwkeurigheid van de kracht-aansturing van ten minste 52 procent voor het heupgewricht en 61 procent voor het kniegewricht. Wanneer beide controllers tegelijk actief waren, leidde dat tot een afname van de interactie energie van ten minste 40 procent op het bovenbeen en 43 procent op het onderbeen. Deze resultaten laten zien dat, wanneer een robot een taak moet uitvoeren die ritmisch is, de nauwkeurigheid van de krachtregelaar en de transparantie kunnen worden vergroot door gebruik te maken van de voorspellende waarde van de AFOs en NFLs. Toekomstige experimenten zullen moeten uitwijzen of deze controllers effectief kunnen worden ingezet in combinatie met de controllers die daadwerkelijk de ondersteuning moeten bieden, zoals degene beschreven in hoofdstuk 3 en 4.

Het merendeel van de ontwikkelde looprobots zijn voorzien van sensoren die gewrichtshoeken en momenten kunnen meten. Deze variabelen kunnen worden gebruikt voor het objectief meten van de door de patiënt uitgevoerde bewegingen en zijn progressie gedurende het revalidatietraject. Tot dusver worden de prestaties van de patiënt tijdens de training vaak gemeten aan de hand van spatiotemporele parameters zoals de staplengte, cadans, stapsymmetrie, bewegingsbereik of geleverde gewrichtsmomenten. Echter, er zijn ook andere parameters die belangrijke informatie kunnen verschaffen gedurende het revalidatieproces. Patiënten met een CVA of een

(gedeeltelijke) dwarslaesie hebben bijvoorbeeld vaak last van een verhoogde gewrichtsstijfheid (impedantie) als gevolg van spasticiteit en/of verhoogde spierspanning, met als gevolg een verminderd loopvermogen. Het tweede doel van dit proefschrift was dan ook het onderzoeken van de mogelijkheden om de LOPES in te zetten als meetinstrument voor dergelijke gewrichtseigenschappen. In hoofdstuk 6 hebben we een nieuwe methode ontwikkeld voor het bepalen van de impedantie over meerdere gewrichten ("multi-joint impedantie"). Bij 8 oudere proefpersonen zijn continue verstoringen aangeboden op de knie en heup, terwijl het verstoorde been vrij kon zwaaien. Met behulp van "Multi-Input Multi-Output" (MIMO) systeem identificatie technieken kon de multi-joint impedantie van het been worden bepaald. Vervolgens is de multi-joint impedantie gemodelleerd in termen van stijfheid- en dempingparameters van de heup en knie, maar ook door het toevoegen van een visco-elastische koppeling tussen beide gewrichten. De gewricht-impedantie is gemeten tijdens relax- en positie-taken. Tijdens de positietaak werd de proefpersoon gevraagd om de beweging van het been, als gevolg van de verstoring, zo laag mogelijk te houden, wat leidde tot een significante toename van de geschatte stijfheid- en dempingparameters. Daarnaast is aangetoond dat er, tijdens het modelleren van beweging van meerdere gewrichten, rekening moet worden gehouden met de genoemde visco-elastische koppeling tussen beide gewrichten. Toekomstige experimenten bij patiënten met een neurologische aandoening zullen moeten bevestigen of de gepresenteerde methode gebruikt kan worden om onderscheid te maken tussen de verschillende niveaus van de stoornis, en of een afname van hun gewrichtsstijfheid ook daadwerkelijk een verbetering in loopfunctie kan verklaren.

De consequenties van de gepresenteerde resultaten, en suggesties voor verder onderzoek worden tot slot besproken in hoofdstuk 8. In dit proefschrift is aangetoond dat robotische ondersteuning, gebaseerd op het AAN principe, goed bruikbaar is. In de verschillende experimenten hebben we laten zien dat actieve participatie, bewegingsvrijheid, en motivatie worden bevorderd door het gebruik van dergelijke controllers. Het gebruik van sensoren en gecompliceerde controllers biedt een oneindige hoeveelheid mogelijkheden om de patiënt te ondersteunen, maar introduceert ook veel nieuwe vragen en uitdagingen. Bij alle interactieve controllers moet bijvoorbeeld worden bepaald hoeveel ondersteuning er wordt aangeboden. Een afname van de ondersteuning vereist een grotere fysieke inspanning van de patiënt. Aangezien de patiënt een beperkt fysiek uithoudingsvermogen heeft, betekent dit dat hij minder lang kan trainen en dus minder stappen kan maken (zie hoofdstuk 3). Toekomstig onderzoek zal moeten uitwijzen hoe trainingsintensiteit en het aantal gemaakte stappen met elkaar samenhangen, en of er sprake is van een optimum. Een soortgelijke afweging geldt ook voor de hoeveelheid ondersteuning en de bewegingsvrijheid die is toegestaan. Het is al aangetoond dat de mogelijkheid om kleine fouten te maken, en die te corrigeren, een positieve invloed heeft op het effect van looptraining, maar de optimale hoeveelheid bewegingsvrijheid is (nog) niet bekend. Ook vragen zoals: wat is de meest effectieve robot revalidatiestrategie, kan robot training gecombineerd worden met andere vormen van neurorevalidatie (functionele elektrostimulatie, ruggenmergstimulatie, medicatie)?, en wie heeft er het

meeste baat bij een bepaald type interventie?, zullen in de toekomst beantwoord moeten worden. Met looprobots is het mogelijk om deze verschillende therapeutische benaderingen op een goed gecontroleerde en reproduceerbare manier te testen. Tegelijkertijd is het met deze robots mogelijk geworden om de effectiviteit van de verschillende strategieën op een gestandaardiseerde en objectieve manier te beoordelen (zoals bijvoorbeeld met de methode beschreven in hoofdstuk 6). In de toekomst zullen grote multicenter trials moeten uitwijzen welke factoren tijdens het revalidatieproces het belangrijks zijn om de klinische effectiviteit te vergroten. Daarnaast zullen dergelijke trials moeten aantonen of het gebruik van looprobots daadwerkelijk leidt tot betere (of snellere) resultaten.

Dankwoord

Dankwoord

In dit laatste hoofdstuk van mijn proefschrift wil ik graag een aantal mensen bedanken die mij hebben begeleid, hebben geholpen bij de experimenten, het proefschrift, of op persoonlijk vlak van onmisbare waarde zijn geweest. Ondanks dat er voor een dankwoord geen maximaal aantal woorden is gedefinieerd, iets waar ik bij het schrijven van de verschillende artikelen (tot grote frustratie) vaak tegenaan ben gelopen, ga ik nog één keer proberen om het kort te houden.

Om te beginnen wil ik alle proefpersonen bedanken die, op welk moment dan ook, een keer in de LOPES hebben plaatsgenomen om deel te nemen aan de verschillende experimenten. Bedankt voor jullie geduld tijdens de soms wat vreemde testen. Deelnemen aan een experiment in een robot die loopbewegingen ondersteunt, om vervolgens een tijdlang op één been te moeten blijven staan lijkt wellicht wat tegenstrijdig. Mijn speciale dank gaat ook uit naar de vrijwilligers voor wie de experimenten een extra opgave was, als gevolg van een hersenbloeding of dwarslaesie. Velen van jullie zijn herhaaldelijk (soms meerdere keren per week) afgereisd naar Enschede om deel te nemen aan de testen. Zonder jullie inzet had ik dit proefschrift niet kunnen schrijven.

Wellicht tegen de gewoonte in ga ik niet verder met het bedanken van mijn promotor, maar richt ik me eerst tot mijn co-promotor. Edwin, zonder jou als dagelijks begeleider had dit traject er waarschijnlijk heel anders uitgezien. De uitdrukking “assist-as-needed”, welke in dit proefschrift herhaaldelijk terugkomt, is ook direct op jou van toepassing. Jouw deur stond altijd open en je was altijd bereid om even van gedachten te wisselen over datgene waar ik op dat moment mee zat. Zeker aan het einde van mijn promotie heb je vaak s ’avonds nog tijd gemaakt om me via Skype van commentaar op artikelen te voorzien. Jouw kritische blik is van grote waarde geweest tijdens dit traject. Ondanks dat we het nooit eens zullen worden over wat de mooiste voetbalclub van Nederland is, hadden onze (werk gerelateerde) discussies meestal wél een uitkomst waar we allebei achter stonden en waar ik mee verder kon. Daarnaast was je op persoonlijk vlak ook altijd erg betrokken en wil ik je bedanken voor je gezelligheid in het lab, op congressen, vakgroepsuitjes en tijdens de talloze demo’s die we samen hebben gegeven. Tot slot, als je ooit nog eens “een beetje een nette” lange broek voor een demo, een “tijdelijke” fiets of een aangifte- adres nodig hebt weet je me te vinden.

Uiteraard wil ik ook mijn promotor bedanken. Herman, jij gaf me de mogelijkheid (en de vrijheid) om dit onderzoek uit te voeren. Je hebt een duidelijke visie en was vaak in staat om me tijdens de werkbesprekingen weer op scherp te zetten, of om belangrijke knopen door te hakken als het onderzoek wat leek vast te lopen. Je input, kritische vragen en opmerkingen heb ik als zeer waardevol ervaren. Ik bewaar leuke herinneringen aan ons tripje door de Zwitserse Alpen na een EVRYON meeting in Lausanne. Nog bedankt dat je me destijds niet hebt achtergelaten terwijl ik heup-diep in de tiefschnee stond.

Wietse, met jou heb ik misschien wel de meeste uurtjes doorgebracht in het lab. We hebben samen leuke experimenten gedaan en vele proefballonnetjes opgelaten. Ik weet niet of het ooit gaat lukken om de EMG's in LOPES onder die van "free walking" te krijgen, maar aan de hoeveelheid controllers waarmee we het hebben geprobeerd heeft het niet gelegen. Voor wat betreft het volume van dit proefschrift ben ik blij met onze gezamenlijke publicatie. In tegenstelling tot ondergetekende ben jij goed in staat om de zaken kort en bondig op te schrijven en zonder jou was hoofdstuk 5 waarschijnlijk net zo lang geworden als de rest. Verder was je een relaxt maatje tijdens de vele reisjes die we voor het EVRYON project hebben gemaakt. Bedankt voor de plezierige samenwerking, en ik wens je alle succes met het afronden van je eigen promotie.

Er zijn meerdere mensen binnen de vakgroep Biomedische Werktuigbouwkunde die ik graag even wil bedanken. Jos en Gijs: hoewel ik niet direct betrokken was bij de ontwikkeling van de LOPES II vond ik het leuk dat ik me mocht mengen in jullie brainstorm sessies. Succes met de verdere ontwikkeling en ik ben ervan overtuigd dat de LOPES II een groot succes wordt. Ramazan and Letianl: thanks for being my roomies, and allowing me to spill my frustrations from time to time. I wish you both the best. Mark: hoewel de tijd simpelweg op was om de experimenten verder uit te bouwen wil ik je toch bedanken voor je hulp bij het opzetten van de pilottesten met de "pusher". Tijdens mijn promotie heb ik een aantal studenten mogen begeleiden. Juliet, Marloes, Daphne, Christos; ik vond het leuk om jullie te mogen begeleiden. Jullie hebben alle vier een belangrijke bijdrage geleverd, aan dit proefschrift, of aan de ontwikkeling van de LOPES in het algemeen. Geert en Wouter; bedankt voor jullie technische ondersteuning. Zonder jullie had de LOPES zeker meer "down time" gehad. Wouter, bedankt voor de vele keren dat je me hebt geholpen bij het vervangen van de kabels van de LOPES. Ik moet nog zien wie ons record van 2 kabels vervangen (en inregelen) binnen het uur gaat verbeteren. Dan de secretaresse van de afdeling. Lianne; bedankt voor het regelen van allerlei zaken waar ik zelf nooit aan gedacht zou hebben. De vanzelfsprekendheid waarmee jij voor iedereen klaar staat moet zeker worden vermeld. Tijdens mijn promotie had ik natuurlijk ook de nodige frustratie met pc's en toebehoren. Gedoe met harde schijven, accu's, licenties, software, noem maar op. Nicolai; bedankt voor je hulp om dit altijd weer zo goed mogelijk op te lossen. To my other colleques: thanks to all of you, for the "vakgroepuitjes", soccer matches, dinners and other get togethers, but mostly for making BW a great place to work. I think the majority of you participated in a LOPES experiment at some point, which is highly appreciated.

This PhD was part of a larger European project. Everyone from the "EVRYON" project (the guys from Pisa, Rome, Lausanne, Budapest, Ljubljana and Delft): thanks! Not only for the scientific collaboration, but also for the good times during project meetings, review meetings, conferences etc. To the guys from Pisa:, I'm still not sure if the frequent visits to Enschede were all initiated strictly out of scientific curiosity, or just to amaze yourselves about the culinary concept of the Dutch kroketten. If you ever want me to send you a box of these frozen delicacies just let me know. Regarding the quality of the coffee in the machines in Enschede: I fully agree….

Dan zijn er een aantal mensen van Het Roessingh die een belangrijke bijdrage hebben geleverd tijdens de experimenten. Bram, Leontien, Martijn: bedankt voor jullie hulp (en gezelligheid) met het begeleiden van de patiënten tijdens de LOPES experimenten. Bertine en Hans: bedankt voor de succesvolle samenwerking die heeft geresulteerd in het artikel dat is opgenomen als hoofdstuk 3.

Ook zijn er twee mensen bij Abbott Medical Optics die ik graag wil bedanken. Theo en Klaas: bedankt voor de interesse die jullie hebben getoond en de flexibiliteit die jullie hebben geboden ten tijde van het afronden van deze promotie.

Gelukkig zijn er ook een aantal clubjes buiten de UT die voor de nodige ontspanning hebben gezorgd. Xoun: ondanks dat mijn betrokkenheid de laatste jaren natuurlijk wat minder was dan tijdens mijn studie, hebben de Ardennen weekendjes, EK's, WK's, gala's, oud en nieuw feesten en kerstdiners voor een flinke dosis afleiding gezorgd. Wat betreft de leden van de "nooit meer stappen in Groningen" Whatsapp-groep, misschien kunnen we nog een keer een uitzondering maken? Rob en Ewout: nu mijn promotie achter de rug is beloof ik dat ik mijn aquaria weer in volle glorie zal herstellen. Ik wacht trouwens nog steeds op die uitnodiging om een keer te gaan 4x4-en. Rob: mooi om te zien met hoeveel enthousiasme de vraag om mijn paranimf te zijn werd beantwoord, ik vind het top dat je erbij bent in december. Kai en Mark: het feit dat jullie altijd dichtbij waren op de UT maakte jullie tot de perfecte proefpersonen als er weer "eventjes" een controller getest moest worden of wanneer er een slachtoffer nodig was voor een demo. Ondanks de vaak last minute aankondiging hebben jullie deze functie vaak, en met verve, vervuld. Ik denk dat jullie mijn demo praatje inmiddels zo vaak hebben gehoord dat we prima een keer hadden kunnen ruilen. Mark: bedankt voor de overload aan spareribs en de gigantische gehaktballen die je mij hebt voorgeschoteld in de tijd dat we samen op de Sterrenstraat hebben gewoond. Het hebben van een huisgenoot met zulke culinaire gaven is echt pure luxe. Daarnaast was je gewoon een hele relaxte huisgenoot. Je staat altijd voor iedereen klaar, en bent altijd overal voor in. Bedankt dus voor je enthousiasme, bij alles. Ook dank aan de leden van InfusiX, voor de vele tripjes die we door de jaren heen hebben gemaakt, dat er nog maar vele mogen volgen. Mijn oude maatjes uit Twello, we zien elkaar te weinig, maar toch zijn er een paar tradities (Sinterklaas, bootje varen..) die we al jaren in stand houden. Bij jullie is het altijd als vanouds gezellig en ik hoop dan ook dat we deze tradities nog jaren in stand blijven houden. Hetzelfde geldt voor de boys van de Borstelweg. Ondanks soms lange periode van afwezigheid vind ik het altijd top om weer aan te kunnen schuiven bij een zomer bbq of een kerstdiner.

Mijn schoonfamilie, Carin&Felix, Sander&Hilde, Remko&Nancy, en de ontelbare hoeveelheid oom en tantes, bedankt voor jullie oprechte interesse. Velen van jullie (inclusief Karin en Johan natuurlijk) hebben zelfs een constructieve bijdrage geleverd aan hoofdstuk 2. Toch leuk om te weten dat in de nieuwe LOPES looppatroontjes worden gebruikt die gebaseerd zijn op de metingen die we hebben gedaan toen jullie een dagje op de UT waren.

En dan natuurlijk mijn eigen familie. Pa, ma, bedankt voor jullie onvoorwaardelijke steun en interesse de afgelopen jaren. Ik kan altijd bij jullie binnenwaaien en jullie staan altijd voor me klaar. Pim, mijn “kleine” broertje. Als ik iets geregeld moet hebben hoef ik maar te bellen. Je bent een echte regelneef, iets waar ik vaak, en dankbaar, gebruik van maak. Bedankt dat je er voor me bent en super dat jij mijn paranimf wilt zijn. Opa, inmiddels 90+, en gelukkig nog altijd van de partij. Ik vind het mooi om te zien hoe fit en betrokken je nog bent. Ik houd een plaatsje voor je vrij op de eerste rij.

Lieve Joyce, de waslijst aan dingen waar ik jou voor moet bedanken is zo lang dat ik hem niet ga opsommen (ik probeerde het immers kort te houden, weer niet gelukt….). Toch wil ik je in het bijzonder bedanken voor de afgelopen maanden. De komst van ons prachtige mannetje, twee maanden voor het afronden van mijn proefschrift maakte de laatste maanden bijzonder hectisch. Toch is er maar één iemand die zo goed de rust weet te bewaren in tijden van stress en chronisch slaapgebrek. Je bent voor mij van onschatbare waarde, en daar ben ik je ontzettend dankbaar voor. Nu we allebei weer in rustig vaarwater zitten kunnen we volop genieten van ons mooie ventje, en van een welverdiende vakantie. Tot slot, Sam; fantastisch dat je er bent, en dat je tijdens het schrijven van dit dankwoord zo lekker naast me op de bank hebt zitten giechelen.

Biography

Biography

Bram Koopman was born in 1982 in Twello, The Netherlands. After his graduation from high school (Etty Hillesum Lyseum, Deventer) in 2001, he moved to Enschede to study Biomedical Engineering at the University of Twente. During his Master he selected "Human Function Technology" as specialization and spend time in Melbourne for his internship at REHAB Tech, a Professional Resource Centre for the Prosthetic, Orthotic and Rehabilitation Engineering industries. His interest for the use of robotic devices for the rehabilitation of neurological patients was gained during his master assignment at the department of Biomechanical Engineering. Under supervision of Herman van de Kooij and Edwin van Asseldonk he graduated cum laude in 2008. Shortly after his graduation he started his PhD research at the department of Biomechanical Engineering on the Evryon project (Evolving Morphologies for Human-Robot Symbiotic Interaction). This project aimed at the development of novel design methodologies for wearable robots that can be can be used for rehabilitation, assistance or human augmentation. In parallel he continued to work on the implementation of assistive strategies and assessment methods for robotic gait trainers. The results of this research are presented in this thesis. In April 2014 he started his new job as project engineer at Abbott Medical Optics, Groningen, The Netherlands.

Publications

Journal publications

B. Koopman, E. H. F. van Asseldonk, H. van der Kooij,"Estimation of human hip and knee multi-joint dynamics using the lopes gait trainer", Submitted to: *IEEE Trans. Neural Syst.* Rehabil. Eng.

B. Koopman†, B. M. Fleerkotte†, J. H. Buurke, E. H. F. van Asseldonk, H. van der Kooij, and J. S. Rietman, "The effect of impedance-controlled robotic gait training on walking ability and quality in individuals with chronic incomplete spinal cord injury: an explorative study," *J. Neuroeng. Rehabil.*, vol. 11, no. 1, pp. 11-26, 2014.

B. Koopman, E. H. F. van Asseldonk, and H. Van der Kooij, "Speed-dependent reference joint trajectory generation for robotic gait support," *J. Biomech*., vol. 47, no. 6, pp. 1447-1458, 2014.

B. Koopman, E. H. F. van Asseldonk, and H. van der Kooij, "Selective control of gait subtasks in robotic gait training: foot clearance support in stroke survivors with a powered exoskeleton," *J. Neuroeng. Rehabil*., vol. 10, no. 1, pp. 10-31, 2013.

M. Donati, N. Vitiello, S. M. M. de Rossi, T. Lenzi, S. Crea, A. Persichetti, F. Giovacchini, **B. Koopman**, J. Podobnik, M. Munih, and M. C. Carrozza, "A flexible sensor technology for the distributed measurement of interaction pressure," *Sensors*, vol. 13, no. 1. pp. 1021-1045, 2013.

R. Ronsse, T. Lenzi, N. Vitiello, **B. Koopman**, E. van Asseldonk, S. M. De Rossi, J. van den Kieboom, H. van der Kooij, M. C. Carrozza, and A. J. Ijspeert, "Oscillator-based assistance of cyclical movements: model-based and model-free approaches," *Med. Biol. Eng. Comput.*, vol. 49, no. 10, pp. 1173-1185, 2011.

S. M. M. de Rossi, N. Vitiello, T. Lenzi, R. Ronsse, **B. Koopman**, A. Persichetti, F. Vecchi, A. J. Ijspeert, H. van der Kooij, and M. C. Carrozza, "Sensing pressure distribution on a lower-limb exoskeleton physical human-machine interface," *Sensors*, vol. 11, no. 1, pp. 207-227, 2011.

† Authors contributed equally

Publications in conference proceedings

B. Koopman, J. H. Meuleman, E. H. F. van Asseldonk, and H. van der Kooij, "Lateral balance control for robotic gait training," in *Proceedings of the IEEE International Conference on Rehabilitation Robotics*, pp.1-6, 2013.

B. Koopman†, W. Van Dijk†, H. Van Der Kooij, and E. H. F. Van Asseldonk, "Improving the transparency of a rehabilitation robot by exploiting the cyclic behaviour of walking," in *Proceedings of the IEEE International Conference on Rehabilitation Robotics*, pp. 1-8, 2013.

R. Ronsse, S. M. M. De Rossi, N. Vitiello, T. Lenzi, **B. Koopman**, H. Van Der Kooij, M. C. Carrozza, and A. J. Ijspeert, "Real-time estimate of period derivatives using adaptive oscillators: Application to impedance-based walking assistance," in *Proceedings of the IEEE International Conference on Intelligent Robots and Systems*, pp. 3362-3368, 2012.

W. van Dijk, **B. Koopman**, R. Ronsse, and H. van der Kooij, "Feed-forward support of human walking," in *Proceedigns of IEEE RAS EMBS Int. Conf. Biomed. Robot. Biomechatronics*, pp. 1955-1960, 2012.

B. Koopman, E. H. F. Van Asseldonk, H. Van Der Kooij, W. Van Dijk, and R. Ronsse, "Rendering potential wearable robot designs with the LOPES gait trainer," in *Proceedings of the IEEE International Conference on Rehabilitation Robotics*, pp. 748-754, 2011.

R. Ronsse, **B. Koopman**, N. Vitiello, T. Lenzi, S. M. M. De Rossi, J. van den Kieboom, E. van Asseldonk, M. C. Carrozza, H. van der Kooij, and A. J. Ijspeert, "Oscillator-based walking assistance: a model-free approach,"in *Proceedings of the IEEE International Conference on Rehabilitation Robotics*, pp. 1-6, 2011.

E. H. F. Van Asseldonk, **B. Koopman**, and H. Van Der Kooij, "Locomotor adaptation and retention to gradual and sudden dynamic perturbations," in *Proceedings of the IEEE International Conference on Rehabilitation Robotics*, pp. 1-5, 2011.

B. Koopman, E. F. van Asseldonk, and H. van der Kooij, "In vivo measurement of human knee and hip dynamics using MIMO system identification," in *Proceedings of the Conference of the IEEE Engineering in Medicine and Biology Society*, pp. 3426-3429, 2010

S. M. De Rossi, N. Vitiello, T. Lenzi, R. Ronsse, **B. Koopman**, A. Persichetti, F. Giovacchini, F. Vecchi, A. J. Ijspeert, H. van der Kooij, and M. C. Carrozza, "Soft artificial tactile sensors for the measurement of human-robot interaction in the rehabilitation of the lower limb," in *Proceedings of the Conference of the IEEE Engineering in Medicine and Biology Society*, pp. 1279-82, 2010.

E. H. F. Van Asseldonk, B**. Koopman**, J. H. Buurke, C. D. Simons, and H. Van Der Kooij, "Selective and adaptive robotic support of foot clearance for training stroke survivors with stiff knee gait," in *Proceedings of the IEEE International Conference on Rehabilitation Robotics*, pp. 602-607, 2009.

H. van der Kooij, **B. Koopman**, and E. H. F. van Asseldonk, "Body weight support by virtual model control of an impedance controlled exoskeleton (LOPES) for gait training," in *Proceedings of the Conference of the IEEE Engineering in Medicine and Biology Society*, pp. 1969-72, 2008.

† Authors contributed equally

Abstracts selected for oral presentation

B. Koopman, E. H. F. van Asseldonk, H. van der Kooij, "Joint Impedance measurement of the hip and knee using the lopes gait trainer," Gepeszet 2012, 8th International Conference on Mechanical Engineering, Budapest, Hungary, 24-24 May, 2012.

B. Koopman, E.H.F. van Asseldonk, H. van der Kooij, "Estimating the impedance of the human leg," 11th IEEE-RAS International Conference on Humanoid Robots (Humanoids 2011), Bled, Slovenia, 26-28 October, 2011.

B. Koopman, E.H.F. van Asseldonk, H. van der Kooij, "Joint impedance measurements of the hip and knee joint using the lopes gait trainer," 3rd Dutch bio-medical engineering conference, Egmond aan Zee, The Netherlands, 21-21 January, 2011.

B. Koopman, E.H.F. van Asseldonk, H. van der Kooij, "In vivo measurement of human knee and hip dynamics using MIMO system identification," 32nd Annual International Conference of the IEEE Engineering in Medicine and Biology Society, Buenos Aires, Argentina, 31 August-4 September, 2010.

B. Koopman, E.H.F. van Asseldonk, H. van der Kooij, "Measuring joint impedance of the human hip and knee joint using MIMO system identification," 4th Annual Symposium of the Benelux Chapter of the IEEE Engineering in Medicine and Biology Society (EMBS), Enschede, The Netherlands, 9-10 November, 2009.

B. Koopman, E.H.F. van Asseldonk, H. van der Kooij, "Adaptive robotic assistance during gait training following stroke," 2nd Dutch bio-medical engineering conference, Egmond aan Zee, The Netherlands, 22-23 January 2009.